RADIOLOGY AND ONCOLOGY

vol.54 no.3

september 2020

CABOMETYX®

(kabozantinib) tablete

60 mg | 40 mg | 20 mg

CABOMETYX® pomembno izboljša PFS, OS in ORR v drugi liniji zdravljenja napredovalega karcinoma ledvičnih celic[1]

- PFS[2]
- OS[2]
- ORR[2]

ORR: objektivna stopnja odziva; OS: celokupno preživetje; PFS: preživetje brez napredovanja bolezni

Referenci: 1. Choueiri TK, Escudier B, Powles T, *et al*. Cabozantinib versus everolimus in advanced renal cell carcinoma (METEOR): final results from a randomised, open-label, phase 3 trial. The Lancet Oncology. 2016;17(7):917-27. **2.** Povzetek glavnih značilnosti zdravila Cabometyx.

Skrajšan povzetek glavnih značilnosti zdravila

▼ Za to zdravilo se izvaja dodatno spremljanje varnosti. Tako bodo hitreje na voljo nove informacije o njegovi varnosti. Zdravstvene delavce naprošamo, da poročajo o katerem koli domnevnem neželenem učinku zdravila.

CABOMETYX 20 mg | 40 mg | 60 mg filmsko obložene tablete
(kabozantinib)

TERAPEVTSKE INDIKACIJE Zdravljenje napredovalega karcinoma ledvičnih celic (KLC) pri predhodno nezdravljenih odraslih bolnikih s srednje ugodnim ali slabim prognostičnim obetom ter pri odraslih bolnikih po predhodnem zdravljenju, usmerjenem v vaskularni endotelijski rastni faktor (VEGF). V monoterapiji zdravljenje hepatocelularnega karcinoma (HCK) pri odraslih bolnikih, ki so se predhodno že zdravili s sorafenibom. **ODMERJANJE IN NAČIN UPORABE** Pri bolnikih s KLC in HCK je priporočeni odmerek 60 mg enkrat na dan. Zdravljenje je treba nadaljevati tako dolgo, dokler bolnik več nima kliničnih koristi od terapije ali do pojava nesprejemljive toksičnosti. Pri sumu na neželene reakcije bo morda treba zdravljenje začasno prekiniti in/ali zmanjšati odmerek. Če je treba odmerek zmanjšati, se priporoča zmanjšanje na 40 mg/dan in nato na 20 mg/dan. Prekinitev odmerka se priporoča pri obravnavi toksičnosti 3. ali višje stopnje po CTCAE (*common terminology criteria for adverse events*) ali nevzdržni toksičnosti 2. stopnje. Zmanjšanje odmerka se priporoča za dogodke, ki bi lahko čez čas postali resni ali nevzdržni. Za priporočila glede prilagoditve odmerka ob pojavu neželenih učinkov glejte celoten povzetek glavnih značilnosti zdravila. Pri blagi ali zmerni ledvični okvari je treba kabozantinib uporabljati previdno. Uporaba se ne priporoča pri hudi ledvični okvari. Pri blagi okvari jeter odmerka ni treba prilagajati. Pri zmerni okvari jeter (Child Pugh B) je priporočljivo skrbno spremljanje celokupne varnosti. Pri bolnikih s hudo okvaro jeter (Child Pugh C) uporaba kabozantiniba ni priporočljiva. Način uporabe: Tablete je treba pogoltniti cele in jih ni dovoljeno drobiti. Bolnikom je treba naročiti, naj vsaj 2 uri pred uporabo zdravila in 1 uro po tem ničesar ne jedo. **KONTRAINDIKACIJE** Preobčutljivost na učinkovino ali katero koli pomožno snov. **POSEBNA OPOZORILA IN PREVIDNOSTNI UKREPI** Večina dogodkov se pojavi zgodaj v teku zdravljenja, zato mora zdravnik bolnika v prvih 8 tednih zdravljenja skrbno spremljati, da oceni, ali je treba odmerek prilagoditi. Dogodki, ki se običajno pojavijo zgodaj, vključujejo hipokalciemijo, hipokaliemijo, trombocitopenijo, hipertenzijo, sindrom palmarno-plantarne eritrodisestezije (PPES), proteinurijo in GI dogodke (bolečine v trebuhu, vnetje sluznice, zaprtje, driska, bruhanje). Pred uvedbo zdravljenja s kabozantinibom je priporočljivo izvesti preiskave delovanja jeter (ALT, AST in bilirubin), vrednosti skrbno spremljati med zdravljenjem in po potrebi prilagoditi odmerek. Bolnike je treba spremljati glede znakov in simptomov jetrne encefalopatije. Bolnike, ki imajo vnetno bolezen črevesja, ki imajo tumorsko infiltracijo prebavil ali so imeli pred posegom na prebavilih zaplete, je treba pred uvedbo zdravljenja skrbno oceniti, nato pa natančno spremljati za pojav simptomov GI perforacij in fistul, vključno z abscesi in sepso. Z uporabo kabozantiniba je treba pri bolnikih, pri katerih se pojavi GI perforacija ali fistula, ki je ni možno ustrezno obravnavati, prenehati. Driska, navzea/bruhanje, zmanjšanje apetita in vnetje ustne sluznice/bolečina v ustni votlini so nekateri od najpogosteje poročanih neželenih učinkov na prebavila. Nemudoma je treba uvesti ustrezne medicinske ukrepe, vključno s podpornim zdravljenjem z antiemetiki, antidiaroiki ali antacidi. Če pomembni neželeni učinki na prebavila vztrajajo ali se ponavljajo, je treba presoditi o prekinitvi odmerjanja, zmanjšanju odmerka ali trajni ukinitvi zdravljenja s kabozantinibom. Kabozantinib je treba uporabljati previdno pri bolnikih, pri katerih obstaja tveganje za pojav venske trombembolije, vključno s pljučno embolijo, in arterijske trombembolije ali imajo te dogodke v anamnezi. Z uporabo je treba prenehati pri bolnikih, pri katerih se razvije akutni miokardni infarkt ali drugi klinično pomembni znaki zapletov trombembolije. Kabozantiniba se ne sme dajati bolnikom, ki hudo krvavijo ali pri katerih obstaja tveganje za hudo krvavitev. Uporaba zaviralcev poti VEGF pri bolnikih s hipertenzijo ali brez nje lahko spodbudi nastanek anevrizem in/ali disekcij arterij. Med zdravljenjem s kabozantinibom je treba spremljati vrednosti trombocitov in odmerek prilagoditi glede na resnost trombocitopenije. Vsaj 28 dni pred načrtovanim kirurškim posegom je treba zdravljenje ustaviti, če je mogoče. Kabozantinib je treba ukiniti pri bolnikih z zapleti s celjenjem rane, zaradi katerih je potrebna zdravniška pomoč. Pred uvedbo kabozantiniba je treba dobro obvladati krvni tlak. Med zdravljenjem je treba vse bolnike spremljati za pojav hipertenzije in jih po potrebi zdraviti s standardnimi antihipertenzivi. V primeru trdovratne hipertenzije, kljub uporabi antihipertenzivov, je treba odmerek kabozantiniba zmanjšati oz. prenehati z zdravljenjem. V primeru hipertenzijske krize je treba zdravljenje ukiniti. Pred uvedbo kabozantiniba je treba opraviti pregled ustne votline in letega v času zdravljenja periodično ponavljati. Ob pojavu osteonekroze čeljusti, je treba prenehati z uporabo kabozantiniba. Pri resni PPES je treba razmisliti o prekinitvi zdravljenja. Nadaljevanje zdravljenja naj se začne z nižjim odmerkom, ko se PPES umiri do 1. stopnje. V času zdravljenja je treba redno spremljati beljakovine v urinu. Če se pri bolniku razvije nefrotični sindrom, je treba z uporabo kabozantiniba prenehati. Pri uporabi kabozantiniba so opazili sindrom posteriorne reverzibilne encefalopatije (PRES). Pri bolnikih s PRES je treba zdravljenje ukiniti. Kabozantinib je treba uporabljati previdno pri bolnikih s podaljšanjem intervala QT v anamnezi, pri bolnikih, ki jemljejo antiaritmike, in pri bolnikih z relevantno obstoječo boleznijo srca, bradikardijo ali elektrolitskimi motnjami. Uporaba kabozantiniba je bila povezana z večjo pojavnostjo elektrolitskih nepravilnosti, zato je priporočljivo spremljati biokemijske parametre in po potrebi uvesti ustrezno nadomestno zdravljenje v skladu s standardno klinično prakso. Bolniki z redko dedno intoleranco za galaktozo, laponsko obliko zmanjšane aktivnosti laktaze ali malabsorpcijo glukoze/galaktoze ne smejo jemati tega zdravila. Plodnost, nosečnost in dojenje: Ženskam v rodni dobi je treba svetovati, da v času zdravljenja s kabozantinibom ne smejo zanositi. Zanositev morajo preprečiti tudi ženske partnerice moških bolnikov, ki uporabljajo kabozantinib. Med zdravljenjem in še vsaj 4 mesece po končanju terapije je treba uporabljati zanesljiv način kontracepcije. Kabozantiniba se ne sme uporabljati med nosečnostjo, razen če zdravljenje ni nujno potrebno zaradi kliničnega stanja ženske. Matere med zdravljenjem in še 4 mesece po končanju terapije ne smejo dojiti. Kabozantinib lahko predstavlja tveganje za plodnost pri moških in ženskah. **INTERAKCIJE** Kabozantinib je substrat za CYP3A4. Pri sočasni uporabi močnih zaviralcev CYP3A4 (npr. ritonavirja, itrakonazola, eritromicina, klaritromicina, soka grenivke) je potrebna previdnost. Kronični sočasni uporabi močnih induktorjev CYP3A4 (npr. fenitoina, karbamazepina, rifampicina, fenobarbitala ali pripravkov zeliščnega izvora iz šentjanževke) se je treba izogibati. Razmisliti je treba o sočasni uporabi alternativnih zdravil, ki CYP3A4 ne inducirajo in ne zavirajo ali pa inducirajo in zavirajo le neznatno. Pri sočasni uporabi zaviralcev MRP2 (npr. ciklosporina, efavirenza, emtricitabina) je potrebna previdnost, saj lahko povzročijo povečanje koncentracij kabozantiniba v plazmi. Učinka kabozantiniba na farmakokinetiko kontraceptivnih steroidov niso preučili, vendar pa se priporoča dodatna kontracepcijska metoda (pregradna metoda). Zaradi visoke stopnje vezave kabozantiniba na plazemske beljakovine je možna interakcija z varfarinom v obliki izpodrivanja s plazemskih beljakovin, zato je treba spremljati vrednosti INR. Kabozantinib morda lahko poveča koncentracije sočasno uporabljenih substratov P-gp v plazmi. Bolnike je treba opozoriti na uporabo substratov P-gp (npr. feksofenadina, aliskirena, ambrisentana, dabigatran eteksilata, digoksina, kolhicina, maraviroka, posakonazola, ranolazina, saksagliptina, sitagliptina, talinolola, tolvaptana) sočasno s kabozantinibom. **NEŽELENI UČINKI** Za popolno informacijo o neželenih učinkih, prosimo, preberite celoten povzetek glavnih značilnosti zdravila Cabometyx. Najpogostejši resni neželeni učinki zdravila v populaciji bolnikov s KLC so bili bolečine v trebuhu, driska, navzea, hipertenzija, embolija, hiponatriemija, pljučna embolija, bruhanje, dehidracija, utrujenost, astenija, zmanjšanje apetita, globoka venska tromboza, omotica, hipomagneziemija in PPES. Najpogostejši resni neželeni učinki zdravila v populaciji bolnikov s HCK so bili jetrna encefalopatija, astenija, utrujenost, PPES, driska, hiponatriemija, bruhanje, bolečine v trebuhu in trombocitopenija. *Zelo pogosti:* anemija, trombocitopenija, hipotiroidizem, zmanjšanje apetita, hipomagneziemija, hipokaliemija, hipoalbuminemija, paragevzija, glavobol, omotica, hipertenzija, krvavitev, disfonija, dispneja, kašelj, driska, navzea, bruhanje, stomatitis, obstipacija, bolečine v trebuhu, dispepsija, bolečina v zgornjem predelu trebuha, PPES, izpuščaj, bolečine v okončinah, utrujenost, vnetje sluznice, astenija, periferni edem, zmanjšanje telesne mase, zvišanje ALT v serumu, zvišanje AST. *Pogosti:* absces, nevtropenija, limfopenija, dehidracija, hipofosfatemija, hiponatriemija, hipokalciemija, hiperkaliemija, hiperbilirubinemija, hiperglikemija, hipoglikemija, periferna nevropatija (vključno s senzorično), tinitus, globoka venska tromboza, venska tromboza, arterijska tromboza, pljučna embolija, GI perforacija, fistula, GERB, hemoroidi, bolečina v ustni votlini, suha usta, disfagija, glosodinija, jetrna encefalopatija, pruritus, alopecija, suha koža, akneiformni dermatitis, sprememba barve las oz. dlak, hiperkeratoza, mišični krči, artralgija, proteinurija, zvišanje ALP v krvi, GGT, kreatinina v krvi, amilaze, lipaze, holesterola v krvi, trigliceridov v krvi. *Občasni:* konvulzije, pankreatitis, holestatični hepatitis, osteonekroza čeljusti, zapleti z ranami. *Neznana pogostnost:* možganska kap, miokardni infarkt, anevrizme in disekcije arterij. **Vrsta ovojnine in vsebina:** Plastenka vsebuje 30 filmsko obloženih tablet. **Režim izdaje:** Rp/Spec **Imetnik dovoljenja za promet z zdravilom:** Ipsen Pharma, 65 quai Georges Gorse, 92100 Boulogne-Billancourt, Francija

Pred predpisovanjem, prosimo, preberite celoten povzetek glavnih značilnosti zdravila!

CAB-300420

IPSEN
Innovation for patient care

SAMO ZA STROKOVNO JAVNOST

CAB0720-03, julij 2020

PharmaSwiss
Choose More Life

PharmaSwiss d.o.o., Brodišče 32, 1236 Trzin
telefon: +386 1 236 47 00, faks: +386 1 236 47 05

RADIOLOGY AND ONCOLOGY

September 2020
Vol. 54 No. 3
Pages 253-370
ISSN 1318-2099
UDC 616-006
CODEN: RONCEM

Publisher

Association of Radiology and Oncology

Aims and Scope

Radiology and Oncology is a multidisciplinary journal devoted to the publishing original and high quality scientific papers and review articles, pertinent to diagnostic and interventional radiology, computerized tomography, magnetic resonance, ultrasound, nuclear medicine, radiotherapy, clinical and experimental oncology, radiobiology, medical physics and radiation protection. Therefore, the scope of the journal is to cover beside radiology the diagnostic and therapeutic aspects in oncology, which distinguishes it from other journals in the field.

Editorial office

Radiology and Oncology
Zaloška cesta 2
P. O. Box 2217
SI-1000 Ljubljana
Slovenia
Phone: +386 1 5879 369
Phone/Fax: +386 1 5879 434
E-mail: gsersa@onko-i.si

Reader for English
Vida Kološa

Secretary
Mira Klemenčič
Zvezdana Vukmirović

Design
Monika Fink-Serša, Samo Rovan, Ivana Ljubanović

Layout
Matjaž Lužar

Printed by
Tiskarna Ozimek, Slovenia

Published quarterly in 400 copies

Beneficiary name: DRUŠTVO RADIOLOGIJE IN ONKOLOGIJE
Zaloška cesta 2
1000 Ljubljana
Slovenia

Beneficiary bank account number: SI56 02010-0090006751
IBAN: SI56 0201 0009 0006 751
Our bank name: Nova Ljubljanska banka, d.d.,
Ljubljana, Trg republike 2,
1520 Ljubljana; Slovenia

SWIFT: LJBASI2X

Subscription fee for institutions EUR 100, individuals EUR 50

The publication of this journal is subsidized by the Slovenian Research Agency.

Indexed and abstracted by:

- *Baidu Scholar*
- *Case*
- *Chemical Abstracts Service (CAS) - CAplus*
- *Chemical Abstracts Service (CAS) - SciFinder*
- *CNKI Scholar (China National Knowledge Infrastructure)*
- *CNPIEC - cnpLINKer*
- *Dimensions*
- *DOAJ (Directory of Open Access Journals)*
- *EBSCO (relevant databases)*
- *EBSCO Discovery Service*
- *Embase*
- *Genamics JournalSeek*
- *Google Scholar*
- *Japan Science and Technology Agency (JST)*
- *J-Gate*
- *Journal Citation Reports/Science Edition*
- *JournalGuide*
- *JournalTOCs*
- *KESLI-NDSL (Korean National Discovery for Science Leaders)*
- *Medline*
- *Meta*
- *Microsoft Academic*
- *Naviga (Softweco)*
- *Primo Central (ExLibris)*
- *ProQuest (relevant databases)*
- *Publons*
- *PubMed*
- *PubMed Central*
- *PubsHub*
- *QOAM (Quality Open Access Market)*
- *ReadCube*
- *Reaxys*
- *SCImago (SJR)*
- *SCOPUS*
- *Sherpa/RoMEO*
- *Summon (Serials Solutions/ProQuest)*
- *TDNet*
- *Ulrich's Periodicals Directory/ulrichsweb*
- *WanFang Data*
- *Web of Science - Current Contents/Clinical Medicine*
- *Web of Science - Science Citation Index Expanded*
- *WorldCat (OCLC)*

This journal is printed on acid- free paper

On the web: ISSN 1581-3207
https://content.sciendo.com/raon
http://www.radioloncol.com

contents

experimental oncology

clinical oncology

radiophysics

review

Transarterial embolization of the external carotid artery in the treatment of life-threatening haemorrhage following blunt maxillofacial trauma

Crt Langel[1], Dimitrij Lovric[1], Ursa Zabret[1], Tomislav Mirkovic[2], Primoz Gradisek[2], Anita Mrvar-Brecko[2], Katarina Surlan Popovic[1]

[1] Institute of Radiology, University Medical Centre Ljubljana, Ljubljana, Slovenia

[2] Department of Anaesthesiology and Surgical Intensive Care, Division of Surgery, University Medical Centre Ljubljana, Ljubljana, Slovenia

Radiol Oncol 2020; 54(3): 253-262.

Received 7 February 2020
Accepted 22 April 2020

Correspondence to: Assoc. Prof. Katarina Šurlan Popović, M.D., Ph.D., Clinical Institute of Radiology, University Medical Centre Ljubljana, Zaloška c 7, 1000 Ljubljana, Slovenia. E-mail: katarina.surlan-popovic@mf.uni-lj.si.

Disclosure: No potential conflicts of interest were disclosed.

Background. Severe bleeding after blunt maxillofacial trauma is a rare but life-threatening event. Non-responders to conventional treatment options with surgically inaccessible bleeding points can be treated by transarterial embolization (TAE) of the external carotid artery (ECA) or its branches. Case series on such embolizations are small; considering the relatively high incidence of maxillofacial trauma, the ECA TAE procedure has been hypothesized either underused or underreported. In addition, the literature on the ECA TAE using novel non-adhesive liquid embolization agents is remarkably scarce.

Patients and methods. PubMed review was performed to identify the ECA TAE literature in the context of blunt maxillofacial trauma. If available, the location of the ECA injury, the location of embolization, the chosen embolization agent, and efficacy and safety of the TAE were noted for each case. Survival prognostic factors were also reviewed. Additionally, we present an illustrative TAE case using a precipitating hydrophobic injectable liquid (PHIL) to safely and effectively control a massive bleeding originating bilaterally in the ECA territories.

Results and conclusions. Based on a review of 205 cases, the efficacy of TAE was 79.4–100%, while the rate of major complications was about 2–4%. Successful TAE haemostasis, Glasgow Coma Scale score ≥ 8 at presentation, injury severity score ≤ 32, shock index ≤ 1.1 before TAE and ≤ 0.8 after TAE were significantly correlated with higher survival rate. PHIL allowed for fast yet punctilious application, thus saving invaluable time in life-threatening situations while simultaneously diminishing the possibility of inadvertent injection into the ECA-internal carotid artery (ICA) anastomoses.

Key words: blunt maxillofacial trauma; external carotid artery injury; intractable bleeding; non-adhesive liquid embolization agent; precipitating hydrophobic injectable liquid, neurointervention

Introduction

Maxillofacial trauma comprises roughly 10% of all trauma cases.[1] It is associated with a wide range of problems, including airway compromise, cervical spine injuries and bleeding.[2] Life-threatening haemorrhage secondary to blunt maxillofacial trauma is considered rare, occurring in 1.2%–4.5% of trauma-related maxillofacial fracture cases.[2-5] The most common origins of haemorrhage in maxillofacial trauma are the internal maxillary artery (IMA), the IMA's distal branches, and the main trunk of the external carotid artery (ECA).[6]

A diverse range of imaging manifestations can present in the setting of blunt carotid artery trauma, including various dissection subtypes (mini-

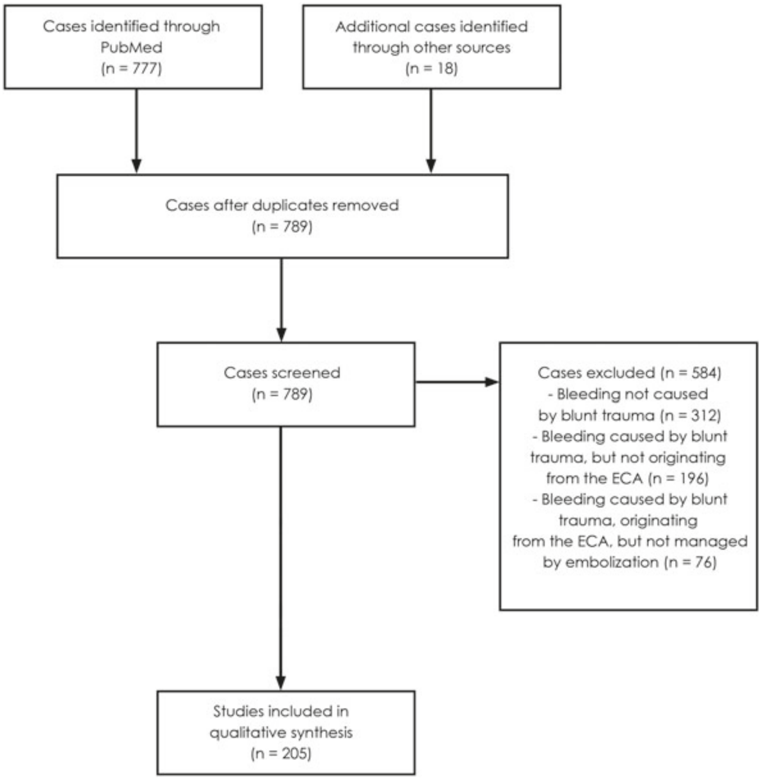

FIGURE 1. A flow diagram based on simplified Preferred Reporting Items for Systematic Reviews and MetaAnalyses (PRISMA) guidelines depicting the number of cases identified, included and excluded. The reasons for the exclusions are also noted.[13]

mal intimal injury, raised intimal flap, dissection with an intramural hematoma, occlusion), pseudoaneurysm, transection with an active haemorrhage, and arteriovenous fistula.[7,8]

In treating severe maxillofacial injuries, airway, breathing and circulation management precede all other procedures. Special care is aimed towards the protection of the airway as the tongue and the soft tissues of the lower face can move backward and obstruct the pharynx due to the decreased level of consciousness, bilateral mandibular fractures, soft tissue swelling and expanding hematomas.[2] Further treatment includes manual compression, nasal packing, coagulopathy correction, cauterization, reduction of the fractures and local vascular control to stop the bleeding from the intra-osseous branches near the fracture lines.[9] Open surgical ligation or transarterial embolization (TAE) of the ECA are available as the most definite options. Advantages of TAE over ligation include rapid access, not necessarily requiring general anaesthesia, superior haemorrhage origin localization using angiography, the ability to control multiple local bleeding points, the ability to perform superselective therapeutic vessel occlusion by cannulating the smaller vessel branches not amenable to open surgical repair, and short procedure time.[10] In addition, ECA ligation oftentimes requires repeat ligation or subsequent TAE to effectively stop the bleeding, whereas TAE is usually efficacious in a single session.[2,11] Furthermore, TAE offers the option to embolize the bleeding origins of a possible concomitant abdominal or other internal haemorrhage in the same session.[12] In certain guidelines, surgical ECA ligation has been completely replaced by TAE for maxillofacial bleeding control.[2]

The initial search data for the review part of this manuscript was processed following a simplified variant of the Preferred Reporting Items for Systematic Reviews and MetaAnalyses (PRISMA) guidelines showing the number of cases identified, included and excluded, plus the reasons for exclusions (Figure 1).[13] The included cases were then analysed in order to obtain the data regarding the use of embolization agents, and the efficacy and safety of the TAE procedure in the context of blunt maxillofacial trauma with bleeding originating from the ECA.

Transarterial embolization of the ECA

Embolization therapy aims at controlling an active bleeding by occluding the feeding artery with an embolization agent (EA).[14] The TAE technique was first suggested by Brooks *et al*. in the 1930s. In the early 1970s, Rosch and Dotter used it for the first time to treat a traumatic vascular injury.[15] It also became an accepted treatment option for a variety of vascular lesions unrelated to trauma, including arteriovenous malformations, glomus tumours, juvenile angiofibromas, and intracranial meningiomas.[16] A pioneer case describing a successful IMA TAE in the treatment of intractable epistaxis was reported by Sokoloff *et al*. in 1974.[17]

Decades of innovation brought about major advances in embolization materials, however, to this day, the principles of the TAE procedure remain largely unaltered.[18] Initially, a vascular access is established by a standard transfemoral approach using the Seldinger technique.[19] Alternatively, brachial or axillary arterial access might be required in case of severe bilateral lower extremity injury.[20] Diagnostic angiography of the whole circulation at risk is then performed, including bilateral common carotid arteries (CCAs), internal carotid arteries (ICAs), vertebral arteries (VAs), and ECAs. If the preliminary computed tomography angiography (CTA) or clinical findings suggest an injury to a specific smaller vessel, e.g. the IMA, the lingual artery or the superficial temporal artery, further microcatheter angiography of these territories is carried out. The purpose is to obtain a general overview of the complete vasculature and to exclude a possible concomitant injury to the CCA, ICA or VA.[21] The vessel that is the source of an active haemorrhage is then therapeutically occluded. The aim of the embolization is to stop the active bleeding, prevent any subsequent rebleeding events, and preserve as much perfusion to the nearby structures as possible, thereby reducing the chance of unnecessary tissue damage. This means embolization is attempted as close to the lesion as possible to avoid occluding the vessels branching off proximally to the embolization site. Circumstances permitting, the culprit vessel should ideally be embolized both distally and proximally to the lesion in order to prevent rebleeding via the collateral circulation.[21] The delivery of the EA is performed under fluoroscopic visualization to the point of contrast medium stasis within the embolized vessel.

Embolization agents

Depending on the vessel calibre, type of vessel injury and other factors, a variety of EAs with differing inherent properties and behaviour may be used. Historically, the first EA was autologous tissue (including blood clots, subcutaneous tissue and muscle) followed by silk threads.[22] Their use gradually declined with the advances in newer EAs, imaging and (micro)catheter technologies.[14,23]

Data gathered in Table 1 indicates coils and gelatine foam (Gelfoam) are the EAs most frequently used for TAE in the context of blunt maxillofacial trauma. There have also been numerous instances of polyvinyl alcohol (PVA), microspheres, and N-butyl-2 cyanoacrylate (NBCA) use. One case of silastic spheres, two cases of Onyx, and a single case of precipitating hydrophobic injectable liquid (PHIL) use have been reported.

Coils are made from platinum or steel, measure 0.2–1.3 mm in diameter and can be supplied in a variety of lengths, shapes and levels of stiffness. They may be bare or fibered with materials such as wool, silk, nylon fibres, polyester, Dacron or PVA.[18] Coils embolize a vessel by physically slowing down the local blood flow, by providing a thrombogenic locus, and by damaging the vessel wall, thus inducing the release of thrombogenic factors. Time to occlusion is typically 5 minutes or less after coil insertion, depending on the type of coil used, the rate of blood flow through the target vessel and the blood's coagulation properties.[18] Larger diameter platinum coils offer good radiopacity, while smaller diameter coils (microcoils) provide for more targeted distal deployment. The possible complications of TAE using coils are non-target vessel occlusion, vessel injury, coil migration, and infection.[18,24] Coils prohibit any future endovascular access distal to the occlusion point, which is particularly relevant in rebleeding events following collateralization.[21]

Gelatine foam (Gelfoam) (Pfizer, Kalamazoo, MI, USA) is a porous material with haemostatic properties prepared from purified porcine skin gelatine. It usually supplied as a block of sponge that needs to be cut into smaller cube- or torpedo-shaped particles prior to embolization. Gelfoam induces foreign body reaction and necrotizing arteritis, resulting in the formation of a thrombus.[25] Gelfoam as a standalone EA provides a temporary vessel occlusion; recanalization typically occurs within 3 weeks to 3 months, but the exact time and the extent cannot reliably be predicted.[23] A combined coils-Gelfoam embolization may be particularly well suited for coagulopathic patients as such vessel occlusion is precise, fast, and permanent.[23] The most significant disadvantage of Gelfoam-only embolization is the reliance on manual preparation of the particles, limiting the reproducibility and predictability of the exact embolization site. Furthermore, air bubbles typically form in the Gelfoam-contrast mixture, presenting a potential risk for an aerobic infection.[18]

Polyvinyl alcohol (PVA) particles (Boston Scientific, Cork, Ireland; Cordis J&J Endovascular, Miami, FL, USA) are irregularly-shaped permanent embolic agents ranging from 100 to 1100 μm in size. The PVA's mechanism of action includes adherence to the vessel wall, induction of an inflammatory reaction, focal angionecrosis and the resulting vessel fibrosis. There is a considerable variability in particle size because fragments smaller than the stated size range are allowed to enter the particulate mixture during production. This in turn increases the risk of distal, non-target embolization as particles tend to lodge in the smallest vessel they can fit in. On the other hand, the PVA particles are also prone to aggregation; this can lead to more proximal vessel occlusion than expected based on the stated size range of the particles.[18]

Microspheres (Embosphere and EmboGold, Merit Medical Systems, South Jordan, UT, USA; Contour SE, Boston Scientific, Natick, MA, USA;

TABLE 1. Data from studies, case series and case reports pertaining to TAE of the ECA or its branches in the treatment of haemorrhage caused by blunt maxillofacial trauma

First author	Year Pub-lished	Case number	Vessel injured	Vessel embolized	Emboli-zation agents used	efficacy (complete cessation of bleeding following TAE of the ECA or its branches)	complications
Bynoe[2]	2003	1	none identified	RL ECA	C GF PVA	100%	partial tongue necrosis
		2	R IMA	R IMA			none
		3	R IMA	RL IMA			none
		4	none identified	RL ECA above LA			none
		5	none identified	RL ECA above LA			groin hematoma
		6	none identified	RL ECA above LA			none
		7	L IMA	L IMA			none
		8	L IMA	L IMA			groin hematoma
		9	L IMA	R ECA above LA, L IMA			none
		10	none identified	R ECA above LA			none
Chen[12]	2009	11	R IMA, R STA	not specified	C GF	100%	could not be assessed
		12	R IMA	not specified	C GF		none
		13	L IMA	not specified	GF		could not be assessed
		14	R IMA	not specified	GF		none
		15	L IMA	not specified	GF		none
		16	RL IMA	not specified	GF		could not be assessed
		17	L ECA	not specified	C GF		none
		18	L IMA	not specified	GF		none
Cogbill[48]	2008	19–39	not discernible due to the merging of blunt and penetrating trauma patients' data	not discernible due to the merging of blunt and penetrating trauma patients' data	C GF	85%	none
Kim[49]	2011	40	not specified	L IMA	PVA	success	none
Komiyama[50]	1998	41	not specified	R SPA	C GF PVA	100%	none
		42	not specified	RL SPA, IOA, FA			none
		43	not specified	L SPA			none
		44	not specified	RL SPA, LPA, ADTA[6], IAA[7], FA, LA			none
		45	not specified	RL SPA, FA			none
		46	not specified	BL SPA, AAA[8]			could not be assessed
		47	not specified	R STA, FA			none
		48	not specified	RL GPA[9], EA			none
		49	not specified	RL SPA, SPAA[10]			none
Kuan[47]	2015	50–76	12 x IMA 6 x FA 6 x LA 5 x MMA[11] 3 x ECA 1 x APA[12] 5x other vessels Note: this statistics also includes one penetrating trauma.	not specified	C GF PVA NBCA	92.3%; data includes one penetrating injury	no serious systemic or neurologic complications

First author	Year Pub-lished	Case number	Vessel injured	Vessel embolized	Emboli-zation agents used	efficacy (complete cessation of bleeding following TAE of the ECA or its branches)	complications
Langel	2020	77	L IMA + R SPA	L ECA + R SPA	C PHIL 25	success	none
Liao[40]	2007	78–112	25 x IMA 5 x MMA 4 x ECA 4 x SPA 4 x STA 2 x APA 1 x FA 1 x SALA 1 x IALA 1 x DPA 5 x other (observed contrast pooling)	not specified	not specified	79.4%	none reported
Liu[3]	2008	113	L STA + L IMA	not specified	GF	success	none reported
Maiorello[51]	2011	114	L FA	L FA	Onyx 18	success	none
Mauldin[52]	1989	115	R ECA	R ECA	C	success	none reported
Mehringer[52]	1982	116–194	not discernible due to the merging of blunt and penetrating trauma patients' data	not discernible due to the merging of blunt and penetrating trauma patients' data	GF PVA silastic spheres	100%	1x cerebral infarction 2x transient occulomotor nerve palsy
Mehrotra[6]	1984	195–196	R IMA	R IMA	GF PVA	success	none reported
			L IMA	L IMA	GF	success	none reported
Noy[38]	2007	197	L IMA, RL FA	L IMA, RL FA	MS NBCA	success	none
Remonda[54]	2000	198	RL IMA	not specified	C PVA NBCA	success	Transient trismus
Thiex[33]	2011	199	L FA	not specified	Onyx	success	none
Wang[55]	2015	200	L STA	not specified	C	100%	none
		201	L FA	not specified	C		none
		202	R STA	not specified	C		none
		203	R STA	not specified	C		none
		204	L STA	not specified	C		none
Wong[56]	2013	205	R IMA	R IMA	NBCA	success	none

Anatomical abbreviations: AAA = anterior auricular artery; ADTA = anterior deep temporal artery; APA = ascending pharyngeal artery; DPA = descending palatine artery; ECA = external carotid artery; FA = facial artery; GPA = greater palatine artery; IAA = inferior alveolar artery; IALA = inferior alveolar artery; IMA = internal maxillary artery; IOA = infraorbital artery; L = left; LPA = lesser palatine artery; MMA = middle meningeal artery; R = right; SALA = superior alveolar artery; SPA = sphenopalatine artery; SPAA = superior posterior alveolar artery; STA = superficial temporal artery

Embolization agent abbreviations: C = coils; GF = Gelfoam; MS = microspheres; PHIL = precipitating hydrophobic injectable liquid; PVA = polyvinyl alcohol particles

Embozene, Celenova, San Antonio, TX, USA; Quadrasphere, Merit Medical Systems, South Jordan, UT, USA; Bead Block and LC Bead, Biocompatibles, Farnham, UK) are smooth globular structures made from an acrylic polymer matrix impregnated with porcine gelatine. They are hydrophilic, non-resorbable, non-aggregating, non-fragmenting spheres sized 40 - 1200 µm. Sizing inside a particular stated size range follows the Gaussian distribution and is thus more predictable than is the case with PVA particles. After lodging in vessels, microspheres induce a histological reaction similar to PVA particles. The most notable downside of using microspheres is the necessity to intermittently agitate the particle-saline suspension prior to application in order to prevent sedimentation.[18,25,26] Also of note is the fact that microspheres of different manufacturers vary in elasticity and, as a consequence, particles of identical size range but different composition occlude vessels at different levels of the vascular tree.[25,27]

NBCA (TruFill, Cordis, Miami Lakes, FL; Histoacryl, B. Braun Aesculap, Tokyo, Japan; Glubran 2, Gem, Viareggio, Lucca, Italy) is a synthetic adhesive liquid EA (glue) that is accompanied by a separately packed tantalum powder, acting as a radiographic opacifier, and ethiodized oil, functioning as a polimerization retardant. All three components are mixed just before deployment. Once the solution is exposed to anionic environment such as blood, polymerization takes place at a rate dependent on the NBCA concentration. NBCA forms a permanent cast obstructing the vessel lumen. This occurs independently of the endogenous coagulation system - an important characteristic when dealing with exsanguinating trauma cases.[18] NBCA glue also induces vessel wall inflammation reaction resulting in fibrosis. The downside of NBCA use is that the catheter may become glued to the vessel wall if not pulled back quickly enough following glue injection. Glue polymerisation can also occur both distally or proximally to the intended occlusion location. NBCA deployment thus requires a skilled operator.[28]

Silastic spheres are the oldest non-absorbable particulate EA, introduced in 1964, and have since been replaced by more modern EAs.[29]

Onyx (Medtronic, Dublin, Ireland) is an ethylene vinyl alcohol (EVOH) copolymer-based non-adhesive liquid EA dissolved in dimethyl sulfoxide (DMSO) with added radiopaque tantalum powder. It was introduced in 1990. As is the case with other DMSO-based non-adhesive liquid EAs, once injected, the DMSO component dissolves into the blood and the copolymer component starts gradually precipitating in a centripetal fashion. The non-adhesive nature allows for long injection times and mid-injection control angiography, if needed. Onyx's final solidification occurs in 5 minutes.[30] There are several drawbacks to this EA, including long pre-injection preparation time (20 minutes of mixer shaking are required to achieve homogenization), a self-hiding effect when used in larger amounts due to high radiopacity, plenty of artefacts in a postinterventional imaging, and the potential to combust or produce sparks during monopolar surgical cauterization.[31,32] In addition, Onyx's dark colour may result in a black discoloration of the skin after superficial embolization or subcutaneous extravasation of the EA.[33,34]

Precipitating hydrophobic injectable liquid (PHIL) (MicroVention, Tustin, CA, USA) is a non-EVOH copolymer-based non-adhesive liquid EA suspended in DMSO with iodine covalently bonded to copolymer to provide radiopacity. It was introduced in 2015. In comparison to Onyx, PHIL is supplied ready-to-use (no shaking is necessary), requires lower volume to achieve the same extent of embolization, is faster to fully precipitate (3 minutes), does not suffer from the self-hiding effect, produces fewer artefacts in postinterventional imaging, is not hazardous to surgical cauterization, and is not dark coloured which diminishes the possibility of skin discoloration.[35,36] PHIL is also more homogenous on fluoroscopy during prolonged injections, but less radiopaque than Onyx once injected.[23]

According to the literature, no cases of blunt trauma-related ECA-territory embolization using other modern non-adhesive liquid EAs, such as Squid (Emboflu, Gland, Switzerland), have so far been reported. In the future, other cutting-edge EAs, such as homogenous microparticles or biodegradable drug-bearing microspheres produced by droplet microfluidics technology, are expected to see regular clinical use.[37]

Efficacy and safety

Various studies and case reports have shown the ECA TAE to be a safe and efficacious method in maxillofacial blunt-trauma related haemorrhage control, although direct comparison of the reviewed literature is rendered difficult by the variations in reporting. Two studies authored by Noy *et al.* and by Hayes *et al.* investigating intractable maxillofacial bleeding of various aetiologies, including but not limited to trauma, enrolling 74 patients in total, found TAE to be efficacious in 89.1 - 90.0%.[38,39] A study by Liao *et al.* focusing exclusively on trauma-related oronasal bleeding enrolling 34 patients discovered TAE to be efficacious in 79.4%.[40] The data collected in Table 1 show that the efficacy of TAE ECA ranges from 79.4% to 100%, with the largest series attaining the perfect success rate comprising 10 cases. These results are similar to the efficacy of non-trauma-related TAE procedures involving the ECA (80%–97%).[41-43]

The complications among the 205 cases reviewed in Table 1 include groin hematoma (2 cases), cerebral infarction (1 case), partial tongue necrosis (1 case), transient occulomotor nerve palsy (1 case), and transient trismus (1 case), indicating an overall complication rate of 3%. However, there is high variability in reporting styles regarding the complications. For example, certain authors limited the reporting only to serious neurologic or systemic complications without further expounding on the exact criterion that delimited the serious complications from the minor ones. Furthermore, complications that could not be assessed might have occurred, e.g. due to patient dying or entering a vegetative state. In addition, it was not possible to determine the risk of publication bias or selective reporting. It is thus safe to assume the overall complication rate to be higher than directly indicated by Table 1 data. Duncan *et al*. found the rate of major complications (comprising cerebral vascular insult only) to be 2% but also reported a rate of minor complications (comprising headache, transient facial pain, paraesthesia, and local groin complications) of 25% in their series of 57 embolizations, of these 3 trauma-related.[44] Cullen and Tami reviewed the literature of 264 cases of IMA embolizations for the treatment of posterior epistaxis and found the rate of major complications (hemiplegia, facial nerve paralysis, cheek necrosis, ICA intimal injury, catheter stuck in a vessel, myocardial infarction) to be 4%, and the rate of minor complications (IMA spasm, hypotension, hematoma, groin bleed, oedema, trismus, paraesthesia, persistent pain, skin slough, palate ulceration, aspiration pneumonia, hepatitis) to be 10%.[45]

The relatively low rate of major complications might be in part due to the rich collateral flow between the ipsilateral and contralateral ECA branches distal to the lingual artery that ensure adequate tissue perfusion in case of one-sided ECA embolization.[46,2] Duncan *et al*. discovered that the complication rate tends to drop with the use of microcatheter techniques. They have also observed a decrease in complication rate in the more recent studies that could be ascribed to factors such as improvement in catheter and guidewire design and increased operator experience.[44]

Survival prognostic factors

Liao *et al.* examined a series of 34 cases of craniofacial trauma requiring TAE and discovered that there was a significant contribution of successful TAE haemostasis to patient survival (p = 0.001). Glasgow Coma Scale score (GCS) ≥ 8 at presentation, injury severity score (ISS) ≤ 32, and shock index (SI; heart rate divided by systolic blood pressure) ≤ 1.1 before TAE and ≤ 0.8 after TAE were also significantly correlated with the patients' higher survival rate ($p < 0.05$). The need to treat a secondary abdominal bleeding origin by laparotomy significantly decreased the rate of survival ($p = 0.023$). The patients' age, the need to perform craniotomy, the bilateral distribution of the bleeding vessels, and the number of the haemorrhaging vessels per patient were not correlated with the patient survival ($p > 0.05$).[40]

Kuan *et al*. confirmed some of the findings by Liao *et al.* and further discovered that patients with initial haemoglobin level lower than 10 g/dL and patients with brain midline shift observed by computed tomography (CT) had statistically higher odds ratios predicting mortality than their counterparts as estimated by univariate logistic regression.[47]

An illustrative case report

A 20-year-old, previously healthy male was brought to the emergency department in 2019 after an accidental 20 m (65 ft), head-first fall to the ground. He had been cleaning windows of his 7th floor dorm room when he lost balance and fell. Eyewitnesses reported the patient had been lying on his stomach after impacting the ground but later managed to roll on his back by himself. A physician-led emergency medical service arrived on the scene in 10 minutes, finding the patient verbally responsive and making an effort to get up. Initial Glasgow Coma Scale (GCS) was an estimated 13. Severe facial trauma compromising the airway and, within a few minutes, cessation of spontaneous respiration necessitated rapid sequence intubation which proved challenging with several failed attempts. Asystole was observed on ECG prompting resuscitation efforts that resulted in the return of spontaneous circulation and sinus rhythm 20 minutes later. Upon arrival at a Level I trauma centre, the patient presented with GCS 5, blood pressure 70/40 mmHg, heart rate 100/min., a multifragment facial fracture (Figure 2A), a ruptured right eye, massive bleeding from the nose and the left ear, a fractured right 4th rib, a fractured left radius, a displaced left femoral fracture and a fractured left tibia. Adhering to our institution's standard trauma protocol, the possible abdominal and thoracic sources

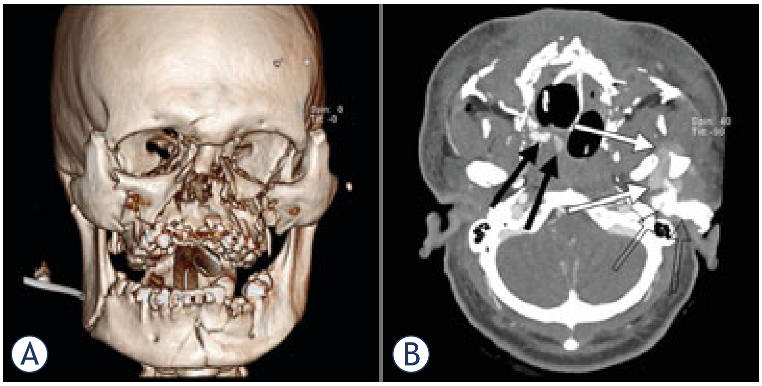

FIGURE 2. (A) A 3D CT reconstruction showing multiple maxillo-facial fractures. (B) An aortocervical CTA showing two small hematomas in the region of the right pterygopalatine fossa and nasal cavity (black arrows) and a cm 3 × 4 cm hematoma in the region of the left masticatory space and deep parotid space (white arrows). Also visible is a hyperdense material used in left ear tamponade (empty arrows).

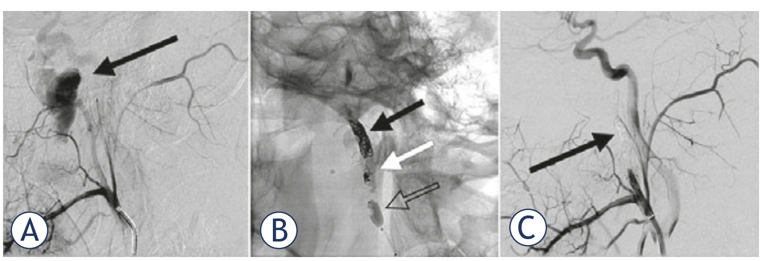

FIGURE 3. (A) A lateral left ECA angiogram showing ECA laceration with 3 × 4 cm pseudoaneurysm continuing into the proximal part of the left IMA. Contrast extravasation can be observed in the vicinity of the pseudoaneurysm. (B) A fluoroscopic view showing left ECA embolization using coils (black arrow) and PHIL 25 liquid embolization agent (white arrow) under balloon flow control (empty arrow). Also of note area small number of stray coils anchored in the vessel in the region of PHIL application (white arrow). (C) A post-embolization lateral left ECA angiogram showing complete exclusion of the ECA distally to the facial artery (black arrow).

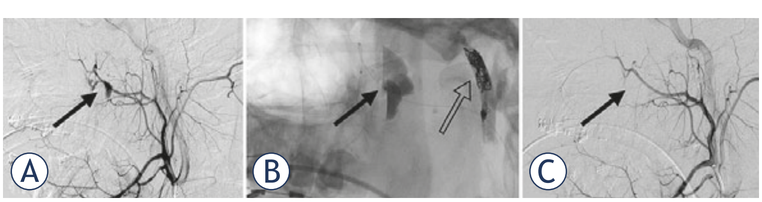

FIGURE 4. (A) A lateral right ECA angiogram showing two pseudoaneurysms in the region of the right pterygopalatine fossa and nasal cavity (black arrows). (B) Fluoroscopy showing microcatether proximally to the hematoma in the right pterygopalatine fossa (black arrow) prior to PHIL 25 application. Also visible is the embolized contralateral ECA (empty arrow). (C) A post-embolization right ECA angiogram showing complete sphenopalatine artery occlusion (black arrow). Also visible are the patent vessels proximally to the embolization.

of major blood loss were excluded. Astonishingly, US, XR, CT and CTA imaging indicated no significant damage to the neurocranium, parenchymal organs or major thoracic or abdominal vessels. Aorto-cervical CTA was then performed, revealing contrast extravasation from the left IMA and the right sphenopalatine artery (SPA) (Figure 2B). This was consistent with the clinical presentation of severe antero-posterior epistaxis and pulsatile bleeding from the left ear. Nasal packing using balloon catheter inserted through the nares into the nasopharynx was performed by an ear, nose and throat (ENT) specialist to successfully control the nose bleeding. Tamponade of the left ear, however, proved to be inadequate with profound bleeding still persisting. Surgical treatment to control the haemorrhage by ligating the left ECA was decided against due to lesion inaccessibility caused by extensive soft tissue damage and swelling. Blood pressure remained low (60/40 mmHg) despite having hitherto administered a total of 5 litres of fluids, including blood transfusion. Tranexamic acid and vasopressors were also applied, to little avail. In these life-threatening circumstances, TAE of the bleeding origins was considered the only remaining option.

The patient was transferred to the neurointerventional suite and a standard right transfemoral vascular access was established. Digital substraction angiography (DSA) showed a laceration of the left ECA with an ensuing 3 × 4 cm pseudoaneurysm continuing into the proximal part of the left IMA (Figure 3A). DSA also showed a right SPA laceration with two small accompanying pseudoaneurysms (Figure 4A). The two culprit arteries were then superselectively catheterized and embolized. ECA embolization was performed using platinum coils and PHIL 25, while the SPA was embolized with PHIL 25 only (Figures 3B and 4B). In the case of the ECA embolization, coils created a mesh scaffold acting as a thrombogenic locus, and PHIL was then added to form a coagulopathy-independent lumen-obliterating cast. PHIL was chosen over other available liquid EAs for its ready-to-use characteristics, saving precious time in an emergency setting. In addition, its lava-like polymerisation properties ensured a well-controlled application, helping prevent any inadvertent injection into the dangerous ECA-internal carotid artery and ECA-vertebral artery anastomoses.

Effort was made to embolize at or just proximal to the laceration point in order to preserve proximal arterial territories. Embolization was continued to the point of arterial stasis. Due to the well-developed left ECA and the resulting high blood flow to the pseudoaneurysm, the ECA embolization was performed under flow control provided by temporary proximal balloon occlusion. No flow control was needed for the SPA embolization. The embolizations of both lesions were immediately followed by complete cessation of the ear bleeding.

Postembolization imaging showed total exclusion of the lacerated vessels (Figures 3C and 4C), complete patency of all proximal vessels, no collateral pathways to the pseudoaneurysm and no other origins of bleeding. There were no procedure-related complications.

To our knowledge, this case is the very first published report of PHIL 25 use for a safe and efficacious management of a massive bleeding originating in the ECA territory. Informed consent was obtained from the patient included in this case report as well as the consent for publication of the individual person's data.

Conclusions

Severe bleeding secondary to blunt maxillofacial trauma is a rare but life-threatening occurrence. Conventional treatment options include manual compression, nasal packing, coagulopathy correction, cauterization, fracture reduction and local vascular control. Open surgical ligation or TAE of the ECA are available as the most definite approaches. Both are similarly efficacious and safe, but TAE offers many advantages, including shorter procedure time, more precise haemorrhage localization, vessel occlusion superselectivity, and the ability to embolize a possible concomitant abdominal or other bleeding during the same session. Major complications of TAE are rare owing to rich collateral blood supply in the ECA territory, with the exception of the lingual artery. The diversion of embolization material into the ICA territories via the ECA-ICA anastomoses is a potentially hazardous complication warranting thorough pre-embolization angiographic overview of the whole vasculature at risk. There are several known factors positively affecting the survival of the maxillofacial trauma patients undergoing ECA TAE, most notably a successful TAE haemostasis, higher GCS, lower ISS, lower SI and higher haemoglobin level on arrival.

Novel non-adhesive liquid EAs such as PHIL allow for faster, more punctilious and coagulopathy-independent application, thus saving invaluable time in life-threatening situations while simultaneously diminishing the possibility of inadvertent injection into the ECA-ICA anastomoses. Prospective randomized clinical studies comparing EAs are warranted to further evaluate their efficacy, safety and feasibility.

References

1. American College of Surgeons, Committee on Trauma. *Advanced trauma life support manual*. Chicago: American College of Surgeons; 1994.
2. Bynoe RP, Kerwin AJ, Parker HH 3rd, Nottingham JM, Bell RM, Yost MJ, et al. Maxillofacial injuries and life-threatening hemorrhage: treatment with transcatheter arterial embolization. *J Trauma* 2003; **55:** 74-79. doi: 10.1097/01.TA.0000026494.22774.A0
3. Liu WH, Chen YH, Hsieh CT, Lin EY, Chung TT, Ju DT. Transarterial embolization in the management of life-threatening hemorrhage after maxillofacial trauma: a case report and review of literature. *Am J Emerg Med* 2008; **26:** 516. e3-5. doi: 10.1016/j.ajem.2007.07.036
4. Thaller SR, Beal SL. Maxillofacial trauma: a potentially fatal injury. *Ann Plast Surg* 1991; **27:** 281-3. doi: 10.1097/00000637-199109000-00015
5. Buchanan RT, Holtmann B. Severe epistaxis in facial fractures. *Plast Reconstr Surg* 1983 **71:** 768-71. doi: 10.1097/00006534-198306000-00003
6. Mehrotra ON, Brown GE, Widdowson WP, Wilson JP. Arteriography and selective embolisation in the control of life-threatening haemorrhage following facial fractures. *Br J Plast Surg* 1984; **37:** 482-5. doi: 10.1016/0007-1226(84)90135-8
7. Sliker CW. Blunt cerebrovascular injuries: imaging with multidetector CT angiography. *RadioGraphics* 2008; **28:** 1689-708. doi: 10.1148/rg.286085521
8. Biffl WL, Moore EE, Offner PJ, Brega KE, Franciose RJ, Burch JM. Blunt carotid arterial injuries: implications of a new grading scale. *J Trauma* 1999; **47:** 845-53. doi: 10.1097/00005373-199911000-00004
9. Ardekian L, Samet N, Shoshani Y, Taicher S. Life-threatening bleeding following maxillofacial trauma. *J Craniomaxillofac Surg* 1993; **21:** 336-8. doi: 10.1016/s1010-5182(05)80493-7
10. Radvany MG, Gailloud P. Endovascular management of neurovascular arterial injuries in the face and neck. *Semin Intervent Radiol* 2010; **27:** 44-54. doi: 10.1055/s-0030-1247888
11. Mahmood S, Lowe T. Management of epistaxis in the oral and maxillofacial surgery setting: an update on current practice. *Oral Surg Oral Med Oral Pathol Oral Radiol Endod* 2003; **95:** 23-9. 10.1067/moe.2003.10
12. Chen YF, Tzeng IH, Li YH, Lo YC, Lin WC, Chiang HJ, et al. Transcatheter arterial embolization in the treatment of maxillofacial trauma induced life-threatening hemorrhages. *J Trauma* 2009; **66:** 1425-30. doi: 10.1097/TA.0b013e3181842046
13. Moher D, Liberati A, Tetzlaff J, Altman DG; PRISMA Group. Preferred reporting items for systematic reviews and meta-analyses: the PRISMA statement. *PLoS Med* 2009; **6:** e1000097. doi: 10.1371/journal.pmed.1000097
14. Hayes SB, Johnson JN, Most Z, Elhammady MS, Yavagal D, Aziz-Sultan MA. Transarterial embolization of intractable nasal and oropharyngeal hemorrhage using liquid embolic agents. *J Neurointerv Surg* 2015; **7:** 537-41. doi: 10.1136/neurintsurg-2014-011101
15. Rosch J, Dotter C T, Brown M J. Selective arterial embolization: a new method for control of acute gastrointestinal bleeding. *Radiology* 1972; **102:** 303-6. doi: 10.1148/102.2.303
16. Brooks B. The treatment of traumatic arteriovenous fistula. *Med J* 1930; **23:** 100-6.
17. Sokoloff J, Wickbom I, McDonald D, Brahme F, Goergen TC, Goldberger LE. Therapeutic percutaneous embolization in intractable epistaxis. *Radiology* 1974; **111:** 285-7. doi: 10.1148/111.2.285
18. Vaidya S, Tozer KR, Chen J. An overview of embolic agents. *Semin Intervent Radiol* 2008; **25:** 204-15. doi: 10.1055/s-0028-1085930

19. Seldinger SI. Catheter replacement of the needle in percutaneous arteriography; a new technique. *Acta Radiol* 1953; **39:** 368-76. doi: 10.3109/00016925309136722

20. Bauer JR, Ray CE. Transcatheter arterial embolization in the trauma patient: a review. *Semin Intervent Radiol* 2004; **21:** 11-22. doi: 10.1055/s-2004-831401

21. Mangla S, Sclafani SJ. External carotid arterial injury. *Injury* 2008; **39:** 1249-56. doi: 10.1016/j.injury.2008.06.012

22. Kunstlinger F, Brunelle F, Chaumont P, Doyon D. Vascular occlusive agents. *AJR Am J Roentgenol* 1981; **136:** 151-6. doi: 10.2214/ajr.136.1.151

23. Lubarsky M, Ray CE, Funaki B. Embolization agents-which one should be used when? Part 1: large-vessel embolization. *Semin Intervent Radiol* 2009; **26:** 352-7. doi: 10.1055/s-0029-1242206

24. Vrachliotis TG, Falagas ME. Infections after endovascular coil embolization. *J Endovasc Ther* 2007; **14:** 805-6. 10.1583/07-2219C.1

25. Sheth RA, Sabir S, Krishnamurthy S, Avery RK, Zhang YS, Khademhosseini A, et al. Endovascular embolization by transcatheter delivery of particles: past, present, and future. *J Funct Biomater* 2017; **8:** E12. doi: 10.3390/jfb8020012

26. Lewis AL, Adams C, Busby W, Jones SA, Wolfenden LC, Leppard SW, et al. Comparative in vitro evaluation of microspherical embolisation agents. *J Mater Sci Mater Med* 2006; **17:** 1193-204. doi: 10.1007/s10856-006-0592-x

27. Liang B, Xiong F, Wu H, Wang Y, Dong X, Cheng S, et al. Effect of transcatheter intraarterial therapies on the distribution of Doxorubicin in liver cancer in a rabbit model. *PLoS One* 2013; **8:** e76388. doi: 10.1371/journal.pone.0076388

28. Niimi Y, Berenstein A, Setton A. Complications and their management during NBCA embolization of craniospinal lesions. *Interv Neuroradiol* 2003; **9:** 157-64. doi: 10.1177/15910199030090S122

29. Berenstein A, Lasjaunias P, Brugge KG. *Surgical neuroangiography*. Vol. 2: Clinical and endovascular treatment aspects in adults. Berlin: Springer-Verlag; 2004.

30. Vollherbst DF, Sommer CM, Ulfert C, Pfaff J, Bendszus M, Mohlenbruch MA. Liquid embolic agents for endovascular embolization: evaluation of an established (Onyx) and a novel (PHIL) embolic agent in an in vitro AVM model. *Am J Neuroradiol* 2017; **38:** 1377-82. doi: 10.3174/ajnr.A5203

31. Siekmann R. Basics and principles in the application of Onyx LD Liquid Embolic System in the endovascular treatment of cerebral arteriovenous malformations. *Interv Neuroradiol* 2005; **11:** 131-40. doi: 10.1177/15910199050110S117

32. Schirmer CM, Zerris V, Malek AM. Electrocautery-induced ignition of spark showers and self-sustained combustion of onyx ethylene-vinyl alcohol copolymer. *Neurosurgery* 2006; **59:** ONS413-8. doi: 10.1227/01.NEU.0000240683.15391.99

33. Thiex R, Wu I, Mulliken JB, Greene AK, Rahbar R, Orbach DB. Safety and clinical efficacy of Onyx for embolization of extracranial head and neck vascular anomalies. *AJNR Am J Neuroradiol* 2011; **32:** 1082-6. doi: 10.3174/ajnr.A2439.

34. Koo HW, Lee JJ. Forehead pigmentation after Onyx embolization for dural arteriovenous fistula presenting with parkinsonism. *Interdiscip Neurosurg* 2020; **19:** 100616. doi: 10.1016/j.inat.2019.100616

35. Leyon JJ, Chavda S, Thomas A, Lamin S. Preliminary experience with the liquid embolic material agent PHIL (Precipitating Hydrophobic Injectable Liquid) in treating cranial and spinal dural arteriovenous fistulas: technical note. *J Neurointerv Surg* 2016; **8:** 596-602. doi: 10.1136/neurintsurg-2015-011684

36. Koçer N, Hanımoğlu H, Batur Ş, Kandemirli SG, Kızılkılıç O, Sanus Z. Preliminary experience with precipitating hydrophobic injectable liquid in brain arteriovenous malformations. *Diagn Interv Radiol* 2016; **22:** 184-9. doi: 10.5152/dir.2015.15283

37. Li W, Zhang L, Ge X, Xu B, Zhang W, Qu L, et al. Microfluidic fabrication of microparticles for biomedical applications. *ChemSoc Rev* 2018; **47:** 5646-83. doi: 10.1039/c7cs00263g

38. Noy D, Rachmiel A, Emodi O, Amsalem Y, Israel Y, Nagler RM. Transarterial embolization in maxillofacial intractable potentially life-threatening hemorrhage. *J Oral Maxillofac Surg* 2017; **75:** 1223-31. doi: 10.1016/j.joms.2017.01.033

39. Hayes SB, Johnson JN, Most Z, Elhammady MS, Yavagal D, Aziz-Sultan MA. Transarterial embolization of intractable nasal and oropharyngeal hemorrhage using liquid embolic agents. *J Neurointerv Surg* 2015; **7:** 537-41. doi: 10.1136/neurintsurg-2014-011101

40. Liao CC, Hsu YP, Chen CT, Tseng YY. Transarterial embolization for intractable oronasal hemorrhage associated with craniofacial trauma: evaluation of prognostic factors. *J Trauma* 2007; **63:** 827-30. doi: 10.1097/TA.0b013e31814b9466

41. Roberson G, Rearden E. Angiography and embolization of the internal maxillary artery for posterior epistaxis. *Arch Otolaryngol*1979; **105:** 333-7. doi: 10.1001/archotol.1979.00790180031006

42. Vitek J. Idiopathic intractable epistaxis: endovascular therapy. *Radiology.* 1991; **181:** 113-6. doi: 10.1148/radiology.181.1.1887018

43. Elahi M, Parnes LS, Fox AJ, Pelz DM, Lee DH. Therapeutic embolization in the treatment of intractable epistaxis. *Arch Otolaryngol Head Neck Surg*1995; **121:** 65-9. doi: 10.1001/archotol.1995.01890010051009

44. Duncan IC, Fourie PA, le Grange CE, van der Walt HA. Endovascular treatment of intractable epistaxis - results of a 4-year local audit. *S Afr Med J* 2004; **94:** 373-8. doi: 10.4102/sajr.v8i3.118

45. Cullen MM, Tami TA. Comparison of internal maxillary artery ligation versus embolization for refractory posterior epistaxis. *Otolaryngol Head Neck Surg* 1998; **118:** 636-42. doi: 10.1177/019459989811800512

46. Burdick TR, Hoffer EK, Kooy T, Ghodke B, Starnes BW, Valji K, et al. Which arteries are expendable? The practice and pitfalls of embolization throughout the body. *Semin Intervent Radiol* 2008; **25:**191-203. doi: 10.1055/s-0028-1085925.

47. Kuan CH, Lin CY, Hsaio JK, Chen JS, Han YY. Prognostic factors of survival from intractable oronasal bleeding after successful transarterial embolization. *J Oral Maxillofac Surg* 2015; **73:** 1790-4. doi: 10.1016/j.joms.2015.03.028

48. Cogbill TH, Cothren CC, Ahearn MK, Cullinane DC, Kaups KL, Scalea TM, et al. Management of maxillofacial injuries with severe oronasal hemorrhage: a multicenter perspective. *J Trauma* 2008; **65:** 994-9. doi: 10.1097/TA.0b013e318184ce12.

49. Kim DY, Dong DK, Park H, Chung J. Endovascular treatment of life-threatening bleeding of bilateral maxillary arteries in a patient with multiple facial bone fractures - a case report. *J Korean Neutrotraumatol Soc* 2011; **7:** 108-111. doi: 10.13004/jknts.2011.7.2.108

50. Komiyama M, Nishikawa M, Kan M, Shigemoto T, Kaji A. Endovascular treatment of intractable oronasal bleeding associated with severe craniofacial injury. *J Trauma* 1998; **44:** 330-4. doi: 10.1097/00005373-199802000-00017

51. Maioriello AV, Stanley DJ, Ho T, Ashley WW. Successful Onyx embolization of life threatening traumatic posterior jugal artery fistula following mandibular fracture. *J Neurointerv Surg* 2012; **4:** e15. doi: 10.1136/neurintsurg-2011-010071

52. Mauldin FW, Cornay WJ 3rd, Mahaley MS Jr, Hicks JN. Severe epistaxis from a false aneurysm of the external carotid artery. *Otolaryngol Head Neck Surg* 1989; **101:** 588-90. doi: 10.1177/019459988910100515

53. Mehringer CM, Hieshima GB, Grinnell VS, Tsai FY, Bentson JR, Hasso AN, et al. Therapeutic embolization for vascular trauma of the head and neck. *AJNR Am J Neuroradiol* 1983; **4:** 137-42. PMID: 6405591

54. Remonda L, Schroth G, Caversaccio M, Lädrach K, Lövblad KO, Zbären P, et al. Endovascular treatment of acute and subacute hemorrhage in the head and neck. *Arch Otolaryngol Head Neck Surg* 2000; **126:** 1255-62. doi: 10.1001/archotol.126.10.1255

55. Wang D, Su L, Han Y, Fan X. Embolization treatment of pseudoaneurysms originating from the external carotid artery. *J Vasc Surg* 2015; **61:** 920-6. doi: 10.1016/j.jvs.2014.10.093.

56. Wong CW, Tan WC, Yeh YT, Chou MC, Yeh CB. Transarterial embolization for traumatic intractable oronasal hemorrhage. *J Emerg Med* 2013; **44:** 1088-91. doi: 10.1016/j.jemermed.2012.06.029

review

Current management of intrahepatic cholangiocarcinoma: from resection to palliative treatments

Ilenia Bartolini[1], Matteo Risaliti[1], Laura Fortuna[1], Carlotta Agostini[1], Maria Novella Ringressi[1], Antonio Taddei[1], Paolo Muiesan[1,2]

[1] Hepatobiliary Unit, Department of Clinical and Experimental Medicine, University of Florence, AOU Careggi, Florence, Italy
[2] Liver Unit, Queen Elizabeth Hospital, Birmingham, UK

Radiol Oncol 2020; 54(3): 263-271.

Received 10 May 2020
Accepted 29 June 2020

Correspondence to: Paolo Muiesan, MD, FRCS, FEBS, Department of Clinical and Experimental Medicine, University of Florence, AOU Careggi, Largo Brambilla 3, 50134, Florence, Italy. E-mail: paolo.muiesan@uhb.nhs.uk

Disclosure: No potential conflicts of interest were disclosed.

Background. Intrahepatic cholangiocarcinoma (ICC) is the second most common liver primary tumour after hepatocellular carcinoma and represents 20% of all the cholangiocarcinomas. Its incidence is increasing and mortality rates are rising. Surgical resection is the only option to cure the disease, despite the high recurrence rates reported to be up to 80%. Intrahepatic recurrences may be still treated with curative intent in a small percentage of the patients. Unfortunately, due to lack of specific symptoms, most patients are diagnosed in a late stage of disease and often unsuitable for resection. Liver transplantation for ICC is still controversial. After the first published poor results, improving outcomes have been reported in highly selected cases, including locally advanced ICC treated with neoadjuvant chemotherapy, when successful in controlling tumour progression. Thus, liver transplantation should be considered a possible option within study protocols. When surgical management is not possible, palliative treatments include chemotherapy, radiotherapy and loco-regional treatments such as radiofrequency ablation, trans-arterial chemoembolization or radioembolization.

Conclusions. This update on the management of ICC focusses on surgical treatments. Known and potential prognostic factors are highlighted in order to assist in treatment selection.

Key words: intrahepatic cholangiocarcinoma; liver resection; liver transplantation

Introduction

Epidemiology

Cholangiocarcinoma is a rare tumour originating from the biliary epithelium. It can arise from the distal biliary tract, at the hepatic hilum or from intrahepatic ducts, beyond second-order biliary ducts. The classification based on the site of origin identifies three entities requiring different treatments and prognoses.[1]

With an incidence of 0.85 per 100,000 worldwide[2], intrahepatic cholangiocarcinoma (ICC) represents up to 20% of all the cholangiocarcinomas. It is the second primary liver tumour following hepatocellular carcinoma (HCC)[1] accounting for 5-30% of all primary liver malignancies.[3,4] Although reports in literature are scarce, its incidence has been rising all over the world in the last three decades.[1,5] Such increase may be associated with a greater prevalence of risk factors but also to improvements in diagnostic tools.[6] Intrahepatic cholangiocarcinoma is a highly invasive tumour, it is frequently multifocal and it is scarcely responsive to treatments. Thus, its mortality rate is about 0.69 per 100,000 and it is increasing along with tumour incidence.[2]

 doi: 10.2478/raon-2020-0045

Well-known risk factors include liver disease and chronic inflammation including cirrhosis, hepatitis B (mostly in Asian countries) and C (mostly in the Western countries), primary sclerosing cholangitis (PSC), biliary tract cysts, intrahepatic biliary stones, toxins, infection with hepatobiliary flukes (frequently in East Asia), metabolic syndrome and obesity.[1,7,8]

Presentation and diagnosis

Intrahepatic cholangiocarcinoma is often clinically silent and there are no specific symptoms in the early stages. Diagnosis is therefore incidental in at least 20-25% of the patients.[1] Symptoms include abdominal pain and, in more advanced cases, weight loss, malaise and asthenia.[1] Jaundice is rarely present (about 15% of the cases) and it can be caused by both external compression and infiltration of the hepatic hilum.[7]

Macroscopically, ICC may present as a mass-forming tumour, with periductal or intraductal growth, or with a combination of these patterns.[9] The mass-forming pattern is the most frequent and it spreads mostly via portal system. Instead, the periductal forms grow mostly through lymphatic vessels.[10] Microscopically, it is composed of bile duct cells with stromal fibrosis and collagen fibres.[1]

Diagnosis can be difficult, clinical suspicion and laboratory exams need to be confirmed by radiologic findings.[11] Laboratory investigations comprehend serum tumour markers including CA19-9 and CEA. The CA 19-9 sensitivity is 62% and its specificity is 63%.[10]

However, tumour markers may be elevated also in presence of tumours different from ICC or in case of benign conditions including cholangitis or cholestasis.[6] Therefore, they are not sensitive enough to be utilised for screening purposes.

Recently, some effort has been placed in the proteomic evaluation of organic fluids and in searching products of cancer cells (including cytokines, enzymes and growth factors) trying to find better biomarkers.[12] Potential serum, urinary and biliary biomarkers have been investigated over the years. Serum markers include trypsinogen-2, IL-6, MUC5AC, cytocheratin-19 fragment (CYFRA 21-1) and progranulin while some of the biliary biomarkers are insulin-like growth factor 1 (IGF1) and microRNA-laden vesicles. However, none of these is currently used in clinical practice.[1,12]

The Ultrasound Sonography (US) is the first imaging test that usually identifies an abdominal mass, but its sensitivity and specificity are operator-dependent. Tumour markers may improve significantly the sensitivity of US. Furthermore, the colour Doppler mode may show portal venous and parenchymal involvement.[13]

Unlike HCC, there are no specific radiological patterns for an imaging-based diagnosis.[3] On Computed Tomography (CT), ICC presents as a predominantly hypodense mass with irregular margins, with a peripheral rim enhancement in the arterial phase. Contrast uptake is progressive on the venous and late phases.[3] The hyper-enhancing pattern on delayed phase reflects stromal fibrosis of interstitial space. Therefore, hyper-attenuating ICCs are more aggressive. Other characteristics of advanced tumours include bile ducts thickening and dilatation, retraction of liver capsule, enlarged regional lymph nodes, vascular invasion and distant metastases.[13]

On contrast-enhanced Magnetic Resonance Imaging (MRI), the ICC is a hypo-intense lesion on T1-weighted images and hyper-intense on T2-weighted images. Central hypo-intensity, on delayed pictures, reflects the presence of fibrosis.[13] The contrast medium uptake in MRI is similar to CT scan. The typical HCC "wash-in and wash-out" pattern is never present, even in case of small tumours.[1,10] The MRI with cholangiopancreatography (MRCP) is the gold standard in the imaging of the biliary tree without the need of invasive techniques (i.e. percutaneous transhepatic cholangiography). The MRI is a powerful tool to evaluate tumour extent and resectability with an accuracy of up to 95%.[13]

However, both CT scan and MRI have low specificity and the diagnosis of small or rare forms of tumour, including mixed HCC-ICC or in presence of PSC, may be difficult by imaging only.[10,14]

Positron emission tomography with 18-fluorodeoxyglucose (FDG-PET) scan is not recommended as a routine staging exam.[14] However, it could be a great tool to discover occult primary tumours, distant or nodal metastasis with a sensitivity and specificity of about 40-55% and 80-87%, respectively.[13] Furthermore, a modification in patient management has been reported in up to 15% of the cases after diagnosis of nodal involvement with FDG-PET.[14,15]

The role of biopsy is still controversial when diagnostic doubt persists after imaging techniques. When a nodule is suitable for resection, most authors suggest that liver biopsy should not be performed because of the risk of seeding.[7,11] Anyhow, there is no strong evidence supporting this risk.[1] Moreover, histological analysis on biopsy is not always able to differentiate a primary from a secondary adenocarcinoma.[16] On the contrary, since distant nodal metastases are a contraindication to liver resection, a biopsy of suspect distant lymph nodes should be performed via endoscopic ultrasound (EUS) with fine-needle aspiration, eventually.[17]

Treatment and prognosis

When technically feasible, surgical resection is the best treatment that can be offered to the patients. In the great majority of them, a major hepatectomy will be necessary to achieve a R0 resection. Nevertheless, reported 5-years survival rates range from 22% and 45%,[5,11,18] mostly due to high recurrence rates (up to 80%).[19-21] Unfortunately, 60 to 88% of the patients with ICC have unresectable tumours due to a late diagnosis.[22,23]

Indications for liver transplantation (LT) for ICC are still controversial. Outcomes of liver transplantation have been changed over the years. In the '90s, a 5-year survival rate of less than 25% was reported.[24-26] Recent papers reported an acceptable 5-years overall survival rate, up to 83%, in highly selected patients.[5,27]

The most important prognostic factors after resection include: tumor-related features (e.g. size and number, vascular and nodal involvement, perineural and periductal invasion and tumour biology)[17], margin status[2], and time-to-recurrence.[21]

Palliative treatments include chemotherapy, radiation therapy or locoregional therapies but all these strategies provide only a modest improvement in prognosis with a median survival inferior to 1 year [5,23,28] and a 5-years survival of less than 10%.[29]

The focus of this paper is on surgical management of ICC with an assessment of prognostic factors for recurrence, which may assist to better select the appropriate treatment for each patient. A brief overview of palliative treatments is also provided.

Surgical management

Surgical resection

Currently, surgical resection is the only accepted treatment for potential cure.[1] Due to the improvements in surgical techniques and advances in perioperative care, surgical indications have been extended in recent years. However, only a minority of patients, 12-40%, are resectable at the time of diagnosis.[11,30]

Surgery aims to achieve complete resection of the tumour with adequate free margins, and, at the same time, leaving a sufficient functional liver remnant. The assessment of resectability is associated with a variety of factors including tumour location and extension, liver function and underlying liver disease and, last but not least, performance status.

In case of involvement of major vascular structures or of first- and second-order biliary branches, a liver resection should be carefully assessed and planned.

Up to half of patients have multifocal disease at presentation.[31] Resection of multifocal ICC is controversial since it usually requires a more demolitive liver resection and it is associated with poorer survival rates. However, multifocality itself should not prevent surgery according to current published evidence.[18,31,32]

On the other hand, distant metastases are a contraindication to surgery. Similarly, metastases of distant lymph nodes are considered a reason for unresectability.[17] In case of suspected infiltration of regional lymph nodes, surgical resection should be assessed carefully given that lymph nodes positivity is one of the most important factors linked to poor prognosis.[29] In 10-20% of the patients, locally advanced tumours may be downstaged and reconsidered for liver resection after neoadjuvant treatments including chemotherapy (based on gemcitabine, cisplatin and paclitaxel) and locoregional procedures.[32] Conversion rate varies between 0% and 53% and up to half of the patients present with stabilized disease.[32]

In presence of cirrhosis, portal pressure should be assessed since clinically significant portal hypertension, defined as an hepatic vein pressure gradient (HVPG) $\geq$ 10 mmHg[33], is a relative contraindication to major resections.[17,20] Further tests to reduce at a minimum the risk of postoperative liver failure include liver function tests, calculation of future liver remnant volume, and evaluation of the presence of fibrosis.[17]

Small tumours or peripherally located lesions can be treated with an atypical or anatomical minor resection. However, in most cases (70-80%), the lesion is multisegmental and a major hepatectomy may be needed.[19] Similarly to HCC, anatomical resections of ICC seem to have better outcomes in terms of survival and recurrence when compared with non-anatomical resections.[34]

A biliary resection and reconstruction is required in about 20-30% of the cases.[19] The necessity of a vascular reconstruction to achieve an R0 resection should not prevent surgery in selected patients. Reames *et al.*, in a multicentric analysis evaluating a total of 1087 patients, reported similar results between patients requiring a caval or portal resection and those who did not.[35]

In case of a predicted small future liver remnant, portal vein embolization can be performed prior to surgery. Liver hypertrophy develops in approximately 40% of patients within 4 weeks. However, 20-30% of these patients will never undergo resection because of tumour progression or inadequate future liver remnant hypertrophy.[17]

The use of ALPPS (Associating Liver Partition and Portal vein ligation for Staged hepatectomy) has been reported for ICC. Liver hypertrophy is achieved faster when compared with PVE and the rate of achievement of second stage is higher with ALPPS compared to other staged procedures, but the cost in terms of morbidity and mortality is significant.[36]

Similarly to other cancers, lymphadenectomy has an undisputed role in staging the disease correctly.[37] For this purpose, a minimum of 6 lymph nodes are required as suggested in the 8th edition of the American Joint Committee on Cancer (AJCC) manual.[38] However, the impact of lymphadenectomy has been previously questioned and only about 50% of patients have been reported to receive a lymphadenectomy.[39] In particular, the therapeutic role of lymphadenectomy is debated although several more recent papers reported a survival benefit.[39] A complete lymphadenectomy is routinely performed by some authors to try to reduce local recurrence but in the subgroup of cirrhotic patients the related high morbidity rates may exceed the benefits.[17]

Minimally invasive surgery for ICC is feasible and safe in selected cases, with the advantages of laparoscopic and robotic techniques and similar oncological outcomes to open surgery.[40,41]

Adjuvant therapy is not fully standardized yet due to the rarity of this disease. However, chemotherapy should be offered to patients with positive nodes at histology though it seems to offer only partial control on lymph node metastatic disease.

Post-operative mortality is less than 5% in high-volume centres.[1] Five-years OS rates after curative surgery range between 22 and 45%. Median survival is reported to be 40 months.[5,11,21,42] Recurrence rates are still very high, ranging from 53% to 80%.[5,21] The reported 1-, 3-, and 5-year disease-free survival is 44%, 18%, and 11%, respectively.[18] The great majority of patients experience disease recurrence within 2 years[5] with a median time to recurrence ranging from 9 to 26 months.[43] However, recurrence has been reported up to 9.5 years after liver resection.[18]

Despite improvements in pre- and intra-operative imaging[21,44], local tumour control may result incomplete, possibly due to unidentified small metastatic lesions at surgery.[5,21] Common extrahepatic sites of recurrence include lungs, abdominal lymph nodes and peritoneum.[21]

In case of intrahepatic only recurrence, further treatments with curative intent may still be possible if an R0 treatment is achievable by surgical resection or radiofrequency ablation.[2,21] However, disease recurrence is the major cause of death in these patients with a disease-specific mortality rate of about 90%.[21]

Liver transplantation

Currently, ICC is a controversial indication for LT.[5,27] The main reasons of such controversy include the shortage of deceased donor organs, the potential of tumour progression whilst waiting for LT after chemotherapy, the high recurrence rates of ICC and the fact that immunosuppression may facilitate recurrence.

Papers from the '90s reported a poor prognosis after liver transplant for ICC with 5-years survival rates of 10-25%.[24,25,45] Furthermore, in most LTs ICC was an incidental diagnosis on the resected specimen, thus patients had not received preoperative adjuvant treatments.[26]

Recently, Sapisochin *et al*. retrospectively looked at 48 patients transplanted for presumed HCC or decompensated cirrhosis but diagnosed as ICC at post-transplant pathology.[27] Fifteen had very early ICC (<2 cm) and 33 had advanced ICC (>2 cm or multifocal). The 5-years OS rate was 65% and 45% for very early and advanced ICC, respectively. Tumour recurrence occurred in 13% of the very early group and in 54.5% of the advanced group, being the main cause of death of the latter. Therefore, LT could be a possible treatment only for cirrhotic patients with very early ICC.[27]

However, the role of neoadjuvant chemotherapy has remained unclear for a long time. Good results in terms of survival (5-years OS rate up to 76%) have been reported in highly selected patients with hilar cholangiocarcinoma who received LT after neoadjuvant chemotherapy or chemo-radiotherapy with good disease control.[46-48] These results encouraged further studies.

In their well-designed prospective case-series, Lunsford *et al*. reported a 1-, 3- and 5-years overall survival rate of 100%, 83.3% and 83.3%, respectively. One-, 3- and 5-years recurrence-free survival was 50% with a median time of recurrence of 7.6 months.

TABLE 1. A comparison between the prognostic factors of the three main recognized staging systems (the Liver Cancer Study Group of Japan [LCSGJ][9], the National Cancer Center of Japan [NCCJ][53], and the American Joint Committee on Cancer [AJCC, 8th edition[38]], Wang *et al.*[49] and Hyder *et al.*[43] nomograms

	Tumor diameter	Number of lesion	Extent of disease	Nodal Invasion	Vascular invasion	Metastatic disease	Other prognostic factors
LCSGJ[9]	Cut-off: 2 cm	Yes	Invasion of the serosa	Yes	Yes	Yes	
NCCJ[53]		Yes		Yes	Yes		Symptoms
AJCC[38]	Cut-off: 5 cm		Yes	Yes	Yes	Yes	
Wang et al.[49]	Yes	Yes		Yes	Yes	Yes	CEA CA19.9
Hyder et al.[43]	Yes	Yes		Yes	Yes		Age Cirrhosis

CA19.9= Carbohydrate Antigen 19.9; CEA = Carcinoembryonic Antigen

Inclusion criteria included: the presence of a locally advanced ICC (> 2 cm or multifocal, confirmed with biopsy or cytology), deemed unresectable after the evaluation of the multidisciplinary team; absence of distant metastasis or major vascular structures involvement; absence of tumour progression after a minimum of 6 months of neoadjuvant chemotherapy or radio-chemotherapy (gemcitabine-based regimens). Prior to proceeding to LT, sampling and frozen section of the hepatic hilum lymph nodes was performed to exclude malignancy.[5]

Despite promising results, the main issue with this paper was related to the highly selected patients and such good prognosis could be a consequence of the indolent behaviour of the disease. Responsiveness to chemotherapy for at least 6 months is a "test of time" and excludes patients with aggressive disease from transplantation. Furthermore, this paper included a small sample size (six patients in 8 years received LT) and the short median follow-up of 36 months.

Further prospective clinical trials taking into account tumour morphology and biology are still needed to draft definite conclusions.

Prognostic factors for recurrence

There are many recognized prognostic factors related to the tumour and to liver resection as well as the previous history of PSC.

Tumour-related factors include size and number, vascular and nodal involvement, perineural and periductal invasion and tumour biology.[17] Serum biomarkers have a controversial role in prognosis establishment.[49]

Most authors recognize tumour size as a prognostic factor for recurrence.[42] Different cut-offs have been reported: 2-3 cm[27], 5 cm[18,19] or 8 cm.[50] In particular, Sapisochin *et al*. stratified the patients into three groups according to tumour size: smaller than 2 cm, between 2 and 3 cm, larger than 3 cm. They found a 5-years OS of 80%, 61% and 42%, respectively.[27] However, some other authors found alternative factors with a stronger prediction potential after resection[10] or LT including not receiving neoadjuvant therapies.[51]

Since multifocality and vascular invasion have a prognostic impact, the American Joint Committee on Cancer (AJCC) classifies both multifocal and single tumours in presence of vascular invasion as T2.[38] Furthermore, multifocality has been reported to significantly correlate with tumour size and differentiation, nodal metastasis and vascular infiltration. Satellitosis seems to confer a worse prognosis when compared with bilateral tumour location although this result may suffer from a selection bias of the patients.[31]

On the contrary, the previously cited paper of Lunsford reported that both volume and number of lesions do not impact on recurrence after LT.[5] However, these different findings may suffer from bias related to the small sample group evaluated.

Node metastasis is an important prognostic factor. Lymph nodes positivity resulted in about 45% of resections and even N0 patients may harbour nodal micrometastases in about 10-20% of the cases.[52]

There are three main recognized staging systems: the Liver Cancer Study Group of Japan (LCSGJ)[9], the American Joint Committee on Cancer (AJCC), 8th edition[38] and the National Cancer Center of Japan (NCCJ)[53,54] (Table 1).

Principal prognostic factors for LCSGJ are tumour diameter with a cut-off of 2 cm, number of lesions, vascular infiltration and invasion of the serosa.[9]

The AJCC, 8th edition[38], applied a cut-off o 5 cm to divide T1 into T1a and T1b.

The NCCJ, Okabayashi and Nathan system[53,54], do not consider tumour diameter as an independent prognostic factor while presence of symptoms, nodal invasion, lesion number and vascular invasion have a prognostic impact. These three systems displayed lack of accuracy in predicting prognosis[10], thus several nomograms have been proposed to predict survival.[43,49] Spolverato *et al*. developed a model to specifically predict cure rate and time necessary to define the patient cured. This cure model included tumour number, size and differentiation, vascular and periductal invasion, nodal positivity and it is easily accessible on internet.[18] Similar results have been previously published.[43,49]

Tumour biology is another fundamental aspect. Grading has been reported to be significantly related with tumour recurrence.[27,29] A high grade of diversity in ICC molecular profile has been reported.[1] Several genetic modifications, epigenetic alterations, gene fusions products (including FGFR2 gene fusion), hormone influences (including evaluation of tumour estrogen sensitivity) and growth factors effects have been assessed and are still under continuous evaluation.[1] The whole-genome analysis helped in understanding two potential altered pathways related with ICC development: activation of the inflammatory response pathway and cellular proliferation pathway, the latter being related with a worse prognosis.[1,55] However, a complete knowledge at the cellular level together with the microenvironment in which tumours develop is far from being achieved.[1] This effort may widen the perspectives in different aspects of tumour management: diagnosis (with the discovery of new circulating biomarkers), treatment allocation (including personalized targeted therapies) and prognosis prediction. For example, while KRAS mutation has been found in patients experiencing recurrence, FGFR gene fusion seems related with an indolent disease.[5,56] Obviously, patients with indolent tumours will have a better prognosis despite the treatments received and they will benefit more from each treatment. The previously reported absence of disease progression during chemotherapy is strictly related with tumour biology.[2,5]

The most important prognostic factor after surgical resection is the state of the margins. Tumour-free margins are related with a significantly better prognosis when compared with infiltrated margins.[2,57]

Finally, time-to-recurrence after surgery with a curative intent has been reported to be itself a prognostic factor.[21] Using a cut-off of 24 months, Zhang *et al*. showed a significantly worse prognosis for patients experiencing early recurrence when compared with those with late recurrence (median OS of 10 and 18 months, respectively).[21] Although recurrence was mainly in the liver, the frequency of extrahepatic localization was higher in the early recurrence group.[21] Furthermore, they found that the size and number of tumours, vascular invasion, presence of satellitosis or surgical margins of less than 1 cm were all associated with the early recurrence pattern at univariate analysis. On the contrary, adjuvant treatments and presence of cirrhosis resulted significantly linked to late recurrence.[21] Interestingly, when further treatments with a curative intent were possible, OS rates resulted similar between the two groups.[21]

Further studies are needed to evaluate with greater detail potential prognostic factors and their weight.

Palliative treatments

Unfortunately, a great majority of the patients present with unresectable disease due to major vascular or bile duct involvement, metastasis or huge burden of disease leading to a potential insufficient future liver remnant.[11] The 5-years survival rate of these patients is less than 10%.[29]

Although ICC tends to develop chemoresistance, systemic therapy is the main treatment in the subset of palliative cures. Chemotherapy could be considered to treat patients with macroscopic residual tumour after surgery, locally advanced or metastatic unresectable tumours or recurrent ICCs. The National Comprehensive Cancer Network guidelines recommend gemcitabine/cisplatin therapy as first-line treatment.[37] In alternative, fluoropyrimidine-based or other gemcitabine-based chemotherapy regimens could be considered.[37] However, the optimal second-line therapy is still controversial.[58] The role of targeted therapy is still under evaluation.[1] Furthermore, a better understanding of the mechanisms that are behind chemoresistance may widen and improve treatment options.

The addition of radiation to chemotherapy is associated with better outcomes in terms of disease-free and overall survival.[59,60] On the contrary, the role of radiotherapy alone for ICC is controversial. Different approaches of radiotherapy are available such as external beam irradiation, brachytherapy with iridium-192, stereotactic body radiotherapy and proton beam irradiation.[59] Technical advances now allow a selective delivery of radiation to the lesion, sparing adjacent tissue. To date there are no randomized trials comparing new techniques with the more conventional ones.

While distant metastasis is a less frequent cause of death, many of these patients die of liver failure caused by tumour-related vascular involvement or biliary obstruction. It is thus important to try to achieve local control of the tumour to improve quality of life.[32] There are no randomized data showing a single optimal local treatment, so a tailored therapy is required. The choice of the best locoregional treatment must consider factors related to the patient (comorbidity, liver function, previous treatments) and to the tumour, such as size, vascularity and its involvement of bile ducts, blood vessels, bowel and chest wall.[32]

Data concerning the use of transarterial embolization therapies for ICC are scarce. These treatments include transarterial chemoembolization (TACE), bland embolization, chemoinfusion (TACI) and radioembolization (TARE, known also as selective internal radiation therapy, SIRT). These therapies are indicated in case of hypervascular lesions and in absence of complete portal vein thrombosis[61] with the exception of TARE that can be used in cases of neoplastic thrombosis. Unfortunately, ICC is typically hypovascular and characterized by fibrous content.[62]

In a retrospective multi-institutional analysis evaluating 198 patients with ICC, partial/complete response or stability of disease was found in 26% and 62% of patients, respectively. Median OS was 13.2 months. Outcomes did not differ on the type of intra-arterial treatment.[63] These results were confirmed by Yang who performed a systematic review including 926 patients.[64] Mean complete radiological response was 10% while partial radiological response was 22.2%. One third of patients suffered from acute toxicity, 30-day mortality was less than 1% and median OS was 13 months. These data showed that transarterial embolization therapies could be safely and effectively used in unresectable cholangiocarcinoma, conferring a survival benefit.[64]

Percutaneous ablation techniques such as radiofrequency or microwave ablation are effective for small lesions (4-5 cm), not located close to major bile ducts or blood vessels or on the liver surface.[65] Irreversible electroporation is a new ablation technique with similar results for small lesions but with no limitations in terms of distance from bile ducts and vessels.[61]

Photodynamic therapy is another palliative treatment that may have a small beneficial effect on survival.[66]

Conclusions

Intrahepatic cholangiocarcinoma is a rare tumour but with an increasing incidence over the years. Unfortunately, mortality rates are rising consensually despite improvements in surgical techniques and perioperative care. When technically feasible and patients are fit, surgical resection is the best option that can be offered. However, survival rates are still discouraging and recurrence rates are high. Liver transplantation may be considered in highly selected patients including those with a very early tumour and cirrhosis or in locally advanced unresectable ICC but stable after neoadjuvant therapy. Unfortunately, the majority of patients present with unresectable disease. Palliative treatments may confer an improvement in survival. However, we should aim at an improved stratification of patients using the known prognostic factors and, hopefully, at a better understanding of biologic cancer profiling. This stratification, together with standardization and improvements in neoadjuvant and adjuvant therapies, may allow a better allocation of treatments and, possibly, an expansion of the indications for surgery in a subset of patients.

References

1. Banales JM, Cardinale V, Carpino G, Marzioni M, Andersen JB, Invernizzi P, et al. Expert consensus document: cholangiocarcinoma: current knowledge and future perspectives consensus statement from the European Network for the Study of Cholangiocarcinoma (ENS-CCA). *Nat Rev Gastroenterol Hepatol* 2016; **13:** 261-80. doi: 10.1038/nrgastro.2016.51
2. Spolverato G, Kim Y, Alexandrescu S, Marques HP, Lamelas J, Aldrighetti L, et al. Management and outcomes of patients with recurrent intrahepatic cholangiocarcinoma following previous curative-intent surgical resection. *Ann Surg Oncol* 2016; **23:** 235-43. doi: 10.1245/s10434-015-4642-9
3. Valls C, Gumà A, Puig I, Sanchez A, Andía E, Serrano T, et al. Intrahepatic peripheral cholangiocarcinoma: CT evaluation. *Abdom Imaging* 2000; **25:** 490-6. doi: 10.1007/s002610000079
4. Khan SA, Toledano MB, Taylor-Robinson SD. Epidemiology, risk factors, and pathogenesis of cholangiocarcinoma. *HPB (Oxford)* 2008; **10:** 77-82. doi: 10.1080/13651820801992641
5. Lunsford KE, Javle M, Heyne K, Shroff RT, Abdel-Wahab R, Gupta N, et al. Liver transplantation for locally advanced intrahepatic cholangiocarcinoma treated with neoadjuvant therapy: a prospective case-series. *Lancet Gastroenterol Hepatol* 2018; **3:** 337-48. doi: 10.1016/S2468-1253(18)30045-1
6. Bertuccio P, Malvezzi M, Carioli G, Hashim D, Boffetta P, El-Serag HB, et al. Global trends in mortality from intrahepatic and extrahepatic cholangiocarcinoma. *J Hepatol* 2019; **71:** 104-14. doi: 10.1016/j.jhep.2019.03.013
7. Bridgewater J, Galle PR, Khan SA, Llovet JM, Park JW, Patel T, et al. Guidelines for the diagnosis and management of intrahepatic cholangiocarcinoma. *J Hepatol* 2014; **60:** 1268-89. doi: 10.1016/j.jhep.2014.01.021

8. Sempoux C, Jibara G, Ward SC, Fan C, Qin L, Roayaie S, et al. Intrahepatic cholangiocarcinoma: new insights in pathology. *Semin Liver Dis* 2011; **31:** 49-60. doi: 10.1055/s-0031-1272839
9. Yamasaki S. Intrahepatic cholangiocarcinoma: macroscopic type and stage classification. *J Hepatobiliary Pancreat Surg* 2003; **10:** 288-91. doi: 10.1007/s00534-002-0732-8
10. Blechacz B, Komuta M, Roskams T, Gores GJ. Clinical diagnosis and staging of cholangiocarcinoma. *Nat Rev Gastroenterol Hepatol* 2011; **8:** 512-22. doi: 10.1038/nrgastro.2011.131
11. Khan SA, Davidson BR, Goldin RD, Heaton N, Karani J, Pereira SP, et al. Guidelines for the diagnosis and treatment of cholangiocarcinoma: an update. *Gut* 2012; **61:** 1657-69. doi: 10.1136/gutjnl-2011-301748
12. Alvaro D. Serum and bile biomarkers for cholangiocarcinoma. *Curr Opin Gastroenterol* 2009; **25:** 279-84. doi: 10.1097/mog.0b013e328325a894
13. Aljiffry M, Walsh MJ, Molinari M. Advances in diagnosis, treatment and palliation of cholangiocarcinoma: 1990-2009. *World J Gastroenterol* 2009; **15:** 4240-62. doi: 10.3748/wjg.15.4240
14. Weber SM, Ribero D, O'Reilly EM, Kokudo N, Miyazaki M, Pawlik TM. Intrahepatic cholangiocarcinoma: expert consensus statement. *HPB (Oxford)* 2015; **17:** 669-80. doi: 10.1111/hpb.12441
15. Lamarca A, Barriuso J, Chander A, McNamara MG, Hubner RA, ÓReilly D, et al. F-fluorodeoxyglucose positron emission tomography. *J Hepatol* 2019; **71:** 115-29. doi: 10.1016/j.jhep.2019.01.038
16. Goodman ZD. Neoplasms of the liver. *Mod Pathol* 2007; **20(Suppl 1):** S49-60. doi: 10.1038/modpathol.3800682
17. Mazzaferro V, Gorgen A, Roayaie S, Droz Dit Busset M, Sapisochin G. Liver resection and transplantation for intrahepatic cholangiocarcinoma. *J Hepatol* 2020; **72:** 364-77. doi: 10.1016/j.jhep.2019.11.020
18. Spolverato G, Vitale A, Cucchetti A, Popescu I, Marques HP, Aldrighetti L, et al. Can hepatic resection provide a long-term cure for patients with intrahepatic cholangiocarcinoma? *Cancer* 2015; **121:** 3998-4006. doi: 10.1002/cncr.29619
19. Endo I, Gonen M, Yopp AC, Dalal KM, Zhou Q, Klimstra D, et al. Intrahepatic cholangiocarcinoma: rising frequency, improved survival, and determinants of outcome after resection. *Ann Surg* 2008; **248:** 84-96. doi: 10.1097/SLA.0b013e318176c4d3
20. Tabrizian P, Jibara G, Hechtman JF, Franssen B, Labow DM, Schwartz ME, et al. Outcomes following resection of intrahepatic cholangiocarcinoma. *HPB (Oxford)* 2015; **17:** 344-51. doi: 10.1111/hpb.12359
21. Zhang XF, Beal EW, Bagante F, Chakedis J, Weiss M, Popescu I, et al. Early versus late recurrence of intrahepatic cholangiocarcinoma after resection with curative intent. *Br J Surg* 2018; **105:** 848-56. doi: 10.1002/bjs.10676
22. Weber SM, Jarnagin WR, Klimstra D, DeMatteo RP, Fong Y, Blumgart LH. Intrahepatic cholangiocarcinoma: resectability, recurrence pattern, and outcomes. *J Am Coll Surg* 2001; **193:** 384-91. doi: 10.1016/s1072-7515(01)01016-x
23. Patel T. Cholangiocarcinoma – controversies and challenges. *Nat Rev Gastroenterol Hepatol* 2011; **8:** 189-200. doi: 10.1038/nrgastro.2011.20
24. Goldstein RM, Stone M, Tillery GW, Senzer N, Levy M, Husberg BS, et al. Is liver transplantation indicated for cholangiocarcinoma? *Am J Surg* 1993; **166:** 768-71. doi: 10.1016/s0002-9610(05)80696-8
25. Pichlmayr R, Weimann A, Oldhafer KJ, Schlitt HJ, Klempnauer J, Bornscheuer A, et al. Role of liver transplantation in the treatment of unresectable liver cancer. *World J Surg* 1995; **19:** 807-13. doi: 10.1007/BF00299775
26. Meyer CG, Penn I, James L. Liver transplantation for cholangiocarcinoma: results in 207 patients. *Transplantation* 2000; **69:** 1633-7. doi: 10.1097/00007890-200004270-00019
27. Sapisochin G, Facciuto M, Rubbia-Brandt L, Marti J, Mehta N, Yao FY, et al. iCCA International Consortium. Liver transplantation for "very early" intrahepatic cholangiocarcinoma: international retrospective study supporting a prospective assessment. *Hepatology* 2016; **64:** 1178-88. doi: 10.1002/hep.28744
28. Valle JW, Furuse J, Jitlal M, Beare S, Mizuno N, Wasan H, et al. Cisplatin and gemcitabine for advanced biliary tract cancer: a meta-analysis of two randomised trials. *Ann Oncol* 2014; **25:** 391-8. doi: 10.1093/annonc/mdt540
29. Mavros MN, Economopoulos KP, Alexiou VG, Pawlik TM. Treatment and prognosis for patients with intrahepatic cholangiocarcinoma: systematic review and meta-analysis. *JAMA Surg* 2014; **149:** 565-74. doi: 10.1001/jamasurg.2013.5137
30. Wu L, Tsilimigras DI, Paredes AZ, Mehta R, Hyer JM, Merath K, et al. Trends in the incidence, treatment and outcomes of patients with intrahepatic cholangiocarcinoma in the USA: facility type is associated with margin status, use of lymphadenectomy and overall survival. *World J Surg* 2019; **43:** 1777-87. doi: 10.1007/s00268-019-04966-4
31. Addeo P, Jedidi I, Locicero A, Faitot F, Oncioiu C, Onea A, et al. Prognostic impact of tumour multinodularity in intrahepatic cholangiocarcinoma. *J Gastrointest Surg* 2019; **23:** 1801-9. doi: 10.1007/s11605-018-4052-y
32. Le Roy B, Gelli M, Pittau G, Allard MA, Pereira B, Serji B, et al. Neoadjuvant chemotherapy for initially unresectable intrahepatic cholangiocarcinoma. *Br J Surg* 2018; **105:** 839-47. doi: 10.1002/bjs.10641
33. Bosch J, Iwakiri Y. The portal hypertension syndrome: etiology, classification, relevance, and animal models. *Hepatol Int* 2018; **12:** 1-10. doi: 10.1007/s12072-017-9827-9
34. Si A, Li J, Yang Z, Xia Y, Yang T, Lei Z, et al. Impact of anatomical versus non-anatomical liver resection on short- and long-term outcomes for patients with intrahepatic cholangiocarcinoma. *Ann Surg Oncol* 2019; **26:** 1841-50. doi: 10.1245/s10434-019-07260-8
35. Reames BN, Ejaz A, Koerkamp BG, Alexandrescu S, Marques HP, Aldrighetti L, et al. Impact of major vascular resection on outcomes and survival in patients with intrahepatic cholangiocarcinoma: a multi-institutional analysis. *J Surg Oncol* 2017; **116:** 133-9. doi: 10.1002/jso.24633
36. De Santibañes M, Boccalatte L, de Santibañes E. A literature review of associating liver partition and portal vein ligation for staged hepatectomy (ALPPS): so far, so good. *Updates Surg* 2017; **69:** 9-19. doi: 10.1007/s13304-016-0401-0
37. National Comprehensive Cancer Network. *NCCN clinical practice guidelines in oncology. Hepatobiliary cancers.* Version 4.2019. [cited 2019 Dec 27]. Available at https://www.36.org/professionals/physician_gls/pdf/hepatobiliary.pdf.
38. Amin MB, Greene FL, Edge SB, Compton CC, Gershenwald JE, Brookland RK, et al. The eighth edition AJCC cancer staging manual: continuing to build a bridge from a population-based to a more "personalized" approach to cancer staging. *CA Cancer J Clin* 2017; **67:** 93-9. doi: 10.3322/caac.21388
39. Sahara K, Tsilimigras DI, Merath K, Bagante F, Guglielmi A, Aldrighetti L, et al. Therapeutic index associated with lymphadenectomy among patients with intrahepatic cholangiocarcinoma: which patients benefit the most from nodal evaluation? *Ann Surg Oncol* 2019; **26:** 2959-68. doi: 10.1245/s10434-019-07483-9
40. Ratti F, Cipriani F, Ariotti R, Gagliano A, Paganelli M, Catena M, et al. Safety and feasibility of laparoscopic liver resection with associated lymphadenectomy for intrahepatic cholangiocarcinoma: a propensity score-based case-matched analysis from a single institution. *Surg Endosc* 2016; **30:** 1999-2010. doi: 10.1097/md.0000000000018307
41. Liu R, Wakabayashi G, Kim HJ, Choi GH, Yiengpruksawan A, Fong Y, et al. International consensus statement on robotic hepatectomy surgery in 2018. *World J Gastroenterol* 2019; **25:** 1432-44. doi: 10.3748/wjg.v25.i12.1432
42. Spolverato G, Kim Y, Ejaz A, Alexandrescu S, Marques H, Aldrighetti L, et al. Conditional probability of long-term survival after liver resection for Intrahepatic cholangiocarcinoma: a multi-institutional analysis of 535 patients. *JAMA Surg* 2015; **150:** 538-45. doi: 10.1001/jamasurg.2015.0219
43. Hyder O, Marques H, Pulitano C, Marsh JW, Alexandrescu S, Bauer TW, et al. A nomogram to predict long-term survival after resection for intrahepatic cholangiocarcinoma: an Eastern and Western experience. *JAMA Surg* 2014; **149:** 432-8. doi: 10.1001/jamasurg.2013.5168
44. Doussot A, Gonen M, Wiggers JK, Groot-Koerkamp B, DeMatteo RP, Fuks D, et al. Recurrence patterns and disease-free survival after resection of intrahepatic cholangiocarcinoma: preoperative and postoperative prognostic models. *J Am Coll Surg* 2016; **223:** 493-505.e2. doi: 10.1016/j.jamcollsurg.2016.05.019
45. Rosen CB, Heimbach JK, Gores GJ. Liver transplantation for cholangiocarcinoma. *Transpl. Int* 2010; **23:** 692-7. doi: 10.1111/j.1432-2277.2010.01108.x

46. Rea DJ, Heimbach JK, Rosen CB, Haddock MG, Alberts SR, Kremers WK, et al. Liver transplantation with neoadjuvant chemoradiation is more effective than resection for hilar cholangiocarcinoma. *Ann Surg* 2005; **242:** 451-61. doi: 10.1097/01.sla.0000179678.13285.fa

47. Heimbach JK, Gores GJ, Haddock MG, Alberts SR, Pedersen R, Kremers W, et al. Predictors of disease recurrence following neoadjuvant chemoradiotherapy and liver transplantation for unresectable perihilar cholangiocarcinoma. *Transplantation* 2006; **82:** 1703-7. doi: 10.1097/01.tp.0000253551.43583.d1

48. Darwish Murad S, Kim WR, Harnois DM, Douglas DD, Burton J, Kulik LM, et al. Efficacy of neoadjuvant chemoradiation, followed by liver transplantation, for perihilar cholangiocarcinoma at 12 US centers. *Gastroenterology* 2012; **143:** 88-98. doi: 10.1053/j.gastro.2012.04.008

49. Wang Y, Li J, Xia Y, Gong R, Wang K, Yan Z, et al. Prognostic nomogram for intrahepatic cholangiocarcinoma after partial hepatectomy. *J Clin Oncol* 2013; **31:** 1188-95. doi: 10.1200/JCO.2012.41.5984

50. Sapisochin G, de Lope CR, Gastaca M, de Urbina JO, López-Andujar R, Palacios F, et al. Intrahepatic cholangiocarcinoma or mixed hepatocellular-cholangiocarcinoma in patients undergoing liver transplantation: a Spanish matched cohort multicenter study. *Ann Surg* 2014; **259:** 944-52. doi: 10.1097/SLA.0000000000000494

51. Hong JC, Petrowsky H, Kaldas FM, Farmer DG, Durazo FA, Finn RS, et al. Predictive index for tumor recurrence after liver transplantation for locally advanced intrahepatic and hilar cholangiocarcinoma. *J Am Coll Surg* 2011; **212:** 514-20. doi: 10.1016/j.jamcollsurg.2010.12.005

52. Clark CJ, Wood-Wentz CM, Reid-Lombardo KM, Kendrick ML, Huebner M, Que FG. Lymphadenectomy in the staging and treatment of intrahepatic cholangiocarcinoma: a population-based study using the National Cancer Institute SEER database. *HPB (Oxford)* 2011; **13:** 612-20. doi: 10.1111/j.1477-2574.2011.00340.x

53. Okabayashi T, Yamamoto J, Kosuge T, Shimada K, Yamasaki S, Takayama T, et al. A new staging system for mass-forming intrahepatic cholangiocarcinoma: analysis of preoperative and postoperative variables. *Cancer* 2001; **92:** 2374-83. doi: 10.1002/1097-0142(20011101)92:9<2374::aid-cncr1585>3.0.co;2-l

54. Nathan H, Aloia TA, Vauthey JN, Abdalla EK, Zhu AX, Schulick RD, et al. A proposed staging system for intrahepatic cholangiocarcinoma. *Ann Surg Oncol* 2009; **16:** 14-22. doi: 10.1245/s10434-008-0180-z

55. Sia D, Hoshida Y, Villanueva A, Roayaie S, Ferrer J, Tabak B, et al. Integrative molecular analysis of intrahepatic cholangiocarcinoma reveals 2 classes that have different outcomes. *Gastroenterology* 2013; **144:** 829-40. doi: 10.1053/j.gastro.2013.01.001

56. Rizvi S, Khan SA, Hallemeier CL, Kelley RK, Gores GJ. Cholangiocarcinoma - evolving concepts and therapeutic strategies. *Nat Rev Clin Oncol* 2018; **15:** 95-111. doi: 10.1038/nrclinonc.2017.157

57. Hyder O, Hatzaras I, Sotiropoulos GC, Paul A, Alexandrescu S, Marques H, et al. Recurrence after operative management of intrahepatic cholangiocarcinoma. *Surgery* 2013; **153**: 811-18. doi: 10.1016/j.surg.2012.12.005

58. Lamarca A, Hubner RA, David Ryder W, Valle JW. Second-line chemotherapy in advanced biliary cancer: a systematic review. *Ann Oncol* 2014; **25:** 2328-38. doi: 10.1093/annonc/mdu162

59. Kim YI, Park JW, Kim BH, Woo SM, Kim TH, Koh YH, et al. Outcomes of concurrent chemoradiotherapy versus chemotherapy alone for advanced-stage unresectable intrahepatic cholangiocarcinoma. *Radiat Oncol* 2013; **8:** 292. doi: 10.1186/1748-717X-8-292

60. Jackson MW, Amini A, Jones BL, Rusthoven CG, Schefter TE, Goodman KA. Treatment selection and survival outcomes with and without radiation for unresectable, localized intrahepatic cholangiocarcinoma. *Cancer J* 2016; **22:** 237-42. doi: 10.1097/PPO.0000000000000213

61. Sieghart W, Hucke F, Peck-Radosavljevic M. Transarterial chemoembolization: modalities, indication, and patient selection. *J Hepatol* 2015; **62:** 1187-95. doi: 10.1016/j.jhep.2015.02.010

62. Boehm LM, Jayakrishnan TT, Miura JT, Zacharias AJ, Johnston FM, Turaga KK, et al. Comparative effectiveness of hepatic artery based therapies for unresectable intrahepatic cholangiocarcinoma. *J Surg Oncol* 2015; **111:** 213-20. doi:10.1002/jso.2378

63. Hyder O, Marsh JW, Salem R, Petre EN, Kalva S, Liapi E, et al. Intra-arterial therapy for advanced intrahepatic cholangiocarcinoma:a multi-institutional analysis. *AnnSurg Oncol* 2013; **20:** 3779-86. doi: 10.1245/s10434-013-3127-y

64. Yang L, Shan J, Shan L, Saxena A, Bester L, Morris DL. Trans-arterial embolisation therapies for unresectable intrahepatic cholangiocarcinoma: a systematic review. *J Gastrointest Oncol* 2015; **6:** 570-88. doi: 10.3978/j.issn.2078-6891.2015.055

65. Han K, Ko HK, Kim KW, Won HJ, Shin YM, Kim PN. Radiofrequency ablation in the treatment of unresectable intrahepatic cholangiocarcinoma: systematic review and meta-analysis. *J Vasc Interv Radiol* 2015; **26:** 943-8. doi: 10.1016/j.jvir.2015.02.024

66. Lu Y, Liu L, Wu JC, Bie LK, Gong B. Efficacy and safety of photodynamic therapy for unresectable cholangiocarcinoma: a meta-analysis. *Clin Res Hepatol Gastroenterol* 2015; **39:** 718-24. doi: 10.1016/j.clinre.2014.10.015

review

Consensus molecular subtypes (CMS) in metastatic colorectal cancer - personalized medicine decision

Martina Rebersek[1,2]

[1] Department of Medical Oncology, Institute of Oncology Ljubljana, Ljubljana, Slovenia
[2] Faculty of Medicine, University of Ljubljana, Ljubljana, Slovenia

Radiol Oncol 2020; 54(3): 272-277.

Received 13 March 2020
Accepted 29 April 2020

Correspondence to: Assist. Prof. Martina Reberšek, M.D., Ph.D., Department of Medical Oncology, Institute of Oncology Ljubljana, Zaloška 2, SI-1000 Ljubljana, Slovenia. E-mail: mrebersek@onko-i.si

Disclosure: No potential conflicts of interest were disclosed.

Background. Colorectal cancer (CRC) is one of the most common types of cancer in the world. Metastatic disease is still incurable in most of these patients, but the survival rate has improved by treatment with novel systemic chemotherapy and targeted therapy in combination with surgery. New knowledge of its complex heterogeneity in terms of genetics, epigenetics, transcriptomics and microenvironment, including prognostic and clinical characteristics, led to its classification into various molecular subtypes of metastatic CRC, called consensus molecular subtypes (CMS). The CMS classification thus enables the medical oncologists to adjust the treatment from case to case. They can determine which type of systemic chemotherapy or targeted therapy is best suited to a specific patient, what dosages are needed and in what order.

Conclusions. CMS in metastatic CRC are the new tool to include the knowledge of molecular factors, tumour stroma and signalling pathways for personalized, patient-orientated systemic treatment in precision medicine.

Key words: metastatic colorectal cancer; heterogeneity; biomarkers; consensus molecular subtypes; CMS1; CMS2; CMS3; CMS4

Introduction

Colorectal cancer (CRC) is still one of the most common types of cancer and one of the lead causes of cancer- related deaths worldwide, as well as in Slovenia. According to the Cancer Registry of Slovenia, there were 1467 new cases of CRC in 2016, of which 871 men and 596 women.[1] The prognosis of these patients has improved significantly over the last decade because of successful preventive screening programme, improved surgical techniques, radiation therapy and systemic treatment for both early and advanced stages. In Slovenia, the incidence of CRC has been declining in the last few years, mainly due to increased awareness and preventive screening programme called SVIT, which has been implemented in Slovenia in 2009. According to the National Cancer Control Program Slovenia, the incidence of CRC has been declining annually. In the last official report from 2015, there were about 400 cases less from 2010 to 2015 (from 1729 cases in 2010 to 1357 cases in 2015).[2]

Metastatic CRC is still an incurable disease for most of the patients, with most commonly liver, lung or lymph nodes and peritoneal metastases. In the past, 15 years ago, median overall survival (mOS) was approximately 12 months and the 5-year survival rate was 13%. However, the survival rate of these patients has increased, mainly due to the combined treatment of metastases with surgery and systemic therapy.[3-5] Long-term survival or even cure can be attained in 20%–50% of the patients who undergo complete R0 resection of liver or lung metastases, and around 70% 5-year survival of these patients can be achieved.[3,4]

However, in the field of systemic therapy there has been a significant progress with new drugs in the recent years. There are more options of initial systemic chemotherapy, oxaliplatin, irinotecan, and fluoropyrimidines, in combination with targeted therapy with anti-epidermal growth factor receptor (EGFR) monoclonal antibodies (cetuximab, panitumumab) in case of *KRAS* wild type tumours or anti-vascular endothelial growth factor (VEGF) inhibitors (monoclonal antibodies bevacizumab, aflibercept, ramucirumab, regorafenib as per oral tyrosine kinase inhibitor).[3-5] The combination of these novel chemotherapy and targeted therapy now extends the mOS up to 40 months.[3-5]

Additionally, testing for new biomarkers enables the usage of new targeted treatment in metastatic CRC patients, such as human epidermal growth factor receptor 2 (HER2/new) amplifications for double HER2 blockade, immunotherapy with anti-programmed cell death protein 1 (PD-1) monoclonal antibodies in high microsatellite instable (MSI) tumours, and neurotrophic tyrosine kinase receptor *(NTRK)* inhibitors in case of *NTRK* gene fusions.[3-5] *BRAF* V600E mutation is associated with poor prognosis under standard treatment of mOS less than 1 year and the responses to targeted therapy of combinations with anti- EGFR, BRAF and MEK inhibitors are promising with longer mOS.[3-5]

Pharmacogenomics' biomarkers such as dihydropyrimidine dehydrogenase, uridine diphosphate glucuronosyltransferase 1A1, excision repair cross complementing rodent repair deficiency complementation group 1, VEGF and thymidylate synthase are also important when planning the treatment and deciding on the type (to choose the alternative systemic therapy), appropriate combination (less toxic) and dosages (to adjust the dose to lower the frequency and grade of the adverse effects) of systemic therapy.[6]

New knowledge about the molecular heterogeneity of CRC, the discovery of biomarkers as predictive factors for disease prognosis and response to systemic treatment, and thus personalized medicine in this field, have also significantly contributed to the prolonged survival rates of patients. Besides gene mutations, tumour stroma and immunity also play a very important role in response to the systemic treatment and the prognosis of the disease.

In 2015, Guinney *et al.* first published the classification of consensus molecular subtypes (CMS), namely MSI immune CMS1, canonical CMS2, metabolic CMS3 and mesenchymal CMS4.[7] The CMS classification includes clinical factors, all pathological and molecular features of the tumour, signalling pathways and immunity. However, it still currently has not translated into regular clinical practice, which could guide the clinicians in their more personalized treatment decisions. At present, the CMSs do not have an impact on clinical decisions, because we do not yet have approved algorithms available for everyday clinical practice

The clinical implications of CMS

Colorectal cancer is genetically and transcriptomically heterogeneous disease. In adjuvant setting for early-stage CRC, there are several gene expression signatures such as ColoPrint, Oncotype DX and others, but they are still not recommended in everyday clinical practice by international guidelines for CRC.[2,3] In metastatic setting, *MSI, RAS* and *BRAF* mutational statuses are routinely tested for prognosis and predictions for systemic treatment. *KRAS* mutational status was the first biomarker in metastatic CRC to predict the response to anti-EGFR inhibitors since 2008. Additionally, mutational status testing in *RAS* gene (*KRAS* and *NRAS* genes) is used in daily clinical practice since 2013. In the past, BRAF mutation was a negative prognostic biomarker for a shorter median OS of 12 months. This was also confirmed in our prospective clinical trial, conducted at the Institute of Oncology Ljubljana between 2010 and 2013, in which we analysed the impact of the molecular biomarkers and histological parameters on survival and response to the first- line systemic therapy of metastatic colorectal cancer patients.[8] Median OS of wild type wt*BRAF* patients was significantly longer than in mutated mt*BRAF* patients, with 59.2 and 27.6 months, respectively, $p = 0.05$.

Today, targeted therapy combining BRAF inhibitors and MEK inhibitors in combination with anti-EGFR inhibitors with mOS of 24 months is approved by FDA, but not by EMA in Europe for the BRAF mutated patients.[2,9] However, metastatic CRC is not a simple disease but rather a heterogeneous one, with different treatment responses and outcomes. Thus, these routinely identified biomarkers provide only some information about tumour biology.

In 2015 Guinney *et al.* in the CRC Subtyping Consortium established four consensus molecular subtypes 1 (CMS1), 2 (CMS2), 3 (CMS3) and 4 (CMS4), based on six independent CRC classification systems.[7] They analysed tumour characteristics of more than 4000 patients, including not only

TABLE 1. Classification of consensus molecular subtypes (CMS). Adopted by Guiney *et al.*[7]

CMS subtype	CMS1 - MSI immune	CMS2 - Canonical	CMS3 – Metabolic	CMS4 - Mesenchymal
Frequency	14%	37%	13%	23%
Characteristics	MSI, CIMP high, hypermutation	SCNA high	Mixed MSI status, SCNA low, CIMP low	SCNA high
	BRAF mutation		KRAS mutation	
	Immune infiltration and activation	WNT and MYC activation	Metabolic deregulation	Stromal infiltration, TGF-β activation, angiogenesis
	Worse survival after relapse			Worse relapse-free and overall survival

CIMP = CpG island methylator phenotype; MSI = microsatellite instable; SCNA = somatic copy number alterations; TGF-β = transforming growth factor beta

their genetic alterations, but also their immune system, cellular metabolism, epithelium, signalling activation, immune tumour infiltration, tumour microenvironment and angiogenesis. The CMS are characterized and named by their main distinguishing features. CMS1 is denoted as MSI immune, presented in 14% of the cases, hypermutated, microsatellite unstable and with strong immune cell infiltration and activation. CMS2 is canonical, presented in 37% of the cases, with marked WNT and MYC signalling activation. CMS3 is called metabolic, presented in 13% of the cases, with epithelial and evident metabolic dysregulation, with *KRAS* mutations and mixed MSI status, low somatic copy number alterations (SCNA) and CpG island methylator phenotype (CIMP). CMS4 is called mesenchymal, presented in 23% of the cases, with prominent transforming growth factor β activation, stromal infiltration and angiogenesis. The main features of CMS subtypes are presented in Table 1.

The CMS subtypes are not classified only by molecular features, but also by clinical features, with prognosis included in its classification.[10-13] Sidedness of the primary tumour is also included. Right-sided tumours, including cecum, ascending colon or transverse colon are characterized by mucinous, signet ring histology, microsatellite instability, hypermethylation, poor differentiation, higher mutation rates of PI3KCA, KRAS and BRAF. They are more frequent in older patients and female patients. Left-sided tumours, including descending colon, sigmoid colon and rectum are characterized by chromosomal aberrations, 18q loss and 20q gain, aneuploidy, p53 mutation, EGFR and HER2 gain, high VEGF-1 mRNA, cyclooxygenase 2 (COX2), high EGFR ligand epiregulin and amphiregulin expression.[10-13]

However, tumour location inside the intestine is even more important than sidedness.[12,14] Namely, CMS1 is more often present in the proximal colon (the cecum, the ascending colon, the transverse colon), CMS2 in the distal colon (the descending colon, the sigmoid colon) and the rectum, CMS3 in the sigmoid colon and the rectum and CMS4 in the distal colon (the descending colon, the sigmoid colon) and the rectum. Tumours of distal colon and rectum appear unique and tumours of the transverse colon appears distinct from other tumours of the right colon.[14] Because of this tumour heterogeneity of different parts of colon and the differences between tumours of colon and rectum, and also intra- tumour heterogeneity of the primary tumour, Fontana *et al*. highlighted the importance of the careful sampling from biopsies or resected primary tumour for each patient to get the right information about his biomarkers.[12]

Since secondary acquired resistance can develop during specific systemic therapy with anti EGFR inhibitors, because of tumour heterogeneity and clonal selection process, it is important to include circulating tumour DNA analyses in evaluation of effectiveness of systemic therapy. This technique can detect genomic alterations in *RAS* and other genes to help adjust systemic therapy before clinical and radiological progression.[11,15-17]

Two recently published papers explain the impact of CMS subtypes on the survival of metastatic CRC patients and the differences to the response to systemic treatment according to CMS subtypes.[18,19] Patients from two phase III clinical trials, the CALBG/SWOG 80405 and the FIRE-3, were included in this analysis. Both clinical trials assessed the combination of anti-VEGFR inhibitor bevacizumab or anti- EGFR inhibitor cetuksimab with different types of chemotherapy - oxaliplatin with 5-FU (FOLFOX) in 75% of the patients in CALGB/SWOG 80405 and irinotecan with 5-FU (FOLFIRI) in all patients in the FIRE- 3.[18-20] Both studies showed that left-sided colorectal cancer responded better to cetuximab-based in combination with irinotecan therapy in case of CMS2 and CMS4 compared to bevacizumab-based therapy, whereas for right-sided tumours this possibility has to be further explored.

Lenz *et al*. have retrospectively analysed the impact of the CMSs on survival of *KRAS* wild type metastatic CRC patients from CALGB/SWOG 80405 clinical study.[18] For the CMS classification, the NanoString panel for the CALBG/SWOG 80405 cohort and the official CMS classifier software were used. Based on the CALGB study results, CMSs are predictive biomarkers for bevacizumab and cetuximab in terms of OS and progression-free survival (PFS). In the CMS2 cohort, patients who received cetuximab had significantly longer OS and slightly improved PFS compared to those who received bevacizumab, although this was not statistically significant. In the CMS1 cohort, patients who received bevacizumab had significantly longer OS and longer PFS compared to the patients who received cetuximab. They concluded that CMS classification is an independent prognostic marker for metastatic CRC patients in the first-line systemic therapy with a combination of chemotherapy with bevacizumab or cetuximab. Patients with CMS1 had the shortest OS and PFS, whereas patients with CMS2 had the longest OS with the lowest risk of death and PFS. They also emphasized the limitations of their analysis to the KRAS wild-type metastatic patients and stated that it was not possible to do a more detailed exploration of the interactions between a specific chemotherapy and targeted therapy. However, in 2019, Aderka *et al*. published a research, studying this topic.[19] The responses of the patients with different CMS subtypes to systemic chemotherapy with oxaliplatin or irinotecan in combination with different targeted therapy, anti- VEGFR inhibitor bevacizumab or anti- EGFR inhibitor cetuximab were analysed. They found that both cytostatics have synergistic effect in combination with cetuximab. Irinotecan upregulates EGFR and promotes the binding of cetuximab and so promotes its antibody-dependent cell-mediated cytotoxicity (ADCC), stimulates the release of IFN-γ and activates dendritic cells, macrophages, T cells and encourages the apoptosis of cancer cells. Furthermore, cetuximab inhibits the tumour's multidrug resistance mechanism for the active metabolite of irinotecan - SN-38 - which accumulates in the cells and thus improves its antitumour effect. The oxaliplatin acts in two ways, as oxaliplatin – DNA adducts and causes DNA oxidative damage. EGRF activation upregulates nucleotide excision repair proteins and base excision repair proteins (*ERCC1)* and in this way neutralises effects of oxaliplatin. The combination of oxaliplatin and anti- EGFR inhibitor cetuximab has a synergistic effect in terms of cetuximab downregulation of *ERCC1* and, which could further improve oxaliplatin activity.[19]

The tumour microenvironment is also an important factor in resistance of CRCs to specific combination of chemotherapy and targeted therapy. The CMS1 and CMS4 tumours have a fibroblast-rich microenvironment.[19] In that case of CMS1 and CMS4 oxaliplatin has an antagonistic action to anti-EGFR inhibitors cetuximab and panitumumab, inducing the release of interleukin 17A from fibroblasts promoting proliferation of cancer stem cells and antagonising the growth suppression and apoptosis of cancer stem cells induced by cetuximab. Activated cancer-associated fibroblasts also secrete transforming growth factor beta (TGF-β) and mediate tumour resistance to anti-EGFR inhibitors by providing an intrinsic EGFR-independent survival pathway to cancer cells. TGF-β also prolongs inhibitory effect on the cetuximab-mediated antibody-dependent cellular cytotoxicity (ADCC), inhibits activation of immune cells, natural killer cells, dendritic cells and macrophages.[19]

In both articles, of Aderka and Lenz, the authors also explained why such differences occur.[18,19] The first significant factor is the previously described synergistic or antagonistic action of the combination of chemotherapy and the biological drug. The second important factor is the sequence of biologicals, bevacizumab and cetuximab, in terms of CMS, which is supported by both studies. If anti VEGFR inhibitor bevacizumab is administrated in first-line systemic treatment, before cetuximab, it reduces the permeability of blood vessels and consequently diffusion and tumour cell binding of cetuximab. The third factor is the half-life of bevacizumab compared to cetuximab, which is also important concerning the sequence of. With a half-life of 21 days, bevacizumab is still active for a period when initiating a second line of cetuximab treatment, reducing the permeability to tumour stroma and the anti-EGFR effect after the first line of bevacizumab. Lastly, in the FIRE-3 study, chemotherapy with only irinotecan hydrochloride (CPT 11) with 5-fluorouracil (5-FU) was used in combination with bevacizumab or cetuksimab; and oxaliplatin with 5-FU was used in 75% in combination with bevacizumab or cetuximab in CALGB study. Thus, researchers concluded that both studies are complementary and not opposing in terms to relevant conclusions from retrospective analyses.[19]

Based on all clinical and molecular knowledge, the mOS for 16 different combinations of oxaliplatin, irinotecan and targeted therapy in first-line treatment was calculated for each CMS subtype. The most effective first- line combination is oxaliplatin with bevacizumab, irinotecan or oxaliplatin with cetuximab, oxaliplatin with cetuximab and irinotecan with cetuximab, in CMS1, CMS2, CMS3 and CMS4 respectively.[19]

Additionally, Stintzing *et al*. conducted an analysis according to CMS classification in terms of objective responses (OR) and PFS from the FIRE-3 clinical trial, in which the first-line therapy was FOLFIRI (irinotecan plus 5-FU) with bevacizumab or cetuximab in *KRAS* wild-type metastatic CRC patients.[20] The retrospective analysis was carried out for *RAS* wild-type metastatic CRC patients. They confirmed the prognostic role of CMS classification in CMS3 and CMS4 subtypes and the predictive role for a better outcome in CMS4 subtype in *RAS* wild-type patients, treated with FOLFIRI and cetuximab. Significantly higher overall response rate (ORR) were seen in CMS2 subtype in the same regimen. OS of patients with CRC subtype CMS4 was significantly longer in treatment with FOLFIRI cetuximab compared to that with FOLFIRI bevacizumab. In patients with CMS3, OS was in favour of FOLFIRI and cetuximab, OS in CMS1 and CMS2 were comparable and independent of targeted therapy.

Lastly, gut microbiome is probably another important biomarker to consider in future studies in treating metastatic CRC patients.[10,21] Gut microbiomes are associated with CMS1 and CMS2 subtypes. It is known that gut microbiome has an important role in carcinogenesis of CRC, showing initial inflammation and modulation of different signalling pathways. Each part of the colon and rectum is characterized by different strains of bacteria. The most important and studied strains were *Fusobcterium nucleatum*, *Escherichia coli* and *Bacteroides fragilis*. Gut microbiome also varies geographically, seven strains are the most important for carcinogenesis, *B. fragilis*, four oral as *F. nucleatum, Parvimonas micra, Porphyromonas asaccharolytica* and *Prevotella intermedia*, *Alistipes finegoldii* and *Thermanaerovibrio acidaminovorans*.[21] Bacterial biomarkers have potential to detect CRC, predict clinical outcome and have a prognostic value.[21] Gut microbiome also mediates the response to chemotherapy, especially of irinotecan, oxaliplatin and 5-flurouracil, prescribed in treatment of metastatic CRC. There are several ways like immunomodulation, metabolism regulation, resistance to chemotherapy, microbial translocation, reduced ecological diversity and others. It also plays an important role in effectiveness of immunotherapy with checkpoint inhibitors in terms of to enhance the action of it. It can be also associated with the adverse effects of immunotherapy, especially with immune-related colitis, depending of the presented strains of bacteria in the gut.[21] Therefore; the knowledge about gut microbiome will have clinical implications for CRC prevention, improvement of treatment responses and reduction of the adverse effects.

Conclusions and future directions

Predictive and prognostic biomarkers are important for personalized medicine and treatment of patients with metastatic CRC and therefore enable better optimization and tailoring of treatment. Pharmacogenomics biomarkers will allow us to adjust and determine the optimum effective dose of the drug for each patient. Gut microbiome is another important biomarker predicting the prognosis of disease and the response to the specific systemic therapy.

CMS subtypes, including molecular heterogeneity at different levels of genetics, epigenetics, transcriptomic, clinical features and more important tumour microenvironment will enable us to estimate the prognosis and make precision medicine individualized for each patient.

In the future, it is important to develop algorithms for everyday clinical practice to determine the CMS subtype for each patient individually, based on patient and tumour characteristics. This will result in the most optimal, patient-tailored treatment to maximize the response, prolong survival, minimize the treatment cost and avoid potential unwanted adverse effects of ineffective therapy.

Acknowledgement

The research was financially supported by The Slovenian Research Agency (ARRS), grant number P3-0321.

References

1. *Cancer in Slovenia 2016*. Ljubljana: Institute of Oncology Ljubljana, Epidemiology and Cancer Registry, Cancer Registry of Republic of Slovenia; 2019.

2. Zakotnik B, Zadnik Z, Žagar T, Primic Žakelj M, Ivanuš U, Jerman T, et al. Reaching sustainable oncology care via the National Cancer Control Program (NCCP). *Ann Oncol* 2019; **30(Suppl 5):** v671-82. doi: 10.1093/annonc/mdz263

3. National Comprehensive Cancer Network. *NCCN clinical practice guidelines in oncology (NCCN guidelines): colon cancer.* Version 1.2020. [cited 2020 Feb 28]. Available at: https://www.nccn.org/professionals/physician_gls/pdf/colon_cancer.pdf

4. Van Cutsem E, Cervantes A, Adam R, Sobrero A, Van Krieken JH, Aderka D, et al. ESMO consensus guidelines for the management of patients with metastatic colorectal cancer. *Ann Oncol* 2016; **27:** 1386-422. doi: 10.1093/annonc/mdw235

5. Modest DP, Pant S, Sartore-Bianchi A. Treatment sequencing in metastatic colorectal cancer. *Eur J Cancer* 2019; **109:** 70-83. doi: 10.1016/j.ejca.2018.12.019

6. Patel JN, Fon MK, Jagosky M. Colorectal cancer biomarkers in the era of personalized medicine. *J Pers Med* 2019; **9**(1). doi: 10.3390/jpm9010003

7. Guinney J, Dienstmann R, Wang X, de Reyniès A, Schlicker A, Soneson C**,** et al. The consensus molecular subtypes of colorectal cancer. *Nat Med* 2015; **21:**1350-6. doi: 10.1038/nm.3967

8. Rebersek M, Mesti T, Boc M, Ocvirk J. Molecular biomarkers and histological parameters impact on survival and response to first- line systemic therapy of metastatic colorectal cancer patients. *Radiol Oncol* 2019; **53:** 85-95. doi: 10.2478/raon-2019-0013

9. Afrasanie VA, Marinca MV, Alexa-Stratulat T, Păduraru M I, Adavidoaiei AM, Miron L, et al. KRAS, NRAS, BRAF, HER2 and microsatellite instability in metastatic colorectal cancer – practical implications for the clinician. *Radiol Oncol* 2019; **53:** 265-74. doi: 10.2478/raon-2019-0033

10. Inamura K. Colorectal cancers: an update on their molecular pathology. *Cancers* 2018; **10:** pii: E26. doi: 10.3390/cancers10010026

11. Dienstmann R, Vermeulen L, Guinney J, Kopetz S, Tejpar S, Tabernero J. Consensus molecular subtypes and the evolution of precision medicine in colorectal cancer. *Nat Rev Cancer* 2017; **17:** 79-92. doi: 10.1038/nrc.2016.126

12. Fontana E, Eason K, Cervantes A, Salazar, R, Sadanandam A. Context matters - consensus molecular subtypes of colorectal cancer as biomarkers for clinical trials. *Ann Oncol* 2019; **30:** 520-7. doi: 10.1093/annonc/mdz052

13. Thanki K, Nicholls ME, GajjarA, Senagore AJ, Qiu S, Szabo C, et al. Consensus molecular subtypes of colorectal cancer and their clinical implications. *Int Biol Biomed J* 2017; **3:** 105-11. PMID: 28825047

14. Loree JM, Pereira AAL, Lam M, Willauer AN, Raghav K, Dasari A, et al. Classifying colorectal cancer by tumor location rather than sidedness highlights a continuum in mutation profiles and consensus molecular subtypes. *Clin Cancer Res* 2018; **24:** 1062-72. doi: 10.1158/1078-0432.CCR-17-2484

15. Dienstmann R, Salazar R, Tabernero J. Molecular subtypes and the evolution on of treatment decisions in metastatic colorectal cancer. *Am Soc Clin Oncol Educ Book*. 2018; **38:** 231-8. doi: 10.1200/EDBK_200929

16. Kato S, Schwaederle MC, Fanta PT, Okamura R, Leichman L, Lippman SC, et al. Genomic assessment of blood- derived circulating tumor DNA in patients with colorectal cancers: Correlation with tissue sequencing, therapeutic response, and survival. *JCO Precis Oncol* 2019; **3:** 1-25. doi: 10.1200/PO.18.00158

17. Siena S, Sartore-Bianchi A, Garcia-Carbonero R, Karthaus M, Smith D, Tabernero J, et al. Dynamic molecular analysis and clinical correlates of tumor evolution within a phase II trial of panitumumab-based therapy in metastatic colorectal cancer. *Ann Oncol* 2018; **29:** 119-26. doi: 10.1093/annonc/mdx504

18. Lenz, HJ, Ou FS, Venook, AP, Hochster HS, Niedzwiecki D, Richard M, et al. Impact of consensus molecular subtype on survival in patients with metastatic colorectal cancer: Results from CALGB/SWOG 80405 (Alliance). *J Clin Oncol* 2019; **37:** 1876-85. doi: 10.1200/JCO.18. 02258

19. Aderka D, Stintzing S, Heinemann V. Explaining the unexplainable: discrepancies in results from the CALGB/SWOG 80405 and FIRE-3 studies. *Lancet Oncol* 2019; **20:** e274-83. doi: 10.1016/S1470-2045(19)30172-X

20. Stintzing S, Wirapati P, Lenz HJ, Neureiter D, Fischer von Weikersthal L, Decker T, et al. Consensus molecular subgroups (CMS) of colorectal cancer (CRC) and 1st-line efficacy of FOLFIRI plus cetuximab or bevacizumab in the FIRE3 (AIO KRK-0306) trial. *Ann Oncol* 2019; **30:** 1796-803. doi: 10.1093/annonc/mdz387

21. Wong SH, Yu J. Gut microbiota in colorectal cancer: mechanisms of action and clinical applications. *Nat Rev Gastroenterol Hepato*l 2019; **16:** 690-704. doi: 10.1038/s41575-019-0209-8

research article

Prognostic role of positron emission tomography and computed tomography parameters in stage I lung adenocarcinoma

Angelo Carretta[1,5], Alessandro Bandiera[1], Piergiorgio Muriana[1], Stefano Viscardi[1], Paola Ciriaco[1], Ana Maria Samanes Gajate[2], Gianluigi Arrigoni[3], Chiara Lazzari[4], Vanesa Gregorc[4], Giampiero Negri[1,5]

[1] Department of Thoracic Surgery, San Raffaele Hospital, Milan, Italy
[2] Department of Nuclear Medicine, San Raffaele Hospital, Milan, Italy
[3] Department of Pathology, San Raffaele Hospital, Milan, Italy
[4] Department of Oncology, San Raffaele Hospital, Milan, Italy
[5] School of Medicine, Vita Salute San Raffaele University, Milan, Italy

Radiol Oncol 2020; 54(3): 278-284.

Received 4 February 2020
Accepted 4 May 2020

Correspondence to: Angelo Carretta, M.D., Department of Thoracic Surgery, San Raffaele Hospital, School of Medicine, Vita Salute San Raffaele University, Via Olgettina, 60 – 20132, Milan, Italy. E-mail angelo.carretta@hsr.it

Disclosure: No potential conflicts of interest were disclosed.

Background. According to the current pathological classification, lung adenocarcinoma includes histological subtypes with significantly different prognoses, which may require specific surgical approaches. The aim of the study was to assess the role of CT and PET parameters in stratifying patients with stage I adenocarcinoma according to prognosis.

Patients and methods. Fifty-eight patients with pathological stage I lung adenocarcinoma who underwent surgical treatment were retrospectively reviewed. Adenocarcinoma *in situ* and minimally-invasive adenocarcinoma were grouped as non-invasive adenocarcinoma. Other histotypes were referred as invasive adenocarcinoma. CT scan assessed parameters were: ground glass opacity (GGO) ratio, tumour disappearance rate (TDR) and consolidation diameter. The prognostic role of the following PET parameters was also assessed: standardized uptake value (SUV) max, SUVindex (SUVmax to liver SUVratio), metabolic tumour volume (MTV), total lesion glycolysis (TLG).

Results. Seven patients had a non-invasive adenocarcinoma and 51 an invasive adenocarcinoma. Five-year disease-free survival (DFS) and cancer-specific survival (CSS) for non-invasive and invasive adenocarcinoma were 100% and 100%, 70% and 91%, respectively. Univariate analysis showed a significant difference in SUVmax, SUVindex, GGO ratio and TDR ratio values between non-invasive and invasive adenocarcinoma groups. Optimal SUVmax, SUVindex, GGO ratio and TDR cut-off ratios to predict invasive tumours were 2.6, 0.9, 40% and 56%, respectively. TLG, SUVmax, SUVindex significantly correlated with cancer specific survival.

Conclusions. CT and PET scan parameters may differentiate between non-invasive and invasive stage I adenocarcinomas. If these data are confirmed in larger series, surgical strategy may be selected on the basis of preoperative imaging.

Key words: adenocarcinoma; lung; surgery; computed tomography; PET

Introduction

The current IASLC/ATS/ERS pathological classification of lung adenocarcinoma includes histological subtypes with different tumour invasiveness and prognosis. In this classification the former term bronchoalveolar carcinoma (BAC) is no longer included and a distinction between adenocarci-

 doi: 10.2478/raon-2020-0034

noma *in situ*, minimally invasive adenocarcinoma and invasive adenocarcinoma with its variants has been established.[1] Patients with adenocarcinoma *in situ* and minimally invasive adenocarcinoma have extremely high survival rates after surgery. Invasive stage I adenocarcinoma is on the other side associated with a relatively high risk of recurrence. Different surgical approaches have therefore been proposed according to the histological features of the tumour, with sublobar resection as a possible treatment option for adenocarcinoma *in situ* and minimally-invasive adenocarcinoma.[2,3] Conversely, major resection is still considered the treatment of choice of early-stage invasive adenocarcinomas.[4] Hence, the identification of pre-operative parameters that allow differentiating neoplastic lesions according to tumour invasiveness is crucial for the planning of surgical treatment. This point is even more important considering the relatively low accuracy in the definition of tumour invasion of the histological analysis obtained after needle biopsy or with intraoperative frozen section.[5,6]

At Computed Tomography (CT), tumours with lepidic growth pattern appear as ground-glass opacities (GGO), which may represent a variable part of the neoplastic lesion, while on the other hand the solid part of the tumour is mainly an expression of invasive adenocarcinoma.[7,8] CT scan derived parameters as GGO ratio, tumour disappearance rate (TDR) and consolidation diameter are an expression of the proportion of ground-glass and solid features of the tumour, and may correlate with histology and clinical behaviour. Previous reports have analysed the correlation of radiologic parameters with tumour invasiveness, but the prognostic role of these factors still has to be completely clarified.[9] Positron emission tomography (PET) derived parameters have also been progressively used in the differential diagnosis and as prognostic factors in patients with adenocarcinoma, the most used of which being the maximum standardized uptake value (SUVmax) of the tumour.[10,11] Moreover, a prognostic role of other PET derived parameters as SUVindex, metabolic tumour value (MTV) and total lesion glycolysis (TLG) was also demonstrated, and some studies showed a better predictive performance of these parameters in comparison with SUVmax.[12,13]

The aim of the current study was to assess the role of CT and PET parameters in the differentiation of non-invasive and invasive adenocarcinomas and in stratifying patients with stage I adenocarcinoma according to their prognosis.

Patients and methods

Patients with pathological stage I lung adenocarcinoma who underwent surgical treatment at our Institution following CT and PET scan evaluation between August 2006 and July 2011 were reviewed. The study was approved by the local Ethics Committee and registered on Clinicaltrials.gov (NCT04202614).

Histological specimens were classified according to the current IASLC/ATS/ERS pathological classification of lung adenocarcinoma.[1] Adenocarcinoma *in situ* and minimally invasive adenocarcinoma were grouped as non-invasive adenocarcinoma. Other histotypes were referred as invasive adenocarcinoma. Tumours were re-staged according to the current 8th edition of the TNM staging system.[14]

Pre-operative imaging work-up included CT scan and whole body PET scan. Nodal involvement in patients with clinical N2/N3 disease was preoperatively excluded by invasive mediastinal assessment (EBUS-TBNA or mediastinoscopy). Major resections were considered the treatment of choice in patients with invasive adenocarcinoma. Wedge resections were performed in the treatment of adenocarcinoma *in situ* and minimally-invasive tumours, and in patients with invasive adenocarcinoma with a functional contraindication to major resection.

The features analysed for all patients were: age, sex, smoking habit, type of surgical resection, tumour histology, stage of disease, morbidity, mortality, overall survival, cancer specific survival and disease free survival, PET-derived and CT scan parameters.

CT scan parameters

CT images were obtained using a commercially available scanner (Toshiba X-press, Toshiba Medical Systems, Tokio, Japan). After infusion of intravenous contrast material spiral acquisition was obtained during breath-hold at the end of inspiration. The chest region was scanned with a detector configuration of 120 kVp, 200 mAs, 1 mm section thickness. The images were assessed using the mediastinal window setting (level, 40 Hounsfield units [HU]; width, 350 HU) and the lung window setting (level, 600 HU; width, 1500 HU).

CT scan assessed parameters were: ground glass opacity (GGO) ratio, tumour disappearance rate (TDR) and consolidation diameter. GGO ratio was defined as the percentage of the tumour with GGO

TABLE 1. Characteristics of 58 surgically-treated patients with stage I adenocarcinoma

	Non-invasive adenocarcinoma (7 patients)	Invasive adenocarcinoma (51 patients)	P
Gender			
Female	4	38	0.178
Male	3	13	
Age (median;range)	67 (46-75)	65 (48-85)	0.530
Type of surgery			
Wedge resection	3	10	0.188
Lobectomy	4	40	
Bilobectomy	0	1	
TNM			
Tis	1	0	0.056
T1aN0	3	9	
T1bN0	1	17	
T1cN0	2	16	
T2aN0	0	9	

appearance (1-[maximum dimension of consolidation on lung windows/maximum dimension of tumour on lung windows]) x 100, TDR% was defined as the ratio between the area of consolidation on mediastinal windows and the area of consolidation on lung window (1-[maximum area of consolidation on mediastinal windows/maximum area of tumour on lung windows]) x 100, consolidation diameter was defined as the maximum diameter of consolidation on lung window.

PET scan parameters

The prognostic role of the following PET-derived parameters was also assessed: standardized uptake value (SUV)max, SUVindex (SUVmax to liver SUVratio), MTV, TLG. PET-derived parameters (SUVmax, SUVindex, MTV and TLG) were calculated with a dedicated software (GE Advantage workstation - GEMS) developed for biomedical images. A volume of interest (VOI) was created for each lesion around the area of FDG uptake enclosing the tumour and SUVmax was obtained. SUVmean and MTV were measured using an automatic isocontour threshold method based on 50% of tumour SUVmax. SUVindex for each neoplastic lesion was calculated according to the method defined by Shiono *et al.*[12] A 6-cm circular region of interest (ROI) was drawn on three consecutive PET slices on the liver parenchyma. Liver SUVmean was defined as the mean of the SUVmax values of the three PET slices. SUVindex was calculated as the ratio of tumour SUVmax to liver SUVmean. TLG was calculated by multiplying MTV by tumour SUVmean.

Statistical analysis

Analysis was performed by SPSS Statistics software, version 18.0 (SPSS Inc., Chicago, IL, USA). Differences between classes of patients were tested for significance with the X^2 or Fisher's exact test for discrete variables and with the Student's t test for continuous variables. Receiver-operating characteristic (ROC) curves for PET and CT derived parameters were generated to define the cut-off values to differentiate non-invasive and invasive tumours and dichotomize patients on the basis of cancer-specific survival. Survival curves were reconstructed according to the Kaplan and Meier method. Differences in survival rates of patients grouped according to selected variables were estimated by means of the log-rank test. The Cox regression analysis was performed to assess the independent value of the significant variables at univariate analysis. Results were considered significant when p-values less than 0.05 were observed. Confidence intervals were calculated at the 95% level.

Results

Fifty-eight patients (41 males, 17 females, mean age 66, range 46 to 85 years) with pathological stage I lung adenocarcinoma entered the study. The characteristics of the patients are depicted in Table 1. Forty-four patients underwent a lobectomy, one patient a bilobectomy and 13 a wedge resection. Seven patients had a non-invasive and 51 an invasive adenocarcinoma. The pathological staging was as follows: Tis in one patient, T1aN0 in 12 cases, T1bN0 in 18 cases, T1cN0 in 18 cases and T2aN0 in 9 cases. The follow-up was complete for all 58 patients. The median follow-up was 60 months (range 3–126). At the end of follow-up thirty-nine patients are alive without evidence of cancer recurrence, 10 patients are alive with evidence of relapse, 4 patients died of cancer recurrence and 5 patients died due to other causes.

Five-year disease-free survival (DFS) and cancer-specific survival (CSS) was 100% and 100% for non-invasive and 70% and 91% for invasive adenocarcinoma, respectively (Figures 1 and 2) (p = 0.115, p = 0.46). Significant differences in GGO ratio, TDR ratio, SUVmax and SUVindex values were observed between non-invasive and invasive adenocarcinoma groups. Mean GGO ratio was 42% in non-invasive and 19% in invasive adenocarcinoma (p = 0.011); mean TDR ratio was 53% in non-invasive and 24% in invasive adenocarcinoma (p = 0.001); mean SUVmax was 2.75 in non-invasive and 7.16 in invasive adenocarcinoma (p = 0.033); mean SUVindex was 0.98 in non-invasive and 3.12 in invasive adenocarcinoma (p = 0.037) (Table 2).

According to the ROC curve analysis optimal GGO ratio and TDR cut-off ratios to distinguish non-invasive from invasive adenocarcinoma were 40% (area under the curve [AUC] 82%, sensitivity 67%, specificity 81%) and 56% (AUC 85%, sensitivity 67%, specificity 96%), respectively; SUVmax and SUVindex cut-off ratios were 2.6 (AUC 81.5%, sensitivity 84%, specificity 71%) and 0.9 (AUC 84%, sensitivity 90%, specificity 71%), respectively. Patients with higher SUVmax and SUVindex values had a significantly higher incidence of less differentiated and larger tumours (Table 3). CSS significantly correlated with SUVmax, SUVindex and TLG. The statistical analysis with ROC curves identified the following best cut-off values to differentiate the patients according to prognosis: SUVmax 8.6, SUVindex 4.08, TLG 9.38. Five-year CSS was 97% in patients with a SUVmax < 8.6 and 81% in patients with a SUVmax > 8.6 (p = 0.036) (Figure 3). Five-year CSS was 97% in patients with a SUVindex < 4.08 and 76% in patients with a SUVindex > 4.08 (p = 0.01) (Figure 4). Five-year CSS was 100% in patients with a TLG < 9.38 and 82% in patients with a TLG > 9.38 (p = 0.02) (Figure 5). The type of surgical resection did not have a prognostic role (Five-year CSS 89% in patients submitted to wedge resection and 93% in patients submitted to major resection, p = 0.822). In particular, in patients submitted to wedge resection a correlation of DFS and CSS with CT and PET parameters was not observed, although patients with a TLG value

TABLE 2. Differences in CT and PET scan parameters according to histology

CT and PET scan parameter	Non-invasive adenocarcinoma	Invasive adenocarcinoma	p
GGO%	42±7.05	19±2.91	0.011
TDR%	53±9.31	24±2.89	< 0.001
Consolidation diameter	13±2.19	21±1.44	0.07
SUVmax	2.75±0.91	7.16±0.73	0.033
SUVindex	0.98±0.25	3.12±0.36	0.037
MTV	3.6±1.74	5.3±0.49	0.293
TLG	12±7.31	19.5±4.34	0.541

GGO = gound-glass opacity; MTV = metabolic tumour volume; SUV = standardized uptake value; TDR = tumour disappearance rate; TLG = total lesion glycolysis

TABLE 3. Characteristics of patient population grouped by standardized uptake value (SUV)max and SUVindex

	SUVmax			SUVindex		
	< 2.6	≥ 2.6	p	< 0.9	≥ 0.9	p
Total No. patients	12	46		10	48	
Histology						
NIA (7)	4	3		5	2	
IA (51)	8	43	0.028	5	46	0.001
Gender						
male	9	32	1.00	6	35	0.458
female	3	14		4	13	
Smoke						
Yes	10	37	1.00	7	40	0.381
No	2	9		3	8	
T						
Tis–T1a	6	7		6	7	
T1b	5	13	0.014	3	15	0.011
T1c	1	17		1	17	
T2a	0	9		0	9	
Grading						
G1	3	1		3	1	
G2	9	38	0.011	7	40	0.004
G3	0	7		0	7	

IA = invasive adenocarcinoma; NIA – Non-invasive adenocarcinoma

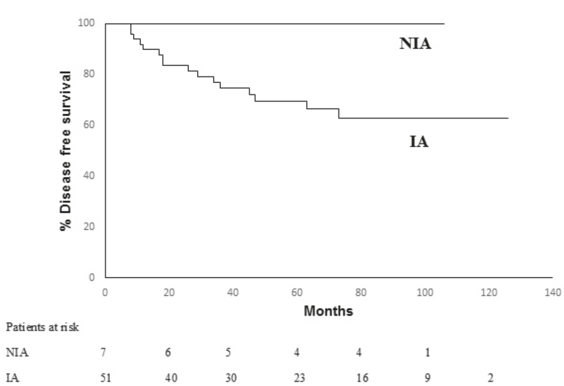

FIGURE 1. Kaplan-Meier disease free survival (DFS) plot for non-invasive and invasive adenocarcinoma (Invasive adenocarcinoma). Five-year DFS (disease free survival) was 100% for non-invasive and 70% for invasive adenocarcinoma (p = 0.115).

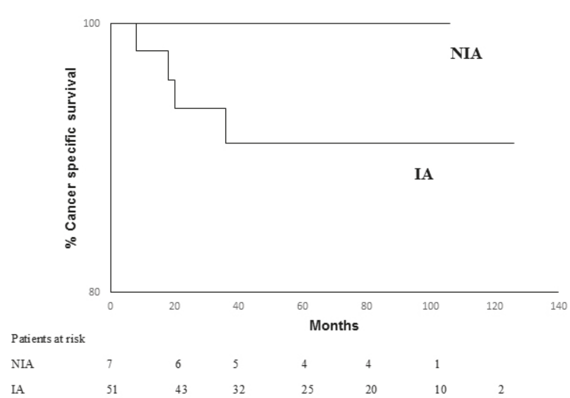

FIGURE 2. Kaplan-Meier cancer specific survival (CSS) plot for non-invasive and invasive adenocarcinoma. Five-year CSS was 100% for non-invasive and 91% for invasive adenocarcinoma (p = 0.46).

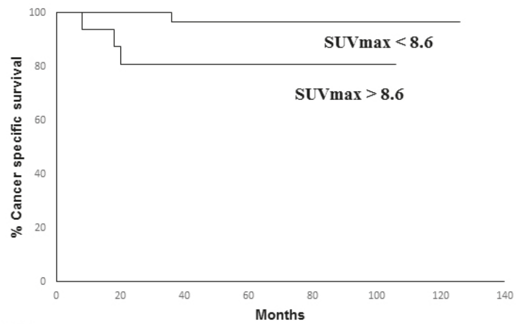

Patients at risk							
SuvMax<8.6	42	42	27	22	18	9	2
SuvMax>8.6	16	12	10	7	6	2	

FIGURE 3. Kaplan-Meier cancer specific survival curves according to SUVmax value. Five-year cancer specific survival (CSS) was 97% in patients with a SUVmax < 8.6 and 81% in patients with a SUVmax > 8.6 (p = 0.036).

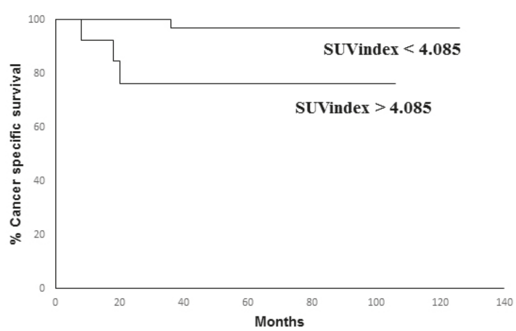

Patients at risk							
SuvIndex<4.085	44	44	30	24	19	10	2
SuvIndex>4.085	14	9	7	5	5	1	

FIGURE 4. Kaplan-Meier cancer specific survival curves (CSS) according to SUVindex value. Five-year CSS was 97% in patients with a SUVindex < 4.08 and 76% in patients with a SUVindex > 4.08 (p = 0.01).

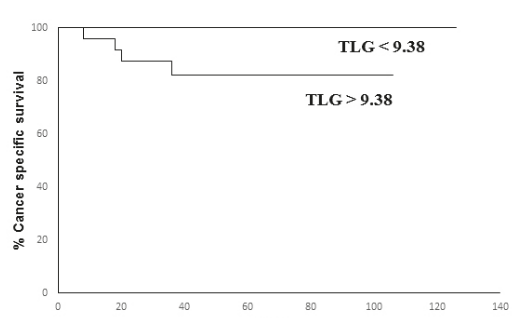

Patients at risk							
TLG<9.38	33	29	24	22	18	9	2
TLG>9.38	25	20	14	8	6	2	

FIGURE 5. Kaplan-Meier cancer specific survival curves (CSS) according to total lesion glycolysis (TLG) value. Five-year CSS was 100% in patients with a TLG < 9.38 and 82% in patients with a TLG > 9.38 (p = 0.02).

under the 9.38 cut-off value tended to have a better survival (p = 0.061). No significant correlation with outcome was identified at multivariate analysis.

Discussion

The current classification of lung adenocarcinoma identifies different histologic subtypes with a clear differentiation between non-invasive and invasive tumours, due to their significantly different prognosis.[1] Preoperative assessment of the invasiveness of stage I adenocarcinoma has become increasingly important for the definition of the ideal surgical treatment. In fact, the standard of care of stage I adenocarcinoma is at present lobectomy with mediastinal lymphadenectomy.[4,15] Conversely, non-invasive lesions may benefit of lung-sparing limited resections. Sublobar resections have in fact been reported as being oncologically equivalent to major anatomical resections in non-invasive and minimally invasive tumours.[2,3] However, tumour invasiveness is hard to be determined at preoperative or intraoperative assessment, since significant limitations exist in the definition of tumour invasiveness in histological specimens obtained by needle biopsy and with intraoperative frozen section.[5,6] Thus, the identification of CT and PET features of non-invasive and invasive tumours may be essential to differentiate invasive and non-invasive lesions, in order to select the optimal surgical treatment.

Previous studies have investigated the role of imaging techniques in distinguishing different adenocarcinoma subtypes. In particular, the proportion of GGO, which reflects the presence of a lepidic pattern, may predict adenocarcinoma invasiveness and prognosis.[7,8,9] In the present retrospective analysis a significant difference in GGO ratio, TDR, SUVmax and SUVindex was observed between non-invasive and invasive adenocarcinoma. These data confirm that CT and PET parameters reflect tumour invasiveness and may be useful for the preoperative differentiation between invasive and non-invasive lesions. Moreover, the combination of PET and CT scan parameters may increase the accuracy of such evaluation.

In our study ROC analysis identified a cut-off value of 40% for GGO ratio to differentiate between invasive and non-invasive adenocarcinoma. These findings are similar to those of a previous study performed by Takahashi *et al*., who identified a GGO ratio of > 50% to differentiate between non-invasive and invasive adenocarcinoma, data confirmed by Honda *et al*.[9,15] More recently, Huang *et al*. have on the other hand observed that a GGO ratio ≥ 75% is a favourable prognostic factor in resected lung adenocarcinoma.[16] Another CT feature analysed in our study which allowed to differentiate between non-invasive and invasive adenocarcinoma was TDR. In our series a TDR value > 56% was more frequently associated with non-invasive adenocarcinoma. In previous studies Takahashi *et al*. reported a TDR cut-off between non-invasive and invasive adenocarcinoma of 75%, while Nakayama *et al.* observed that a TDR > 50% was a favourable prognostic factor in resected pulmonary adenocarcinoma.[9,17] The results of our analysis confirm the role of these CT scan derived parameters in the definition of tumour invasiveness.

We also analysed the role of PET derived parameters in predicting invasive tumour features in resected stage I adenocarcinomas. SUV is the most widely used parameter in the diagnosis and prognostic analysis of lung cancer.[10,11,18] However, despite its usefulness in diagnosis, staging and prognostic assessment, the role of SUV in predicting tumour invasiveness in adenocarcinoma has not been completely investigated. Furthermore, the use of SUV is impaired by two major factors: it depends on biologic and technological variables that limit its reproducibility, and is not representative of the neoplastic volume.[19] Shiono *et al.* therefore proposed to correct the value of lung cancer SUV using the liver as internal control (SUVindex).[12] The present study demonstrated that SUVindex was also a predictive factor for recurrence in stage I adenocarcinoma. The cut-off values of SUVmax and SUVindex which allowed to differentiate between invasive and non-invasive adenocarcinomas were 2.6 and 0.9, respectively. In a previous study Hattori *et al.* identified a SUVmax < 1 as a cut-off value to predict adenocarcinoma *in situ*.[20]

Considering cancer specific survival, the univariate statistical analysis in our series demonstrated that SUVmax, SUVindex and TLG could be identified as prognostic factors. The best cut-off values to differentiate the patients according to prognosis were: SUVmax 8.6, SUVindex 4.08, TLG 9.38. Similar results concerning the SUVmax value were observed in a previous study by Lee *et al*., where patients with a SUVmax ≤ 9.5 had a significantly higher overall and disease-free survival.[18] Dichotomizing the patients according to the cut-off values of SUVmax, SUVindex and TLG it was therefore possible to stratify the groups of patients according to their prognosis. Patients with parameters over the cut-off value of SUVmax, SUVindex and TLG had in fact a worse CSS. These data confirm the prognostic role of these PET derived parameters. Besides considering the advantages of SUVindex in terms of reproducibility, it is also important to highlight the role of TLG, which seems to be a promising prognostic factor as it is representative of both tracer uptake and metabolic tumour burden.

Considering the results of our study and previous data of the literature, it is reasonable to try to discriminate preoperatively between non-invasive and invasive adenocarcinoma by integrating CT and PET parameters. The association of CT and PET parameters could in fact allow improving the preoperative differential diagnosis of invasive and non-invasive tumours in order to differentiate the surgical approach. Moreover, PET derived parameters as SUVmax, SUVindex and TLG may play an additional role to that of histology in the definition of the prognosis of patients with stage I adenocarcinoma.

The present study, aiming at focusing the attention on both CT and PET parameters in providing prognostic information in stage I adenocarcinoma, has some limitations, being a retrospective and single-institution study based on a relatively limited series of patients. In particular, the two groups of patients (non-invasive and invasive tumours) were relatively unbalanced, a point which could have limited the results. Even so, the advantage of a single-institution study is that the methodology to assess CT and PET parameters could be homogeneous and clinical data were uniform. Further studies with a larger cohort of patients are nevertheless required to confirm the results of our analysis.

References

1. Travis WD, Brambilla E, Nicholson AG, Yatabe Y, Austin JHM, Beasley MB, et al. The 2015 World Health Organization classification of lung tumors. Impact of genetic, clinical and radiologic advances since the 2004 classification. *J Thoracic Oncol* 2015; **10:** 1243-60. doi: 10.1097/JTO.0000000000000630
2. Tsutani Y, Miyata Y, Nakayama H, Okumura S, Adachi S, Yoshimura M, et al. Appropriate sublobar resection choice for ground glass opacity-dominant clinical stage Ia lung adenocarcinoma. *Chest* 2014; **145:** 66-71. doi: 10.1378/chest.13-1094
3. Moon Y, Lee KY, Moon SW, Park JK. Sublobar resection margin width does not affect recurrence of clinical N0 non-small cell lung cancer presenting as GGO-predominant nodule of 3 cm or less. *World J Surg* 2017; **41:** 472-9. doi: 10.1007/s00268-016-3743-3
4. Khullar OV, Liu Y, Gillespie T, Higgins KA, Ramalingam S, Lipscomb J, et al. Survival after sublobar resection versus lobectomy for clinical stage IA lung cancer: an analysis from the National Cancer Data Base. *J Thorac Oncol* 2015; **10:** 1625-33. doi: 10.1097/JTO.0000000000000664
5. He P, Yao G, Guan Y, Lin Y, He J. Diagnosis of lung adenocarcinoma in situ and minimally invasive adenocarcinoma from intraoperative frozen sections: an analysis of 136 cases. *J Clin Pathol* 2016; **69:** 1076-80. doi: 10.1136/jclinpath-2016-203619

6. Walt AE, Marchevsky AM. Root cause analysis of problems in the frozen section diagnosis of in situ, minimally invasive, and invasive adenocarcinoma of the lung. *Arch Pathol Lab Med* 2012; **136:** 1515-21. doi: 10.5858/arpa.2012-0042-OA

7. Lee HY, Lee KS. Ground-glass opacity nodules: histopathology, imaging evaluation, and clinical implications. *J Thorac Imaging* 2011; **26:** 106-18. doi: 10.1097/RTI.0b013e3181fbaa64

8. Liu Y, Sun H, Zhou F, Su C, Gao G, Ren S, et al. Imaging features of TSCT predict the classification of pulmonary preinvasive lesion, minimally and invasive adenocarcinoma presented as ground glass nodules. *Lung Cancer* 2017; **108:** 192-7. doi: 10.1016/j.lungcan.2017.03.011

9. Takahashi M, Shigematsu Y, Ohta M, Tokumasu H, Matsukura T, Hirai T. Tumor invasiveness as defined by the newly proposed IASCL/ATS/ERS classification has prognostic significance for pathologic stage Ia lung adenocarcinoma and can be predicted by radiologic parameters. *J Thorac Cardiovasc Surg* 2014; **147:** 54-9. doi: 10.1016/j.jtcvs.2013.08.058

10. Zhou J, Li Y, Zhang Y, Liu G, Tan H, Hu Y, et al. Solitary ground-glass opacity nodules of stage Ia pulmonary adenocarcinoma: combination of 18F-FDG PET/CT and high resolution computed tomography features to predict invasive adenocarcinoma. *Oncotarget* 2017; **8:** 23312-21. doi: 10.18632/oncotarget.15577

11. Uehara H, Tsutani Y, Okumura S, Nakayama H, Adachi S, Yoshimura M. Prognostic role of positron emission tomography and high-resolution computed tomography in clinical stage Ia lung adenocarcinoma. *Ann Thorac Surg* 2013; **96:** 1958-65. doi: 10.1016/j.athoracsur.2013.06.086

12. Shiono S, Abiko M, Okazaki T, Chiba M, Yabuki H, Sato T. Positron emission tomography for predicting recurrence in stage I lung adenocarcinoma: standardized uptake value corrected by mean liver standardized uptake value. *Eur J CardioThorac Surg* 2011; **40:** 1165-9. doi: 10.1016/j.ejcts.2011.02.041

13. Melloni G, Gajate AMS, Sestini S, Gallivanone F, Bandiera A, Landoni C, et al. New positron emission tomography derived parameters as predictive factor for recurrence in resected stage I non-small cell lung cancer. *Eur J Surg Oncol* 2013; **39:** 1254-61. doi: 10.1016/j.ejso.2013.07.092

14. Brierley JD, Gospodarowicz MK, Wittekind C. *UICC TNM classification of malignant Tumours*. 8th Edition. Oxford: Wiley-Blackwell; 2017. p. 105-12.

15. Honda T, Kondo T, Murakami S, Saito H, Oshita F, Ito H, et al. Radiographic and pathological analysis of small lung adenocarcinoma using the new IASLC classification. *Clin Radiol* 2013; **68:** e21-6 doi: 10.1016/j.crad.2012.09.002

16. Huang TW, Lin KH, Huang HK, Chen YI, Ko KH, Chang CK, et al. The role of the ground-glass opacity ratio in resected lung adenocarcinoma. *Eur J Cardiothorac Surg* 2018; **54:** 229-34. doi: 10.1093/ejcts/ezy040

17. Nakayama H, Yamada K, Saito H, Oshita F, Ito H, Kameda Y, et al. Sublobar resection for patients with peripheral small adenocarcinomas of the lung: surgical outcome is associated with features on computed tomographic imaging. *Ann Thorac Surg* 2007; **84:** 1675-79. doi: 10.1016/j.athoracsur.2007.03.015

18. Lee HY, Lee SW, Lee KS, Jeong JY, Choi JY, Kwon OJ, et al. Role of CT and PET Imaging in predicting tumor recurrence and survival in patients with lung adenocarcinoma: a comparison with the International Association for the Study of Lung Cancer/American Thoracic Society/European Respiratory Society classification of lung adenocarcinoma. *J Thorac Oncol* 2015; **10:** 1785-94 doi: 10.1097/JTO.0000000000000689

19. Nair VS, Krupitskaya Y, Gould MK. Positron emission tomography 18F-Fluorodeoxyglucose uptake and prognosis in patients with surgically treated, stage I non-small cell lung cancer: a systematic review. *J Thorac Oncol* 2009; **4:** 1473-9. doi: 10.1097/JTO.0b013e3181bccbc6

20. Hattori A, Suzuki K, Matsunaga T, Fukui M, Tsushima Y, Takamochi K, et al. Tumor standardized uptake value on positron emission tomography is a novel predictor of adenocarcinoma in situ for c-Stage IA lung cancer patients with a part-solid nodule on thin-section computed tomography scan. *Interact Cardiovasc Thorac Surg* 2014; **18:** 329-34. doi: 10.1093/icvts/ivt500

research article

[^{18}F]FDG PET immunotherapy radiomics signature (iRADIOMICS) predicts response of non-small-cell lung cancer patients treated with pembrolizumab

Damijan Valentinuzzi[1,2], Martina Vrankar[3,4], Nina Boc[3], Valentina Ahac[3], Ziga Zupancic[3], Mojca Unk[3], Katja Skalic[3], Ivana Zagar[3], Andrej Studen[1,2], Urban Simoncic[1,2], Jens Eickhoff[5], Robert Jeraj[1,2,6]

[1] Jožef Stefan Institute, Ljubljana, Slovenia
[2] Faculty of Mathematics and Physics, University of Ljubljana, Ljubljana, Slovenia
[3] Institute of Oncology Ljubljana, Ljubljana, Slovenia
[4] Faculty of Medicine, University of Ljubljana, Ljubljana, Slovenia
[5] Department of Biostatistics and Medical Informatics, University of Wisconsin, Madison, WI, USA
[6] Department of Medical Physics, University of Wisconsin, Madison, WI, USA

Radiol Oncol 2020; 54(3): 285-294.

Received 30 April 2020
Accepted 5 June 2020

Correspondence to: Prof. Robert Jeraj, Ph.D., Department of Medical Physics, University of Wisconsin, 1111 Highland Avenue, Madison, WI 53705, USA. Phone: +1 608 263 8619; E-mail: rjeraj@wisc.edu

Disclosure: No potential conflicts of interest were disclosed.

Background. Immune checkpoint inhibitors have changed the paradigm of cancer treatment; however, non-invasive biomarkers of response are still needed to identify candidates for non-responders. We aimed to investigate whether immunotherapy [^{18}F]FDG PET radiomics signature (iRADIOMICS) predicts response of metastatic non-small-cell lung cancer (NSCLC) patients to pembrolizumab better than the current clinical standards.

Patients and methods. Thirty patients receiving pembrolizumab were scanned with [^{18}F]FDG PET/CT at baseline, month 1 and 4. Associations of six robust primary tumour radiomics features with overall survival were analysed with Mann-Whitney U-test (MWU), Cox proportional hazards regression analysis, and ROC curve analysis. iRADIOMICS was constructed using univariate and multivariate logistic models of the most promising feature(s). Its predictive power was compared to PD-L1 tumour proportion score (TPS) and iRECIST using ROC curve analysis. Prediction accuracies were assessed with 5-fold cross validation.

Results. The most predictive were baseline radiomics features, e.g. Small Run Emphasis (MWU, p = 0.001; hazard ratio = 0.46, p = 0.007; AUC = 0.85 (95% CI 0.69–1.00)). Multivariate iRADIOMICS was found superior to the current standards in terms of predictive power and timewise with the following AUC (95% CI) and accuracy (standard deviation): iRADIOMICS (baseline), 0.90 (0.78–1.00), 78% (18%); PD-L1 TPS (baseline), 0.60 (0.37–0.83), 53% (18%); iRECIST (month 1), 0.79 (0.62–0.95), 76% (16%); iRECIST (month 4), 0.86 (0.72–1.00), 76% (17%).

Conclusions. Multivariate iRADIOMICS was identified as a promising imaging biomarker, which could improve management of metastatic NSCLC patients treated with pembrolizumab. The predicted non-responders could be offered other treatment options to improve their overall survival.

Key words: anti-PD-1; [^{18}F]FDG PET/CT; non-small-cell lung cancer; radiomics analysis; iRADIOMICS

Introduction

In spite of the advances in lung cancer treatment, prognosis for patients has been poor with a 5-year survival rate around 15%.[1] A new hope has come with renaissance of immunotherapy, such as programmed death-1 antibodies (anti-PD-1), which invigorate a patient's immune system to fight

 doi: 10.2478/raon-2020-0042

against malignant cells.[2] In non-small-cell lung cancer (NSCLC), which represents 85% of all lung cancer cases, treatment outcomes of anti-PD-1 immunotherapy are significantly better compared to conventional cytotoxic therapies. In selected patient population, response rates can be over 40%.[3] The responding patients usually achieve durable benefit and prolonged survival. Occasionally, even complete remissions of metastatic disease are observed, but such complete responses are still in minority.

Due to possible unusual response patterns (e.g. pseudoprogression), treatment response assessment in immunotherapy is challenging.[4] The most routinely used methods are Response Evaluation Criteria in Solid Tumours (RECIST) and its modification for use in immunotherapy (iRECIST), among others.[5] Although iRECIST was found superior to RECIST in identifying pseudoprogression, iRECIST is a late response assessment method, because anatomical changes observed on computed tomography are usually delayed, and the suspicion of progressive disease needs to be confirmed with an additional scan 1–2 months after the first assessment.[6] Importantly, studies have shown that none of the RECIST-based endpoints could be used as valid surrogates for overall survival (OS) in anti-PD-1 trials, while the correlation of iRECIST-based endpoints with OS is yet to be explored.[7,8] Since the molecular and functional tumour changes are known to appear faster compared to anatomical changes, several immunotherapy response assessment methods, based on 2-deoxy-2-[fluorine-18] fluoro-D-glucose positron emission tomography/computed tomography ([^{18}F]FDG PET/CT), have been proposed.[9-12] However, there is still a lack of sufficient evidence to infer, which method, if any, might be the most appropriate for the routine clinical use.[13-15]

Recently, research into the identification of new biomarkers for use in immunotherapy has also increased. Various predictive and prognostic biomarkers of response have been identified, including tumour PD-1 ligand (PD-L1) expression, tumour mutation burden, tumour infiltrating lymphocytes density, mismatch repair deficiency, microsatellite instability, and gut microbiota.[16,17] However, the reports from different studies sometimes oppose each other, therefore the current biomarkers need further validation.[18] Moreover, most of them require invasive biopsies, and are impractical or too expensive for a routine clinical use. On the other hand, few immunotherapy clinical studies examined possible non-invasive imaging biomarkers, but there is still a lack of research performed in NSCLC patients.[14] Three retrospective anti-PD-1 studies showed associations of pre-treatment sum of maximum standardized uptake values (SUV_{max}) of all lesions (SUV_{maxwb})[19], SUV_{max} of the most avid lesion[20], and volumetric parameters (metabolic tumour volume [MTV], and total lesion glycolysis [TLG])[21], with NSCLC patient response as defined by RECIST. However, significant correlations of these features with OS were not observed. There is also a lack of clinical studies in immunotherapy investigating more sophisticated image analysis methods such as radiomics analysis. Radiomics analysis harnesses the full power of medical imaging by extracting numerous quantitative features, hypothesized to reflect more deeply the tumour phenotype, as well as the genotype.[22,23] Recent anti-PD-(L)1 radiomics studies have shown associations of CT radiomics signatures with tumour immune phenotype[24], hyperprogression[25], and progression-free survival (PFS)[26]. Moreover, two studies also examined the predictive value of PET radiomics features. Polverari *et al*. observed significant differences in tumour heterogeneity (as defined by kurtosis and skewness) between patients with progressive disease (PD) and non-PD[21], while the study by Mu *et al*. proposed a combined PET and CT radiomics signature for predicting patient PFS and OS.[27] In these studies (except Polverari *et al*.), data mining using vast number of features (up to 1160) was performed in order to build multivariate radiomics signatures containing up to eight features. Although on one hand, such approach might allow for a more precise quantification of tumour characteristics, on the other hand, the so obtained predictive models could be prone to overfitting, and probably too complex and non-intuitive for a successful clinical translation. Moreover, it is also well known that a lot of radiomics features are not suitable candidates for biomarkers, for example due to an excessive test-retest variability.[28]

The primary aim of our prospective study was to determine whether immunotherapy [^{18}F]FDG PET radiomics signature (iRADIOMICS) predicts response of stage IV NSCLC patients to pembrolizumab better than the current routinely used clinical standards (PD-L1 immunohistochemistry, and iRECIST). To overcome the aforementioned pitfalls, we deliberately analysed only a small subset of radiomics features, which were previously proven to be robust and reliable according to test-retest variability[28], and built iRADIOMICS with minimum number of features.

Patients and methods

Patients

Thirty consecutive patients who met the following inclusion criteria were enrolled from January 2017 – March 2019 at the Institute of Oncology Ljubljana (Slovenia): ≥ 18 years old, cytologically or histologically confirmed stage IV NSCLC (8th TNM classification of the International Association for the Study of Lung Cancer), no history of other malignancies, PD-L1 tumour proportion score (TPS) > 1% (assessed by a validated immunohistochemistry assay), Eastern Cooperative Oncology Group criteria (ECOG) performance status 0–2. Enrolment required approval of the multidisciplinary tumour board that the patient was a candidate for treatment with pembrolizumab. The study (NCT04007068) was approved by the institutional review board committee and the National Ethics Committee (KME 117/02/17). All patients gave informed consent to participate.

Study protocol

All patients underwent standard diagnostic procedures including clinical examination and blood tests. Baseline [18F]FDG PET/CT was performed ≤ 4 weeks before treatment, and follow-up [18F]FDG PET/CTs were performed 1 month (± 5 days) and 4 months (± 14 days) after treatment initiation. Patients were treated with pembrolizumab until progression, clinical benefit, or unaccepted toxicities. Pembrolizumab dosage was 2 mg/kg or 200 mg/patient (depending on the guidelines at the time of treatment), intravenously, every three weeks (q3w). Patients could also receive palliative radiotherapy in case of symptomatic lesions. Such treatment intervention required approval of the multidisciplinary tumour board.

Imaging acquisition and analysis

Patients fasted for at least 6 hours before intravenous application of 3.7 MBq/kg [18F]FDG and remained seated or recumbent for 60 minutes. Data acquisition was performed on a Biograph 40 mCT (Siemens Healthcare, Erlangen, Germany) with the following parameters: CT (tube current 100 kV, tube voltage 80 mAs, Care dose 4D and Care kV dose modulation, collimation 16×1.2 mm, pitch 1.2, reconstruction using 3 mm slice thickness in 2 mm increment, abdominal window, B40f kernel), [18F]FDG PET (acquired from skull base to mid-thigh, 2 minutes per bed position, reconstruction using TruX+TOF (UltraHD-PET) algorithm, 2 iterations per 21 subsets, matrix size 200×200, 3 mm slice thickness, 2.5 mm pixel size). Two physicians segmented the lesions semi-automatically in 3D Slicer using SUV > 4.0 g/ml as the threshold. The segmentations were then examined by an experienced radiologist and, if necessary, manually edited. The radiologist also performed iRECIST assessment. All researchers involved in tumour segmentations were blinded to the outcome of the study.

Feature extraction

At first, eight [18F]FDG radiomics features were extracted from primary tumours, including three volume-based features (volume, maximum standardized uptake value (SUV_{max}), total SUV (SUV_{total})) and five texture-based heterogeneity features, derived from Grey-Level Co-occurrence Matrix (GLCM) (Sum Entropy, Entropy-GLCM, Difference Entropy) and Grey-Level Run Length Matrix (GLRLM) (Small Run Emphasis (SRE), Run Percentage).[29,30] Importantly, these five texture-based features were deliberately chosen, because they were identified as very robust and reliable, based on test-retest variability in a prospective multicentre study of NSCLC tumours imaged with [18F]FDG PET/CT.[28] Feature definitions and their intuitive explanations are summarized in Table S1. Feature extraction was performed using an in-house software, see references.[31-33] Briefly, features were extracted using a voxel-based method. The image was discretized into 256 grey levels. For each voxel, the feature was calculated over a 5 × 5 voxel patch in axial, coronal, and sagittal planes, and averaged over the three planes for each voxel. The final feature was calculated by averaging over all voxels. After examining the correlation between features using Pearson correlation coefficient, we excluded SUV_{total} and Run Percentage from further analysis, because they were too closely correlated with other features (Figure S1).

Statistical analysis

Response was defined based on overall survival (OS), the gold standard end-point in immunotherapy[8], therefore OS was the primary outcome measure in our study. OS was defined as the time from initiation of pembrolizumab until death from any cause. Patients with OS > 14.9 months were defined as responders. The selected threshold was median OS in the multicentre KEYNOTE-10 study (subgroup of NSCLC patients with PD-L1 TPS > 50%, treated with pembrolizumab dose 2 mg/kg)).[34] Although the inclusion criteria in our study was PD-L1 TPS > 1%, the majority of patients (26/30, 87%) had PD-L1 TPS > 50%, resulting in comparable median OS (15.95 months).

Mann-Whitney U-test and Fisher exact test were used to investigate the differences in radiomics features and demographic data between the responders and non-responders. Receiver operating characteristic (ROC) curve analysis was used to assess the predictive power of each radiomics feature. Univariate and multivariate Cox proportional hazards (Cox PH) regression analyses were used to study the relationship between the radiomics features and OS. A multivariate Cox PH model was constructed utilizing forward selection, considering univariate predictors of level $p < 0.05$. The results of the variable selection procedure were confirmed using backward selection based on the Akaike Information Criterion (AIC). Since the hazard ratio depends on the unit of the measurement, all radiomics features were normalized into z-scores.[35] Probability of OS as a function of time was analysed with Kaplan-Meier diagrams, and the difference between survival curves was tested with the log-rank test.

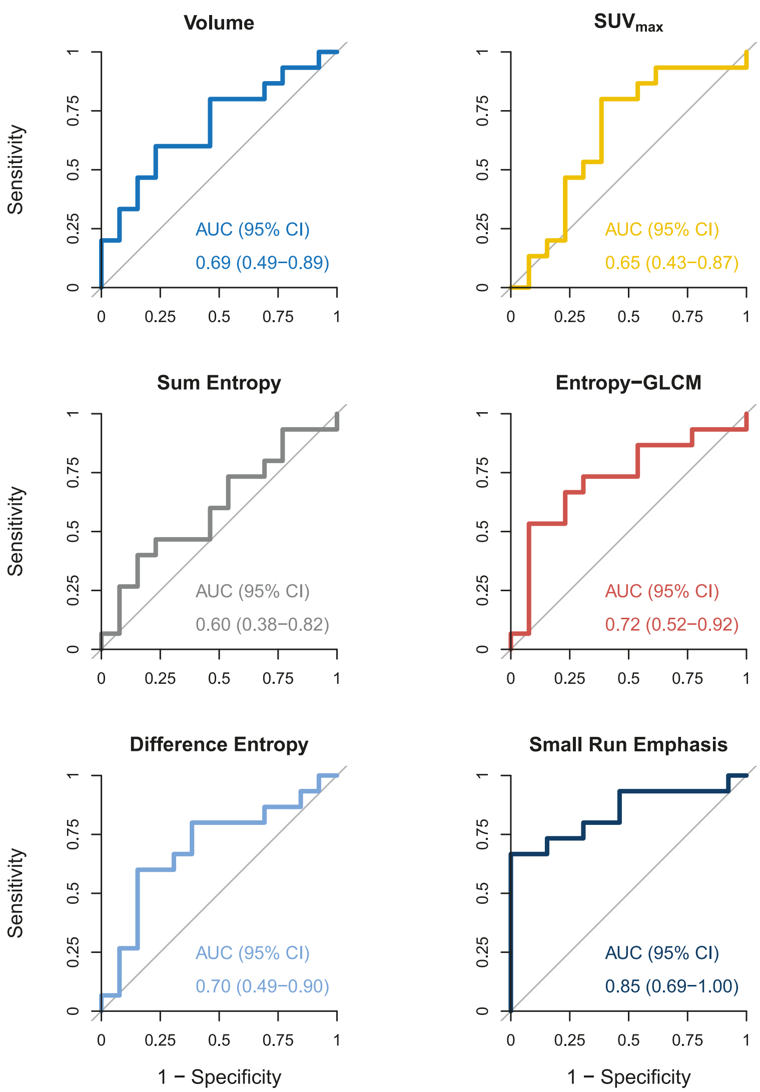

FIGURE 1. Baseline radiomics features of primary tumours – Receiver operating characteristic curve (ROC) analysis. For each radiomics feature, the area under the ROC curve (AUC) with the corresponding 95% confidence interval (CI) is reported. AUC of 0.8 or above indicates a high level of predictive power, while an AUC of 0.6 or less indicates poor level of predictive power.

iRADIOMICS, iRECIST, and PD-L1 signatures were constructed using univariate or multivariate logistic regression analyses. The iRADIOMICS signatures consisted of the most promising radiomics features. The iRECIST signature consisted of one categorical variable with five ordered iRECIST response categories.[5] The predictive power of each model was assessed by calculating the area under the curve (AUC) of the corresponding ROC analysis. The accuracy of each model (percentage of correctly classified patients) was assessed with repeated (10×) 5-fold cross validation, so that the patients were randomly split into five groups: at each validation step, four unique groups were chosen to train the model and the remaining group was used to validate accuracy of model predictions.

A planned sample size of 30 evaluable patients was deemed to be sufficient for evaluating the predictive power of each model. Specifically, assuming an anticipated response rate of 50%, a sample size of 30 evaluable patients provided >85% power to detect an AUC of at least 0.80 (high predictive power) at the two-sided 0.05 significance level under the null hypothesis that the AUC is at most 0.5. All analyses were performed in R (3.5.3.) and were considered statistically significant if $p < 0.05$.

Results

Patient demographic and clinical data

Thirty patients were enrolled in the study. Median follow-up time (time to censoring) was 21.4 months. A full list of demographic characteristics is presented in Table 1. The examination of demographic data did not reveal any significant differences between the responders and non-responders.

Individual radiomics features as predictors of overall survival (OS)

We analysed radiomics features extracted from primary tumours at baseline, month 1, and month

TABLE 1. Patient demographic and clinical data. The data is presented for all patients, responders (overall survival [OS] > 14.9 months), and non-responders (OS < 14.9 months). The reported p-value is the result of Mann-Whitney U-test (MWU) (continuous variables) and Fisher exact test (categorical variables) comparing differences between responders and non-responders

Characteristic	All patients median (range)	Responders (OS > 14.9 months) median (range)	Non-responders (OS < 14.9 months) median (range)	p-value
Number of patients	30	16	14	
Age [years]	65 (46–77)	67 (48–76)	61 (46–77)	0.298
PD-L1 TPS [%]	75 (3–100)	77.5 (3–100)	75 (10–100)	0.933
Sex				**0.715**
Female	15	9	6	
Male	15	7	8	
Histology				**0.532**
Adenocarcinoma	17	8	9	
Squamous cell carcinoma	8	4	4	
Other	5	4	1	
Smoking status				**0.672**
Never	1	0	1	
Former > 3 years ago	12	7	5	
Former < 3 years ago	5	3	2	
Until current disease	8	3	5	
Current smoker	4	3	1	
ECOG PS				**0.162**
0	8	2	6	
1	18	12	6	
2	4	2	2	
Line of treatment (immunotherapy)				**0.096**
1st	15	10	5	
2nd	13	4	9	
3rd	2	2	0	
Palliative RT during treatment				**0.657**
No	24	12	12	
Yes	6	4	2	

ECOG PS = Eastern Cooperative Oncology Group performance status; RT = radiotherapy; TPS = tumour proportion score (TPS)

4. Two patients did not have primary tumours, excluding them from this analysis (N = 28). The analysis of the features extracted at baseline is presented in Table 2 and Figure 1. Neither standard volume-based features (volume, SUV_{max}) were able to discriminate responders from non-responders. Among the texture-based features, Entropy-GLCM (p = 0.046) and Small Run Emphasis (SRE) (p = 0.001) were found to be significantly different between the two groups. ROC curve analysis revealed SRE having high level of predictive power (AUC = 0.85 (95% CI 0.69–1.00)), while the predictive power of other features was moderate (0.6 < AUC < 0.8).

At month 1, only volume was significantly different between the responders and non-responders (p = 0.035, AUC = 0.75 (0.55-0.95)), while none of the radiomics features reached high level of predictive power (AUC < 0.8). At month 4, none of the features were significantly different between responders and non-responders, and all radiomics features had AUC < 0.7.

To further explore the impact of baseline radiomics features on OS, we performed Cox proportional

TABLE 2. Baseline radiomics features of primary tumours – Mann-Whitney U-test (MWU) and receiver operating characteristic (ROC) curve analysis. Patients were dichotomized into 2 groups: responders (OS > 14.9 months) and non-responders (OS < 14.9 months). For each radiomics feature median value, range, p-value of MWU, and the area under the ROC curve (AUC) with the corresponding 95% confidence interval (CI), are reported. See also Figure 1

Feature	Responders (OS > 14.9 months) median (range)	Non-responders (OS < 14.9 months) median (range)	p-value	AUC (95% CI)
Volume [cm³]	27.9 (2.64–351)	44.4 (7.81–792)	0.098	0.69 (0.49–0.89)
SUV_{max} [g/ml]	20.6 (5.21–32.1)	15.6 (9.54–37.0)	0.185	0.65 (0.43–0.87)
Sum entropy	3.69 (3.53–3.77)	3.7 (3.54–3.76)	0.387	0.60 (0.38–0.82)
Entropy-GLCM	**4.07 (3.99–4.15)**	**4.11 (4.03–4.14)**	**0.046**	**0.72 (0.52–0.92)**
Difference entropy	2.98 (2.74–3.07)	2.89 (2.74–3.06)	0.080	0.70 (0.49–0.90)
Small Run Emphasis (SRE)	**0.0382 (0.00962–0.0615)**	**0.0163 (0.00854–0.0303)**	**0.001**	**0.85 (0.69–1.00)**

GLCM = Grey-Level Co-occurrence Matrix; SUV_{max} = maximum standardized uptake value

TABLE 3. Baseline radiomics features of primary tumours – univariate and multivariate Cox proportional hazards regression analysis (Cox PH). For each radiomics feature, the hazard ratio (HR), corresponding 95% confidence interval (CI), and p-value of univariate analysis are reported. The 2-variable multivariate regression model was chosen based on the Akaike information criterion (AIC). In order to achieve comparable HRs, all radiomics features were normalized into z-scores

Feature	Univariate HR (95% CI)	Univariate p-value	Multivariate HR (95% CI)	Multivariate p-value
Volume	**1.6 (1.1–2.4)**	**0.015**		
SUV_{max}	0.77 (0.46–1.3)	0.320		
Sum Entropy	0.96 (0.60–1.5)	0.860		
Entropy-GLCM	1.4 (0.82–2.3)	0.230		
Difference entropy	**0.62 (0.40–0.97)**	**0.037**	**0.54 (0.31–0.93)**	**0.026**
Small Run Emphasis (SRE)	**0.46 (0.26–0.81)**	**0.007**	**0.39 (0.20–0.76)**	**0.006**

GLCM = Grey-Level Co-occurrence Matrix; SUV_{max} = maximum standardized uptake value

hazards (Cox PH) regression analysis (Table 3). In univariate analysis, volume (hazard ratio (HR) = 1.6, p = 0.015), Difference Entropy (HR = 0.62, p = 0.037), and SRE (HR = 0.46, p = 0.007) showed statistically significant relationship with patient OS. Multivariate Cox PH regression model with the lowest AIC consisted of Difference Entropy (HR = 0.54, p = 0.026) and SRE (HR = 0.39, p = 0.006). As shown in Figure S1, SRE and Difference Entropy also exhibited low correlation (ϱ = 0.20), confirming that these two features were independent predictors of survival.

For the feature SRE, which was found to be the most informative in all statistical tests, we performed Kaplan-Meier survival analysis for baseline SRE where patients were dichotomized by the median (Figure 2). Survival probability was significantly different between groups (p = 0.015). Median OS of the patients with SRE < SRE_{median} was 10.4 months (95% CI 6.0 months–not reached), while median OS of the patients with SRE ≥ SRE_{median} was not reached (95% CI 15.9 months–not reached).

Ability of iRADIOMICS, iRECIST, and PD-L1 signatures to predict patient overall survival

Finally, we examined the predictive power of iRADIOMICS (baseline), iRECIST (month 1 and 4), and PD-L1 (baseline) signatures. 25 patients, which had both baseline and month 1 scans available, were suitable for this analysis. Two patients were excluded because they had no primary tumours (impossible to extract iRADIOMICS), and three other patients had no month 1 scans (impossible to assess iRECIST). For the three additional patients, who died before the scheduled month 4 scanning, we used month 1 iRECIST assessment for the construction of month 4 iRECIST signature. Otherwise, the statistics of month 4 iRECIST signature could

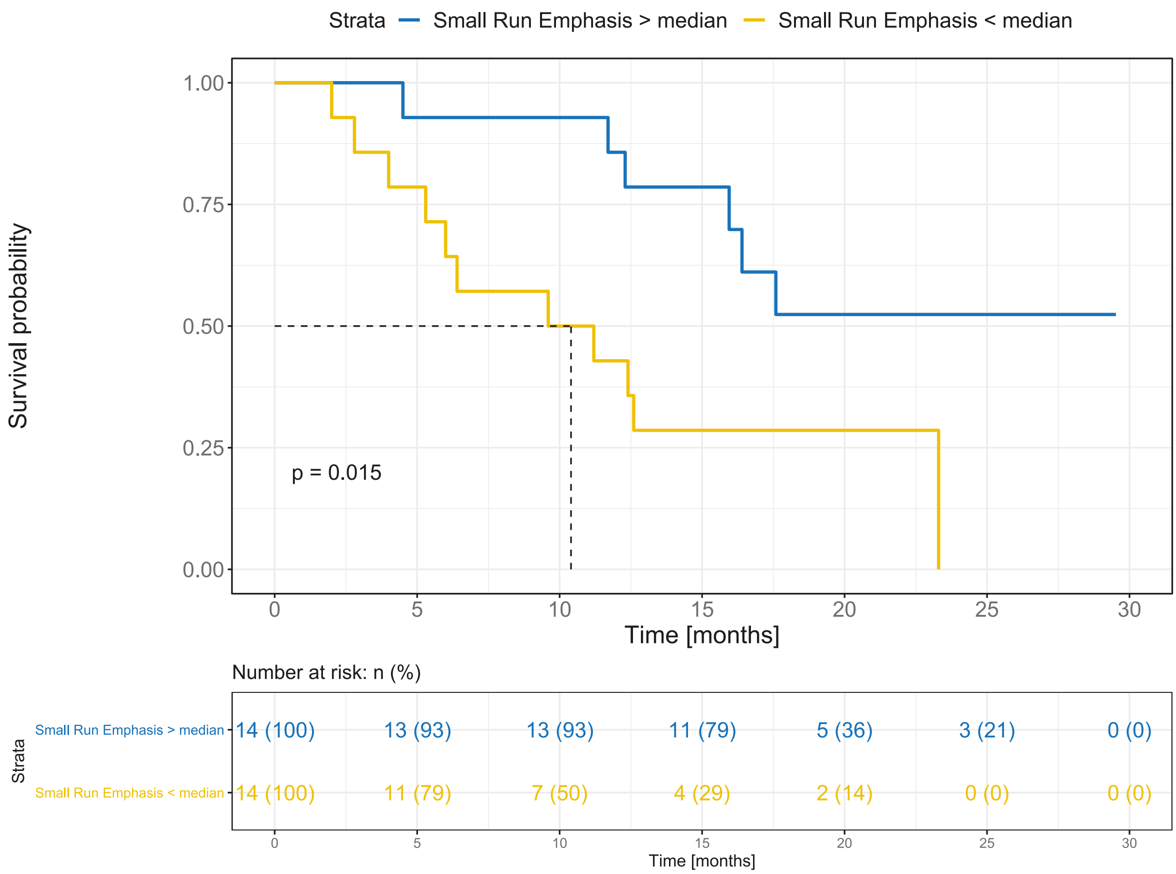

FIGURE 2. Kaplan-Meier diagram – Small Run Emphasis (SRE). Blue: patients with SRE ≥ SRE_{median}, yellow: patients with SRE < SRE_{median}. The reported p-value is the result of log-rank test.

be biased due to the exclusion of hyperprogressive patients. The results are presented in Figure 3. PD-L1 TPS showed poor predictive power (AUC = 0.60 (0.37-0.83)). The AUC of iRECIST signatures were 0.79 (0.62–0.95) and 0.86 (0.72–1.00) for month 1 and month 4, respectively. On the other hand, the AUC of the univariate iRADIOMICS at baseline was 0.81 (0.62–0.99), which was comparable to iRECIST at month 1. The highest predictive power was achieved by the multivariate baseline iRADIOMICS (consisting of SRE and Difference Entropy) with AUC = 0.90 (0.78–1.00). Model coefficients of iRADIOMICS are summarized in Table S2.

To further validate the predictive ability of all models, the accuracy of predictions was calculated using 5-fold cross validation. PD-L1 TPS achieved poor accuracy of only 53% (standard deviation SD = 18%). iRECIST signatures at month 1 and month 4 correctly classified 76% (16%) and 76% (17%) of patients, respectively. The accuracy of univariate iRADIOMICS at baseline was slightly lower, 73% (18%). The highest accuracy was achieved by multivariate baseline iRADIOMICS, which correctly classified 78% (18%) of patients.

Additionally, we performed a sensitivity study by repeating the same analyses either with a subset of 22 patients, who were scanned at all three time-points (excluding hyperprogressive patients who died before month 4), or by using all available data at each specific time-point (resulting in different number of analysed patients at baseline, month 1 and month 4), but the change of the results was negligible. In each scenario, multivariate iRADIOMICS reached AUC around 0.90 with accuracy up to 80%, and always performed better than the other models.

Discussion

New biomarkers of response to immunotherapy are urgently needed. In NSCLC, PD-L1 TPS is still the only predictive biomarker routinely used in clinics, in spite of the growing evidence sug-

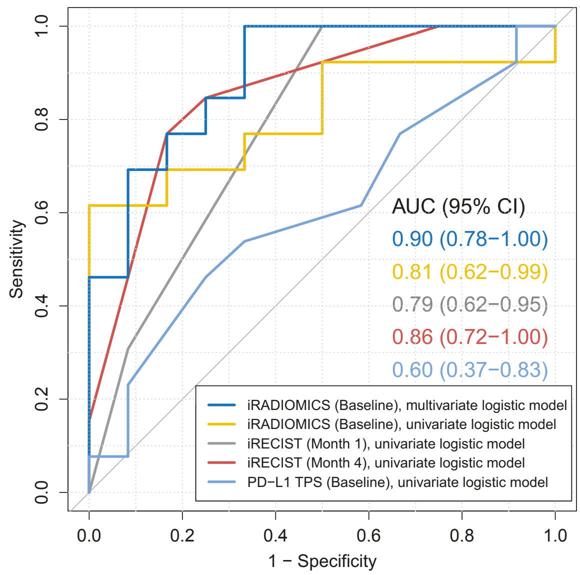

FIGURE 3. Receiver operating characteristic (ROC) curve analysis. Blue: baseline iRADIOMICS multivariate logistic model (independent variables: Small Run Emphasis [SRE], Difference Entropy), yellow: baseline iRADIOMICS univariate logistic model (independent variable: SRE), grey: month 1 iRECIST univariate logistic model (independent variable: iRECIST response category), red: month 4 iRECIST univariate logistic model (independent variable: iRECIST response category). For each model, area under curve (AUC) and 95% confidence interval (CI) are reported.

gesting that it is far from optimal.[36] Among the reasons for its questionable predictive power are inconsistent measurement methodologies, intra-tumour PD-L1 expression heterogeneity, and the fact that immune cells infiltrating the tumour can express PD-L1.[37] Even in our study, the survival predictions based on PD-L1 TPS performed poorly. Additionally, because it is not clear to what extent the current standards for treatment response assessment (RECIST, iRECIST) correlate with overall survival (OS), the duration of treatment, as well as the decision about cessation of anti-PD-1 immunotherapy, rely on the subjective judgment of the treating physician, which is mainly based on the observed immune-related adverse events and achieved clinical benefit.

We aimed to address these issues with the use of [^{18}F]FDG PET/CT imaging, since it is widely used, affordable, and non-invasive. When we examined the predictive ability of individual radiomics features, we found that some of the features showed high predictive power at baseline, while at month 1 and month 4 their informative value decreased significantly. This is consistent with a number of studies suggesting that intrinsic tumour characteristics, such as tumour histopathology, tumour microenvironment, and immune contexture, most likely have a major impact on response to immunotherapy.[16,17,38] The most dominant feature was Small Run Emphasis (SRE), which was able to discriminate responders from non-responders to anti-PD-1 therapy, it had a significant relationship with patient OS, and high predictive power. In patients with SRE > SRE_{median}, the probability of survival by Kaplan-Meier analysis was also significantly higher. Although studies have shown that texture-based features might reflect tumour heterogeneity on macroscopic, cellular, or even molecular or genomic level[39], their clear relationship with the underlying biology still needs to be elucidated. However, from the definitions of texture features used in our study we can infer that at baseline, primary tumours of responders have finer and more homogeneous metabolic structure, as reflected by higher SRE and lower Entropy-GLCM, respectively. See Table S1 for formal mathematical definitions, as well as intuitive descriptions of the studied texture features. In terms of underlying biology we could speculate that these findings might reflect tumours with spatially more homogeneous clonal structure, more homogeneous intrinsic infiltration of immune cells, more homogeneous tumour microenvironment, or fewer hypoxic or necrotic regions. Interestingly, this finding is in agreement with the study by Polverari *et al*., where patients with progressive disease (PD) exhibited higher tumour heterogeneity at baseline (reflected by higher kurtosis and skewness), compared to non-PD patients. On the other hand, the finding is at odds with the study by Mu *et al*., where heterogeneous tumours presumably had a higher chance to achieve durable clinical benefit.[27] However, heterogeneous tumour phenotype in this study was inferred from two components of eight-variable radiomics signature, making intuitive conclusions about the underlying tumour biology even more difficult compared to our study. In agreement with the study by Takada *et al*., we also observed the trend of higher SUV_{max} among the responding patients, although it was not statistically significant.[20] A similar lack of statistical significance of SUV_{max}, or even the opposite trend, was observed by other groups, therefore the predicitve value of SUV_{max} should be considered highly questionable.[13,19,21]

We analysed only primary tumours, yet neglected lymph nodes (LN) and distant metastases (DM). The main reason for this approach is that radiomics analyses might not accurately quantify intra-tumour heterogeneity of small lesions due to the partial volume effects, which could be even more pronounced in PET imaging with limited spatial resolution.[40] However, inclusion of LN and DM in future predictive models could additionally improve their predictive power and accuracy. Especially an [^{18}F]FDG PET signal of LN might be connected with the cancer immunity cycle, possibly capturing the processes that occur in LN after the initiation of anti-PD-1 therapy, including T cell priming and activation.[41]

The analysis of the predictive ability of iRECIST, PD-L1, and iRADIOMICS signatures revealed some interesting aspects. First, the response to anti-PD-1 therapy seems to occur fast, as iRECIST signature was able to predict the response of 76% of patients already at month 1, while the predictive ability at month 4 had not improved. These results suggest that treatment response assessment could be performed as soon as 1 month after treatment initiation. Moreover, its satisfactory ability to predict OS indicates that clinical decisions about (dis) continuation of anti-PD-1 therapy could (at least in part) rely on iRECIST assessment rather than purely on the observed clinical benefit. However, the correlation of other iRECIST-based endpoints with patient survival should be further explored.

Lastly, the iRADIOMICS was found superior to PD-L1 and iRECIST both in terms of predictive power and, importantly, timing. From the clinical point of view, each additional month (or day) of an ineffective therapy can be crucial for metastatic NSCLC patients. The fact that the iRADIOMICS was able to correctly predict the response of almost 80% of patients before therapy, could have an important clinical impact. The predicted non-responders to pembrolizumab could be offered other treatment options to improve their OS. However, the predictive ability of iRADIOMICS needs to be confirmed in future independent studies with a higher number of patients.

Our study compared the predictive power of baseline biomarkers (iRADIOMICS and PD-L1) to the early treatment response assessment method (iRECIST) – single point vs. multiple point assessment. However, from the practical standpoint, the baseline prediction is desirable to the treatment response assessment as it is earlier and allows more time for favourable clinical decision making. Potentially the two approaches could be combined, but such study would require higher number of patients to secure clinical significance because of more degrees of freedom (variables).

Acknowledgments

The authors acknowledge the financial support from the Slovenian Research Agency (research core funding P1-0389), and the University of Wisconsin Carbone Cancer Center (support grant P30 CA014520).

Trial registration: ClinicalTrials.gov NCT04007068. Registered 5 July 2019 (retrospectively registered).

References

1. Siegel RL, Miller KD, Jemal A. Cancer statistics, 2019. *CA Cancer J Clin* 2019; **69:** 7-34. doi: 10.3322/caac.21551
2. Hoos A. Development of immuno-oncology drugs – from CTLA4 to PD1 to the next generations. *Nat Rev Drug Discov* 2016; **15:** 235-47. doi: 10.1038/nrd.2015.35
3. Reck M, Rodríguez-Abreu D, Robinson AG, Hui R, Csőszi T, Fülöp A; KEYNOTE-024 investigators, et al. Pembrolizumab versus chemotherapy for PD-L1-positive non-small-cell lung cancer. *N Engl J Med* 2016; **375:** 1823-33. doi: 10.1056/NEJMoa1606774
4. Vrankar M, Unk M. Immune RECIST criteria and symptomatic pseudoprogression in non-small cell lung cancer patients treated with immunotherapy. *Radiol Oncol* 2018; **52:** 365-9. doi:10.2478/raon-2018-0037
5. Seymour L, Bogaerts J, Perrone A, et al. iRECIST: guidelines for response criteria for use in trials testing immunotherapeutics. *Lancet Oncol* 2017; **18:** e143-52. doi: 10.1016/S1470-2045(17)30074-8
6. Tazdait M, Mezquita L, Lahmar J, Ferrara R, Bidault F, Ammari S, et al. Patterns of responses in metastatic NSCLC during PD-1 or PDL-1 inhibitor therapy: comparison of RECIST 1.1, irRECIST and iRECIST criteria. *Eur J Cancer* 2018; **88:** 38-47. doi: 10.1016/j.ejca.2017.10.017
7. Mushti SL, Mulkey F, Sridhara R. Evaluation of overall response rate and progression-free survival as potential surrogate endpoints for overall survival in immunotherapy trials. *Clin Cancer Res* 2018; **24:** 2268-2275. doi: 10.1158/1078-0432.CCR-17-1902
8. Nie RC, Chen FP, Yuan SQ, Luo YS, Chen S, Chen YM, et al. Evaluation of objective response, disease control and progression-free survival as surrogate end-points for overall survival in anti-programmed death-1 and anti-programmed death ligand 1 trials. *Eur J Cancer* 2019; **106:** 1-11. doi: 10.1016/j.ejca.2018.10.011
9. Cho SY, Lipson EJ, Im HJ, Rowe SP, Gonzalez EM, Blackford A, et al. Prediction of response to immune checkpoint inhibitor therapy using early-time-point 18F-FDG PET/CT imaging in patients with advanced melanoma. *J Nucl Med* 2017; **58:** 1421-8. doi: 10.2967/jnumed.116.188839
10. Anwar H, Sachpekidis C, Winkler J, Kopp-Schneider A, Haberkorn U, Hassel JC, et al. Absolute number of new lesions on 18F-FDG PET/CT is more predictive of clinical response than SUV changes in metastatic melanoma patients receiving ipilimumab. *Eur J Nucl Med Mol Imaging* 2018; **45:** 376-83. doi: 10.1007/s00259-017-3870-6
11. Goldfarb L, Duchemann B, Chouahnia K, Zelek L, Soussan M. Monitoring anti-PD-1-based immunotherapy in non-small cell lung cancer with FDG PET: introduction of iPERCIST. *EJNMMI Res* 2019; **9:** 8. doi: 10.1186/s13550-019-0473-1
12. Ito K, Teng R, Schöder H, Humm JL, Ni A, Michaud L, et al. 18 F-FDG PET/CT for monitoring of ipilimumab therapy in patients with metastatic melanoma. *J Nucl Med* 2019; **60:** 335-41. doi: 10.2967/jnumed.118.213652
13. Kaira K, Higuchi T, Naruse I, Arisaka Y, Tokue A, Altan B, et al. Metabolic activity by 18F–FDG-PET/CT is predictive of early response after nivolumab in previously treated NSCLC. *Eur J Nucl Med Mol Imaging* 2018; **45:** 56-66. doi: 10.1007/s00259-017-3806-1

14. Aide N, Hicks RJ, Le Tourneau C, Lheureux S, Fanti S, Lopci E. FDG PET/CT for assessing tumour response to immunotherapy. *Eur J Nucl Med Mol Imaging* 2019; **46:** 238-50. doi: 10.1007/s00259-018-4171-4

15. Rossi G, Bauckneht M, Genova C, Rijavec E, Biello F, Mennella S, et al. Comparison between 18F-FDG-PET- and CT-based criteria in non-small cell lung cancer (NSCLC) patients treated with Nivolumab. *J Nucl Med* 2019; [Ahead of print]. doi: 10.2967/jnumed.119.233056

16. Yi M, Jiao D, Xu H, Liu Q, Zhao W, Xinwei Han H, et al. Biomarkers for predicting efficacy of PD-1/PD-L1 inhibitors. *Mol Cancer* 2018; **17:** 129. doi: 10.1186/s12943-018-0864-3

17. Zou W, Wolchok JD, Chen L. PD-L1 (B7-H1) and PD-1 pathway blockade for cancer therapy: Mechanisms, response biomarkers, and combinations. *Sci Transl Med* 2016; **8:** 328rv4. doi: 10.1126/scitranslmed.aad7118

18. Shukuya T, Carbone DP. Predictive markers for the efficacy of anti–PD-1/PD-L1 antibodies in lung cancer. *J Thorac Oncol* 2016; **11:** 976-88. doi: 10.1016/j.jtho.2016.02.015

19. Evangelista L, Cuppari L, Menis J, Bonanno L, Reccia P, Frega S, et al. 18F-FDG PET/CT in non-small-cell lung cancer patients: a potential predictive biomarker of response to immunotherapy. *Nucl Med Commun* 2019; **40:** 802-7. doi: 10.1097/MNM.0000000000001025

20. Takada K, Toyokawa G, Yoneshima Y, Tanaka K, Okamoto I, Shimokawa M, et al. 18F-FDG uptake in PET/CT is a potential predictive biomarker of response to anti-PD-1 antibody therapy in non-small cell lung cancer. *Sci Rep* 2019; **9:** 1-7. doi: 10.1038/s41598-019-50079-2

21. Polverari, G. Ceci F, Bertaglia V, Reale MC, Rampado O, Gallio E, et al. 18F-FDG PET parameters and radiomics features analysis in advanced NSCLC treated with immunotherapy as predictors of therapy response and survival. *Cancers* 2020;. **12:** 1163. doi: 10.3390/cancers12051163

22. Lambin P, Rios-Velazquez E, Leijenaar R, Carvalho S, van Stiphout RG, Granton P, et al. Radiomics: extracting more information from medical images using advanced feature analysis. *Eur J Cancer* 2012; **48:** 441-6. doi: 10.1016/j.ejca.2011.11.036

23. Thawani R, McLane M, Beig N, Ghose S, Prasanna P, Velcheti V, et al. Radiomics and radiogenomics in lung cancer: a review for the clinician. *Lung Cancer* 2018; **115:** 34-41. doi: 10.1016/j.lungcan.2017.10.015

24. Sun R, Limkin EJ, Vakalopoulou M, Dercle L, Champiat S, Han SR, et al. A radiomics approach to assess tumour-infiltrating CD8 cells and response to anti-PD-1 or anti-PD-L1 immunotherapy: an imaging biomarker, retrospective multicohort study. *Lancet Oncol* 2018; **19:** 1180-91. doi: 10.1016/S1470-2045(18)30413-3

25. Tunali I, Gray JE, Qi J, Abdalah M, Jeong DK, Guvenis A, et al. Novel clinical and radiomic predictors of rapid disease progression phenotypes among lung cancer patients treated with immunotherapy: an early report. *Lung Cancer* 2019; **129:** 75-9. doi: 10.1016/j.lungcan.2019.01.010

26. Dercle L, Fronheiser M, Lu L, Du S, Hayes W, Leung DK, et al. Identification of non-small cell lung cancer sensitive to systemic cancer therapies using radiomics. *Clin Cancer Res* 2020. [Aheqad of print]. doi: 10.1158/1078-0432.CCR-19-2942

27. Mu W, Tunali I, Gray JE, Qi J, Schabath MB, Gillies RJ. Radiomics of 18F-FDG PET/CT images predicts clinical benefit of advanced NSCLC patients to checkpoint blockade immunotherapy. *Eur J Nucl Med Mol Imaging* 2020; **47:** 1168-82. doi: 10.1007/s00259-019-04625-9

28. Desseroit MC, Tixier F, Weber WA, Siegel BA, Le Rest CC, Visvikis D, et al. Reliability of PET/CT shape and heterogeneity features in functional and morphologic components of non-small cell lung cancer tumors: a repeatability analysis in a prospective multicenter cohort. *J Nucl Med* 2017; **58:** 406-11. doi: 10.2967/jnumed.116.180919

29. Tang X. Texture information in run-length matrices. *IEEE Trans image Process* 1998; **7:** 1602-9. doi: 10.1109/83.725367

30. Haralick RM, Shanmugam K, Dinstein I. Textural features for image classification. *IEEE Trans Syst Man Cybern* 1973; **3:** 610-21. doi: 10.1109/TSMC.1973.4309314

31. Lin C, Harmon S, Bradshaw T, Eickhoff J, Perlman S, Liu G, et al. Response-to-repeatability of quantitative imaging features for longitudinal response assessment. *Phys Med Biol* 2019; **64:** 025019. doi: 10.1088/1361-6560/aafa0a

32. Galavis PE, Hollensen C, Jallow N, Paliwal B, Jeraj R. Variability of textural features in FDG PET images due to different acquisition modes and reconstruction parameters. *Acta Oncol* 2010; **49:** 1012-6. doi: 10.3109/0284186X.2010.498437

33. Chen S, Harmon S, Perk T, et al. Diagnostic classification of solitary pulmonary nodules using dual time 18F-FDG PET/CT image texture features in granuloma-endemic regions. *Sci Rep*. 2017; **7:** 9370. doi: 10.1038/s41598-017-08764-7

34. Herbst RS, Baas P, Kim D-W, Felip E, Pérez-Gracia JL, Han JY, et al. Pembrolizumab versus docetaxel for previously treated, PD-L1-positive, advanced non-small-cell lung cancer (KEYNOTE-010): a randomised controlled trial. *Lancet* 2016; **387:** 1540-50. doi: 10.1016/S0140-6736(15)01281-7

35. Kickingereder P, Burth S, Wick A, Götz M, Eidel O, Schlemmer HP, et al. Radiomic profiling of glioblastoma: identifying an imaging predictor of patient survival with improved performance over established clinical and radiologic risk models. *Radiology*. 2016; **280:** 880-9. doi: 10.1148/radiol.2016160845

36. Gubens MA, Davies M. NCCN guidelines updates: new immunotherapy strategies for improving outcomes in non-small cell lung cancer. *J Natl Compr Canc Netw* 2019; **17:** 574-8. doi: 10.6004/jnccn.2019.5005

37. McLaughlin J, Han G, Schalper KA, Carvajal-Hausdorf D, Pelekanou V, Rehman J, et al. Quantitative assessment of the heterogeneity of PD-L1 expression in non-small-cell lung cancer. *JAMA Oncol* 2016; **2:** 46. doi: 10.1001/jamaoncol.2015.3638

38. Galon J, Mlecnik B, Bindea G, Angell HK, Berger A, Lagorce C, et al. Towards the introduction of the 'immunoscore' in the classification of malignant tumours. *J Pathol* 2014; **232:** 199-209. doi: 10.1002/path.4287

39. Aerts HJWL, Velazquez ER, Leijenaar RTH, Parmar C, Grossmann P, Carvalho S, et al. Decoding tumour phenotype by noninvasive imaging using a quantitative radiomics approach. *Nat Commun* 2014; **5:** 4006. doi: 10.1038/ncomms5006

40. Yip SSF, Aerts HJWL. Applications and limitations of radiomics. *Phys Med Biol* 2016; **61:** R150-66. doi: 10.1088/0031-9155/61/13/R150

41. Chen DS, Mellman I. Oncology meets immunology: the cancer-immunity cycle. *Immunity* 2013; **39:** 1-10. doi: 10.1016/j.immuni.2013.07.012

42. Santos TA, Maistro CEB, Silva CB, Oliveira MS, Franca MC, Castellano G. MRI texture analysis reveals bulbar abnormalities in Friedreich ataxia. *Am J Neuroradiol* 2015; **36:** 2214-8. doi: 10.3174/ajnr.A4455

43. Galloway MM. Texture analysis using gray level run lengths. *Comput Graph Image Process* 1975; **4:** 172-9. doi: 10.1016/s0146-664x(75)80008-6

research article

Improvement of the primary efficacy of microwave ablation of malignant liver tumors by using a robotic navigation system

Jan Schaible[1], Benedikt Pregler[1], Niklas Verloh[1], Ingo Einspieler[1], Wolf Bäumler[1], Florian Zeman[2], Andreas Schreyer[3], Christian Stroszczynski[1], Lukas Beyer[1]

[1] Department of Radiology, University Medical Center Regensburg, Regensburg, Germany

[2] Center for Clinical Studies, University Medical Center Regensburg, Regensburg, Germany

[3] Department of Radiology, Hospital Brandenburg, Brandenburg, Germany

Radiol Oncol 2020; 54(3): 295-300.

Received 17 February 2020
Accepted 3 May 2020

Correspondence to: Dr. Jan Schaible, Department of Radiology, University Hospital Regensburg, 93053 Regensburg, Germany.
E-mail: jan.schaible@ukr.de

Disclosure: No potential conflicts of interest were disclosed.

Background. The aim of the study was to assess the primary efficacy of robot-assisted microwave ablation and compare it to manually guided microwave ablation for percutaneous ablation of liver malignancies.

Patients and methods. We performed a retrospective single center evaluation of microwave ablations of 368 liver tumors in 192 patients (36 female, 156 male, mean age 63 years). One hundred and nineteen ablations were performed between 08/2011 and 03/2014 with manual guidance, whereas 249 ablations were performed between 04/2014 and 11/2018 using robotic guidance. A 6-week follow-up (ultrasound, computed tomography and magnetic resonance imaging) was performed on all patients.

Results. The primary technique efficacy outcome of the group treated by robotic guidance was significantly higher than that of the manually guided group (88% *vs*. 76%; $p = 0.013$). Multiple logistic regression analysis indicated that a small tumor size (≤ 3 cm) and robotic guidance were significant favorable prognostic factors for complete ablation.

Conclusions. In addition to a small tumor size, robotic navigation was a major positive prognostic factor for primary technique efficacy.

Key words: interventional radiology; robotic assistance; microwave ablation; liver tumor

Introduction

Local ablation therapy has been established as a suitable alternative to resection for the treatment of tumors in the liver, lung, kidney and bone. It is considered a curative treatment for hepatocellular carcinoma (HCC) and can prolong the survival of patients with unresectable colorectal liver metastases.[1,2]

In recent years, microwave ablation (MWA), which is a thermal ablation method, has increasingly been used as an alternative to radiofrequency ablation (RFA). Although there are only a few studies that have compared MWA and RFA, MWA seems to have an advantage for the treatment of large tumors and tumors near vessels owing to its higher energy output.[3-5] Although the local recurrence rate has decreased owing to technological advances such as the development of multi-applicator systems for MWA and increasing application experience, surgical resection still seems superior with respect to local tumor control.[6-9]

To achieve optimal therapy results with the best possible local tumor control, it is extremely important to obtain complete ablation while maintaining a sufficient safety distance.[10] Although there are still no uniform guidelines for the minimum safety margin (distance between treated tumor and ablation margin), most operators assume a safety margin of approximately 0.5–1 cm.[11-13] To achieve this, the microwave applicator (antenna) must be positioned with millimeter precision, which can be very challenging, especially in the case of several overlapping ablation areas. In addition to the common freehand placement, modern navigation systems have been introduced to allow 3D planning and precise antenna placement.[14,15]

Unfortunately, there are only a few studies of the use of navigation systems, and often only with a small number of patients. Although it has been shown that modern navigation systems enable very accurate antenna placement, it is not yet clear whether this also leads to improved primary efficacy of the technique.[14,16,17] Therefore, the aim of this study was to compare the primary efficacy of robotic-guided ablation with that of manually guided ablation, as evidenced by magnetic resonance imaging (MRI) follow-up after 6 weeks.

Patients and methods

Study design and participant selection

The indications for percutaneous tumor ablation were established by a multi-disciplinary tumor board. The following exclusion criteria were applied: coagulation disorders not amendable to substitution; portal vein, hepatic vein or inferior vena cava invasion; extrahepatic metastases; and multifocal hepatic disease not amenable to complete ablation.

A total of 192 patients underwent either freehand or robotic guided microwave ablation from 08/2011 to 11/2018, inclusive. All procedures were performed by the same three experienced interventional radiologists (*blinded*).

Ethical approval

This single-center retrospective observational study was approved by the local ethics committee. All procedures performed in studies involving human participants were in accordance with the ethical standards of the institutional and/or national research committee and with the 1964 Helsinki declaration and its later amendments and the guidelines for Good Clinical Practice from the International Conference on Harmonization. Informed consent was obtained from all individual participants included in the study.

Navigation system and thermoablation procedure

All microwave ablations were performed under general anesthesia. During CT scans and antenna positioning, control of the respiratory movement was performed by temporary tube disconnection. Arterial and portal venous helical CT scans (Somatom 16 or Definition Egde, Siemens Healthcare, Forchheim, Germany) with a slice thickness of 1 mm were acquired.

CT fluoroscopy was used for ablations without navigation support, an acquisition mode that allows continuous image update using in-room table control. After the initial 2-phase planning CT, the antenna was placed during repeated temporary breath holds. To verify the correct antenna placement, one unenhanced CT was obtained before starting the ablation. If necessary, the antenna was repositioned until the whole tumor volume was covered.

When using robot navigation, the initial CT data was sent to the navigation system (Maxio, Perfint Healthcare, Chennai, India).[18,19] The desired ablation area and the antenna entry point were defined using the planning software, and the trajectory was visualized. If necessary, multiple antenna positions were planned with overlapping ablation zones. After approval of the plan, the robotic arm was automatically positioned over the patient and the antenna was positioned using the targeting device during breath hold. The probes were pushed forward manually along the preplanned path while held by the robotic needle holder. Before ablation, a CT scan was performed and the antenna position was verified by overlaying it with the planned trajectory. Consistent docking and absolute registration of the robotic device was performed using a base plate fixed on the ground. The navigation system is connected to the local PACS as a DICOM node. The images are automatically pushed to the navigation system by an auto transfer task after successful reconstruction of the 1mm images in the CT scanner.

For ablation, either the Acculis Microwave Tissue Ablation (MTA) System (AngioDynamics, Latham, NY, USA; Accu2i pMTA Applicator 1.8 mm diameter in 14 or 19 cm length) or the Emprint Ablation System (Medtronic, Minneapolis, USA; Emprint™ Percutaneous Antennas 1.8 mm diameter in 15 or 20 cm length) was used, depending on tumor configuration and relationship to the surrounding tissue. By comparison of the expected ablation zone in the unenhanced scan (typically

TABLE 1. Patient characteristics

	Age, years				Sex, n, (%)		Treated tumors per patient, n		Tumor entity, n (%)			
	Min.	Mean (SD)	Median (IQR)	Max.	Male	Female	Median (IQR)	Max.	HCC	CRC	CCC	Other
Patients (n = 192)	15	65.03 (23.56)	64.00 (57.75, 72.00)	83	156 (81)	36 (19)	1.00 (1.00, 2.00)	9	139 (72)	29 (15)	7 (4)	17 (9)

CCC = cholangiocellular carcinoma; CRC = colorectal liver metastasis; HCC = hepatocellular carcinoma; IQR = interquartile range; SD = standard deviation

TABLE 2. Tumors treated using freehand and robotic guidance

Ablation technique	Long axis, mm			Liver segment, n (%)									Device, n (%)		Primary efficacy, n (%)	
	Min	Mean (SD)	Max	I	II	III	IVa	IVb	V	VI	VII	VIII	Acculis	Emprint	Complete	In-complete
Freehand (n = 119)	4	19.79 (12.42)	85	1 (1)	10 (8)	16 (13)	16 (13)	9 (8)	13 (11)	17 (14)	15 (13)	22 (18)	65 (55)	54 (45)	9 (76)	28 (24)
Robotic guidance (n = 249)	3	18.78 (10.78)	64	6 (2)	24 (10)	20 (8)	26 (10)	16 (6)	38 (15)	36 (14)	36 (14)	47 (19)	143 (57)	106 (43)	219 (88)	30 (12)

SD = standard deviation

hypodense) to the initial tumor in the planning scan. If there was suspicion of insufficient ablation margin repositioning was performed.

After ablation and track ablation, all patients underwent a noncontrast multislice CT scan of the liver to detect complications.

Imaging follow-up

All patients underwent our standard follow-up scheme after 6 weeks including CT, MRI with hepatospecific contrast agent and ultrasound. Further follow-up investigations were only carried out using MRI and ultrasound for radiation protection. The radiographic adjudication/visual assessment of the complete success of the ablation was retrospectively determined in consensus by two experienced radiologists (*blinded*). The primary technique efficacy was defined as the percentage of the target tumors that were successfully eradicated following the initial procedure as evidenced in the 6-week follow up according to the standardization of terminology by Ahmed *et al*. [20]

Statistical analysis

R 3.51 was used to perform all statistical calculations. A p-value of $p \leq 0.05$ was considered the cut-off point of statistical significance. For multivariate analysis of primary efficacy using nested data (multiple ablations per patient in some cases), we applied generalized estimation equations (GEEs).

Results

Patient characteristics

A total of 192 patients (156 male) were included in the study (Table 1). The median age was 64 years (range: 57–72). In total, 264 ablation sessions were performed with a median number of treatment sessions per patient of 1 (range: 1–4). 137 patients required one session, 41 patients required two sessions and the remaining patients required three or more sessions. The median number of tumors treated per patient was 1 (range: 1–9).

Tumor characteristics

A total of 368 tumors spread across all liver segments were treated using MWA and either robotic-assistance or CT fluoroscopy (Table 2). The two most frequent tumor entities were hepatocellular carcinoma (n = 271) and liver metastasis of colorectal carcinoma (n = 54), followed by cholangiocellular carcinoma (n = 18). The median tumor size was 16 mm, with 59 tumors larger than 30 mm.

Primary technique efficacy and prognostic factors

The primary efficacy rate using robotic guidance was 88%, i.e., 219 of the 249 tumors were covered completely by the ablation volume. Needle repositioning was necessary in 92 of 249 ablations (37%). In contrast, the primary efficacy rate for freehand

TABLE 3. Influence of tumor characteristics on primary efficacy

Predictor		Estimate	Std.err	Wald	p-value
Long axis, mm	≤ 30	Reference			
	> 30	− 0.8717	0.3657	5.68	**0.0171**
Guidance	Freehand	Reference			
	Robotic	0.8064	0.3256	6.13	**0.0133**
Tumor entity	HCC	Reference			
	CRC	0.2922	0.4483	0.42	0.5145
	CCC	0.0665	0.6524	0.01	0.9188
	Other	0.0832	0.5228	0.03	0.8736
Liver segment	I	Reference			
	II	− 0.3956	1.0798	0.13	0.7141
	III	− 0.0449	1.1025	0.00	0.9675
	IVa	0.2688	1.1180	0.06	0.8100
	IVb	− 0.2539	1.1597	0.05	0.8267
	V	0.5961	1.1285	0.28	0.5974
	VI	0.9036	1.1736	0.59	0.4413
	VII	0.0656	1.1090	0.00	0.9528
	VIII	− 0.1069	1.0929	0.01	0.9221

CCC = cholangiocellular carcinoma; CRC = colorectal liver metastasis; HCC = hepatocellular carcinoma; Wald = $\chi 2$ test for the coefficients

TABLE 4. Monte Carlo simulation of primary technique efficacy rate depending on tumor size and antenna guidance

Long axis, mm	Guidance	CI-2.5%	Median	CI-97.5%
≤ 30	Freehand	0.60	0.75	0.86
> 30	Freehand	0.34	0.55	0.76
≤ 30	Robotic	0.78	0.87	0.92
> 30	Robotic	0.55	0.74	0.87

CI-2.5% and CI-97.5% = the central interval bounds at the lower 2.5 and upper 97.5 percentiles, respectively; Median = the simulated distribution's median

ablation was 76% (91 of 119 tumors). Logistic regression was performed to investigate whether tumor characteristics (size, entity and location) and the type of guidance (robotic or freehand) can impact primary technique efficacy (Table 3).

Compared with tumor size ≤ 3 cm, tumor size > 3 cm was a significantly unfavorable prognosticator of primary technique efficacy (odds ratio 0.42; p = 0.02). Compared with freehand antenna placement, robotic guidance was a significant favorable prognostic factor (odds ratio 2.24; p = 0.01). Table 4 shows estimations of the primary technique efficacy for robotic and freehand guidance.

Adverse events

141 (80.11%) of the robotic-guided and 62 (70.45%) of the CT-fluoroscopy-guided procedures were performed without any adverse events. Grade I (mild), II (moderate) and III (severe) adverse events occurred in 9 (5.11%), 6 (3.41%) and 1 (0.57%) of the robotic-guided procedures, respectively, and 3 (3.41%), 3 (3.41%) and 1 (1.14%) of the freehand-guided procedures, respectively.

Grade IV (life-threatening) adverse events occurred in 1 (0.57%) of the robotic-guided procedures and 2 (2.27%) of the freehand-guided procedures. The patient in the robotic-guided group suffered an injury to the 10th intercostal artery during ablation, which led to persistent bleeding and had to be treated with embolization. One of the patients in the freehand group, who had previously undergone partial liver resection and a consecutive Chilaiditi situation, had a perforation of a prolapsed intestinal loop that had to be surgically overstitched. The other patient in the freehand group suffered from bleeding from the 7th and 8th intercostal artery after ablation, which had to be closed by embolization.

Treatment-related patient death (Grade V) occurred in 1 (0.57%) of the robotic-guided procedures and 0 (0.00%) of the freehand guided procedures. A patient that had a previous liver and kidney transplant developed severe cholangitis two days after ablation and subsequent liver and kidney failure with lactate acidosis, which could not be controlled despite ultima ratio crush hepatectomy.

There was no significant difference in the frequency of adverse events (p = 0.07) between the two groups.

Discussion

In recent years, the importance of local ablative procedures for the treatment of liver tumors has steadily increased. It is well-known that an initial complete response is associated with improved survival from hepatocellular carcinoma and colorectal liver metastasis.[10,21] Therefore, the exact placement of the antenna is critically important to achieve complete ablation with a sufficient safety margin.

Navigation procedures are increasingly used to assist with accurate antenna placement. We have also switched from manual guidance to navigation in almost all cases. Only in very few cases (tumor right below diaphragm or right next to stomach) we switched to manual placement for better control. Although a very high accuracy of the robot-supported placement has already been shown[14,18] until now, it has not been clear whether this improves the primary efficacy, i.e., the percentage of target tumors successful eradicated.

Studies have shown that the robotic-guided approach improves the accuracy of targeting the tumor, reduces patient radiation dose and increases procedural performance when compared with conventional non-navigated antenna placement.[14,22-24] Other studies claim that there is no statistically significant reduction in the dose between the robotic-assisted and conventional method.[25] In one of our earlier studies, we showed that robotic assistance for liver tumor ablation reduces the patient radiation dose and allows a fast positioning of the microwave applicator with high accuracy.[18] Due to the small number of patients (n = 46) we could not show any significant difference in the primary efficacy rate. In one of our previous studies, we were able to show that additional overhead does not save time in the case of only one tumor, and that savings can only be expected in complex procedures.[26]

Although these previous studies have shown that antenna placement is highly accurate when using a robotic-guided navigation system, the impact of higher accuracy on the technical efficacy has not been investigated. In this study, we show for the first time in a large patient population (249 tumors ablated using robotic assistance) that robotic guidance is associated with a significantly higher technical success rate (primary efficacy rate using robotic guidance was 88%, primary efficacy rate for freehand ablation was 76%). From our point of view, this difference is very remarkable, because we had many years of expertise in manual guidance and still managed to achieve this improvement with the new type of navigation.

Although the large patient population indicates a high significance, some limitations have to be discussed. One aspect that needs to be considered is that interindividual differences could play a role. However, from our point of view, the high experience and the large number of ablations of each interventionalist speak against great interindividual differences. In addition, the learning curve also plays a role, which undoubtedly occurs over time, as Beermann *et al.* also stated.[27]

In summary, our study was the first to show that robotic-guided antenna placement goes hand in hand with a higher primary efficacy.

References

1. Kokudo N, Hasegawa K, Akahane M, Igaki H, Izumi N, Ichida T, et al. Evidence-based clinical practice guidelines for hepatocellular carcinoma: The Japan Society of Hepatology 2013 update (3rd JSH-HCC Guidelines). *Hepatol Res* 2015; **45:** n/a-n/a. doi: 10.1111/hepr.12464
2. Ruers T, Van Coevorden F, Punt CJ, Pierie JE, Borel-Rinkes I, Ledermann JA, et al. Local treatment of unresectable colorectal liver metastases: results of a randomized Phase II trial. *JNCI J Natl Cancer Inst* 2017; **109:** 9. doi: 10.1093/jnci/djx015
3. Facciorusso A, Di Maso M, Muscatiello N. Microwave ablation versus radiofrequency ablation for the treatment of hepatocellular carcinoma: a systematic review and meta-analysis. *Int J Hyperth* 2016; **32:** 339-44. doi: 10.3109/02656736.2015.1127434
4. Vogl TJ, Farshid P, Naguib NN, Zangos S, Bodelle B, Paul J, et al. Ablation therapy of hepatocellular carcinoma: a comparative study between radiofrequency and microwave ablation. *Abdom Imaging* 2015; **40:** 1829-37. doi: 10.1007/s00261-015-0355-6
5. Abdelaziz AO, Nabeel MM, Elbaz TM, Shousha HI, Hassan EM, Mahmoud SH, et al. Microwave ablation versus transarterial chemoembolization in large hepatocellular carcinoma: prospective analysis. *Scand J Gastroenterol* 2015; **50:** 479-84. doi: 10.3109/00365521.2014.1003397
6. Chu KF, Dupuy DE. Thermal ablation of tumours: biological mechanisms and advances in therapy. *Nat Rev Cancer* 2014; **14:** 199-208. doi: 10.1038/nrc3672
7. van Amerongen MJ, Jenniskens SFM, van den Boezem PB, Fütterer JJ, de Wilt JHW. Radiofrequency ablation compared with surgical resection for curative treatment of patients with colorectal liver metastases – a meta-analysis. *HPB* 2017; **19:** 749-56. doi: 10.1016/j.hpb.2017.05.011
8. Wang Y, Luo Q, Li Y, Deng S, Wei S, Li X. Radiofrequency ablation versus hepatic resection for small hepatocellular carcinomas: a meta-analysis of randomized and nonrandomized controlled trials. *PLoS One* 2014; **9:** e84484. doi: 10.1371/journal.pone.0084484
9. Xu Q, Kobayashi S, Ye X, Meng X. Comparison of hepatic resection and radiofrequency ablation for small hepatocellular carcinoma: a meta-analysis of 16,103 patients. *Sci Rep* 2015; **4:** 7252. doi: 10.1038/srep07252
10. Sala M, Llovet JM, Vilana R, Bianchi L, Solé M, Ayuso C, et al. Initial response to percutaneous ablation predicts survival in patients with hepatocellular carcinoma. *Hepatology* 2004; **40:** 1352-60. doi: 10.1002/hep.20465
11. Kurilova I, Gonzalez-Aguirre A, Beets-Tan RG, Erinjeri J, Petre EN, Gonen M, et al. Microwave ablation in the management of colorectal cancer pulmonary metastases. *Cardiovasc Intervent Radiol* 2018; **41:** 1530-44. doi: 10.1007/s00270-018-2000-6
12. Ke S, Ding XM, Qian XJ, Zhou YM, Cao BX, Gao K, et al. Radiofrequency ablation of hepatocellular carcinoma sized > 3 and ≤ 5 cm: is ablative margin of more than 1 cm justified? *World J Gastroenterol* 2013; **19:** 7389-98. doi: 10.3748/wjg.v19.i42.7389
13. Schaible J, Pregler B, Baümler W, Einspieler I, Jung EM, Stroszczynski C, et al. Safety margin assessment after microwave ablation of liver tumors: inter- and intrareader variability. *Radiol Oncol* 2020; 54(3): 295-300.; **54:** 57-61. doi: 10.2478/raon-2020-0004
14. Mbalisike EC, Vogl TJ, Zangos S, Eichler K, Balakrishnan P, Paul J. Image-guided microwave thermoablation of hepatic tumours using novel robotic guidance: an early experience. *Eur Radiol* 2015; **25:** 454-62. doi: 10.1007/s00330-014-3398-0
15. Bale R, Widmann G, Schullian P, Haidu M, Pall G, Klaus A, et al. Percutaneous stereotactic radiofrequency ablation of colorectal liver metastases. *Eur Radiol* 2012; **22:** 930-37. doi: 10.1007/s00330-011-2314-0
16. Beyer LP, Michalik K, Niessen C, Platz Batista da Silva N, Wiesinger I, Stroszczynski C, et al. Evaluation of a robotic assistance-system for percutaneous computed tomography-guided (CT-guided) facet joint injection: a phantom study. *Med Sci Monit* 2016; **22:** 3334-9. doi: 10.12659/MSM.900686
17. Solomon SB, Patriciu A, Bohlman ME, Kavoussi LR, Stoianovici D. Robotically driven interventions: a method of using CT fluoroscopy without radiation exposure to the physician. *Radiology* 2002; **225:** 277-82. doi: 10.1148/radiol.2251011133

18. Beyer LP, Pregler B, Niessen C, Dollinger M, Graf BM, Müller M, et al. Robot-assisted microwave thermoablation of liver tumors: a single-center experience. *Int J Comput Assist Radiol Surg* 2016; **11:** 253-9. doi: 10.1007/s11548-015-1286-y

19. Beyer LP, Pregler B, Michalik K, Niessen C, Dollinger M, Müller M, et al. Evaluation of a robotic system for irreversible electroporation (IRE) of malignant liver tumors: initial results. *Int J Comput Assist Radiol Surg* 2017; **12:** 803-9. doi: 10.1007/s11548-016-1485-1

20. Ahmed M, Solbiati L, Brace CL, Breen DJ, Callstrom MR, Charboneau JW, et al Image-guided tumor ablation: standardization of terminology and reporting criteria - 10-year update. *Radiology* 2014; **273:** 241-60. doi: 10.1148/radiol.14132958

21. Solbiati L, Ahmed M, Cova L, Ierace T, Brioschi M, Goldberg SN. Small liver colorectal metastases treated with percutaneous radiofrequency ablation: local response rate and long-term survival with up to 10-year follow-up. *Radiology* 2012; **265:** 958-68. doi: 10.1148/radiol.12111851

22. Koethe Y, Xu S, Velusamy G, Wood BJ, Venkatesan AM. Accuracy and efficacy of percutaneous biopsy and ablation using robotic assistance under computed tomography guidance: a phantom study. *Eur Radiol* 2014; **24:** 723-30. doi: 10.1007/s00330-013-3056-y

23. Hiraki T, Matsuno T, Kamegawa T, Komaki T, Sakurai J, Matsuura R, et al. Robotic insertion of various ablation needles under computed tomography guidance: accuracy in animal experiments. *Eur J Radiol* 2018; **105:** 162-7. doi: 10.1016/j.ejrad.2018.06.006

24. Heerink WJ, Ruiter SJS, Pennings JP, Lansdorp B, Vliegenthart R, Oudkerk M, et al. Robotic versus freehand needle positioning in CT-guided ablation of liver tumors: a randomized controlled trial. *Radiology* 2019; **290:** 826-32. doi: 10.1148/radiol.2018181698

25. Abdullah BJJ, Yeong CH, Goh KL, Yoong BK, Ho GF, Yim CCW, et al. Robotic-assisted thermal ablation of liver tumours. *Eur Radiol* 2015; **25:** 246-57. doi: 10.1007/s00330-014-3391-7

26. Beyer LP, Lürken L, Verloh N, Haimerl M, Michalik K, Schaible J, et al. Stereotactically navigated percutaneous microwave ablation (MWA) compared to conventional MWA: a matched pair analysis. *Int J Comput Assist Radiol Surg* 2018; **13:** 1991-7. doi: 10.1007/s11548-018-1778-7

27. Beermann M, Lindeberg J, Engstrand J, Galmén K, Karlgren S, Stillström D, et al. 1000 consecutive ablation sessions in the era of computer assisted image guidance – lessons learned. *Eur J Radiol Open* 2019; **6:** 1-8. doi: 10.1016/j.ejro.2018.11.002

research article

Simplified perfusion fraction from diffusion-weighted imaging in preoperative prediction of *IDH1* mutation in WHO grade II-III gliomas: comparison with dynamic contrast-enhanced and intravoxel incoherent motion MRI

Xiaoqing Wang[1], Mengqiu Cao[1], Hongjin Chen[2], Jianwei Ge[2], Shiteng Suo[1], Yan Zhou[1]

[1] Department of Radiology, Renji Hospital, School of Medicine, Shanghai Jiao Tong University, Shanghai, China,
[2] Department of Neurosurgery, Renji Hospital, School of Medicine, Shanghai Jiao Tong University, Shanghai, China

Radiol Oncol 2020; 54(3): 301-310.

Received 23 March 2020
Accepted 13 May 2020

Correspondence to: Yan Zhou, Department of Radiology, Renji Hospital, School of Medicine, Shanghai Jiao Tong University, 160 Pujian Road, Pudong New District, Shanghai, China. E-mail: clare1475@hotmail.com

Disclosure: No potential conflicts of interest were disclosed.

Background. Effect of isocitrate dehydrogenase 1 (*IDH1*) mutation in neovascularization might be linked with tissue perfusion in gliomas. At present, the need of injection of contrast agent and the increasing scanning time limit the application of perfusion techniques. We used a simplified intravoxel incoherent motion (IVIM)-derived perfusion fraction (*SPF*) calculated from diffusion-weighted imaging (DWI) using only three b-values to quantitatively assess *IDH1*-linked tissue perfusion changes in WHO grade II-III gliomas (LGGs). Additionally, by comparing accuracy with dynamic contrast-enhanced (DCE) and full IVIM MRI, we tried to find the optimal imaging markers to predict *IDH1* mutation status.

Patients and methods. Thirty patients were prospectively examined using DCE and multi-b-value DWI. All parameters were compared between the *IDH1* mutant and wild-type LGGs using the Mann–Whitney U test, including the DCE MRI-derived K^{trans}, v_e and v_p, the conventional apparent diffusion coefficient ($ADC_{0,1000}$), IVIM-derived perfusion fraction (*f*), diffusion coefficient (*D*) and pseudo-diffusion coefficient (*D**), *SPF*. We evaluated the diagnostic performance by receiver operating characteristic (ROC) analysis.

Results. Significant differences were detected between WHO grade II-III gliomas for all perfusion and diffusion parameters ($P < 0.05$). When compared to *IDH1* mutant LGGs, *IDH1* wild-type LGGs exhibited significantly higher perfusion metrics ($P < 0.05$) and lower diffusion metrics ($P < 0.05$). Among all parameters, *SPF* showed a higher diagnostic performance (area under the curve 0.861), with 94.4% sensitivity and 75% specificity.

Conclusions. DWI, DCE and IVIM MRI may noninvasively help discriminate *IDH1* mutation statuses in LGGs. Specifically, simplified DWI-derived *SPF* showed a superior diagnostic performance.

Key words: *IDH1* mutation; glioma perfusion; diffusion-weighted MRI; dynamic contrast-enhanced MRI; intravoxel incoherent motion; 2016 WHO CNS tumor classification

Introduction

Gliomas, the most common primary intracranial neoplasms in humans, are classified as grade I–IV based on histopathological criteria. Different from grade IV, also known as glioblastoma, the outcome of grade II-III gliomas (lower-grade gliomas, LGGs) are highly variable. Published survival duration of LGGs ranged from 1 to over 15 years, reflecting molecular heterogeneity of these tumors.[1-5] The 2016 revised fourth edition of the World Health Organization (WHO) classification of tumors of

 doi: 10.2478/raon-2020-0037

the central nervous system defines a large subset of gliomas based on molecular alterations, among which mutation of isocitrate dehydrogenase (*IDH1*) has shown to be the most important, for this mutation is thought to be a predictor of early steps in gliomagenesis. It has been shown that 70%–90% of LGGs- carry *IDH1* mutations, and that *IDH1* mutant glioma have a survival benefit associated with the maximal surgical resection, and the use of radiation and chemical therapy.[6-8] Hence, assessing grade II and III gliomas by genetic alteration, which might be helpful for patient prognosis and clinical treatment, is now a common clinical practice.

The *IDH1* gene plays an important role in tumor angiogenesis and vasculogenesis, which have been recognized as hallmarks of histopathological growth and progression of gliomas.[9-11] Therefore, preoperative assessment of tumor perfusion by MRI may give insight into the *IDH1* mutation status, thus aiding in clinical decision making. Several MR perfusion techniques have been developed to evaluate the degree of tissue vascularization. Dynamic contrast-enhanced (DCE) MRI and intravoxel incoherent motion (IVIM) MRI are two common MR perfusion techniques with distinct imaging mechanisms.[11-15]

Using rapid T1-weighted imaging to measure the changes resulting from gadolinium contrast agent leakage in and out of the extracellular extravascular space, DCE MRI enables the determination of several hemodynamic parameters, including the volume transfer constant (K^{trans}), the extravascular extracellular volume fraction (v_e), and the vascular plasma volume fraction (v_p).[11,16] Previous studies have demonstrated the clinical potential of DCE MRI in glioma grading and differential diagnosis.[17,18] However, the need for an intravenous injection of contrast agent limits its clinical application in patients with renal dysfunction or individuals who are allergic to gadolinium.

IVIM MRI is a variant of conventional diffusion-weighted imaging (DWI) in that images at multiple b-values are required to fit the two-component mathematical model. In this model, the effect of microcirculation of blood in the capillary network (characterized by the pseudo-diffusion coefficient D^*) is separated from the pure water diffusion component (characterized by the diffusion coefficient D). More than eight b-values are typically needed to fully characterize biexponential signal attenuation, thus increasing the scanning time. Some simplified models based on IVIM theory with fewer b-values have been proposed. Both the full and simplified IVIM models have shown their abilities in characterizing tumor perfusion and assessing the glioma grade.[19-21]

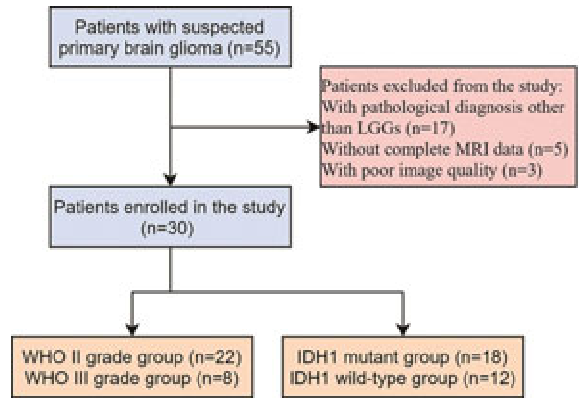

FIGURE 1. Flowchart of study design.

The purpose of our study, therefore, was to determine the association of the three b-value DWI-derived simplified perfusion fraction (*SPF*) with tumor perfusion and to compare the performance with DCE and IVIM MRI-derived parameters in the preoperative prediction of *IDH1* mutation status in LGGs using surgical and histopathological findings as a standard of reference.

Patients and methods

Patient enrollment

This prospective single-center study was performed in accordance with the principle of the Declaration of Helsinki and was approved by the local ethics committee. Written informed consent was obtained from all subjects prior to study enrollment. The flowchart of the study design is demonstrated in Figure 1.

From April 2018 to March 2019, 55 patients who were suspected of primary brain tumors were prospectively enrolled in the study. All patients underwent initial MRI at the same unit and were then underwent neurosurgical resection at our hospital. Excluded from the study were 17 patients with pathological diagnosis other than LGGs, five patients without complete DCE MRI or IVIM data, and three patients due to poor image quality associated with head movement. Finally, a total of 30 patients (13 women, 17 men; average age, 44.73 years; age range, 19–78 years) with histopathologically confirmed LGGs (WHO II glioma, $n = 22$; WHO III glioma, $n = 8$) were enrolled. The descriptive statistics are shown in Table 1.

MRI acquisition protocols

MRI of all patients was performed on a 3.0-T MRI unit (Signa HDxt; GE Medical Systems, Milwaukee, WI, USA) using a standard 8-channel head coil. The advanced MRI protocol included DCE MRI and DWI with 10 b-values (0–1000 s/mm^2). Conventional protocol—T1- and T2-weighted imaging with fast spin-echo sequences (T1WI, T2WI), T2 fluid-attenuated inversion recovery (FLAIR) sequence, and contrast-enhanced T1WI— were performed during the same examination.

Three-dimensional DCE MRI of head was performed after intravenous administration of a gadopentetate dimeglumine (Magnevist; Bayer Healthcare, Berlin, Germany, 0.1 mmol per kilogramof body weight) at a rate of 4 ml/s via a power injector (Spectris; Medrad, Pittsburgh, PA, USA). Precontrast scans with four dynamics were collected before gadopentetate dimeglumine was injected. The detailed parameters of the pre- and postcontrast scans were as follows: repetition time (TR)/echo time (TE), 3.3 ms/1.3 ms, flip angle, 15°; matrix, 256 × 160; field of view (FOV), 220 × 220 mm; section thickness, 2 mm; number of sections, 40; and total scanning time, 4 min.

DWI was acquired before contrast injection. Ten b-values (0, 20, 50, 80, 150, 200, 300, 500, 800, and 1000 s/mm^2) were applied with a fat-suppressed single-shot echo-planar sequence in three orthogonal directions sequentially, they were averaged two times, and then trace images were generated. The other imaging parameters were: TR/TE, 3000 ms/106 ms; matrix, 192 × 192; FOV, 260 × 260 mm; section thickness/gap, 5/1 mm; number of signal averages, 2; number of sections, 15. The multi-b-value DWI was acquired at 5 min and 36 s, and if separately, 2 min and 11 s for three-b-value DWI.

MR image analysis

DCE MRI analysis

Pharmacokinetic parameters (K^{trans}, v_e, v_p) were calculated off-line by using commercially available software (MIStar; Apollo Medical Imaging, Melbourne, VIC, Australia) according to the two-compartment Tofts model.[22] Preprocessing for the perfusion data included semiautomatic selection of arterial input function (AIF). The AIF was obtained independently for every patient from the intracranial internal carotid artery. Parametric maps of K^{trans}, v_e, and v_p were generated on a pixel-by-pixel basis.

TABLE 1. Patient characteristics

Characteristic	*IDH1* mutants (*n* = 18)	*IDH1* wild-type (*n* = 12)
Mean age (y)[a]	42.8 (22–67)	47.9 (19–78)
Sex distribution (M/F)[b]	10/8	7/5
WHO grade		
II	15	7
III	3	5
Histologic type		
Astrocytoma	12	5
Oligodendroglioma	3	0
Oligoastrocytoma	0	1
Anaplastic astrocytoma	1	3
Anaplastic oligodendroglioma	1	2
Anaplastic oligoastrocytoma	1	1

* Mean (range) or count is reported; a = significant difference in age was noted between isocitrate dehydrogenase 1 (*IDH1*) mutant and wild-type groups (P = 0.020); b = no significant difference in sex distribution was noted between *IDH1* mutant and wild-type groups (P = 0.769)

F = female; M = male

DWI analysis

DWI data were performed with a program in MATLAB (MATLAB 2017a; MathWorks, Natick, MA, USA) programming tool. Full IVIM features - the diffusion coefficient (D), pseudo-diffusion coefficient (D^*), and the perfusion fraction (f)—were extracted by fitting the biexponential model using all b-values as follows:

$$S_b = S_0[f_{exp}(-bD^*) + (1 - f)\,exp(-bD)],$$

where S_b stands for the signal intensity in present b-value and S_0 stands for the signal intensity in the absence of diffusion gradient.

The monoexponential DWI model used in calculating the ADC value can be written as follows:

$$ADC_{low,high} = -ln\,(S_{low}/S_{high})/\,(b_{low} - b_{high}),$$

where S_{high} is signal intensity at b_{high} and S_{low} is signal intensity at b_{low}, respectively. As the b-value has a differential sensitivity to Brownian motion of water protons, $ADC_{0,200}$ represents mixed diffusion and perfusion effects and $ADC_{200,1000}$ is almost purely related to diffusion.[23,24] The b-value scheme was chosen following previous recommendations[25-27] which indicated that the effects of diffusion and microcapillary perfusion are both reflected within low b-values (b < 200 s/mm^2), while for higher b-values (b > 200 s/mm^2), a large proportion of measured signal in each imaging voxel was caused by tissue diffusion. When a typical b-value (1000 s/mm^2) was used, the contribution of perfusion has

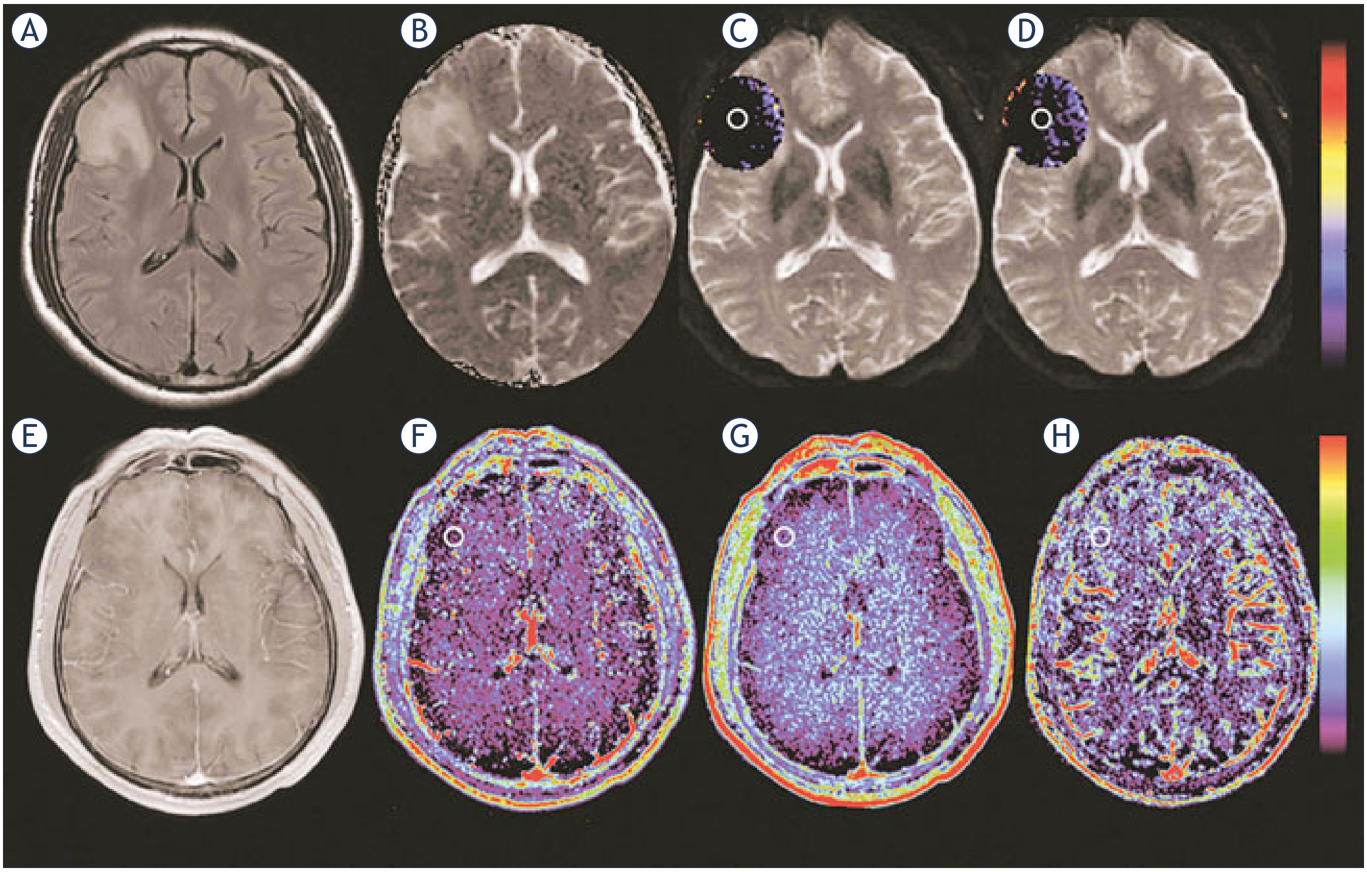

FIGURE 2. Images obtained in a 44-year-old man with astrocytoma (isocitrate dehydrogenase 1 [*IDH1*] mutant glioma). **(A)** Fluid-attenuated inversion recovery (FLAIR) image shows a heterogeneous hyperintense lesion in the right frontal lobe. **(B)** Apparent diffusion coefficient $(ADC)_{0,1000}$ map shows increased *ADC* value in the lesion. **(C, D)** Intravoxel incoherent motion (IVIM) perfusion fraction (*f*) and simplified perfusion fraction (*SPF*) maps show no increased values in the corresponding area of the hyperintense lesion as shown in **(A)**. **(E)** On contrast-enhanced T1-weighted image, the lesion is non-enhancing. **(F-H)** Dynamic contrast-enhanced (DCE) MRI parametric maps of volume transfer constant (K^{trans}), extravascular extracellular volume fraction (v_e) and vascular plasma volume fraction (v_p) show no increased values in the lesion. Regions of interest are marked on parametric maps.

TABLE 2. Parameters derived from dynamic contrast-enhanced (DCE) MRI and diffusion-weighted imaging (DWI) between WHO grade II and III gliomas

Parameter	Grade II	Grade III	*P*-value
K^{trans} (min^{-1})	0.067 ± 0.048	0.116 ± 0.064	0.013
v_e	0.071 ± 0.057	0.401 ± 0.344	0.018
v_p	0.036 ± 0.020	0.051 ± 0.018	0.035
$ADC_{0,1000}$ (×10^{-3} mm^2/s)	1.093 ± 0.203	0.904 ± 0.184	0.028
SPF (%)	10.78 ± 4.378	16.391 ± 5.471	0.012
D (×10^{-3} mm^2/s)	1.194 ± 0.261	0.949 ± 0.169	0.021
*D** (×10^{-3} mm^2/s)	6.692 ± 1.564	8.618 ± 2.215	0.037
f (%)	3.315 ± 1.536	6.380 ± 3.419	0.020

* *P*-values are considered significant at $P < 0.05$.

ADC = apparent diffusion coefficient; *D* = diffusion coefficient; *D** = pseudo-diffusion coefficient; *f* = perfusion fraction; K^{trans} = volume transfer constant; v_e = extravascular extracellular volume fraction; v_p = vascular plasma volume fraction; *SPF* = simplified perfusion fraction

faded away entirely. The *ADC* thus appears to be a sensitive index of diffusion component. On the other hand, since a b-value of 1000 s/mm^2 is small enough, high image quality may be guaranteed and the kurtosis effect may be avoided. As the contribution of kurtosis is greater when b-value is beyond 1000 s/mm^2.[28,29] Therefore, the relative proportion of the perfusion component in the whole diffusion pool, named *SPF*, can be determined as follows (20):

$$SPF = (ADC_{0,200} - ADC_{200,1000})/ADC_{0,200}.$$

Region of interest analysis

The regions of interest (ROIs) were drawn by two readers who have 6(M.C.) and 19(Y.Z.) years of experience in neuroradiology, respectively, and con-

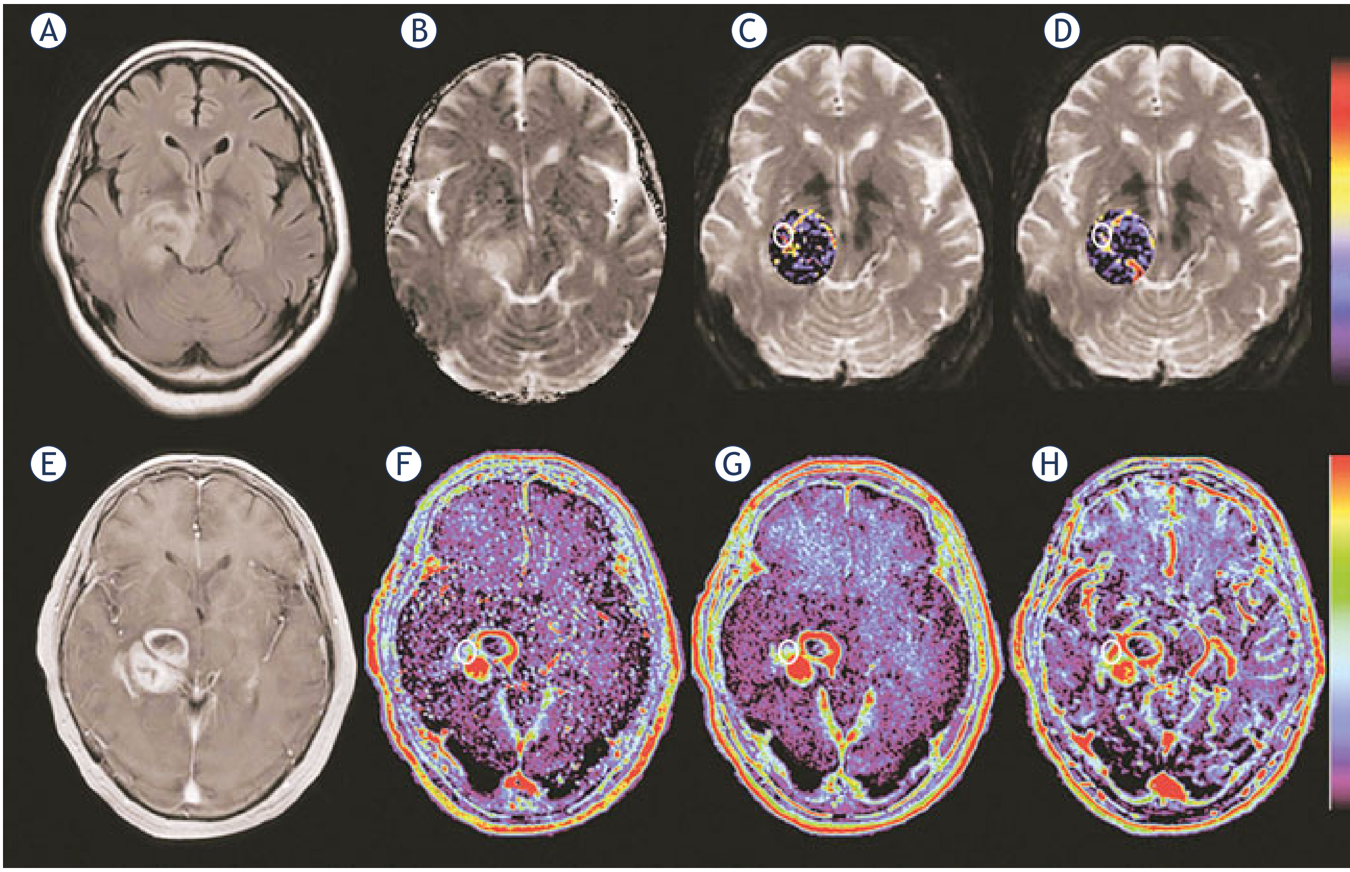

FIGURE 3. Images obtained in a 72-year-old woman with astrocytoma (isocitrate dehydrogenase 1 [*IDH1*] wildtype glioma). **(A)** FLAIR shows a heterogeneous hyperintense lesion in the right hemisphere. **(B)** Apparent diffusion coefficient $(ADC)_{0,1000}$ map shows a mixed pattern of high and intermediate *ADC* values in the lesion. **(C, D)** Intravoxel incoherent motion (IVIM) perfusion fraction (*f*) and simplified perfusion fraction (*SPF*) maps show markedly increased *f* and *SPF* values in the corresponding area of the contrast-enhanced lesion as shown in **(E)**. **(E)** On contrast-enhanced T1-weighted image, the lesion is vividly enhanced. **(F-H)** Dynamic contrast-enhanced (DCE) MRI parametric maps of volume transfer constant (K^{trans}), extravascular extracellular volume fraction (v_e) and vascular plasma volume fraction (v_p) show obviously increased values in the corresponding area of the contrast-enhanced lesion. Regions of interest are marked on parametric maps.

sensus was researched. Both readers were blinded to the histopathological results and other clinical data, including age and gender. Following previous studies[30,31], an elliptical ROI (20–340 mm^2) was placed by each doctor on parametric maps of the solid tumor area as much as possible to include the portion with the minimum values of diffusion (D and $ADC_{0,1000}$) and maximum values of perfusion (*SPF*, *f*, *D**, K^{trans}, v_p, and v_e). For correlation analysis between *SPF* and other perfusion parameters, the similar-sized ROIs used for *SPF* images were placed in the corresponding area of DCE images and IVIM images. T1-weighted contrast-enhanced images where contrast agent leakage in tumors was observed were used as a reference to define the ROIs on parametric maps.[32,33] The study used *ADC* images combined with T1-weighted, T2-weighted, and FLAIR images to determine the ROI of tumor

TABLE 3. Parameters derived from dynamic contrast-enhanced (DCE) MRI and diffusion-weighted imaging (DWI) between isocitrate dehydrogenase 1 (*IDH1*) mutant and wild-type gliomas

Parameter	*IDH1* mutant	*IDH1* wild-type	*P*-value*
K^{trans} (min^{-1})	0.054 ± 0.024	0.123 ± 0.073	0.007
v_e	0.052 ± 0.035	0.121 ± 0.080	0.007
v_p	0.032 ± 0.015	0.051 ± 0.022	0.015
$ADC_{0,1000}$ (×10^{-3} mm^2/s)	1.123 ± 0.185	0.923 ± 0.199	0.009
SPF (%)	9.572 ± 3.437	16.332 ± 4.925	< 0.001
D (×10^{-3} mm^2/s)	1.108 ± 0.245	0.959 ± 0.146	0.047
*D** (×10^{-3} mm^2/s)	6.546 ± 1.757	8.196 ± 1.794	0.020
f (%)	3.080 ± 1.581	5.712 ± 2.924	0.005

* *P*-values are considered significant at $P < 0.05$

ADC = apparent diffusion coefficient; *D* = diffusion coefficient; *D** = pseudo-diffusion coefficient; K^{trans} = volume transfer constant; *f* = perfusion fraction; *SPF* = simplified perfusion fraction; v_e = extravascular extracellular volume fraction; v_p = vascular plasma volume fraction

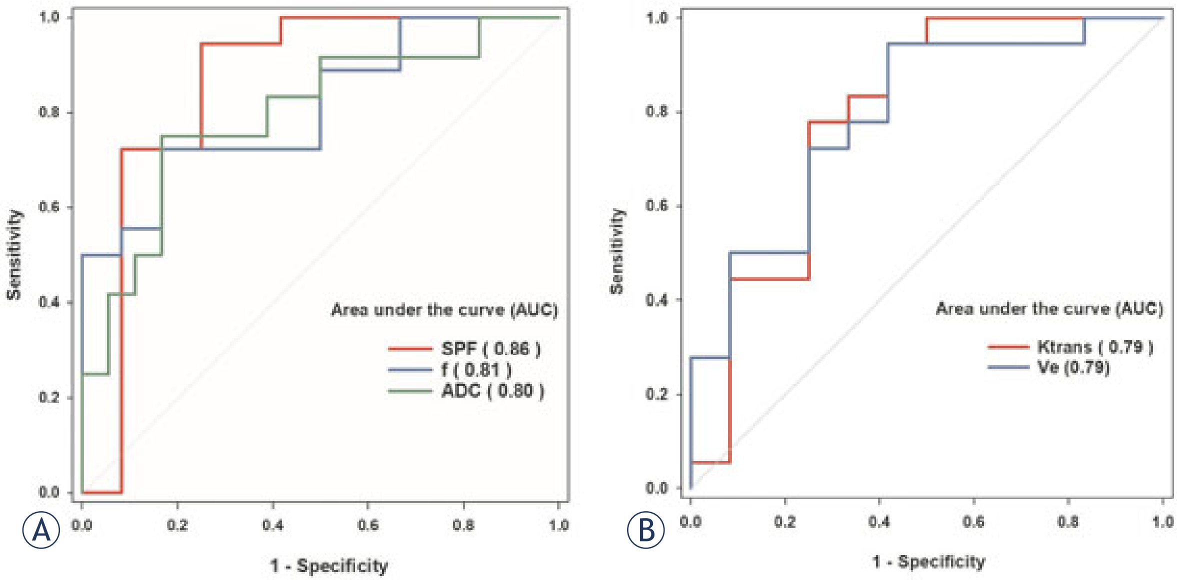

FIGURE 4. Receiver operating characteristic (ROC) curves and corresponding area under the curve values for **(A)** diffusion-weighted imaging (DWI) parameters (simplified perfusion fraction [*SPF*], perfusion fraction [*f*], apparent diffusion coefficient $[ADC]_{0,1000}$) and **(B)** dynamic contrast-enhanced (DCE) MRI parameters (transfer constant [K^{trans}], extravascular extracellular volume fraction [v_e] and vascular plasma volume fraction [v_p]) in the differentiation of isocitrate dehydrogenase 1 (*IDH1*) mutant and wildtype gliomas. *SPF* showed the highest diagnostic performance with the area under the curve value of 0.86.

area in nonenhancing lesion. Special care was taken to exclude necrosis, cysts, hemorrhage, calcification, and intralesional macrovessels.

Statistical analysis

Statistical analysis was performed using commercial software (SPSS version 22, IBM Corporation, Armonk, NY, USA and MedCalc, version 11.4.2.0, MedCalc Software, Mariakerke, Belgium). The relationship between perfusion parameters was analyzed with Spearman rank correlation. We considered correlation coefficients < 0.4, 0.4–0.6, 0.6–0.8, and > 0.8 to indicate week, moderate, strong, and very strong correlation, respectively. The unpaired t-test and Mann–Whitney U test were used to determine the difference in DWI, DCE and IVIM MRI parameters between WHO grade II and III gliomas, as well as between *IDH1* mutant and wild-type gliomas, according to the data normality (Kolmogorov-Smirnov test). ROC curves were constructed to evaluate the ability to identify different *IDH1* mutation statuses. Area under the curve (AUC) values of < 0.7, 0.7–0.9, and

TABLE 4. Diagnostic performance of parameters for differentiation between isocitrate dehydrogenase 1 (*IDH1*) mutant and wild-type gliomas

Parameter	AUC (95% CI)	Sensitivity (%)	Specificity (%)	Cutoff value
K^{trans} (min^{-1})	0.773 (0.563–0.983)	77.8	75.0	> 0.062
v_e	0.760 (0.569–0.951)	94.4	58.3	> 0.119
v_p	0.680 (0.451–0.909)	55.6	91.7	> 0.029
$ADC_{0,1000}$ (×10^{-3} mm^2/s)	0.718 (0.531–0.904)	83.3	75.0	≤ 1.002
SPF (%)	0.861 (0.686–0.959)	94.4	75.0	> 14.500
D (×10^{-3} mm^2/s)	0.727 (0.541–0.913)	72.2	83.3	> 1.065
*D** (×10^{-3} mm^2/s)	0.690 (0.493–0.886)	44.4	91.4	≤ 5.959
f (%)	0.810 (0.658–0.963)	72.2	83.3	> 3.617

ADC = apparent diffusion coefficient; *D* = diffusion coefficient; *D** = pseudo-diffusion coefficient; *f* = perfusion fraction;*K^{trans} = volume transfer constant; *SPF* = simplified perfusion fraction; v_e = extravascular extracellular volume fraction; v_p = vascular plasma volume fraction

> 0.9 were considered to indicate low, medium, and high diagnostic performance, respectively. Differences between AUC values were analyzed by using the Delong method (34). Optimal thresholds were determined by maximizing the Youden index ((specificity + sensitivity) − 1). A *P*-value less than 0.05 was considered to indicate statistical significance.

Results

In terms of histology, 16 patients had astrocytomas, three had oligodendrogliomas, one had an oligoastrocytoma, four had anaplastic astrocytomas, three had anaplastic oligodendrogliomas, and three had anaplastic oligoastrocytomas. Intercorrelation analysis between perfusion parameters revealed a significant association for *SPF* and *f* ($\varrho = 0.768$, $P < 0.001$). The study also found a moderate correlation between *SPF* and v_e ($\varrho = 0.548$, $P = 0.002$) and between *SPF* and K^{trans} ($\varrho = 0.535$, $P = 0.002$).

The statistical data of DCE MRI and DWI-derived parameters in differentiating WHO grade II and III gliomas are summarized in Table 2. Perfusion-related parameters including K^{trans}, v_e, v_p, *f*, *D**, and *SPF* were all significantly higher in WHO grade III gliomas than in WHO grade II gliomas (all $P < 0.05$), while *ADC* and *D* values were both significantly lower in WHO grade III gliomas (both $P < 0.05$).

Representative cases of *IDH1* mutant and wild-type LGGs are shown in Figures 2 and 3. The mean values ± standard deviations of DCE MRI and DWI-derived parameters for the *IDH1* mutant and wild-type tumors in the whole LGGs group, are summarized in Table 3. Compared with *IDH1* mutant LGGs, *IDH1* wild-type LGGs exhibited significantly higher perfusion values, that is, K^{trans}, v_e, v_p, *f*, *D**, and *SPF* (all $P < 0.05$), and significantly lower diffusion values, that is, *ADC* and *D* (both $P < 0.05$). In the WHO grade II subgroup, v_p and *SPF* differed significantly between *IDH1* mutant and wild-type tumors ($P = 0.018$ and $P = 0.049$, respectively), whereas in the WHO grade III subgroup, only *f* showed a significant difference ($P = 0.014$).

The results of ROC curve analysis are presented in Figure 4 and Table 4. For differentiation between *IDH1* mutant and wild-type LGGs, the ROC curve analysis showed that among all parameters, *SPF* gave the highest AUC value (0.86), followed by *f* (0.81) and *ADC* (0.80), though no significant difference in AUC values was found ($P > 0.05$). The optimal *SPF* threshold for *IDH1* mutation discrimination was 14.5%, with a sensitivity and specificity of 94.4% and 75.0%, respectively.

Discussion

In this study, an analysis of DWI, DCE, and IVIM MRI was performed to evaluate the tissue diffusion and perfusion characteristics to identify histological and molecular profiles of LGGs. Our results showed that diffusion and perfusion metrics exhibited substantial differences between WHO grade II and III gliomas, as well as between *IDH1* mutant and wild-type LGGs. Among all parameters, the simplified DWI-derived perfusion fraction showed higher efficacy in *IDH1* mutation detection, indicating that this recently developed three-b-value DWI approach may serve as a surrogate method for LGGs molecular diagnosis.

DWI, DCE, and IVIM MRI-derived parameters showed significant differences between grade II and III gliomas. Diffusion-related parameters, including *ADC* and *D* values, were significantly lower in WHO grade III gliomas; this result is in line with those of previous studies.[19,35] It is now well established that *ADC* is strongly correlated with cellularity and the nuclear cytoplasmic ratio in tumor tissue[36-38], both of which are important criteria in the histopathological grading of gliomas.

Notably, perfusion-related parameters, especially *SPF*, *f*, and K^{trans}, showed a relatively good performance for glioma grading compared with diffusion parameters. This is most likely due to the increased perfusion feature in higher grade gliomas; K^{trans} reflects the volume transfer constant of a contrast agent from the plasma space to the extravascular extracellular space.[39,40] In higher-grade gliomas, active angiogenesis and incomplete basement membrane of tumor neovasculature lead to an increment in microvascular permeability, thus a high K^{trans} value. A previous study[13] showed that *SPF* and IVIM-derived *f* correlated well with DCE MRI-derived K^{trans} and were useful in differentiating high- from low-grade gliomas. Our results further show that *f* and *SPF* also exhibited significant differences between WHO grade II and III gliomas.

Over the last decade, studies have shown that gliomas with *IDH* mutation are less aggressive and more sensitive to chemotherapy, contributing to a longer overall survival.[41-44] Therefore, *IDH* plays a key role in the determination of the glioma molecular phenotype. Zhao *et al.*[45] have shown that compared with *IDH1* mutant gliomas, *IDH1* wild-type gliomas are characterized by increased neoangiogenesis and a higher nuclear cytoplasmic ratio due to the infiltrative nature. Higher vascular proliferation leads to stronger perfusion effects. In this study, DWI, DCE, and IVIM MRI-derived perfusion parameters all showed significant differences between *IDH1* mutant and wild-type LGGs. Elevated perfusion was observed in *IDH1* wild-type LGGs, which is in agreement with several previous reports using other perfusion imaging techniques.[46-48] For example, Kickingereder *et al.*[46] and Brendle *et al.*[48] performed dynamic susceptibility contrast and arterial spin labeling perfusion-weighted imaging on patients with LGGs, respectively, and both found significantly higher cerebral blood flow values in *IDH1* wild-type LGGs. This could be explained by considering the molecular function of *IDH1*. Cui *et al.*[49] and Reis *et al.*[50] suggested that *IDH1* mutation is associated with decreased invasiveness and reduced angiogenesis via downregulation of the Wnt/β-catenin signaling pathway. Furthermore, the accumulation of 2-hydroxyglutarate, an oncometabolite produced upon *IDH1* mutation, has been shown to affect hypoxia-inducible factor (HIF) levels and the HIF response and may, consequently, reduce hypoxia-induced neovascularization.[51]

According to our ROC curve analysis, the simplified DWI-derived perfusion fraction showed a superior diagnostic accuracy as a predictor for *IDH1* mutation in LGGs compared to the full IVIM-derived *f*. This result suggests that the three-b-value simplified DWI approach could save substantial scanning time compared with the full IVIM approach, with no loss of diagnostic efficiency. Additionally, both simplified and full IVIM perfusion performed better than DCE MRI. These two perfusion methods represent different aspects of vasculature. IVIM measures microscopic translational motions associated with microcirculation of blood in the capillary network, while DCE MRI measures capillary leakage of gadolinium contrast agent based on pharmacokinetic modeling. When WHO grade II and III gliomas were analyzed separately, we found *SPF* exhibited a statistically significant difference in assessing *IDH1* mutation status of WHO grade II tumors, whereas f helped assess WHO grade III tumors. However, these preliminary results must be interpreted with caution due to the small sample size. Besides perfusion, diffusion parameters like $ADC_{0,1000}$ were also predictive of *IDH1* mutation in LGGs, with a lower diffusion coefficient found in *IDH1* wild-type tumors. Our findings are in agreement with the existing literature regarding their association.[47,52]

Our study has several limitations. First, the cohort was relatively small, especially that of WHO grade III LGGs ($n = 8$). Therefore, we may have underestimated some associations, such as the association between perfusion-related metrics and *IDH1* mutation status, in WHO grade III gliomas. A further prospective study with a larger cohort should be performed to validate our results. Second, estimation bias may occur as a result of different cutoff b-values for IVIM analysis. Therefore, the set of b-values needs to be further optimized for brain tumors. Finally, the placement of ROIs was subjective and specific to a limited area on MRI. Automatic segmentation and image analysis of the entire tumor volume may improve preoperative risk stratification.

In conclusion, DWI, DCE, and IVIM MRI can be used as quantitative perfusion methods in preoperative *IDH1* mutation prediction in LGGs. Specifically, the simplified DWI-derived perfusion fraction showed a superior diagnostic performance, which holds the potential to serve as a contrast-free and time-saving alternative in the clinical setting. However, further validation in a large patient population is warranted.

Acknowledgements

YZ, STS, MQC, XQW contributed to the conception and design of the study. Data collection and evaluation were carried out by HJC, MQC, XQW as well as JWG. Statistical analyses and visualization were performed by XQW and STS. The manuscript was written by XQW, STS, YZ and MQC. All authors critically reviewed and approved the manuscript.

This work was supported by the National Natural Science Foundation of China [grant numbers 81501458, 81701642, 81571650, and 81901693); Shanghai Science and Technology Committee Medical Guide Project (western medicine) (grant number17411964300); Shanghai Municipal Education Commission-Gaofeng Clinical Medicine Grant Support (grant number 20172013); Medical Engineering Cross Research Foundation of Shanghai Jiao Tong University (grant number YG2015QN37, YG2017QN47) and Incubating Program for Clinical Research and Innovation of Ren Ji Hospital, School of Medicine, Shanghai Jiao Tong University (PYIII-17-027).

References

1. Cancer Genome Atlas Research N, Brat DJ, Verhaak RGW, Aldape KD, Yung WKA, Salama SR, et al. Comprehensive, integrative genomic analysis of diffuse lower-grade gliomas. *The N Engl J Med* 2015; **372:** 2481-98. doi: 10.1056/NEJMoa1402121

2. Chang EF, Clark A, Jensen RL, Bernstein M, Guha A, Carrabba G, et al. Multiinstitutional validation of the University of California at San Francisco Low-Grade Glioma Prognostic Scoring System. *J Neurosurg* 2009; **111:** 203-10. doi: 10.3171/2009.2.Jns081101

3. Chang EF, Smith JS, Chang SM, Lamborn KR, Prados MD, Butowski N, et al. Preoperative prognostic classification system for hemispheric low-grade gliomas in adults. *J Neurosurg* 2008; **109:** 817-24. doi: 10.3171/jns/2008/109/11/0817

4. Karim AB, Maat B, Hatlevoll R, Menten J, Rutten EH, Thomas DG, et al. A randomized trial on dose-response in radiation therapy of low-grade cerebral glioma: European Organization for Research and Treatment of Cancer (EORTC) Study 22844. *Int J Radiat Oncol Biol Phys* 1996; **36:** 549-56. doi: 10.1016/s0360-3016(96)00352-5

5. van den Bent MJ. Practice changing mature results of RTOG study 9802: another positive PCV trial makes adjuvant chemotherapy part of standard of care in low-grade glioma. *Neuro Oncol* 2014; **16:** 1570-4. doi: 10.1093/neuonc/nou297

6. Delfanti RL, Piccioni DE, Handwerker J, Bahrami N, Krishnan A, Karunamuni R, et al. Imaging correlates for the 2016 update on WHO classification of grade II/III gliomas: implications for IDH, 1p/19q and ATRX status. *J Neurooncol* 2017; **135:** 601-9. doi: 10.1007/s11060-017-2613-7

7. Beiko J, Suki D, Hess KR, Fox BD, Cheung V, Cabral M, et al. IDH1 mutant malignant astrocytomas are more amenable to surgical resection and have a survival benefit associated with maximal surgical resection. *Neuro Oncol* 2014; **16:** 81-91. doi: 10.1093/neuonc/not159

8. Villani V, Merola R, Vidiri A, Fabi A, Carosi M, Giannarelli D, et al. Temozolomide low-dose chemotherapy in newly diagnosed low-grade gliomas: activity, safety, and long-term follow-up. *Tumori* 2017; **103:** 255-60. doi: 10.5301/tj.5000565

9. Carmeliet P, Jain RK. Molecular mechanisms and clinical applications of angiogenesis. *Nature* 2011; **473:** 298-307. doi: 10.1038/nature10144

10. Onishi M, Ichikawa T, Kurozumi K, Date I. Angiogenesis and invasion in glioma. *Brain Tumor Pathol* 2011; **28:** 13-24. doi: 10.1007/s10014-010-0007-z

11. Gaddikeri S, Gaddikeri RS, Tailor T, Anzai Y. Dynamic contrast-enhanced MR imaging in head and neck cancer: techniques and clinical applications. *AJNR Am J Neuroradiol* 2016; **37:** 588-95. doi: 10.3174/ajnr.A4458

12. Roberts HC, Roberts TP, Brasch RC, Dillon WP. Quantitative measurement of microvascular permeability in human brain tumors achieved using dynamic contrast-enhanced MR imaging: correlation with histologic grade. *AJNR Am J Neuroradiol* 2000; **21:** 891-9.

13. Knopp EA, Cha S, Johnson G, Mazumdar A, Golfinos JG, Zagzag D, et al. Glial neoplasms: Dynamic Contrast-enhanced T2*-weighted MR imaging. *Neuroradiology* 1999; **211:** 791-8. doi: 10.1148/radiology.211.3.r99jn46791.

14. Hino T, Togao O, Hiwatashi A, Yamashita K, Kikuchi K, Momosaka D, et al. Clinical efficacy of simplified intravoxel incoherent motion imaging using three b-values for differentiating high- and low-grade gliomas. *PLoS One* 2018; **13:** e0209796-e. doi: 10.1371/journal.pone.0209796

15. Wang X, Chen XZ, Shi L, Dai JP. Glioma grading and IDH1 mutational status: assessment by intravoxel incoherent motion MRI. *Clin Radiol* 2019; **74:** 651.e7-651.e14. doi: 10.1016/j.crad.2019.03.020

16. Koh DM, Collins DJ, Orton MR. Intravoxel incoherent motion in body diffusion-weighted MRI: reality and challenges. *AJR Am J Roentgenol* 2011; **196:** 1351-61. doi: 10.2214/AJR.10.5515

17. Awasthi R, Rathore RK, Soni P, Sahoo P, Awasthi A, Husain N, et al. Discriminant analysis to classify glioma grading using dynamic contrast-enhanced MRI and immunohistochemical markers. *Neuroradiology* 2012; **54:** 205-13. doi: 10.1007/s00234-011-0874-y

18. Lu S, Gao Q, Yu J, Li Y, Cao P, Shi H, et al. Utility of dynamic contrast-enhanced magnetic resonance imaging for differentiating glioblastoma, primary central nervous system lymphoma and brain metastatic tumor. *Eur J Radiol* 2016; **85:** 1722-7. doi: 10.1016/j.ejrad.2016.07.005

19. Togao O, Hiwatashi A, Yamashita K, Kikuchi K, Mizoguchi M, Yoshimoto K, et al. Differentiation of high-grade and low-grade diffuse gliomas by intravoxel incoherent motion MR imaging. *Neuro Oncol* 2016; **18:** 132-41. doi: 10.1093/neuonc/nov147

20. Cao M, Suo S, Han X, Jin K, Sun Y, Wang Y, et al. Application of a simplified method for estimating perfusion derived from diffusion-weighted MR imaging in glioma grading. *Front Aging Neurosci* 2018; **9:** 432. doi: 10.3389/fnagi.2017.00432

21. Conklin J, Heyn C, Roux M, Cerny M, Wintermark M, Federau C. A simplified model for intravoxel incoherent motion perfusion imaging of the brain. *AJNR Am J Neuroradiol* 2016; **37:** 2251-7. doi: 10.3174/ajnr.A4929

22. Shukla-Dave A, Lee NY, Jansen JFA, Thaler HT, Stambuk HE, Fury MG, et al. Dynamic contrast-enhanced magnetic resonance imaging as a predictor of outcome in head-and-neck squamous cell carcinoma patients with nodal metastases. *Int J Radiat Oncol Biol Phys* 2012; **82:** 1837-44. doi: 10.1016/j.ijrobp.2011.03.006

23. Thoeny HC, de Keyzer F, Vandecaveye V, Chen F, Sun X, Bosmans H, et al. Effect of vascular targeting agent in rat tumor model: dynamic contrast-enhanced versus diffusion-weighted MR imaging. *Radiology* 2005; **237:** 492-9. doi: 10.1148/radiol.2372041638

24. Teruel JR, Goa PE, Sjøbakk TE, Østlie A, Fjøsne HE, Bathen TF. A simplified approach to measure the effect of the microvasculature in diffusion-weighted MR imaging applied to breast tumors: preliminary results. *Radiology* 2016; **281:** 373-81. doi: 10.1148/radiol.2016151630

25. Federau C, Maeder P, O'Brien K, Browaeys P, Meuli R, Hagmann P. Quantitative measurement of brain perfusion with intravoxel incoherent motion MR imaging. *Radiology* 2012; **265:** 874-81. doi: 10.1148/radiol.12120584

26. Suo S, Cao M, Zhu W, Li L, Li J, Shen F, et al. Stroke assessment with intravoxel incoherent motion diffusion-weighted MRI. *NMR Biomed* 2016, **29:** 320-8. doi: 10.1002/nbm.3467

27. Zhang Q, Wang Y-X, Ma HT, Yuan J. Cramér-Rao bound for intravoxel incoherent motion diffusion weighted imaging fitting. *Conf Proc IEEE Eng Med Biol Soc* 2013; **2013:** 511-4. doi: 10.1109/EMBC.2013.6609549

28. While PT, Teruel JR, Vidić I, Bathen TF, Goa PE. Relative enhanced diffusivity: noise sensitivity, protocol optimization, and the relation to intravoxel incoherent motion. *MAGMA* 2018; **31:** 425-38. doi: 10.1007/s10334-017-0660-x

29. Wu W-C, Chen Y-F, Tseng H-M, Yang S-C, My P-CJER. Caveat of measuring perfusion indexes using intravoxel incoherent motion magnetic resonance imaging in the human brain. *Eur Radiol* 2015; **25:** 2485-92. doi: 10.1007/s00330-015-3655-x

30. Chung WJ, Kim HS, Kim N, Choi CG, Kim SJ. Recurrent glioblastoma: optimum area under the curve method derived from dynamic contrast-enhanced T1-weighted perfusion MR imaging. *Radiology* 2013; **269:** 561-8. doi: 10.1148/radiol.13130016

31. Han X, Suo S, Sun Y, Zu J, Qu J, Zhou Y, et al. Apparent diffusion coefficient measurement in glioma: Influence of region-of-interest determination methods on apparent diffusion coefficient values, interobserver variability, time efficiency, and diagnostic ability. *J Magn Reson Imaging* 2017; **45:** 722-30. doi: 10.1002/jmri.25405

32. Park JE, Kim HS, Park KJ, Kim SJ, Kim JH, Smith SA. Pre-and posttreatment glioma: comparison of amide proton transfer imaging with MR spectroscopy for biomarkers of tumor proliferation. *Radiology* 2015; **278:** 514-23. doi: 10.1148/radiol.2015142979

33. Bisdas S, Braun C, Skardelly M, Schittenhelm J, Teo TH, Thng CH, et al. Correlative assessment of tumor microcirculation using contrast-enhanced perfusion MRI and intravoxel incoherent motion diffusion-weighted MRI: is there a link between them? *NMR Biomed* 2014; **27:** 1184-91. doi: 10.1002/nbm.3172

34. DeLong ER, DeLong DM, Clarke-Pearson DL. Comparing the areas under two or more correlated receiver operating characteristic curves: a nonparametric approach. *Biometrics* 1988; **44:** 837-45.

35. Zou T, Yu H, Jiang C, Wang X, Jiang S, Rui Q, et al. Differentiating the histologic grades of gliomas preoperatively using amide proton transfer-weighted (APTW) and intravoxel incoherent motion MRI. *NMR Biomed* 2018; 31. doi: 10.1002/nbm.3850

36. Sugahara T, Korogi Y, Kochi M, Ikushima I, Shigematu Y, Hirai T, et al. Usefulness of diffusion-weighted MRI with echo-planar technique in the evaluation of cellularity in gliomas. *J Magn Reson Imaging* 1999; **9:** 53-60. doi: 10.1002/(sici)1522-2586(199901)9:1<53::Aid-jmri7>3.0.Co;2-2

37. Matsumoto Y, Kuroda M, Matsuya R, Kato H, Shibuya K, Oita M, et al. In vitro experimental study of the relationship between the apparent diffusion coefficient and changes in cellularity and cell morphology. *Oncol Rep* 2009; **22:** 641-8. doi: 10.3892/or_00000484

38. Chen L, Liu M, Bao J, Xia Y, Zhang J, Zhang L, et al. The Correlation between apparent diffusion coefficient and tumor cellularity in patients: a meta-analysis. *PLoS One* 2013; **8:** e79008. doi: 10.1371/journal.pone.0079008

39. Provenzale JM, York G, Moya MG, Parks L, Choma M, Kealey S, et al. Correlation of relative permeability and relative cerebral blood volume in high-grade cerebral neoplasms. *AJR Am J Roentgenol* 2006; **187:** 1036-42. doi: 10.2214/AJR.04.0676

40. Mills SJ, Patankar TA, Haroon HA, Balériaux D, Swindell R, Jackson A. Do cerebral blood volume and contrast transfer coefficient predict prognosis in human glioma? *AJNR Am J Neuroradiol* 2006; **27:** 853-8.

41. Houillier C, Wang X, Kaloshi G, Mokhtari K, Guillevin R, Laffaire J, et al. IDH1 or IDH2 mutations predict longer survival and response to temozolomide in low-grade gliomas. *Neurology* 2010; **75:** 1560-6. doi: 10.1212/WNL.0b013e3181f96282

42. Beiko J, Suki D, Hess KR, Fox BD, Cheung V, Cabral M, et al. IDH1 mutant malignant astrocytomas are more amenable to surgical resection and have a survival benefit associated with maximal surgical resection. *Neuro Oncol* 2014; **16:** 81-91. doi: 10.1212/WNL.0b013e3181f96282

43. Eckel-Passow JE, Lachance DH, Molinaro AM, Walsh KM, Decker PA, Sicotte H, et al. Glioma groups based on 1p/19q, IDH, and TERT promoter mutations in tumors. *N Engl J Med* 2015; **372:** 2499-508. doi: 10.1056/NEJMoa1407279

44. Cohen AL, Holmen SL, Colman H. IDH1 and IDH2 mutations in gliomas. *Curr Neurol Neurosci Rep* 2013; **13:** 345. doi: 10.1007/s11910-013-0345-4

45. Zhao S, Lin Y, Xu W, Jiang W, Zha Z, Wang P, et al. Glioma-derived mutations in IDH1 dominantly inhibit IDH1 catalytic activity and induce HIF-1alpha. *Science* 2009; **324:** 261-5. doi: 10.1126/science.1170944

46. Kickingereder P, Sahm F, Radbruch A, Wick W, Heiland S, Deimling Av, et al. IDH mutation status is associated with a distinct hypoxia/angiogenesis transcriptome signature which is non-invasively predictable with rCBV imaging in human glioma. *Sci Rep* 2015; **5:** 16238. doi: 10.1038/srep16238

47. Leu K, Ott GA, Lai A, Nghiemphu PL, Pope WB, Yong WH, et al. Perfusion and diffusion MRI signatures in histologic and genetic subtypes of WHO grade II–III diffuse gliomas. *J Neurooncol* 2017; **134:** 177-88. doi: 10.1007/s11060-017-2506-9

48. Brendle C, Hempel JM, Schittenhelm J, Skardelly M, Tabatabai G, Bender B, et al. Glioma grading and determination of IDH mutation status and ATRX loss by DCE and ASL perfusion. *Clin Neuroradiol* 2018; **28:** 421-8. doi: 10.1007/s00062-017-0590-z

49. Cui D, Ren J, Shi J, Feng L, Wang K, Zeng T, et al. R132H mutation in IDH1 gene reduces proliferation, cell survival and invasion of human glioma by downregulating Wnt/β-catenin signaling. *Int J Biochem Cell Biol* 2016; **73:** 72-81. doi: 10.1016/j.biocel.2016.02.007

50. Reis M, Czupalla CJ, Ziegler N, Devraj K, Zinke J, Seidel S, et al. Endothelial Wnt/β-catenin signaling inhibits glioma angiogenesis and normalizes tumor blood vessels by inducing PDGF-B expression. *J Exp Med* 2012; **209:** 1611-27. doi: 10.1084/jem.20111580

51. Koivunen P, Lee S, Duncan CG, Lopez G, Lu G, Ramkissoon S, et al. Transformation by the (R)-enantiomer of 2-hydroxyglutarate linked to EGLN activation. *Nature* 2012; **483:** 484-8. doi: 10.1038/nature10898

52. Villanueva-Meyer JE, Wood MD, Choi BS, Mabray MC, Butowski NA, Tihan T, et al. MRI Features and IDH mutational status of grade II diffuse gliomas: impact on diagnosis and prognosis. *AJR Am J Roentgenol* 2018; **210:** 621-8. doi: 10.2214/AJR.17.18457

research article

The feasibility of ultrasound-guided vacuum-assisted evacuation of large breast hematomas

Sa'ed Almasarweh[1], Mazen Sudah[1], Sarianna Joukainen[2], Hidemi Okuma[1], Ritva Vanninen[1,3], Amro Masarwah[1]

[1] Kuopio University Hospital, Diagnostic Imaging Center, Department of Clinical Radiology, Kuopio, Finland

[2] Kuopio University Hospital, Department of Plastic Surgery, Division Surgery, Kuopio, Finland

[3] University of Eastern Finland, Cancer Center of Eastern Finland, Kuopio, Finland

Radiol Oncol 2020; 54(3): 311-316.

Received 3 May 2020
Accepted 27 May 2020

Correspondence to: Sa'ed Almasarweh, Department of Clinical Radiology, Kuopio University Hospital, Puijonlaaksontie 2, P.O. Box 100, FI-70029 Kuopio, Finland. E-mail: saadn.masarweh@gmail.com

Disclosure: No potential conflicts of interest were disclosed.

Background. Breast hematoma is an often underrated and disregarded post-procedural complication in the literature. Current treatment modalities are comprised of either surgical or expectant therapy, while percutaneous procedures play a smaller role in their treatment. We aimed to examine the efficacy of vacuum-assisted evacuation (VAE) in the treatment of clinically significant large breast hematomas as an alternative to surgery.

Patients and methods. We retrospectively analysed patients that underwent breast interventions (surgical and percutaneous), who later developed clinically significant large hematomas and underwent a trial of VAE of hematoma in our hospital within the period of four years. Patient and procedure characteristics were acquired before and after VAE. Success of intervention was based on ≥ 50% clearance of hematoma volume and patients' subjective resolution of symptoms. All patients were followed clinically and by ultrasound if needed at different intervals depending on the severity of presenting symptoms.

Results. Eleven patients were included in the study. The mean largest diameter of hematomas was 7.9 cm and mean surface area was 32.4 cm^2. The mean duration of the procedure was 40.5 min. In all patients VAE of hematoma was implemented successfully with no complications. Control visits showed no major residual hematoma or seroma formation.

Conclusions. Our results show that VAE of hematoma can be implemented as a safe alternative to surgery in large, clinically significant hematomas, regardless of aetiology or duration. The procedure carries less risk, stress and cost with the added benefit of outpatient treatment when compared to surgical treatment.

Key words: breast hematoma; vacuum assisted breast biopsy; hematoma evacuation; breast

Introduction

Complications following therapeutic, reconstructive, or aesthetic breast surgeries as well as percutaneous procedures, both biopsies and excisions, are important considerations for women undergoing or pursuing these options. In general, the most common local complications following routine breast interventions are inherent to the surgery itself *e.g.* infection, pain, hematoma, delayed healing, and abnormal scarring. Risk factors for complications include smoking, obesity, larger breasts, anticoagulant treatments, and older age.[1]

Early clinically significant postoperative hematomas typically develop within the first 12 to 48 hours after surgery.[2] Immediate reoperation is usually indicated in expanding hematomas, hemodynamic instability, and jeopardized flap viability.[3] Less commonly, a hematoma appears days or weeks after surgery and may be associated with minor injury or trauma to the breast, with the majority identified within the first 14 days. Late hematomas can also occur and are thought to be related to direct trauma, clotting disorders, overactivity, and use of intraoperative corticosteroids.[4,5] Postprocedural hematomas are not uncommon, yet most of them are small and resolve spontaneously. Large, clinically more significant hematomas in the late postoperative period are infrequent. Symptomatic, painful, or infected hematomas are treated surgically since hematomas with dense contents or clots do not drain with needle aspirations or drains are blocked immediately.[6]

If a clinically significant hematoma does occur, an evacuation is advised. Expectant management is not favoured due to the lengthy nature of spontaneous liquefaction and discomfort that patients report, which eventually leads to fibrosis and distortion of breast tissue.[7] Surgical management is aimed at the rapid decompression of the closed wound space through exploration, drainage and establishing haemostasis. After evacuation the wound is thoroughly irrigated and closed in order to preserve the cosmetic aspect of the breast.[8] Percutaneous drainage of the hematoma during the first 24 hours of hematoma formation might be challenging, on the assumptions that an organized clot would have already been formed. Partial liquefaction occurs 6 to 7 days after the formation of the hematoma, which is considered as the best interval for percutaneous evacuation.[9]

Breast imaging-guided interventions are widely used in daily practice *e.g.* core biopsy and vacuum assisted breast biopsy and excision (VABB and VABE) to diagnose different types of imaging findings and remove benign or risk lesions. The larger the needle used for biopsy and the number of cores obtained, the more likely complications will appear.[10] Significant vascular damage is more probable in VABB or VABE procedures.[11] Recently it was reported that VABB can be used as a treatment modality for clinically significant hematoma in patients with small hematomas less than 4cm in size.[6] The effectiveness of vacuum-assisted evacuation of large breast hematomas has not been previously reported.

In this study we aimed to investigate ultrasound-guided vacuum-assisted evacuation (VAE) of breast hematoma as a safe, viable, time and resource-sparing treatment modality for larger (> 5 cm) breast hematomas irrespective of aetiology. This technique could decrease the rate of multiple operations and eliminate added morbidity of surgery and anaesthesia while yielding satisfactory therapeutic results.

Patients and methods

Patients

All VAE of hematomas performed in our institution between February 2016 and February 2020 were retrospectively retrieved from the regional picture archiving and communication system (PACS) and the clinical data of these patients were also retrieved from the local digital archives. In our institution, hematomas that do not fulfil the criteria for immediate surgery, cause discomfort and unsettling symptoms for the patients (considerable pain, pressure symptoms, local infection and prolonged healing) or patients who refuse surgical intervention are offered a trial of VAE of hematoma. The Chair of the Hospital District waived the need for written informed consent from the patients due to the retrospective nature of this study. All clinical investigations were conducted according to the relevant guidelines and the principles expressed in the Declaration of Helsinki.

Data collection

The total amount of breast surgeries, VABB and VABE as well as postoperative haemorrhagic complications requiring surgical intervention were retrieved from the hospital's digital information systems.

All medical records of patient undergoing VAE procedures were also reviewed and the following parameters were recorded and included in a database: Age, type of breast procedure, time interval between previous procedure and VAE of hematoma, symptoms exhibited pre- as well as post-VAE, medications, comorbidities, size of hematoma and the estimated residual volume after the procedure, echogenicity of hematoma at time of VAE, gauge of the needle used, complications during or after the procedure and findings at control. The total duration of the procedure was measured from the time the patient has entered the ultrasound room until discharge.

Procedure

In Kuopio University Hospital (KUH), automated VABB procedures were introduced in 2015. With experience in VABB, VABE was gradually introduced and consequently evacuation of large hematomas was offered as an alternative to surgery. The procedures were carried out with EnCor™ Breast Biopsy System (BD Bard, Tempe, AZ, USA). US-guided interventions were performed using

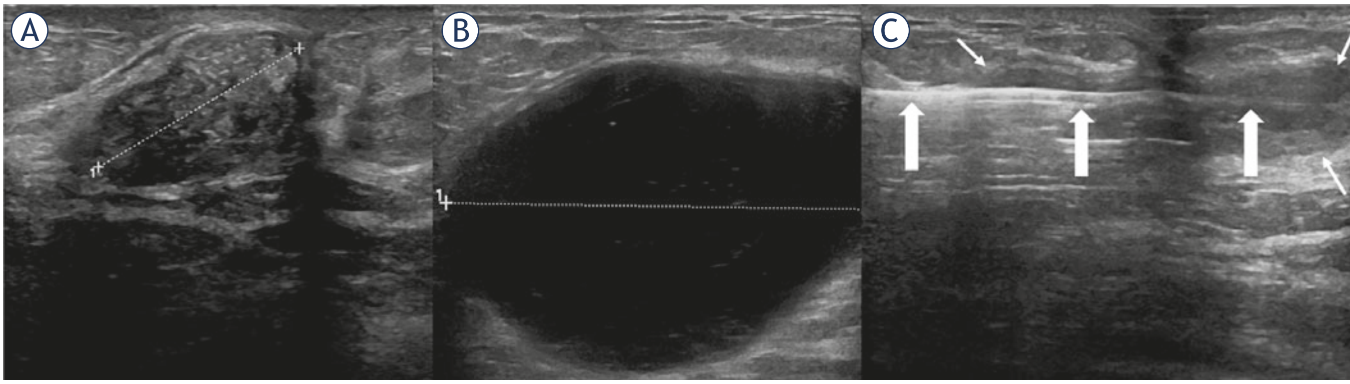

FIGURE 1. Illustration of a vacuum assisted evacuation of hematoma in patient number 9. Vacuum assisted excision of a discordant lesion **(A)** at core biopsy resulted in a palpable painful hematoma. Ultrasound image of the 5.5x4.0 cm hematoma **(B)**. Complete evacuation of the hematoma with sparing of hematoma wall **(C)**; Large arrows indicate needle's shaft and small white arrows indicate hematoma wall

a Logiq E9 class US scanner (GE, Wauwatosa, Wisconsin, USA) equipped with a 5–15 MHz linear array transducer. All procedures were performed by, or under the supervision of, a breast radiologist with over 25 years of experience in multimodality breast imaging and interventions. No change in patients' medications was required. After thorough local disinfection, application of aseptic measures as well as the injection of local anaesthetic through the insertion channel (lidocaine with adrenaline; max 10 ml) a small skin incision was made. An EnCor™ 7/10G vacuum needle was then inserted into the base of the hematoma. The needle's cutting blade was opened, and continuous suction was applied until the hematoma emptied and its walls collapsed (Figure 1). Residual hematomas in side-pockets were ignored. In the case of incomplete hematoma aspiration (less than 50%) due to large, blocking or hard clots, the blade was used to fragment the fibrotic tissue through multiple biopsy samples. Sample container was continuously flushed with saline during the aspiration-fragmentation procedure to avoid blockage, and the container would be changed if filled with accumulated material as needed. The walls of the hematoma were carefully avoided during any fragmentation procedure to avoid possible rebleeding. After the procedure, the area of the breast with hematoma was manually compressed for at least 10 minutes, longer, if the patient received anti-coagulants. The use of a tight sports-brassiere was recommended for a minimum of 24 hours with compression pads over the area of the hematoma to prevent rebleeding or major seroma formation. Since 2019 we continued to provide fully adjustable and flexible breast compression wraps to all patients. Patients were then discharged.

Some hematomas were longer than the shaft of the vacuum needle, thus separate insertions from opposite sides were implemented to complete the procedure. Otherwise, procedures were completed through single insertion.

Success of intervention was based on clearance of a targeted ≥ 50% of hematoma's volume, visually estimated by the operator, patients' subjective assessment of symptom resolution and the resolution of hematoma without the need for surgery during follow-up. All patients were followed clinically and by US if needed at different intervals depending on the severity of presenting symptoms.

Results

During the recruitment period, a total of 1208 breast operations and 358 VABB or lesion excision procedures were performed. We detected a total of 44 clinically large hematomas as complications. Of the 1208 operative patients, 33 had early postoperative bleeding and had to undergo surgical evacuation while 8 patients suffered from delayed hematoma formation. Therefore, the reoperation rate for early postoperative bleeding was 2.7% (33/1208) and the rate of late hematomas treated with VBE was 0.7% (8/1208). On the other hand, of the 358 patients that have undergone VABB and excision procedures, 3 patients were later diagnosed to have clinically relevant hematomas with an incidence rate of 0.84% (3/358).

Altogether 11 consecutive patients who have been diagnosed with breast hematoma and treated with the VAE system were included in the analysis. Patients had a mean age of 59 years (range 38-85) and their characteristics are presented in Table 1.

TABLE 1. Characteristics of patients with hematoma

Patient	Age (yrs)	Wait time* (days)	Intervention	Medications	Size (cm)
1	42	14	BLES	Anti-Coagulant	6 x 4
2	67	1	VABB	None	8 x 4
3	38	36	Surgery	None	6 x 3
4	48	78	Surgery	None	6 x 5
5	49	21	Surgery	None	5.5 x 3
6	51	34	Surgery	Anti-Platelet and hydrocortisone	7 x 6.5
7	84	15	Surgery	Anti-Platelet	12 x 2.5
8	71	597	Surgery	None	5.5 x 3.5
9	85	51	VABE	Anti-Coagulant	5.5 x 4
10	60	29	Surgery	None	20 x 5
11	53	22	Surgery	None	5.5 x 5

* Wait time = number of days between surgical intervention/biopsy and VAE of hematoma;

BLES = breast lesion excision system; VABB = vacuum assisted breast biopsy; VABE = vacuum assisted breast-lesion excision

TABLE 2. Hematoma characteristics pre- and post-vacuum assisted evacuation (VAE)

Patient	Size pre-VAE (in cm)	Estimated decrease in size post-VAE (percentage)	Symptoms
1	6 x 4	> 50%	Resolution
2	8 x 4	> 50%	Resolution
3	6 x 3	100%	Resolution
4	6 x 5	100%	Resolution
5	5.5 x 3	100%	Resolution
6	7 x 6.5	80%	Resolution
7	12 x 2.5	70%	Resolution
8	5.5 x 3.5	90%	Resolution
9	5.5 x 4	100%	Resolution
10	20 x 5	80%	Resolution
11	5.5 x 5	100%	Resolution

Of the 11 participants, 3 patients had hematomas as complications after percutaneous interventional procedures and 8 patients after surgeries, of which 5 were reduction mammoplasties. The mean number of days between the initial intervention and VAE of hematoma of 10 patients was 30 days with an outlier of 597 days due to an idiopathic late developing complicated hematoma in a mastectomy site after radiotherapy. One of these patients had a slowly progressive hematoma after VABB and refused surgical evacuation. Regarding symptoms prior to evacuation, all patients reported pain, 45.5% prolonged healing (n = 5), 45.5% mass effect (n = 5), 18.2% infection (n = 2).

Of the ultrasound imaging of the hematomas taken prior to VAE of hematoma, 7/11 were hypoechoic, 1/11 was hyperechoic and 3/11 had mixed echogenicity. All hematomas underwent unsuccessful aspiration trials with fine needles (G18–23). The mean duration of the VAE procedure was 40.5 min (range 19–62). One patient was taking aspirin alone, one aspirin and hydrocortisone, one patient was taking Warfarin, one patient taking Dabigatran and one patient taking Apixaban.

One patient had a massive two-sided communicating 20 x 5 and 12 x 4 cm hematoma, therefore in this analysis, we included only the largest portion. The mean maximum diameter of the evacuated hematomas was 7.9 cm and an average surface area of 32.4cm^2. The gauge of the VAE probes was a choice between 7G or 10G. Most of the procedures were performed using 7G-sized needles (n = 8) owing to the larger size of the treated hematomas. Four patients underwent ultrasound-guided aspiration of the hematoma cavity due to post-evacuation seroma formation 1–7 days after VAE procedure. No complications were reported post-evacuation or aspiration procedures.

The parameters before as well as after VAE of hematoma are depicted in Table 2. All patients underwent regular follow-up after evacuation. Upon follow-up, all cases were deemed successfully treated with no major hematoma residue or seroma formation.

Discussion

One of the most common complications in breast interventions is hematoma formation, which remains grossly underrated and disregarded in the literature, especially when its frequency is taken into consideration. Breast hematomas can range from small mammographically-detected hematomas to large clinically significant hematomas that can cause severe discomfort to patients. Our results suggest that Vacuum-assisted evacuation of hematoma is a time-sparing, cost-effective and successful method of evacuation for small as well as large breast hematomas regardless of aetiology.

Our patient population was comprised of both post-biopsy and post-surgical patients, thus expanding the aetiological factors to not only include biopsy-induced hematomas. In our study we included all consecutive patients treated in our institution presenting with hematomas of different

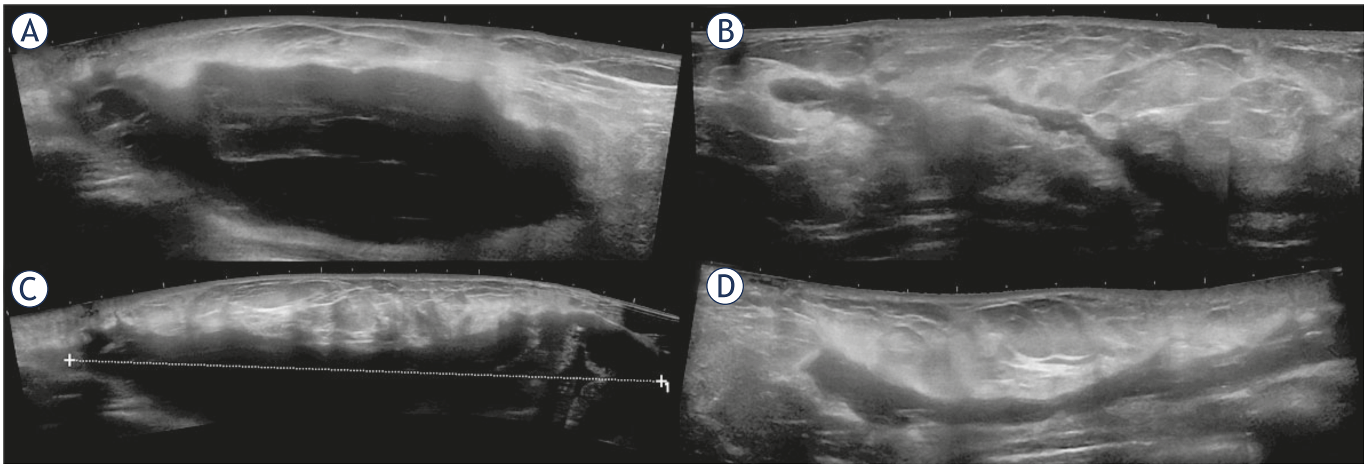

FIGURE 2. Patient number 10 with massive two-sided communicating hematoma treated through separate punctures. Image **(A)** represents a panoramic view of the cranial aspect of the 12 cm long hematoma and image **(B)** represents a panoramic view after the evacuation. Image **(C)** represents the caudal 20 cm long hematoma and correspondingly image **(D)** shows the view after treatment.

sizes. This goes to prove that VAE can be implemented in clinically large significant hematomas. It is stipulated that percutaneous drainage of acute hematomas should be attempted between days 7–14 after formation of hematoma, in order to allow time for hematoma liquefaction. Moreover, delayed hematomas, *i.e.* hematomas developing 6 months or more post-intervention, are always evacuated surgically.[7] In our study the wait time was variable, in that the procedure timing was not set on a set-point schedule, rather on different time-intervals regarding date of hematoma formation. Furthermore, one large delayed hematoma was evacuated successfully after 597 days (1.64 years), proving that even delayed hematomas can be successfully treated with VAE of hematoma irrespective of duration.

While the true incidence of large clinically significant hematomas remains unknown, findings from this study show that it is relatively uncommon. The treatment of breast hematomas in the literature is suggested as either surgical or expectant. Both treatment modalities impose certain risks and added morbidity for the patient. Patients face problems such as added costs, the ordeal of going through surgery or stress due to the aesthetic and psychological impact of the procedure. Moreover, expectant therapies may pose future diagnostic difficulties.[9]

A recent report evaluated the efficacy of the VABB system in evacuating symptomatic hematomas after VABB excision of benign breast lesions in 8 patients. Evacuation was successful in all the cases and no technique-related complications were observed.[6] However, the inclusion criteria were restricted to hematomas observed post-VABB or VABE and not post-surgical complications, which limits the patient population on which this technique can be used. Moreover, 75% (6/8) of hematomas were smaller than 4 cm with a largest maximum diameter of 5.6 cm. This means that most clinically significant breast hematomas that are difficult to handle conservatively were excluded. The study failed to address whether this technique could be attempted on larger and more difficult to evacuate hematomas, which would otherwise need to be evacuated surgically.

Vacuum-assisted biopsies are also currently implemented as a treatment modality for small palpable or non-palpable benign or risk lesions, by assuring rapid and complete excision of these lesions to be better histopathologically evaluated and therefore obviating the need for therapeutic surgery or continuous follow-up.[12] Minimally invasive management of many B3 lesions with VABE continues to be a suitable alternative to first-line surgical excision in most cases.[13] In this study, we wanted to study the efficacy of automatic VABE system in removing symptomatic clinically significant hematomas. Not only are VABE systems faster with less implications on patients, but the endogenous vacuum capability, the large bore size as well as the slicing mechanism of the probe could be used to evacuate organized hematomas, which otherwise would be difficult to aspirate percutaneously and would need surgical drainage and evacuation.

Evacuations were performed immediately upon request and without prior scheduling as our patients presented with acute symptoms and the procedure offered immediate relief. Furthermore, most of these patients were discharged immediately after the procedure. No change in anticoagulant medications were required as the procedures were quite straightforward without any excision of fibroglandular breast tissues. The tip of the blade is very sharp and penetrates even denser tissues easily, hence special care should be applied in handling the needle inside the hematoma cavity in order not to induce any damage to the cavity walls. Due to the large size of the needles, we regularly chose the shortest insertion pathway and used a combination of local anaesthetic with adrenaline to reduce any possible bleeding consequences.

The obvious limitations of the study are the small number of patients and the retrospective nature. This study needs to be validated on a larger scale to include more patients with a more controlled inclusion and outcome criteria. Furthermore, the volume of the evacuated part of the hematoma was not measured during the procedure due to the continuous saline flush used in our practice and could not be retrospectively accurately verified.

To conclude, this study shows that VAE procedure is a successful, time-conserving, easily implemented interventional treatment modality for both small and large breast hematomas that would decrease the morbidity, costs and inconvenience of repeated surgery.

References

1. Araco A, Gravante G, Araco F, Delogu D, Cervelli V, Walgenbach K. A retrospective analysis of 3,000 primary aesthetic breast augmentations: postoperative complications and associated factors. *Aesthetic Plast Surg* 2007; **31:** 532-9. doi: 10.1007/s00266-007-0162-8
2. Seth AK, Hirsch EM, Kim JY, Dumanian GA, Mustoe TA, Galiano RD, et al. Hematoma after mastectomy with immediate reconstruction: an analysis of risk factors in 883 patients. *Ann Plast Surg* 2013; **71:** 20-3. doi: 10.1097/SAP.0b013e318243355f
3. Phan R, Rozen WM, Chowdhry M, Fitzgerald O'Connor E, Hunter-Smith DJ, Ramakrishnan VV. Risk factors and timing of postoperative hematomas following microvascular breast reconstruction: A prospective cohort study. *Microsurgery* 2020; **40:** 99-103. doi: 10.1002/micr.30473
4. Collins JB, Verheyden CN. Incidence of breast hematoma after placement of breast prostheses. *Plast Reconstr Surg* 2012; **129:** 413e-20e. doi: 10.1097/PRS.0b013e3182402ce0
5. Handel N, Cordray T, Gutierrez J, Jensen JA. A long-term study of outcomes, complications, and patient satisfaction with breast implants. *Plast Reconstr Surg* 2006; **117:** 757-67; discussion 768-72. doi: 10.1097/01.prs.0000201457.00772.1d.
6. Guzman-Aroca F, Berna-Serna JD, Garcia-Ortega AA, Hernandez-Gomez D, Berna-Mestre JD. A new management technique for symptomatic haematomas following therapeutic vacuum-assisted biopsy. *J Clin Med* 2019; **8:** 1493. doi: 10.3390/jcm8091493
7. Smith B. Complications of Breast Surgery. In: Cance WG, editor. *Breast surgery* Amsterdam: IOS Press; 2001. p. 95-102.
8. Vitug AF, Newman LA. Emergencies in breast surgery. *Surg Clin North Am* 2007; **87:** 431-51. doi: 10.1016/j.suc.2007.01.005
9. Polverini A, Kruper L. Surgical Emergencies in Breast Surgery. In: Fong Y, editor. *Surgical Emergencies in the Cancer Patient.* New York: Springer International Publishing; 2017. p. 431-51.
10. Zagouri F, Gounaris A, Liakou P, Chrysikos D, Flessas I, Bletsa G, et al. Vacuum-assisted breast biopsy: more cores, more hematomas? *In Vivo* 2011; **25:** 703-5.
11. Bick U, Trimboli RM, Athanasiou A, Balleyguier C, Baltzer PAT, Bernathova M, et al. Image-guided breast biopsy and localisation: recommendations for information to women and referring physicians by the European Society of Breast Imaging. *Insights Imaging* 2020; **11:** 12. doi: 10.1186/s13244-019-0803-x
12. Park HL, Hong J. Vacuum-assisted breast biopsy for breast cancer. *Gland Surg* 2014; **3:** 120-7. doi: 10.3978/j.issn.2227-684X.2014.02.03
13. Rageth CJ, O'Flynn EAM, Pinker K, Kubik-Huch RA, Mundinger A, Decker T, et al. Second International Consensus Conference on lesions of uncertain malignant potential in the breast (B3 lesions). *Breast Cancer Res Treat* 2019; **174:** 279-96. doi: 10.1007/s10549-018-05071-1.

research article

Analysis of damage-associated molecular pattern molecules due to electroporation of cells in vitro

Tamara Polajzer[1], Tomaz Jarm[1], Damijan Miklavcic[1]

[1] Faculty of Electrical Engineering, University of Ljubljana, Ljubljana, Slovenia

Radiol Oncol 2020; 54(3): 317-328.

Received 18 June 2020
Accepted 7 July 2020

Correspondence to: Prof. Damijan Miklavčič, Ph.D., Faculty of Electrical Engineering, University of Ljubljana, Tržaška 25, SI-1000 Ljubljana, Slovenia. E-mail: damijan.miklavcic@fe.uni-lj.si

Disclosure: No potential conflicts of interest were disclosed.

Background. Tumor cells can die via immunogenic cell death pathway, in which damage-associated molecular pattern molecules (DAMPs) are released from the cells. These molecules activate cells involved in the immune response. Both innate and adaptive immune response can be activated, causing a destruction of the remaining infected cells. Activation of immune response is also an important component of tumor treatment with electrochemotherapy (ECT) and irreversible electroporation (IRE). We thus explored, if and when specific DAMPs are released as a consequence of electroporation *in vitro*.

Materials and methods. In this *in vitro* study, 100 µs long electric pulses were applied to a suspension of Chinese hamster ovary cells. The release of DAMPs – specifically: adenosine triphosphate (ATP), calreticulin, nucleic acids and uric acid was investigated at different time points after exposing the cells to electric pulses of different amplitudes. The release of DAMPs was statistically correlated with cell permeabilization and cell survival, e.g. reversible and irreversible electroporation.

Results. In general, the release of DAMPs increases with increasing pulse amplitude. Concentration of DAMPs depend on the time interval between exposure of the cells to pulses and the analysis. Concentrations of most DAMPs correlate strongly with cell death. However, we detected no uric acid in the investigated samples.

Conclusions. Release of DAMPs can serve as a marker for prediction of cell death. Since the stability of certain DAMPs is time dependent, this should be considered when designing protocols for detecting DAMPs after electric pulse treatment.

Key words: electroporation; pulsed electric field treatment; damage-associated molecular pattern molecules; immunogenic cell death; electrochemotherapy

Introduction

Electroporation or pulsed electric field (PEF) treatment can cause changes in membrane permeability, which allows molecules, that are otherwise membrane impermeable, to cross the plasma membrane. In reversible electroporation the damage to cell membrane is repaired, enabling the cell to reestablish its metabolism and survive. This type of electroporation is used in multiple therapies. Electrochemotherapy (ECT) is one of such widely used therapies in which the increased cell membrane permeability enables chemotherapeutic drug to enter the cell and thus potentiates the cytotoxicity of the drug.[1,2] In irreversible electroporation (IRE) the damage to the cells however is too severe for the cells to recover which leads to cell death. While the cells are destroyed, the integrity of tissue like vessels, nerves and extracellular matrix remains preserved[3,4], making this therapy very appealing for ablation of tumor and other tissues, otherwise unsuitable for surgical removal or thermal ablation such as radiofrequency ablation or cryo-ablation.[5,6]

In ECT eight square 100 μs electrical pulses, with an amplitude of 100-1000 V are usually used to induce a reversible membrane permeabilization. For IRE, more pulses (80-100 pulses) at higher amplitude (up to 3000 V) are required, to overwhelm the reparative capacity of the cells which leads to cell death.[7] From morphological, biochemical, and functional perspectives, different cell death pathways/types can be activated.[8] Historically, based on morphological changes, three different forms of cell death were defined: apoptosis (cell shrinkage, chromatin condensation, formation of apoptotic bodies); autophagy (cytoplasmic vacuolization); and necrosis (loss of plasma membrane integrity).[8,9] Such classification is still employed, but in newer classification based on genetic, biochemical, pharmacological and functional differences, cell death is either accidental (uncontrollable death caused by disassembly of the plasma membrane) or regulated (activation of signal transduction). Depending on signaling pathways different types of regulated cell death are being characterized, e.g. intrinsic and extrinsic apoptosis, necroptosis, ferroptosis, pyroptosis, immunogenic cell death, lysosome-dependent cell death, mitochondrial permeably transition driven necrosis and many others gathered and described by Galluzi *et al*..[10] In electroporation studies, cell death has been most extensively explored in the range of nanosecond pulse treatment, where the majority of studies confirmed cell death by apoptosis (intrinsic and extrinsic) and only few studies indicated necrosis.[11,12] Both pathways were confirmed also in microsecond pulse treatment.[13-9] Nevertheless, in recent studies new cell death types were also detected like pyroptosis[20], necroptosis[20,21] and immunogenic cell death.[22-29]

In IRE [18,30-34] and ECT with either bleomycin or cisplatin[26,35-37] used for cancer treatment, involvement and importance of host immune response was demonstrated, counteracting tumor escape mechanisms.[29,38,39] After these therapies, dying tumor cells can release specific molecules, which are being recognized by the cells of immune system. These molecules can activate the innate and adaptive immune response, leading to the destruction of the remaining tumor cells in the body[40] and inducing long-lasting protective antitumor immunity.[41] Some studies even suggest that immunogenic effect of IRE is more pronounced than in other ablation therapies like radiofrequency ablation[31] and cryoablation.[32] Evidence suggests that administration of immune-stimulating molecules can even enhance the local effectiveness of ECT[35] and IRE[29,42-44] allowing simultaneous treatment of distant tumors.

Our immune system consists of two complementary and closely collaborative systems, an innate (non-specific) and an adaptive (antigen-specific) system. Activation of immune system is essential for our survival, as it distinguishes and eliminates potentially harmful molecules, even the ones that derive from the host/our own tissues. Well known are the pathogen-associated molecules (PAMPs), which are present on microbes and are being recognized by cells of the innate immune system when they bind to pattern recognition receptors (PRRs). The same pathways are activated by the host's damage-associated molecular pattern molecules (DAMPs), which act as endogenous damage signal in case of cell death or response to stress, leading to inflammatory response.[45-47] Release of DAMPs characterizes immunogenic cell death (ICD). Most of DAMPs are normally located intracellularly[48], where under normal physiological conditions have an important intracellular role. When a cell is damaged or dies, DAMPs are actively or passively exposed or released to extracellular space.[49-51] The release of DAMPs is often accompanied by cytokines, chemokines and other inflammatory mediators.[52] In extracellular space DAMPs have a completely different function, as they are being recognized by pattern recognition receptors (PRRs), such as TRLs, NOD-like, PRLs and RAGE receptors on immune cells.[50,53] Binding of DAMPs to these receptors stimulates innate immune response through promoting the release of pro-inflammatory mediators and recruiting immune cells (dendritic cells, macrophages, T cells and neutrophils). Usually, the exposure of different DAMPs depends on endoplasmic reticulum stress, followed by reactive oxygen species (ROS) production.[41] Release of DAMPs correlates with the degree of trauma.[54] Some DAMPs can even be involved in tissue repair pathway.[55-57] It depends on DAMPs and their triggered pathways, together with cytokines and growth factor to determine, if mild acute inflammation and wound healing [56,58] or severe inflammation and fibrosis will follow.[59]

Electroporation causes an increase in membrane permeability and allows molecules, for which the membrane is usually impermeable, including DAMPs, to cross it. ATP, one of the main DAMPs, was even used as an indicator of cell membrane permeabilization in the first electroporation studies.[60] In recent years reports on electroporation studies have started to emerge investigating the immunogenic cell death caused by electroporation. Studies detected DAMPs, like ATP, high-mobility group box 1 protein (HMGB1) release and calreticulin externalization, as they are the gold standard for predicting the ICD in cancer cells.[41] So far mostly single (or a small subset of) DAMPs were studied. Most studies involved nanosecond pulse treatment[22-25], whereas studies using microsecond[26,29], millisecond[28] and H-FIRE pulse treatments[27] are even more scarce. For now, different DAMPs were investigated at different intervals after electroporation ranging from 30 min to 72 hours, using different types of cancer cells.

Because in both ECT and IRE the immune system response is essential for successful and complete tumor eradication, we decided to explore if and when specific DAMPs are released in response to electroporation *in vitro*. The experiments were performed using 100 µs long pulses, as they are most commonly used in ECT treatment and in IRE for soft tissue ablation.

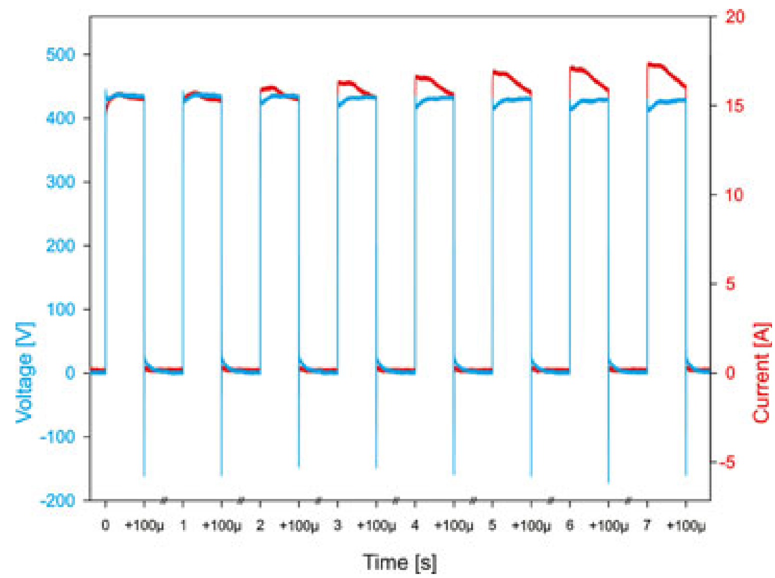

FIGURE 1. Application of 500 V pulses. Blue line shows voltage and red line shows current. Due to sequencing, all eight pulses are in one picture, separated by //.

Materials and methods

Cell preparation

Chinese hamster ovary (CHO-K1) from European Collection of Authenticated Cell Cultures were grown in culture flasks (TPP, Switzerland) filled with HAM F-12 growth medium (PAA, Austria) at 37°C with a humidified 5% CO_2. The growth medium was enriched with 10% fetal bovine serum (FBS) (Sigma-Aldrich, Germany), L-glutamine (StemCell, Canada) and antibiotics penicillin/streptomycin (PAA, Austria) and gentamycin (Sigma-Aldrich, Germany). At 70% confluency, cells were detached with trypsin solution (10x trypsin-EDTA (PAA, Austria) 1:9 diluted in Hank's basal salt solution (StemCell, Canada), which was inactivated after 3 minutes by the growth medium. After 5 minutes of centrifugation at 180 g and 22°C supernatant was removed. Cell were mixed with the growth medium to obtain cell density at $2x10^6$ cells/ml.

Electric pulse generation

Laboratory prototype pulse generator (University of Ljubljana), based on H-bridge digital amplifier with 1 kV MOSFETs (DE275-102N06A, IXYS, USA), described in [61] was used. Eight 100 µs long monopolar electric pulses with repetition frequency 1 Hz and amplitude of 0–600 V (0-3 kV/cm; voltage to distance ratio) with increments of 100 V (and additional increments in the permeabilization assay) were applied between stainless steel 304 plate electrodes (d = 2 mm). Oscilloscope HDO6104A-MS, differential probe HVD3206A and the current probe CP031A, all from LeCroy, USA, were used to monitor the delivered pulses, i.e. voltage and current. The delivered voltage was approximately 10-15% lower than the value set on the pulse generator and the current was in the range of 3-21 A. When pulses with high amplitudes were applied (Figure 1), current decreased slightly during the pulse, presumingly due to electrochemistry at electrode-electrolyte interface reducing the available interface area for ion exchange between the metal electrode and the electrolyte and possibly also due to ion depletion at the said interface.

Results

First, the permeabilization and the survival curves were obtained to determine experimental points for the studies on release of DAMPs. Permeabilization and survival curves are presented in all figures showing the concentration of various DAMPs to visualize how the presence of DAMPs is related to changes in permeabilization and cell viability. In figures the permeabilization and survival curves are shown only at pulse amplitudes tested for the presence of DAMPs; in steps of 50 V in the range of pulses where changes in permeabilization occur and in steps of 100 V above 200 V.

The concentration of ATP in supernatant was first measured with fluorescent method 30 minutes and

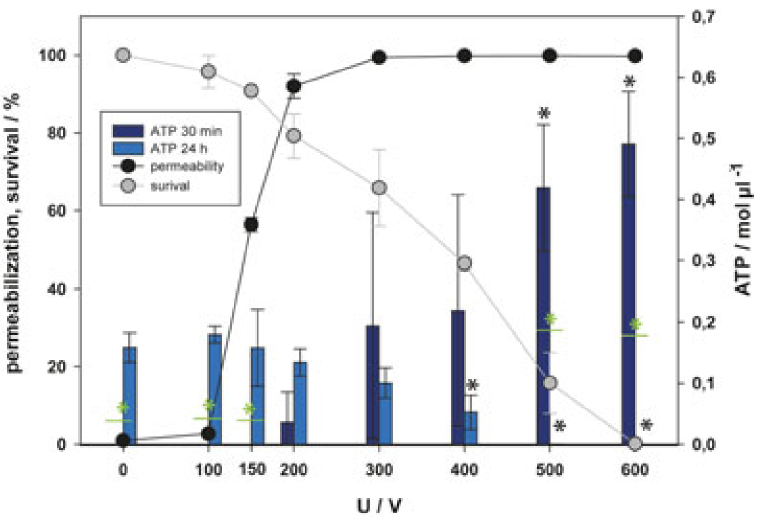

FIGURE 2. Release of adenosine triphosphate (ATP) as a function of electric pulse amplitude determined by fluorescent assay. Two-time points after electroporation were assessed. Permeabilization and survival curves are also presented. Black and green asterisks (*) indicate statistically significant differences between the samples at different voltages and the corresponding control at 0 V (one-way analysis of variance [ANOVA] followed by Holm-Sidak post-hoc test, ($p < 0.05$) and within the pair of samples at different voltages (t-test, $p < 0.05$), respectively).

24 hours after electroporation (Figure 2). At 30 minutes the concentration of ATP in supernatant was detected at 200 V. However, statistical difference between the control and the treatment groups (obtained by one-way analysis of variance [ANOVA] followed by the post-hoc test) was only detected at 500 V and above. The concentration of ATP in supernatant grew with increasing pulse amplitude, which after 24 hours led to decreased cell viability; e.g. correlation between the cell survival and ATP concentration in supernatant detected after 30 min is quite strong and negative; R = -0.864. Also, weak correlation between cell permeabilization and ATP concentration in supernatant (R = 0.594) confirms, that ATP presence in supernatant is more strongly correlated with the irreversible than the reversible electroporation. It may indicate that strong ATP release from cells leads to cell death.

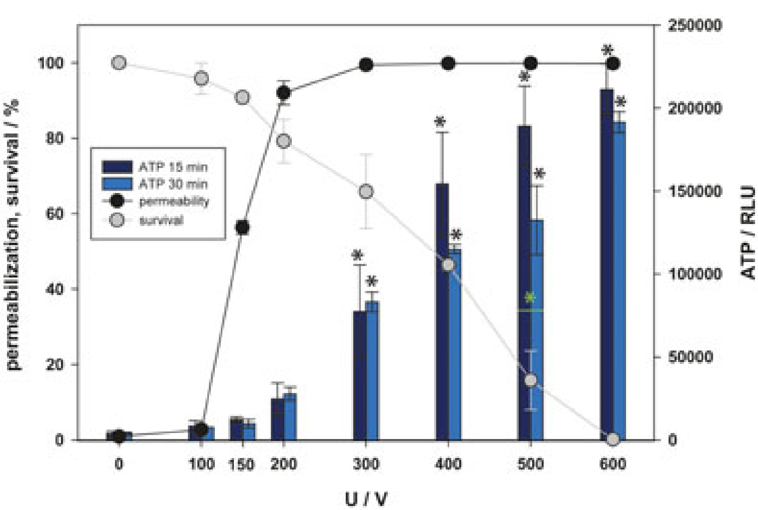

FIGURE 3. Release of adenosine triphosphate (ATP), as a function of electric pulse amplitude determined by luminescence assay. Two-time points after electroporation were assessed. Permeabilization and survival curves are also presented. Black and green asterisks (*) indicate statistically significant differences between the samples at different voltages and the corresponding control at 0 V (one-way analysis of variance [ANOVA] followed by Holm-Sidak post-hoc test, ($p < 0.05$) and within the pair of samples at different voltages (t-test, $p < 0.05$), respectively).

After 24 hours (Figure 2) the lowest ATP concentration was achieved at the pulse amplitude resulting in death of most cells (500, 600 V). The concentration of ATP at these points is statistically different to the results obtained 30 minutes after pulse treatment. After 24 hours the concentration of ATP had decreased with the lower viability, but statistical differences between the control and the treatment groups were present from 400 to 600 V. At 24 hours there is a positive statistical correlation between the cell survival and concentration of ATP in supernatant (R = 0.888), which is stronger than the correlation to permeabilization (R = -0.695).

Since no ATP was detected in supernatant within the range of reversible electroporation after 30 minutes using the fluorescent method (Figure 2), we also used a more sensitive luminescent method (Figure 3). Furthermore, since ATP analysis showed that 24 h after treatment ATP is not detected in all samples, we were also interested in how fast ATP was degraded. Scuderi *et at*. showed complete resealing of plasma membrane 10 minutes after pulse treatment using 8 x 100 µs pulses.[63] Thus, another time point for ATP measurement was chosen, *i.e.* 15 minutes after (Figure 3). With more sensitive luminescent detection assay, ATP was detected in supernatant already at 100 V, however statistically significant difference to control was only detected at 300 V and higher. These results are more reliable due to higher assay sensitivity however even with this method statistically significant amount of ATP in supernatant is detected in the range of irreversible electroporation, as increased electric field/voltage kills more cells more ATP is present in the extracellular space. This is also confirmed by a strong correlation between the survival and the amount of ATP in supernatant, R = -0.947 for 15 min and R = -0.964 for 30 min, and much weaker correlation between the permeabilization and the amount of ATP (R = 0.704 for 15 min and R = 0.728 for 30 min). In our results, only one significant difference was found in detected ATP amount between 15 and 30 minutes after pulse treatment at 500 V. Since this difference was not detected for all the experimental points (voltages), we believe that ATP in extracellular space is not degraded in this first 30 minutes after pulse treatment.

Calreticulin (CRT) is an endoplasmic reticulum protein which needs to be transferred to the outer leaflet of the plasma membrane in order to act as a DAMP. Externalization of calreticulin to outer membrane in an active process involving also its transport across the cell. Due to this active and time demanding process the externalization of calreticulin was investigated 4 and 24 hours (also used in previous studies[23-25,28]) after pulse treatment (Figure 4) on viable cells (determined by propidium iodide [PI] staining). Calreticulin was first detected at 300 V and its fluorescence increased with increasing voltage of pulses. Furthermore, the lowest viability at 600 V with < 5% of viable cell has the strongest signal of calreticulin after 4 and 24 hours. This could indicate the amount of externalized calreticulin per viable cell increases with the level of stress (amplitude of applied electric pulses). Furthermore, analysis shows a strong correlation between survival determined by MTS test and externalization of calreticulin, as survival decreased, the detection of calreticulin increased (R = -0.801 for 4h and R = -0.946 for 24h) and weak correlation between permeabilization and externalization of calreticulin was observed (R = 0.535 for 4h and R = 0.556 for 24h). Since calreticulin was detected only in viable cells (determined by PI) additional information on viability was obtained, and results were normalized to control (0 V) for each investigated time point separately. Except for the results at 300 V, no statistically significant difference between 4 and 24 hours was detected at any other experimental point, suggesting that calreticulin can be detected 4 hours after pulse treatment and that expression of the protein remains stable for the next 20 hours.

Until now, nucleic acids (in the role of DAMPs) have not been investigated in relation to electroporation. Most of RNA (except fresh transcripted mRNA) is located in cytoplasm, while DNA is located in the cell nucleus. The concentration of RNA and DNA in supernatant has been detected 15, 30 minutes and 24 hours after electroporation like in ATP assay (Figure 5 and 6). Concentration of DNA/RNA started to rise from 400 V up (Figure 5 and 6). This happened at the same pulse amplitudes where after 24 hours cell viability was affected, indicating the amount of nucleic acid occurs in the range of cell death, *i.e.* irreversible electroporation. Exposure of cells to higher pulse amplitudes caused higher release of nucleic acids, which after 24 h resulted in lower cell viability. This is confirmed also by a strong negative correlation between survival and

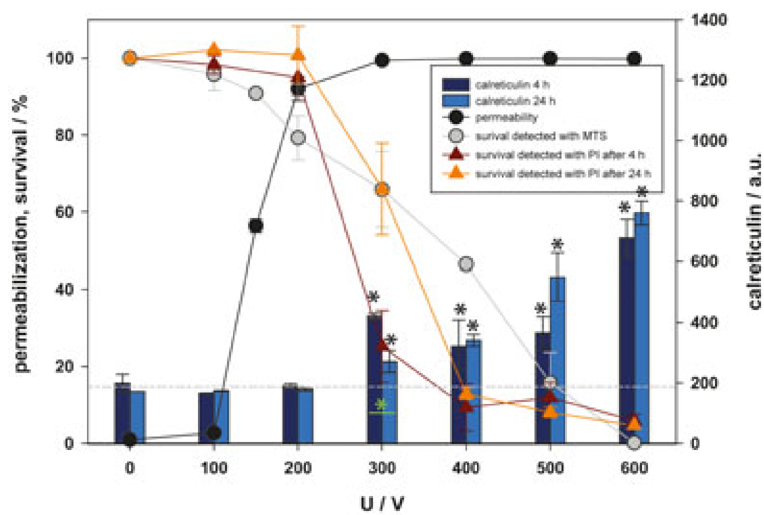

FIGURE 4. Externalization of calreticulin as a function of electric pulse amplitude. Two-time points after electroporation were assessed. Permeabilization and survival (MTS) curves are also presented. Survival detected by propidium iodide (PI) protocol is normalized to control and presented with red (4 hours after pulse treatment) and orange (24 hours after pulse treatment) line. Approximate baseline of calreticulin is presented with -----. Black and green asterisks (*) indicate statistically significant differences between the samples at different voltages and the corresponding control at 0 V (one-way analysis of variance [ANOVA] followed by Holm-Sidak post-hoc test, ($p < 0.05$) and within the pair of samples at different voltages (t-test, $p < 0.05$), respectively).

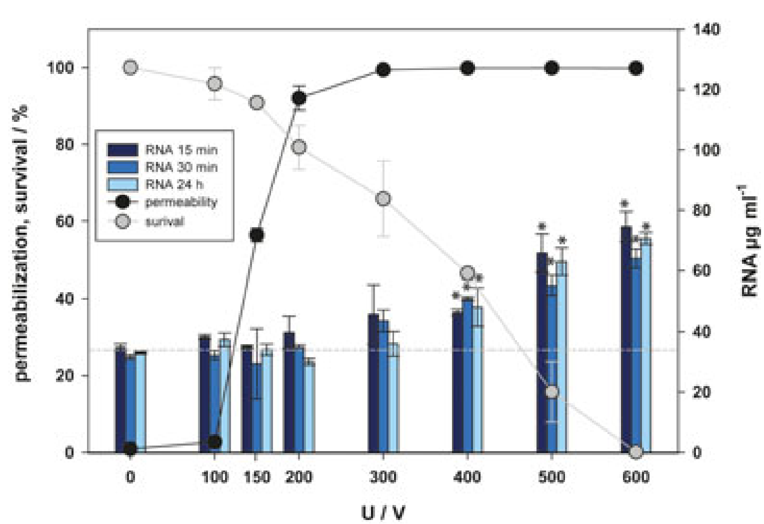

FIGURE 5. Release of RNA as a function of electric pulse amplitude. Three-time points after electroporation were assessed. Permeabilization and survival curves are also presented. Approximate baseline of RNA is presented with -----. Black and green asterisks (*) indicate statistically significant differences between the samples at different voltages and the corresponding control at 0 V (one-way analysis of variance [ANOVA] followed by Holm-Sidak post-hoc test, ($p < 0.05$) and within the pair of samples at different voltages (t-test, $p < 0.05$), respectively).

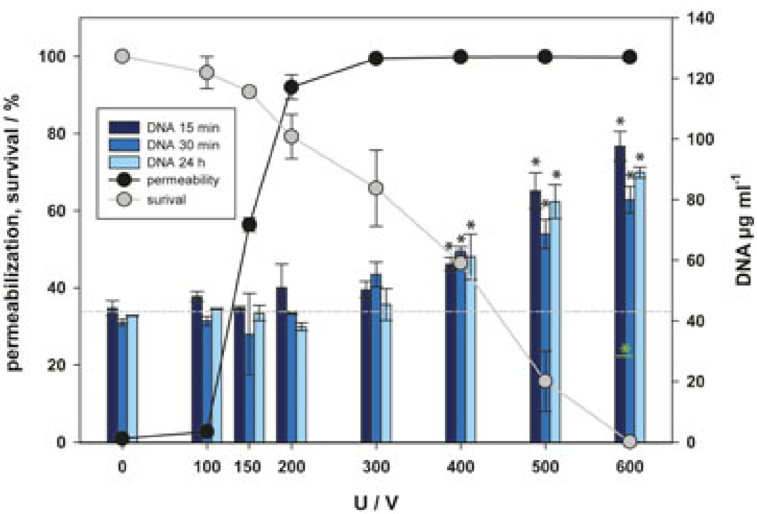

FIGURE 6. Release of DNA as a function of electric pulse amplitude. Three-time points after electroporation were assessed. Permeabilization and survival curves are also presented. Approximate baseline of DNA is presented with -----. Black and green asterisks (*) indicate statistically significant differences between the samples at different voltages and the corresponding control at 0 V (one-way analysis of variance [ANOVA] followed by Holm-Sidak post-hoc test, ($p < 0.05$) and within the pair of samples at different voltages (t-test, $p < 0.05$) respectively.

release of RNA (R = -0.909 for 15 min, R = -0.909 for 30 min, R = -0.919 for 24 h) and weak correlation between permeabilization and release of RNA (R = 0.584 for 15 min, R = 0.696 for 30 min, R is not significant for 24 h), respectively. Similarly, for DNA, a strong correlation between survival and release of DNA (R = -0.935 for 15 min, R = -0.919 for 30 min, R = -0.928 for 24 h) and a weak correlation between

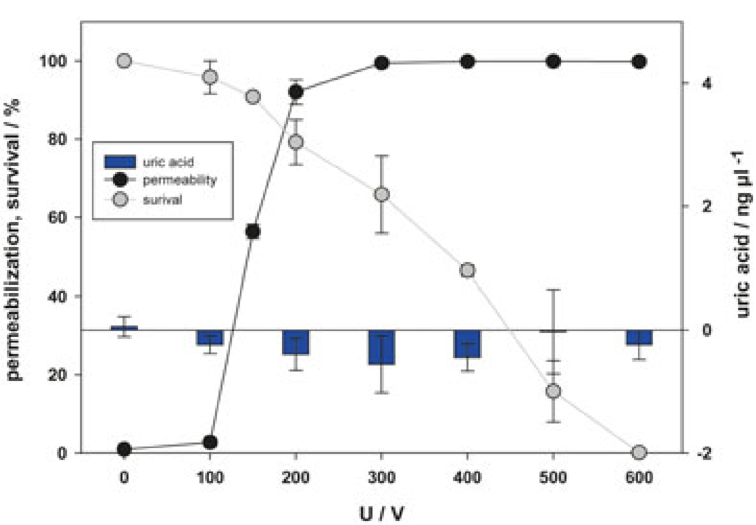

FIGURE 7. Release of uric acid as a function of electric pulse amplitude. Amount of uric acid was analysed 24 hours after pulse treatment in supernatant. Permeabilization and survival curves are also presented. No statistical difference was detected.

permeabilization and release of DNA (R = 0.571 for 15 min, R = 0.689 for 30 min, R is not significant for 24 h) was found. This correlation may indicate that loss of nucleic acids results in cell death.

Comparison of the concentration of RNA detected in supernatant 15, 30 minutes and 24 hours after pulse treatment did not show any significant differences. Comparison of the concentration of DNA detected in supernatant 15, 30 minutes and 24 hours after pulse treatment showed only significant differences between 15 and 30 minutes at 600 V, yet interestingly this was not the case between 15/30 minutes and 24 hours after pulse treatment. According to our results, the released nucleic acids *in vitro* are stable and are not degraded within 24 hours after pulse treatment.

We also tried to detect uric acid, another well know DAMP molecule. The release of uric acid in supernatant was analyzed 24 hours after pulse treatment (Figure 7). In our experiments we were however unable to detect any uric acid in supernatant after pulse treatment. Initial experiments were also performed after 30 minutes, but results were the same (data not shown).

Discussion

Besides the induced membrane permeabilization, followed by cell death, activation of the immune response seems to be an important component in effectiveness of ECT[26,35-37] and IRE[18,30-34] treatment *in vivo*. Activation of the immune system can be triggered by a special type of cell death, called immunogenic cell death (ICD) in which DAMPs are the key mediators.[64] Presence of DAMPs after pulse treatment has been detected in different types of cancer cells and normal tissues.[22-29] However, only one study was performed with 100 us pulses, which are predominantly used in ECT and IRE.[26] The authors investigated release of ATP, calreticulin and HMGB1 due to electroporation pulses alone, bleomycin alone and combination of electroporation pulses and bleomycin. Their study demonstrated the release of ATP and calreticulin after pulse treatment, but how this correlates to reversible and/or irreversible electroporation remained elusive. This question is addressed in our study, were release/detection of different DAMPs was correlated with permeabilization and survival curve *in vitro*.

Detected amounts of DAMPs were correlated to cell membrane permeabilization determined by PI assay immediately after pulse treatment and cell survival, analyzed 24 hours after treatment by

MTS test, *i.e.* to reversible and irreversible electroporation, respectively. It is generally believed that membrane permeabilization and cell survival after pulse treatment are causally related, *i.e.* in IRE cell death occurs due to membrane permeabilization and loss of cell homeostasis (in this study correlation coefficient between the two is -0.680) and in ECT increased accumulation of drug leads to increased cell cytotoxicity.

In ECT and IRE it was also demonstrated that the immune response plays an important role in achieving therapeutic effect.[33-36] We have therefore determined different DAMPs at different times after exposing the cells to electric pulses and determined whether the concentrations of extracellular DAMPs were better correlated to cell death or to membrane permeabilization. While activation inflammatory response and activation of immune system is desired in cancer therapies, on the other hand it can be a wanted or an unwanted effect in gene therapy.[68,69] In DNA vaccination therapies, changed permeability of cell membrane enhances the introduction of DNA vaccine inside of cell and the presence of DAMPs additionally activates inflammatory response, which leads to enhanced production of antibodies, thus enhancing the efficiency of vaccination.[65-67] Nevertheless, in most cases of gene therapy, the immune response in unwanted, as it may destroy the transfected cells and prevent transgenic protein expression.[68,69] By now many DAMPs have been identified and the number is still increasing. Most known are the HMGB1, nucleic acids, proteins like heat-shock proteins, S100 and calreticulin, purine metabolites like ATP and uric acid and saccharides. A list of know DAMPs and their receptors is given by Roh and Sohn.[48]

ATP is a well-known molecule in biology and biochemistry for being a universal energy source in the cell and necessary for multiple cell processes and cell metabolism. Interestingly, first studies of electroporation and increase in plasma membrane permeability involved adenosine triphosphate ATP detection in electroporation buffer.[70] The released ATP is also considered a DAMP. In our study two types of ATP detection methods with different sensitivities were used.[71,72] In a previous study performed by Calvet *et al*.[26] using the same pulses as in our study, the release of ATP was detected 30 minutes after the treatment. We were able to confirm their observations with the fluorescence and the luminescence method (Figures 2 and 3 respectively). Furthermore, the investigation of the effects at different pulse amplitudes showed that the release of ATP increases with increasing amplitude. This was expected, as ATP release was previously used as a permeability marker after electroporation.[70] However, in our results statistical differences between the control and the treatment groups were not detected in the range where the permeabilization curve is ascending, but was detected only in the range of pulse amplitudes at which all cells were already permeabilized and many were dead. Since ANOVA analysis is less sensitive when large amount of samples with big differences between them are analyzed, additional ANOVA was performed, taking into account only the results from 0 to 300 V (e.g. where permeabilization changes from 0 to 100%). Now additional analysis showed that statistical differences between control and the treatment groups are present at 200 V and above in luminescent method, suggesting ATP release as possible membrane permeabilization detection method. In the fluorescence method, this statistical difference was obtained only at 300 V. Such difference in analysis and also a bigger ratio of ATP between the control and the treatment groups indicates that the luminescence method is more sensitive method than the fluorescence method. Taken into consideration ATP release at all investigated voltages (also the one leading to cell death after 24 hours) the release of ATP is more strongly correlated to cell death/irreversible electroporation (R = 0.888) than permeability/reversible electroporation (R = -0.695).

24 hours after pulse treatment (Figure 2) the highest amount of ATP was detected in the supernatant of control sample and the amount of ATP decreased with increasing pulse amplitude. This can be explained by homeostasis of ATP in living cells. In a living homeostatic cell most of the ATP is located intracellularly, however in considerably lower concentration ATP is also present in extracellular space.[73] When cells are damaged, considerable release of ATP molecule affects ATP pumps, causing depletion of intracellular K^+ and accumulation of intracellular NA^+ and Ca^{2+} and leading to cell death.[74] A previous study showed that electroporation pulses cause ATP depletion, which in 24 results in lower viability, presumingly by affecting Ca^{2+}-ATPase.[75] In our study the effect on survival was also confirmed by very strong positive correlation between survival/irreversible electroporation and amount of ATP detected in supernatant (R = 0.888). Nevertheless, we need to consider, that some of the ATP detected in supernatant could be from the cells damaged due to cell handling during experiment. In extracellular space ATP is degraded by nucleotides like CD39 and CD37, which convert

ATP through ADP and AMP to adenosine[73], which explains why ATP was detected 30 minutes at very high voltages (500, 600 V), but was no longer detected after 24 hours (Figure 2). This can also explain why Calvet *et al.*[26], was unable to detect ATP 30 hours after pulse treatment alone, however it does not explain, why ATP was still detected when bleomycin alone or in combination with electroporation pulses was used. How fast ATP degrades in extracellular space, remains unknown. Our results do not indicate that ATP degrades within the first 30 minutes after pulse treatment, since no difference between 15 and 30 minutes after pulse treatment was detected. In a different study[76] the results for ATP 4 hours after pulse treatment was lower in samples exposed to pulse treatment than in the control. If this is taken into consideration together with our results, then ATP degradation *in vitro* occurs somewhere between 30 minutes and 4 hours after pulse treatment.

Calreticulin was another molecule of interest in our study. This highly conserved protein has major functions in lumen of the endoplasmic reticulum (ER). It is involved in correct folding of proteins that are produced in endoplasmic reticulum[77] and in regulation of calcium metabolism, as it affects Ca^{2+} capacity of the ER stores.[78] In the early phase of cell death, activated ER stress leads to translocation of calreticulin to cells surface trough ER-Golgi pathway or lysosome exocytosis.[79,80] Calreticulin, as DAMP, was investigated previously in electroporation studies.[22-26,28] In Calvets's study[26], which used the same pulses as in our study (eight 100 μs pulses), calreticulin was determined 30 hours after treatment using different treatments. Calreticulin was detected on the plasma membrane after electroporation pulses alone or in combination with bleomycin (ECT), yet no externalization was detected in cells threated with bleomycin alone. Since only calreticulin, exposed on the cell surface acts as a DAMP, only viable cells (determined by PI) were taken into analysis. The presence of calreticulin on the cell surface was previously detected already 4 hours after electroporation with millisecond pulses[28], thus we assumed 4 hours is sufficient time for calreticulin to transfer to cells surface. Additionally, calreticulin was detected also 24 after pulse treatment. In our study calreticulin was investigated 4 and 24 hours after treatment (Figure 4), which is after the resealing of cell membrane.[63] Even though calreticulin was detected on the surface of live cells, it was detected only in the range of irreversible electroporation. Additionally, calreticulin detection increased with decreasing cell viability (less viable cells), implicating that bigger stress or in this case pulse amplitude causes more calreticulin molecules to be externalized to cell surface. Nevertheless, since it is believed that externalization of calreticulin occurs in early phase of cell death[79,80], it is possible that cell determined as viable would die within next hours.

In comparison to ATP, calreticulin is more stable. Only at 300 V the difference between 4 and 24 hours was statistically significant. Stability of externalized calreticulin was previously also confirmed in another in vitro study.[24] Nevertheless, *in vivo* study shows expression is the strongest between four and six hours, and diminishes 24 h after the treatment.[28]

So far studies investigating DAMPs, released by the electroporation treatment, included ATP, calreticulin and HMGB1. In addition to ATP and calreticulin we also included other known DAMPs in our study, namely nucleic acids and uric acid, which so far have not been investigated as DAMPs after electroporation. Inside the cells nucleic acids are the source of genetic information. As DAMPs in extracellular space nucleic acids bind to TLR receptors. Bound DNA can even attract HMGB1 (a non-histone nuclear protein, which can be actively or passively released into extracellular space, where it acts as a DAMP[81]) and together they form complexes stimulating dendritic cells to produce type 1 interferon (non-specific immune response), which can lead to anti-DNA autoantibody production (specific immune response).[82] Nucleic acids (RNA and DNA) can be detected in supernatant already within minutes after pulse treatment (Figure 5,6). Nevertheless, we need to consider – based on the control, 0 V in Figures 5 and 6, that some of the nucleic acids detected in supernatant could be from the cells damaged due to cell handling during experiment. Since RNA is more abundantly present in cells than DNA[83,84], the same was expected to be the case in the supernatant after pulse treatment. However, the amount of detected DNA in our samples was bigger than that of RNA. Since RNA is more prone to degradation than DNA[84], it is possible that some of the RNA was destroyed during the process of analysis. Nevertheless, the amount of released nucleic acids increases with increasing voltage of electric pulses to which the cells were exposed. Our results indicate that the release of nucleic acids (RNA and DNA) occurs in the range of irreversible electroporation; *i.e.* pulse amplitudes that lead to cell death as determined by MTS test at 24 h post treatment. This was confirmed also by very strong negative correlation between the cell survival and the release for RNA and DNA.

Uric acid is a product of purine metabolism within the cell, like degradation of nucleic acids, and is released from injured and dying cells.[85] A molecule that is soluble inside the cell, accumulates in extracellular space, where it is transformed in insoluble crystal of monosodium urate, stimulating the maturation of dendritic cells and T-cell response.[85,86] Here, the presence of uric acid after electroporation was investigated for the first time. Presence of uric acid in supernatant was investigated 24 hours after electroporation treatment (Figure 7). We expected uric acid to show a similar behavior in pulse parameter dependency as other DAMPs. However, we did not detect uric acid in supernatant after pulse treatment. Standard curve was obtained, therefore Uric Acid Assay Kit worked. Maybe uric acid production did not happen or uric acid was still inside of cells and not yet in supernatant as predicted. Furthermore, we found no existing data on CHO cells and uric acid in the literature, so maybe formation of uric acid in ovarian cells does not occur.

With respect to the results obtained, detection of DAMPs and its correlation to cell membrane permeabilization and cell survival seems to be more complex than initially thought. Even a DAMP like ATP, which can be released due to electroporation alone is better correlated to cell survival than membrane permeabilization (Tables 1, 2). A recent study performed by Ringel-Scaia *et al.*[27], in which multiple signaling pathways were analyzed, showed that the cell and cell population is a dynamic system which changes with time. Two hours after pulse treatment RNA analyses showed activation of immunosuppressive pathway, cell injury and apoptosis. With time these genes became less pronounces and after 24 hours change in gene expression indicated proinflammatory response, cell repair and necrosis/pyroptosis. This explains changes in DAMPs detection hours after pulse treatment, including the presence and absence of different DAMPs and its correlation with cell survival. Since statistical correlations between DAMP release and cell survival is much stronger than with membrane permeabilization, involvement of immune system in IRE can be explained. However, activation of immune system was demonstrated also in ECT treatments, were reversible electroporation is used. How can that be, if correlation between membrane permeabilization and released DAMPs is weak or does not even exist? Modeling[87] and *in vivo* experiments[88] show that application of

TABLE 1. Correlation (R) between survival and release of damage-associated molecular pattern molecules (DAMPs) after pulse treatment. Investigated time points for each molecule are presented in the bottom row. Correlation was evaluated with Pearson correlation coefficient and survival was analyzed via MTS assay 24 hours after pulse treatment

	R *vs.* survival (MTS)				
PI	-0.680				
ATP		-0.947 (L)	-0.964 (L)/-0.864 (F)		0.888 (F)
DNA		-0.935	-0.919		-0.928
RNA		-0.909	-0.909		-0.919
CRT				-0.801	-0.946
uric acid					NS
time points after EP	*3 min*	*15 min*	*30 min*	*4 h*	*24 h*

ATP = adenosine triphosphate; CRT = calreticulin; (F) = fluorescence assay; (L) = luminescence assay; NS = no statistical significance; PI = propidium iodide

TABLE 2. Correlation (R) between permeabilization and release of damage-associated molecular pattern molecules (DAMPs) after pulse treatment. Investigated time points for each molecule are present in the bottom row. Correlation was evaluated with Pearson correlation coefficient and permeabilization was analyzed by propidium iodide (PI) assay 3 minutes after pulse treatment

	R vs permeabilization (PI)				
MTS					-0.680
ATP		0.704	0.728 (L)/0.594 (F)		-0.695 (F)
DNA		0.571	0.689		NS
RNA		0.584	0.696		NS
CRT				0.535	0.556
uric acid					NS
time points after EP	*3 min*	*15 min*	*30 min*	*4 h*	*24 h*

ATP = adenosine triphosphate; CRT = calreticulin; (F) = fluorescence assay; (L) = luminescence assay; NS = no statistical significance

nominally reversible electroporation pulses such as those used for ECT of tumors still causes some cell death by means of irreversible electroporation in tissue close to the electrodes, due to inhomogeneous electric field distribution, which can thus lead to the release of DAMPs and activation of the immune system.

The aim of this study was to explore, if and when specific DAMPs are released as a consequence of electroporation and if the release of DAMPs can be correlated to reversible and/or irreversible electroporation. Even though detection of certain DAMPs remains uncertain, others show strong correlation to cell survival/irreversible electroporation and much weaker correlation to membrane permeabilization/reversible electroporation. Release of DAMPs could perhaps serve as a predictor of cell death. In addition, it may indicates that the stability of certain DAMPs is questionable and thus their presence and detectability is time dependent. This needs to be taken into consideration when designing protocols to detect DAMPs after electroporation treatment. Finally, to obtain a better insight of DAMP release with respect to electroporation treatment other cell types including also cancer cell types should be investigated.

Acknowledgements

Authors would like to thank L. Vukanović and D. Hodžić for their help in the cell culture laboratory and Dr. Matej Reberšek for help with pulse recording and image production. The research was supported by Medtronic and the Slovenian Research Agency (research core funding No. IP-0510, P2-0249 and grant to young researcher Tamara Polajžer).

References

1. Orlowski S, Belehradek J, Paoletti C, Mir LM. Transient electropermeabilization of cells in culture. Increase of the cytotoxicity of anticancer drugs. *J Biochem Pharmacol Res* 1988; **3:** 4727-33. doi: 10.1016/0006-2952(88)90344-9

2. Mir LM. Bases and rationale of the electrochemotherapy. *EJC Suppl* 2006; **4:** 38-44. doi: 0.1016/j.ejcsup.2006.08.005

3. Scheffer HJ, Nielsen K, De Jong MC, Van Tilborg AJM, Vieveen JM, Bouwman A, et al. Irreversible electroporation for nonthermal tumor ablation in the clinical setting: a systematic review of safety and efficacy. *J Vasc Interv Radiol* 2014*;* **25:** 997-1011. doi: 10.1016/j.jvir.2014.01.028

4. Phillips M, Maor E, Rubinsky B. Nonthermal irreversible electroporation for tissue decellularization. *J Biomech Eng* 2010; **132:** 091003. doi: 10.1115/1.4001882

5. Davalos RV, Mir LM, Rubinsky B. Tissue ablation with irreversible electroporation. *Ann Biomed Eng* 2005; **3:** 223-31. doi: 10.1007/s10439-005-8981-8

6. Chen X, Ren Z, Zhu T, Zhang X, Peng Z, Xie H, et al. Electric ablation with irreversible electroporation (IRE) in vital hepatic structures and follow-up investigation. *Sci Rep* 2015; **5:** 16233. doi: 10.1038/srep16233

7. Jiang C, Davalos RV, Bischof JC. A review of basic to clinical studies of irreversible electroporation therapy. *IEEE Trans Biomed Eng* 2015; **62:** 4-20. doi: 10.1109/TBME.2014.2367543

8. Galluzzi L, Maiuri MC, Vitale I, Zischka H, Castedo M, Zitvogel L, et al. Cell death modalities: classification and pathophysiological implications. *Cell Death Differ* 2007; **14:** 1237-43. doi: 10.1038/sj.cdd.4402148

9. Schweichel JU, Merker HJ. The morphology of various types of cell death in prenatal tissues. *Exp Teratol* 1973; **7:** 253-66. doi: 10.1002/tera.1420070306

10. Galluzzi L, Vitale I, Aaronson SA, Abrams JM, Adam D, Agostinis P, et al. Molecular mechanisms of cell death: recommendations of the nomenclature committee on cell death 2018. *Cell Death Differ* 2018; **25:** 486-541. doi: 10.1038/s41418-017-0012-4

11. Batista Napotnik T, Rebersek M, Vernier PT, Mali B, Miklavcic D. Effects of high voltage nanosecond electric pulses on eukaryotic cells (in vitro): a systematic review. *Bioelectrochemistry* 2016; **110:** 1-12. doi: 10.1016/j.bioelechem.2016.02.011

12. Beebe SJ. Regulated and apoptotic cell death after nanosecond electroporation. In: Miklavčič D, editor. *Handbook of electroporation*. Heidelberg: Springer International Publishing; 2017. p. 511-28. doi: 10.1007/978-3-319-32886-7_146

13. Chai W, Zhang W, Wei Z, Xu Y, Shi J, Luo X, et al. Irreversible electroporation of the uterine cervix in a rabbit model. *Biomed Microdevices* 2017; **19:** 103. doi: 10.1007/s10544-017-0248-2

14. Kim HB, Sung CK, Baik KY, Moon KW, Kim HS, Yi JH, et al. Changes of apoptosis in tumor tissues with time after irreversible electroporation. *Biochem Biophys Res Commun* 2013; **435:** 651-6. doi: 10.1016/j.bbrc.2013.05.039

15. Lee EW, Loh CT, Kee ST. Imaging guided percutaneous irreversible electroporation: Ultrasound and immunohistological correlation. *Technol Cancer Res Treat* 2007; **6:** 287-93. doi: 10.1177/153303460700600404

16. Lee EW, Wong D, Tafti BA, Prieto V, Totonchy M, Hilton J, et al. Irreversible electroporation in eradication of rabbit VX2 liver tumor. *J Vasc Interv Radiol* 2012; **23:** 833-40. doi: 10.1016/j.jvir.2012.02.017

17. Zhang Z, Li W, Procissi D, Tyler P, Omary RA, Larson AC. Rapid dramatic alterations to the tumor microstructure in pancreatic cancer following irreversible electroporation ablation. *Nanomedicine* 2014; **9:** 1181-92. doi: 10.2217/nnm.13.72

18. José A, Sobrevals L, Ivorra A, Fillat C. Irreversible electroporation shows efficacy against pancreatic carcinoma without systemic toxicity in mouse models. *Cancer Lett* 2012; **317:** 16-23. doi: 10.1016/j.canlet.2011.11.004

19. Al-Sakere B, André F, Bernat C, Connault E, Opolon P, Davalos RV, et al. Tumor ablation with irreversible electroporation. *PLoS One* 2007; **2:** e1135. doi: 10.1371/journal.pone.0001135

20. Zhang Y, Lyu C, Liu Y, Lv Y, Chang TT, Rubinsky B. Molecular and histological study on the effects of non-thermal irreversible electroporation on the liver. *Biochem Biophys Res Commun* 2018; **500:** 665-70. doi: 10.1016/j.bbrc.2018.04.132

21. López-Alonso B, Hernáez A, Sarnago H, Naval A, Güemes A, Junquera C, et al. Histopathological and ultrastructural changes after electroporation in pig liver using parallel-plate electrodes and high-performance generator. *Sci Rep* 2019; **9:** 2467. doi: 10.1038/s41598-019-39433-6

22. Nuccitelli R, Berridge JC, Mallon Z, Kreis M, Athos B, Nuccitelli P. Nanoelectroablation of murine tumors triggers a cd8-dependent inhibition of secondary tumor growth. *PLoS One* 2015; **10:** e0134364. doi: 10.1371/journal.pone.0134364

23. Nuccitelli R, McDaniel A, Anand S, Cha J, Mallon Z, Berridge J, et al. Nanopulse stimulation is a physical modality that can trigger immunogenic tumor cell death. *J Immunother Cancer* 2017; **5:** 32. doi: 10.1186/s40425-017-0234-5

24. Guo S, Jing Y, Burcus NI, Lassiter BP, Tanaz R, Heller R, et al. Nano-pulse stimulation induces potent immune responses, eradicating local breast cancer while reducing distant metastases. *Int J Cancer* 2018; **142:** 629-40. doi: 10.1002/ijc.31071

25. Rossi A, Pakhomova ON, Mollica PA, Casciola M, Mangalanathan U, Pakhomov AG, et al. Nanosecond pulsed electric fields induce endoplasmic reticulum stress accompanied by immunogenic cell death in murine models of lymphoma and colorectal cancer. *Cancers* 2019; **11:** 2034. doi: 10.3390/cancers11122034

26. Calvet CY, Famin D, André FM, Mir LM. Electrochemotherapy with bleomycin induces hallmarks of immunogenic cell death in murine colon cancer cells. *Oncoimmunology* 2014; **3:** e28131. doi: 10.4161/onci.28131

27. Ringel-Scaia VM, Beitel-White N. Lorenzo MF, Brock RM, Huie KE, Coutermarsh-Ott S. High-frequency irreversible electroporation is an effective tumor ablation strategy that induces immunologic cell death and promotes systemic anti-tumor immunity. *EBioMedicine* 2019; **44:** 112-25. doi: 10.1016/j.ebiom.2019.05.036

28. Schultheis K, Smith, TRF, Kiosses WB, Kraynyak KA, Wong A, Oh J, et al. Delineating the cellular mechanisms associated with skin electroporation. *Hum Gene Ther Methods* 2018; **29:** 177-88. doi: 10.1089/hgtb.2017.105

29. Zhao J, Wen X, Tian L, Li T, Xu C, Wen X, et al. Irreversible electroporation reverses resistance to immune checkpoint blockade in pancreatic cancer. *Nat Commun* 2019; **10:** 1-14. doi: 10.1038/s41467-019-08782-1

30. Vogl TJ, Wissniowski TT, Naguib NNN, Hammerstingl RM, Mack MG, Münch S, et al. Activation of tumor-specific T lymphocytes after laser-induced thermotherapy in patients with colorectal liver metastases. *Cancer Immunol Immunother* 2019; **58:** 1557-63. doi: 10.1007/s00262-009-0663-1

31. Bulvik BE, Rozenblum N, Gourevich S, Ahmed M, Andriyanov AV, Galun E, et al. Irreversible electroporation versus radiofrequency ablation: a comparison of local and systemic effects in a small-animal model. *Radiology* 2016; **280:** 413-24. doi: 10.1148/radiol.2015151166

32. White SB, Zhang Z, Chen J, Gogineni VR, Larson AC. Early immunologic response of irreversible electroporation versus cryoablation in a rodent model of pancreatic cancer. *J Vasc Interv Radiol* 2018; **29:** 1764-9. doi: 10.1016/j.jvir.2018.07.009

33. Scheffer HJ, Stam AGM, Geboers B, Vroomen LGPH, Ruarus A, de Bruijn B, et al. Irreversible electroporation of locally advanced pancreatic cancer transiently alleviates immune suppression and creates a window for antitumor T cell activation. *Oncoimmunology* 2019; **8:** 1652532. doi: 10.1080/2162402X.2019.1652532

34. Pandit H, Hong YK, Li Y, Rostas J, Pulliam Z, Li *P,* et al. Evaluating the regulatory immunomodulation effect of irreversible electroporation (ire) in pancreatic adenocarcinoma. *Ann Surg Oncol* 2019; **26:** 800-6. doi: 10.1245/s10434-018-07144-3

35. Calvet CY, Mir LM. The promising alliance of anti-cancer electrochemotherapy with immunotherapy. *Cancer Metastasis Rev* 2016; **35:** 165-77. doi: 10.1007/s10555-016-9615-3

36. Sersa G, Teissie J, Cemazar M, Signori E, Kamensek U, Marshall G, et al. Electrochemotherapy of tumors as in situ vaccination boosted by immunogene electrotransfer. *Cancer Immunol Immunother* 2015; **64:** 1315-27. doi: 10.1007/s00262-015-1724-2

37. Serša G, Miklavcic D, Cemazar M, Belehradek J, Jarm T, Mir LM. Electrochemotherapy with CDDP on LPB sarcoma: comparison of the anti- tumor effectiveness in immunocompetent and immunodeficient mice. *Bioelectrochem Bioenerg* 1997; **43:** 279-83. doi: 10.1016/S0302-4598(96)05194-X

38. Gerlini G, Tun-Kyi A, Dudli C, Burg G, Pimpinelli N, Nestle FO. Metastatic melanoma secreted IL-10 down-regulates CD1 molecules on dendritic cells in metastatic tumor lesions. *Am J Pathol* 2004; **165:** 1853-63. doi: 10.1016/S0002-9440(10)63238-5

39. Gerlini G, Di Gennaro P, Mariotti G, Urso C, Chiarugi A, Pimpinelli N, et al. Indoleamine 2,3-dioxygenase cells correspond to the BDCA2 plasmacytoid dendritic cells in human melanoma sentinel nodes. *J Investig Dermatol* 2010; **130:** 898-901. doi: 10.1038/jid.2009.307

40. Geboers B, Scheffer HJ, Graybill PM, Ruarus AH, Nieuwenhuizen S, Puijk RS, et al. High-voltage electrical pulses in oncology: irreversible electroporation, electrochemotherapy, gene electrotransfer, electrofusion, and electroimmunotherapy. *Radiology* 2020; **295:** 192190. doi: 10.1148/radiol.2020192190

41. Zhou J, Wang G, Chen Y, Wang H, Hua Y, Cai Z. Immunogenic cell death in cancer therapy: Present and emerging inducers. *J Cell Mol Med* 2019; **23:** 4854-65. doi: 10.1111/jcmm.14356

42. Alnaggar M, Lin M, Mesmar A, Liang S, Qaid A, Xu K, et al. Allogenic natural killer cell immunotherapy combined with irreversible electroporation for stage iv hepatocellular carcinoma: survival outcome. *Cell Physiol Biochem* 2018; **48:** 1882-93. doi: 10.1159/000492509

43. Yang Y, Qin Z, Du D, Wu Y, Qiu S, Mu F, et al. Safety and short-term efficacy of irreversible electroporation and allogenic natural killer cell immunotherapy combination in the treatment of patients with unresectable primary liver cancer. *Cardiovasc Intervent Radiol* 2019; **42:** 48-59. doi: 10.1007/s00270-018-2069-y

44. Lin M, Liang S, Wang X, Liang Y, Zhang M, Chen J. Percutaneous irreversible electroporation combined with allogeneic natural killer cell immunotherapy for patients with unresectable (Stage III/IV) pancreatic cancer: a promising treatment. *J Cancer Res Clin Oncol* 2017; **143:** 2607-18. doi: 10.1007/s00432-017-2513-4

45. Diercks GFH, Kluin PM. Basic principles of the immune system and autoimmunity. In: Jonkman FM, editor. *Autoimmune bullous diseases.* Heidelberg: Springer International Publishing; 2016. p. 3-12. doi: 10.1007/978-3-319-23754-1_1

46. Kellie S, Al-Mansour Z. Overview of the immune system. In: Skwarczynski M, Toth I, editors. *Micro- and nanotechnology in vaccine development*. Elsevier Inc; 2017. p. 63-81. doi: 10.1016/B978-0-323-39981-4.00004-X

47. Chaplin DD. Overview of the immune response. *J Allergy Clin Immunol* 2010; **125:** S3. doi: 10.1016/j.jaci.2009.12.980

48. Roh JS, Sohn DH. Damage-associated molecular patterns in inflammatory diseases. *Immune Netw* 2018; **18:** e27. doi: 10.4110/in.2018.18.e27

49. Obeid M, Tesniere A, Ghiringhelli F, Fimia GM, Apetoh L, Perfettini JL, et al. Calreticulin exposure dictates the immunogenicity of cancer cell death. *Nat Med* 2007; **13:** 54-61. doi: 10.1038/nm1523

50. Kato J, Svensson CI. Role of extracellular damage-associated molecular pattern molecules (DAMPs) as mediators of persistent pain. *Prog Mol Biol Transl Sci* 2015; **131:** 251-79. doi: 10.1016/bs.pmbts.2014.11.014

51. Bianchi ME. DAMPs, PAMPs and alarmins: all we need to know about danger. *J Leukoc Biol* 2007; **81:**1-5. doi: 10.1189/jlb.0306164

52. Chan JK, Roth J, Oppenheim JJ, Tracey KJ, Vogl T, Feldmann M. Science in medicine Alarmins : awaiting a clinical response. *J Clin Invest* 2012; **122:** 2711-9. doi: 10.1172/JCI62423.tification

53. Rock KL, Lai JJ, Kono H. Innate and adaptive immune responses to cell death. *Immunol Rev* 2011; **243:** 191-205. doi: 10.1111/j.1600-065X.2011.01040.x

54. Stoecklein VM, Osuka A, Lederer JA. Trauma equals danger - damage control by the immune system. *J Leukoc Biol* 2012; **92:** 539-51. doi: 10.1189/jlb.0212072

55. Wynn TA, Ramalingam TR. Mechanisms of fibrosis: therapeutic translation for fibrotic disease. *Nat Med* 2012; **18:** 1028-40. doi: 10.1038/nm.2807

56. Straino S, Di Carlo A, Mangoni A, De Mori R, Guerra L, Maurelli R. High-mobility group box 1 protein in human and murine skin: involvement in wound healing. *J Invest Dermatol* 2008; **128:** 1545-53. doi: 10.1038/sj.jid.5701212

57. Yang S, Xu L, Yang T, Wang F. High-mobility group box-1 and its role in angiogenesis. *J Leukoc Biol* 2014; **95:** 563-74. doi: 10.1189/jlb.0713412

58. Zampell JC, Yan A, Avraham T, Andrade V, Malliaris S, Aschen S, et al. Temporal and spatial patterns of endogenous danger signal expression after wound healing and in response to lymphedema. *Am J Physiol Cell Physiol* 2011; **300:** 1107-21. doi: 10.1152/ajpcell.00378.2010

59. Duffield JS, Lupher M, Thannickal VJ, Wynn TA. Host responses in tissue repair and fibrosis. *Annu Rev Pathol* 2013; **8:** 241-76. doi: 10.1146/annurev-pathol-020712-163930

60. Rols MP, Teissié J. Electropermeabilization of mammalian cells. Quantitative analysis of the phenomenon. *Biophys J* 1990; **58:** 1089-98. doi: 10.1016/S0006-3495(90)82451-6

61. Sweeney DC, Reberšek M, Dermol J, Rems L, Miklavčič D, Davalos RV. Quantification of cell membrane permeability induced by monopolar and high-frequency bipolar bursts of electrical pulses. *Biochim Biophys Acta Biomembr* 2016; **1858:** 2689-98. doi: 10.1016/j.bbamem.2016.06.024

62. Batista Napotnik T, Miklavčič D. In vitro electroporation detection methods – an overview. *Bioelectrochemistry* 2018; **120:** 166-82. doi: 10.1016/j.bioelechem.2017.12.005

63. Scuderi M, Rebersek M, Miklavcic D, Dermol-Cerne J. The use of high-frequency short bipolar pulses in cisplatin electrochemotherapy in vitro. *Radiol Oncol* 2019; **53:** 194-205. doi: 10.2478/raon-2019-0025

64. O'Brien MA, Power DG. Clover AJP, Bird B, Soden DM, Forde PF. Local tumour ablative therapies: opportunities for maximising immune engagement and activation. *Biochim Biophys Acta* 2014; **184:** 510-23. doi: 10.1016/j.bbcan.2014.09.005

65. Babiuk S, Baca-Estrada ME, Foldvari M, Middleton DM, Rabussay D, Widera G, et al. Increased gene expression and inflammatory cell infiltration caused by electroporation are both important for improving the efficacy of DNA vaccines. *J Biotechnol* 2004; **110:** 1-10. doi: 10.1016/j.jbiotec.2004.01.015

66. Roos AK, Moreno S, Leder C, Pavlenko M, King A, Pisa P. Enhancement of cellular immune response to a prostate cancer DNA vaccine by intradermal electroporation. *Mol Ther* 2006; **13:** 320-7. doi: 10.1016/j.ymthe.2005.08.005

67. Chiarella P, Massi E, De Robertis M, Sibilio A, Parrella P, Fazio VM, et al. Electroporation of skeletal muscle induces danger signal release and antigen-presenting cell recruitment independently of DNA vaccine administration. *Expert Opin Biol Ther* 2008; **8:** 1645-57. doi: 10.1517/14712598.8.11.1645

68. Bessis N, Garcia Cozar FJ, Boissier MC. Immune responses to gene therapy vectors: influence on vector function and effector mechanisms. *Gene Ther* 2004; **11(Suppl 1):** S10-7.. doi: 10.1038/sj.gt.3302364

69. Shirley JL, de Jong YP, Terhorst C, Herzog RW. Immune responses to viral gene therapy vectors. *Mol Ther* 2020; **28:** 709-22. doi: 10.1016/j.ymthe.2020.01.001

70. Rols MP, Teissié J. Electropermeabilization of mammalian cells. Quantitative analysis of the phenomenon. *Biophys J* 1990; **58:** 1089-98. doi: 10.1016/S0006-3495(90)82451-6

71. Fan F, Wood KV. Bioluminescent assays for high-throughput screening. *Assay Drug Dev Technol* 2007; **5:** 127-36. doi: 10.1089/adt.2006.053

72. Wood KV. The bioluminescence advantage. [cited 2020 May 12]. Available at: https://worldwide.promega.com/resources/pubhub/enotes/the-bioluminescence-advantage/

73. Falzoni S, Donvito G, Di Virgilio F. Detecting adenosine triphosphate in the pericellular space. *Interface Focus* 2013; **3:** 2012. doi: 10.1089/adt.2006.053

74. Wang XQ, Xiao AY, Sheline C, Hyrc K, Yang A, Goldberg MP, et al. Apoptotic insults impair Na+, K+-ATPase activity as a mechanism of neuronal death mediated by concurrent ATP deficiency and oxidant stress. *J Cell Sci* 2003; **116:** 2099-110. doi: 10.1242/jcs.00420

75. Hansen EL, Sozer EB, Romeo S, Frandsen SK, Vernier PT, Gehl J. Dose-dependent ATP depletion and cancer cell death following calcium electroporation, relative effect of calcium concentration and electriamount strength. *PLoS One* 2015; **10:** e0122973. doi: 10.1371/journal.pone.0122973

76. Ashdown CP, Johns SC, Aminov E, Unanian M, Connacher W, Friend J, et al. Pulsed low-frequency magnetic fields induce tumor membrane disruption and altered cell viability. *Biophys J* 2020; **118:** 1552-63. doi: 10.1016/j.bpj.2020.02.013

77. Krause KH, Michalak M. Calreticulin. *Cell* 1997; **88:** 439-43. doi: 10.1016/s0092-8674(00)81884-x

78. Gelebart P, Opas M, Michalak M. Calreticulin, a Ca2+-binding chaperone of the endoplasmic reticulum. *Int J Biochem Cell Biol* 2005; **37:** 260-6. doi: 10.1016/j.biocel.2004.02.030

79. Panaretakis T, Kepp O, Brockmeier U, Tesniere A, Bjorklund AC, Chapman DC, et al. Mechanisms of pre-apoptotic calreticulin exposure in immunogenic cell death. *Embo J* 2009; **28:** 578-90. doi: 10.1038/emboj.2009.1

80. Kranz P, Neumann F, Wolf A, Classen F, Pompsch M, Ocklenburg T, et al. PDI is an essential redox-sensitive activator of PERK during the unfolded protein response (UPR). *Cell Death Dis* 2017; **8:** e2986. doi: 10.1038/cddis.2017.369

81. Hou W, Zhang Q, Yan Z, Chen R, Zeh HJ, Kang R, et al. Strange attractors: DAMPs and autophagy link tumor cell death and immunity. *Cell Death Dis* 2013; **4:** e966. doi: 10.1038/cddis.2013.493

82. Pisetsky DS. The origin and properties of extracellular DNA: from PAMP to DAMP. *Clin Immunolog* 2012; **144:** 32-40. doi: 10.1016/j.clim.2012.04.006

83. Shinohara K, Toné S, Ejima T, Ohigashi T, Ito A. Quantitative distribution of DNA, RNA, histone and proteins other than histone in mammalian cells, nuclei and a chromosome at high resolution observed by scanning transmission soft x-ray microscopy (stxm). *Cells* 2019; **8:** 164. doi: 10.3390/cells8020164

84. Mackenzie RJ. DNA vs. RNA – 5 key differences and comparison. Technology Networks. [cited 2020 Jun 9]. Available at: https://www.technologynetworks.com/genomics/lists/what-are-the-key-differences-between-dna-and-rna-296719.

85. Shi Y, Evans JE, Rock KL. Molecular identification of a danger signal that alerts the immune system to dying cells. *Nature* 2003; **425:** 516-21. doi: 10.1038/nature01991

86. Shi Y, Galusha SA, Rock KL. Cutting Edge: elimination of an endogenous adjuvant reduces the activation of cd8 t lymphocytes to transplanted cells and in an autoimmune diabetes model. *J Immunol* 2006; **176:** 3905-8. doi: 10.4049/jimmunol.176.7.3905

87. Miklavcic D, Semrov D, Mekid H, Mir LM. A validated model of in vivo electric field distribution in tissues for electrochemotherapy and fo: DNA electrotransfer for gene therapy. *Biochim Biophys Acta Gen Subj* 2000; **1523:** 73-83. doi: 10.1016/S0304-4165(00)00101-X

88. Zmuc J, Gasljevic G, Sersa G, Edhemovic I, Boc N, Seliskar A, et al. Large liver blood vessels and bile ducts are not damaged by electrochemotherapy with bleomycin in pigs. *Sci Rep* 2019; **9:** 3649. doi: 10.1038/s41598-019-40395-y

research article

Impact of COVID-19 on cancer diagnosis and management in Slovenia – preliminary results

Vesna Zadnik[1,3], Ana Mihor[1], Sonja Tomsic[1], Tina Zagar[1], Nika Bric[1], Katarina Lokar[1], Irena Oblak[2,3]

[1] Epidemiology and Cancer Registry, Institute of Oncology Ljubljana, Ljubljana, Slovenia
[2] Department of Radiation Oncology, Institute of Oncology Ljubljana, Ljubljana, Slovenia
[3] Faculty of Medicine, University of Ljubljana, Ljubljana, Slovenia

Radiol Oncol 2020; 54(3): 329-334.

Received 8 July 2020
Accepted 15 July 2020

Correspondence to: Prof. Vesna Zadnik, M.D., Ph.D., Epidemiology and Cancer Registry, Institute of Oncology Ljubljana, Zaloška cesta 5, SI-1000 Ljubljana, Slovenia. E-mail: vzadnik@onko-i.si

Disclosure: No potential conflicts of interest were disclosed.

Background. The COVID-19 pandemic has disrupted the provision and use of healthcare services throughout the world. In Slovenia, an epidemic was officially declared between mid-March and mid-May 2020. Although all non-essential health care services were put on hold by government decree, oncological services were listed as an exception. Nevertheless, as cancer control depends also on other health services and additionally major changes in people's behaviour likely occurred, we aimed to analyse whether cancer diagnosis and management were affected during the COVID-19 epidemic in Slovenia.

Methods. We analysed routine data for the period November 2019 through May 2020 from three sources: (1) from the Slovenian Cancer Registry we analysed data on pathohistological and clinical practice cancer notifications from two major cancer centres in Ljubljana and Maribor; (2) from the e-referral system we analysed data on all referrals in Slovenia issued for oncological services, stratified by type of referral; and (3) from the administrative data of the Institute of Oncology Ljubljana we analysed data on outpatient visits by type as well as on diagnostic imaging performed.

Results. Compared to the November 2019 – February 2020 average, the decrease in April 2020 was about 43% and 29% for pathohistological and clinical cancer notifications; 33%, 46% and 85% for first, control and genetic counselling referrals; 19% (53%), 43% (72%) and 20% (21%) for first (and control) outpatient visits at the radiotherapy, surgery and medical oncology sectors at the Institute of Oncology Ljubljana, and 48%, 76%, and 42% for X-rays, mammograms and ultrasounds performed at the Institute, respectively. The number of CT and MRI scans performed was not affected.

Conclusions. Significant drops in first referrals for oncological services, first visits and imaging studies performed at the Institute, as well as cancer notifications in April 2020 point to a possibility of a delayed cancer diagnosis for some patients during the first surge of SARS-CoV-2 cases in Slovenia. The reasons for the delay cannot be ascertained with certainty and could be linked to health-seeking behaviour of the patients, the beliefs and practices of doctors and/or the health system management during the epidemic. Drops in control referrals and control visits were expected and are most likely due to the Institute of Oncology Ljubljana postponing non-essential follow-ups through May 2020.

Key words: cancer; COVID; delay in diagnosis; referral

Introduction

Many cancer experts have highlighted the problem of access to and utilisation of cancer care services during and after the COVID-19 pandemic.[1–3] Control measures are effective at containing the spread of disease, and once extensive community transmission of the virus occurs they undoubtedly contribute to preserving cancer services through protecting the health system from collapsing, although they are expected to also have negative effects for cancer control. In Slovenia, a middle

 doi: 10.2478/raon-2020-0048

European country of approximately two million inhabitants with universal health care, the response to COVID-19 epidemic was swift and included changes in the functioning of the health care system that potentially affected cancer diagnosis and management.

An overview of the COVID-19 epidemic in Slovenia

The first confirmed COVID-19 patient in Slovenia was registered on the 4th of March 2020. The first cases were imported, though soon, secondary, tertiary and quaternary transmissions of the novel virus were detected and on the 12th of March, the Health Minister following the advice of the National Institute of Public Health (NIPH) declared an epidemic, which meant the activation of the Slovenian Pandemic Plan. Control measures implemented thereafter were strict and introduced rapidly with the aim of mitigating the spread of COVID-19. On the 16th of March, all schools and educational institutions were closed, all public transport services stopped and all non-essential services shut. Soon after, all gatherings of people were prohibited, with the exception of members of the same household, working from home was encouraged and restrictions on movement of people were put in place limiting movement to within their municipality (lock-down).

Measures concerning the provision of health care services were enacted through the *Ordinance on temporary measures in health care to contain and control the COVID-19 epidemic*[4] from the 20th of March, which stipulated that all non-essential ambulatory visits (those not referred as needing urgent or very fast management) and elective surgery appointments be put on hold. Oncological services were listed as an exception, though all preventive care activities were also put on hold by decree, meaning all three cancer screening programmes (cervical, breast and colorectal cancer) were temporarily stopped. Screening was stopped also in other countries.[5,6] At the Institute of Oncology Ljubljana, the only tertiary comprehensive cancer centre, COVID-19 preventive measures were being continually introduced and adapted starting on 26th of February. A triage, at first only physical and later also via telephone, was set up to screen patients for COVID-19 symptoms, relative escorts of patients to the hospital and visits of hospitalised patients were not allowed, except for dying patients, while non-essential follow-up visits and surgeries were postponed through May. Despite this, work at the Institute continued almost uninterrupted. Similar measures were taken by oncology departments across Europe[7,8] and many highlighted the need for stricter measures and more testing with the aim of keeping cancer clinics COVID-free given reports of the higher risk COVID-19 poses to people with cancer[9] and in order to maintain the provision of oncological services.[10,11]

Towards the end of March, the epidemic peaked with daily cases starting to decrease. In the second half of April, easing of control measures in the country started and on the 9th of May, the government lifted restrictions on provision of healthcare services. Following this, on the 15th of May Slovenia declared an end to the epidemic. During this time, the Institute of Oncology Ljubljana continued with normal follow-up and surgeries, also introducing working Saturdays to make up for the delay in these services. Furthermore, cancer screening programmes gradually began sending invitations again and were operating close to or at full capacity in June 2020.

Aim of the study

In light of severe restrictions in movement of individuals, cancellation of non-essential health care services and ensuing behavioural responses among the population, there might be collateral consequences of COVID-19 related measures for cancer control, despite the Institute of Oncology Ljubljana having retained almost normal functioning. In order to gain a quick and timely understanding of how cancer care in Slovenia has been affected by the COVID-19 epidemic, we carried out an analysis on readily available, up-to-date and reliable data sources.

Methods

We carried out an analysis of data from the Slovenian Cancer Registry, the e-referral system of Slovenia, managed by the NIPH, and the administrative hospital data of the Institute of Oncology Ljubljana. Using this data, we evaluated referrals for first and control oncological examination and treatment from all levels of healthcare, as well as cancer diagnosis and treatment at tertiary level only. The observed period was from November 2019 through May 2020.

The Slovenian Cancer Registry is one of the oldest cancer registries in Europe, operating since 1950. In 2018, the transition from passive to active registration started, which allows for up-to-date data on cancer notifications. This is an important feature, considering the need for real-time analysis of data to be able to inform decision-makers regarding the measures for COVID-19 control. From the Cancer Registry, we extracted data on monthly cancer notifications from the two major oncological centres in Slovenia, the Institute of Oncology Ljubljana and the University Medical Centre Maribor which are included in the active registration. The Ljubljana and Maribor oncological centres cover a major part of newly diagnosed cancers in Slovenia. Two types of cancer notifications were evaluated: those from pathohistological departments and those from clinical setting.

The second source was the NIPH e-referral system. We accessed the data from the e-referral system on all monthly referrals issued in Slovenia for selected types of oncological health services as coded in the Codebook of healthcare services, namely the Oncological examination – first, Oncological examination – control and Oncological genetic testing and counselling. As Slovenia has a gate-keeping system in place, where secondary and tertiary care is only possible through referrals, this means the number of referrals is an accurate reflection of demand for specialist oncological care.

Finally, from the administrative data of the Institute of Oncology Ljubljana we analysed data on monthly patient visits, stratified according to first and control outpatient visits, and data on cancer diagnostic imaging, namely the monthly number of X-rays, mammograms, ultrasounds, CT and MRI scans performed.

Results and discussion

Referral for oncological examination and treatment

Figure 1 shows the time trend of monthly referrals during November 2019 – May 2020 where a significant reduction in the number of referrals can be seen in April, with a somewhat smaller reduction in March. The reduction was seen for all types of referrals, though significantly more pronounced for control referrals compared to first referrals, whereas referring for oncological genetic testing and counselling stopped almost completely. Compared to the November – February average, the decrease in April was about 33%, 46% and 85% for first, control and genetic counselling referrals, respectively. In May, the number of all types of referrals started rising again.

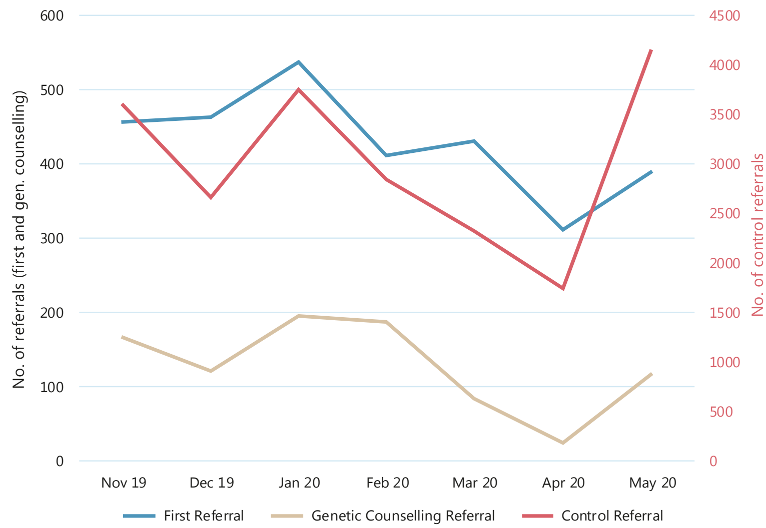

FIGURE 1. Referrals for oncological services stratified by first referral, control referral and referral for genetic counselling in Slovenian health-care system between November 2019 and May 2020.

The drop in control referrals can most likely be explained as a consequence of the cancer institutes' policies to defer non-essential control visits. All patients were notified about their deferral and thus there was probably lower demand for control referrals from patients though other reasons could also play a role. Oncological genetic testing and counselling is a preventive service, meaning that doctors were probably less likely to refer patients for this type of care, since the decree on health care stipulated these services are temporarily dis-

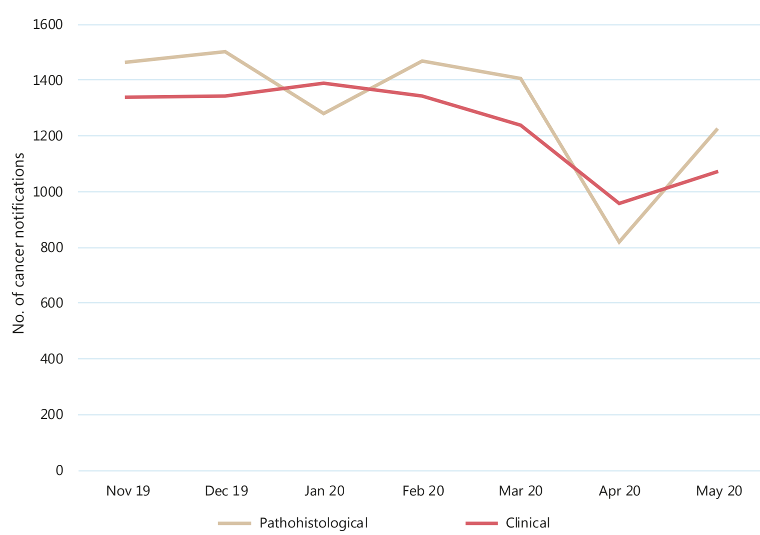

FIGURE 2. All cancer notifications from pathohistological and clinical departments at the Institute of Oncology Ljubljana and University Medical Centre Maribor between November 2019 and May 2020.

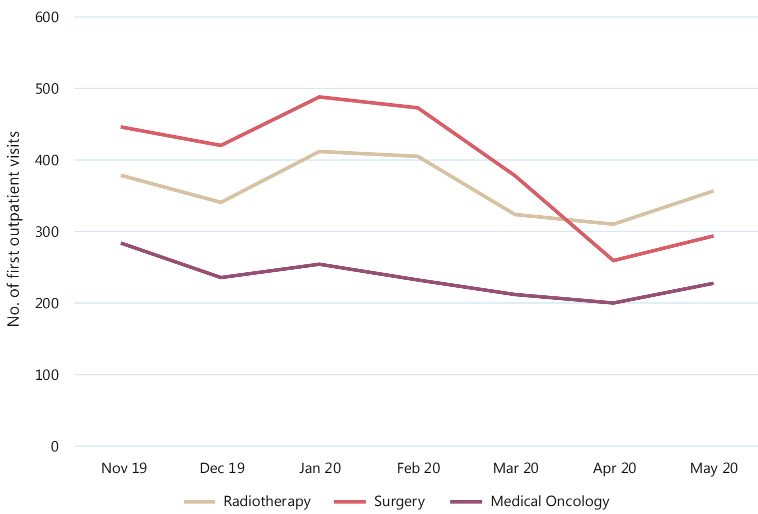

FIGURE 3. First outpatient visits to the Institute of Oncology Ljubljana stratified by type of sector (radiotherapy, surgery, and medical oncology) between November 2019 and May 2020.

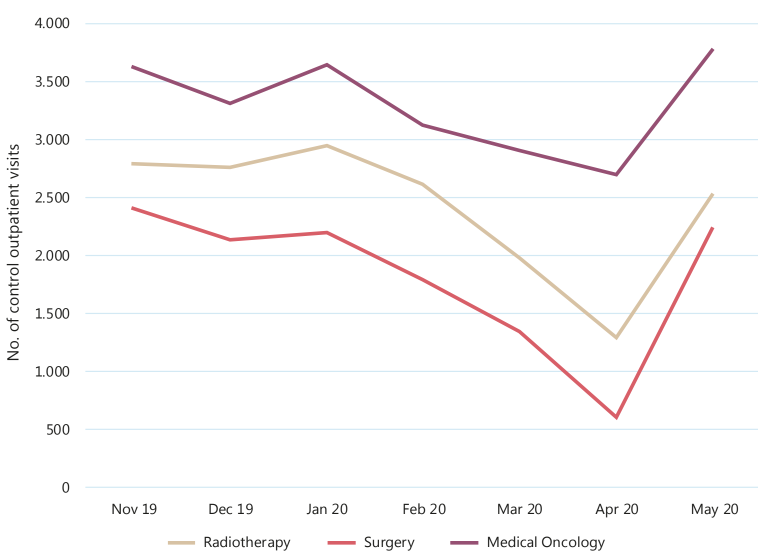

FIGURE 4. Control outpatient visits to the Institute of Oncology Ljubljana stratified by type of sector (radiotherapy, surgery, and medical oncology) between November 2019 and May 2020.

continued, even though oncological services were clearly listed as an exception. Patients themselves were also less likely to seek services for non-urgent care during lock-down. The reasons behind the drop in first referrals are difficult to determine. It is possible that, compared to pre-epidemic period, during lock-down, people were less likely to seek medical care even if they experienced symptoms of disease. On the other hand, access to primary and secondary level care could have been so disrupted that some patients could not get through to their doctors in order to complain about their issues. Another factor could be that primary level doctors were less likely to refer symptomatic patients for secondary and tertiary diagnostics because these services were not freely available and most of the first symptoms of cancer are rather unspecific. A combination of these factors was likely at play. As a result, we fear that fewer cancers were diagnosed in early stages.

Other countries have reported similar findings. In the UK, a dermatology service found a reduction in referrals for skin cancer of more than 50% in April 2020 compared to April 2019. Additionally, they analysed referrals for other types of cancer in their hospital and found similar reductions for a wide range of cancers, most pronounced for colorectal cancer.[12] Also in the UK, others have shown that in the whole country, urgent referrals for cancer from GPs fell by 60% in April.[13] In Italy, the referrals for BRCA testing to a genetic laboratory had decreased by about 60%.[14]

Delay in diagnosis

Figure 2 shows the trend in the number of cancer notifications from pathohistological and clinical departments sent to the Cancer Registry from the two main cancer centres, Institute of Oncology Ljubljana and University Medical Centre Maribor. Again, the same pattern can be observed with the largest decrease observed for April and an upward trend in May. Compared to the November 2019 – February 2020 average, the decrease in April was about 43% and 29% for pathohistological and clinical cancer notifications, respectively.

The absolute number of new notifications is not equivalent to the number of newly diagnosed cancers because a cancer case can be reported to the Cancer Registry more than once from different healthcare providers that come into contact with a patient with a cancer, while on the other hand, a small part of notifications turn out not to be malignant cases after additional investigations by the Cancer Registry. Despite this, the relative decline in new notifications can be interpreted as a decrease in newly diagnosed cancers. Roughly, this means in April there were about a third fewer cancers diagnosed in Slovenia compared to the average pre-epidemic period. The reasons for the lower number of cancer notifications are likely related to the drop in referrals. It is not surprising therefore, that the maximum drop in referrals and the maximum drop in newly diagnosed cancers are concurrent. Perhaps the time shift might have been visible if we stratified the data into weeks instead of months, because it takes a week or two for patients who are referred for oncological exam to be diagnosed with cancer. No doubt, another factor for the drop in notifications was the temporary two-month long complete cessation of all three cancer screening programmes, though at the moment it is not possible to quantify what proportion of delayed cancer diagnoses could be attributed to lack of access to cancer screening.

Our results are in line with a study from the Netherlands, where the Netherlands Cancer Registry recorded a decrease in weekly pathological cancer notifications between the end of February and start of April 2020. The decrease was observed for all age groups and all cancer groups but was largest (max. 60%) for skin cancer (excluding basal cell carcinoma), followed by breast cancer (max. 50%). The largest weekly decrease for all cancers excluding skin cancer was approximately a quarter.[15] Fewer cancer diagnoses were reported also in Italy. A Pathologic Anatomy Unit in the province of Macerata recorded a decrease in pathohistological diagnoses of cancer during weeks 11-20 (March and April) of 2020 compared to the same period in 2018 and 2019. Unlike in the Netherlands, they did not observe a decrease for malignant melanoma but observed the highest drops for prostate (75%), bladder (66%) and colorectal cancer (62%). Clinically relevant delay was considered only for colorectal cancer. Interestingly, screening for colorectal cancer was disrupted in Italy but was more preserved for breast cancer, which saw a reduction of (only) 25%.[16]

Diagnostics and treatment

Administrative data from the Institute of Oncology Ljubljana are presented in Figures 3–5. Compared to the November 2019 – February 2020 average, the decrease in first outpatient visits in April 2020 was 19%, 43% and 20% at the radiotherapy, surgery and medical oncology sectors of the Institute, respectively, whereas for control outpatient visits, these numbers were 53%, 72% and 21%.

Visits to the medical oncology department, where patients receive active chemotherapy treatment, were least affected. The largest drop in both first and control visits can be observed for the surgical department. These results are expected, as all truly elective surgeries at the Institute were postponed, though we cannot say if a part of the decrease in the first visits could also to a minor degree reflect less patients having been diagnosed

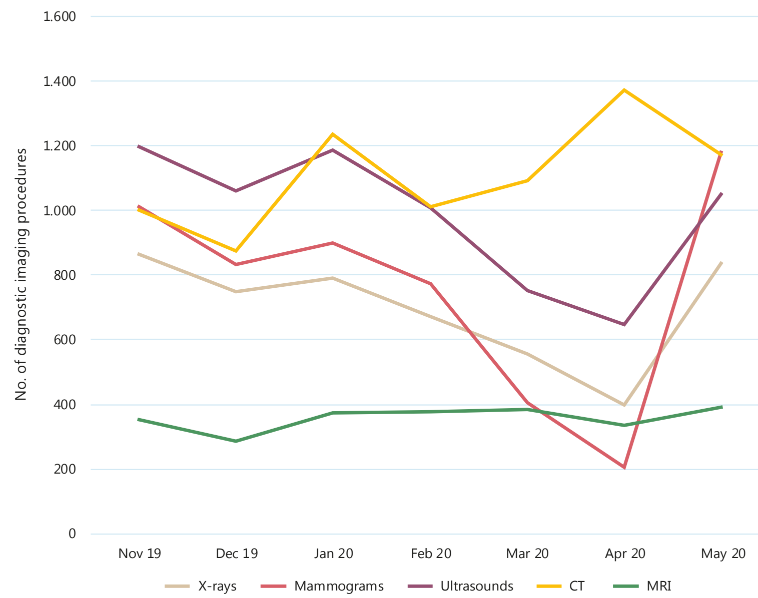

FIGURE 5. The number of X-rays, mammograms, ultrasounds, CT and MRI scans performed at the Institute of Oncology Ljubljana between November 2019 and May 2020.

with cancer and planned for surgery as part of their primary treatment. The decline in first visits to radiotherapy and medical oncology departments was small but could also point to fewer (newly diagnosed) patients being treated. In general, reductions in control outpatient visits were expected due to either postponing non-essential follow-up visits or carrying them out as telehealth visits. For radiotherapy, it might be also indicative of the rationalisation in radiotherapy regimes (such as fewer fractions of radiotherapy).

Outpatient visits to oncological centres must have declined across Europe, though we could not find any already published European study which reported on the number of cancer outpatient visits. A report from the US shows that oncology outpatient visits had fallen by as much as 47% in April 2020.[17]

Regarding diagnostic imaging, in April 2020 compared to the November 2019 – February 2020 average, there were also significant reductions in X-rays (48%), mammograms (76%) and ultrasounds (42%) performed at the Institute. This could again point to fewer patients being in the diagnostic process though there were changes in the functioning of the Institute that could also have contributed to this result. The numbers of CT and MRI scans were not affected. The reduction in diagnostic imaging was thus most pronounced for mammography, which is only in part linked to the suspension of breast cancer screening, as mammograms within the screening programme are tallied separately.

Conclusions

Significant drops in first oncological referrals, first outpatient visits, x-rays, mammograms and ultrasounds as well as cancer notifications from the two major cancer centres all point to a delay in diagnosis and treatment of cancer for some patients during the COVID-19 epidemic in Slovenia. The reasons that lead to this decline cannot be assessed in our study but are presumed to be a combination of COVID-19 related factors on the side of the patients and doctors as well as the health care system and its management during the peak of the crisis. To what extent the pausing of screening programmes influenced cancer diagnosis should be evaluated at least after six months of restarting the programmes. The drop in control referrals and visits is not as relevant clinically and was an expected outcome in light of the decision to postpone non-urgent care. Long-term studies are needed in order to evaluate what the effects of the perceived delay in diagnosis and treatment during the COVID-19 epidemic will be in terms of classical cancer burden indicators, such as poorer survival or a shift toward more advanced stage at diagnosis for specific cancer types. For example, projections for the US show that cumulative excess deaths from colorectal and breast cancers between 2020 and 2030 could be around 1%[18], highlighting the need for extreme caution when deciding on what measures to adopt if/when subsequent surges in COVID-19 cases occur so as to not significantly disrupt cancer control services also in the future.

References

1. Amit M, Tam S, Bader T, Sorkin A, Benov A. Pausing cancer screening during the severe acute respiratory syndrome coronavirus 2 pandemic: should we revisit the recommendations? *Eur J Cancer* 2020; **134:** 86-9. doi: 10.1016/j.ejca.2020.04.016
2. Vanni G, Pellicciaro M, Materazzo M, Palombi L, Buonomo OC. Breast cancer diagnosis in coronavirus-era: alert from italy. *Frontiers Oncol* 2020; **10**: 938. doi: 10.3389/fonc.2020.00938
3. Vrdoljak E, Sullivan R, Lawler M. Cancer and coronavirus disease 2019; how do we manage cancer optimally through a public health crisis? *Eur J Cancer* 2020; **132:** 98-9. doi: 10.1016/j.ejca.2020.04.001
4. Ordinance on interim measures in the field of health activities to contain and control the COVID-19 epidemic.[Slovenian]. *Uradni list Republike Slovenije*; 32/20; Ljubljana; 2020. [cited 2020 Jun 30]. Available at https://www.uradni-list.si/glasilo-uradni-list-rs/vsebina/2020-01-0645/odlok-o-zacasnih-ukrepih-na-podrocju-zdravstvene-dejavnosti-zaradi-zajezitve-in-obvladovanja-epidemije-covid-19
5. Del Vecchio Blanco G, Calabrese E, Biancone L, Monteleone G, Paoluzi OA. The impact of COVID-19 pandemic in the colorectal cancer prevention. *Int J Colorectal Dis* 2020; [Ahead of print] 4 Jun 2020. doi:10.1007/s00384-020-03635-6
6. World Health Organization. *Rapid assessment of service delivery for NCDs during COVID-19 pandemic*. Geneva; 2020.
7. Fong D, Rauch S, Petter C, Haspinger E, Alber M, Mitterer M. Infection rate and clinical management of cancer patients during the COVID-19 pandemic: experience from a tertiary care hospital in northern Italy. *ESMO Open* 2020; **5:** e000810. doi: 10.1136/esmoopen-2020-000810
8. van de Haar J, Hoes LR, Coles CE, Seamon K, Fröhling S, Jäger D, et al. Caring for patients with cancer in the COVID-19 era. *Nat Med* 2020; **26:** 665-71. doi: 10.1038/s41591-020-0874-8
9. Liang W, Guan W, Chen R, Wang W, Li J, Xu K, *et al.* Cancer patients in SARS-CoV-2 infection: a nationwide analysis in China. *Lancet Oncol* 2020; **21:** 335-7. doi: 10.1016/S1470-2045(20)30096-6
10. Restivo A, De Luca R, Spolverato G, Delrio P, Lorenzon L, D'Ugo D, et al. The need of COVID19 free hospitals to maintain cancer care. *Eur J Surg Oncol* 2020; **46:** 1186-7. doi: 10.1016/j.ejso.2020.04.003
11. Mahase E. Covid-19: cancer research urges mass testing to enable care to continue during pandemic. *BMJ* 2020; **369:** m1561. doi: 10.1136/bmj.m1561
12. Earnshaw CH, Hunter HJA, McMullen E, Griffiths CEM, Warren RB. Reduction in skin cancer diagnosis, and overall cancer referrals, during the COVID-19 pandemic. *Br J Dermatol* 2020; [Ahead of print] 4 Jun 2020. doi:10.1111/bjd.19267
13. Mahase E. Covid-19: Urgent cancer referrals fall by 60%, showing "brutal" impact of pandemic. *BMJ* 2020; **369:** m2386. doi: 10.1136/bmj.m2386
14. Minucci A, Scambia G, Santonocito C, Concolino P, Urbani A. BRCA testing in a genomic diagnostics referral center during the COVID-19 pandemic. *Mol Biol Rep* 2020; **47:** 4857-60. doi: 10.1007/s11033-020-05479-3
15. Dinmohamed AG, Visser O, Verhoeven RHA, Louwman MWJ, van Nederveen FH, Willems SM, et al. Fewer cancer diagnoses during the COVID-19 epidemic in the Netherlands. *Lancet Oncol* 2020; **21:** 750-1. doi: 10.1016/S1470-2045(20)30265-5
16. De Vincentiis L, Carr RA, Mariani MP, Ferrara G. Cancer diagnostic rates during the 2020 'lockdown', due to COVID-19 pandemic, compared with the 2018–2019: an audit study from cellular pathology. *J Clin Pathol* 2020; [Ahead of print] 19 June 2020. doi: 10.1136/jclinpath-2020-206833
17. Mehrotra A, Chernew M, Linetsky D, Hatch H, Cutler D. The impact of the COVID-19 pandemic on outpatient visits: a rebound emerges. *To the Point (blog), Commonwealth Fund* 2020; Published Online First: 19 May 2020. [cited 2020 Jun 30]. Available at: https://www.commonwealthfund.org/publications/2020/apr/impact-covid-19-outpatient-visits. doi: https://doi.org/10.26099/ds9e-jm36
18. Sharpless NE. COVID-19 and cancer. *Science* 2020; **368:** 1290. doi: 10.1126/science.abd3377

research article

Breast cancer risk based on adapted IBIS prediction model in Slovenian women aged 40-49 years - could it be better?

Tjasa Oblak[4], Vesna Zadnik[1,2], Mateja Krajc[3,4], Katarina Lokar[1], Janez Zgajnar[2,5]

[1] Epidemiology and Cancer Registry, Institute of Oncology Ljubljana, Ljubljana, Slovenia
[2] University of Ljubljana, Faculty of Medicine, Ljubljana, Slovenia
[3] Cancer Genetic Clinic, Institute of Oncology Ljubljana, Ljubljana, Slovenia
[4] Faculty of Health Sciences, University of Primorska, Izola, Slovenia
[5] Department of Surgical Oncology, Institute of Oncology Ljubljana, Ljubljana, Slovenia

Radiol Oncol 2020; 54(3): 335-340.

Received 25 March 2020
Accepted 7 May 2020

Correspondence to: Prof. Janez Žgajnar, M.D, Ph.D., Department of Surgical Oncology, Institute of Oncology Ljubljana, Zaloška cesta 2, SI-1000 Ljubljana, Slovenia. E-mail: jzgajnar@onko-i.si

Disclosure: No potential conflict of interest were disclosed.

Background. The aim of the study was to assess the proportion of women that would be classified as at above-average risk of breast cancer based on the 10 year-risk prediction of the Slovenian breast cancer incidence rate (S-IBIS) program in two presumably above-average breast cancer risk populations in age group 40-49 years: (i) women referred for any reason to diagnostic breast centres and (ii) women who were diagnosed with breast cancer aged 40–49 years. Breast cancer is the commonest female cancer in Slovenia, with an incidence rate below European average. The Tyrer-Cuzick breast cancer risk assessment algorithm was recently adapted to S-IBIS. In Slovenia a tailored mammographic screening for women at above average risk in age group 40–49 years is considered in the future. S-IBIS is a possible tool to select population at above-average risk of breast cancer for tailored screening.

Patients and methods. In 357 healthy women aged 40–49 years referred for any reason to diagnostic breast centres and in 367 female breast cancer patients aged 40–49 years at time of diagnosis 10-years breast cancer risk was calculated using the S-IBIS software. The proportion of women classified as above-average risk of breast cancer was calculated for each subgroup of the study population.

Results. 48.7% of women in the Breast centre group and 39.2% of patients in the breast cancer group had above-average 10-year breast cancer risk. Positive family history of breast cancer was more prevalent in the Breast centre group ($p < 0.05$).

Conclusions. Inclusion of additional risk factors into the S-IBIS is warranted in the populations with breast cancer incidence below European average to reliably stratify women into breast cancer risk groups.

Key words: breast cancer; early detection; risk prediction model; tailored screening

Introduction

Breast cancer is the most common cancer in women with more than 2 million new cases diagnosed worldwide in the year 2018 and therefore represents a major public health problem. In Europe alone, the number of women diagnosed with breast cancer in 2018 was approximately 523 000 with an estimated age-standardized incidence rate of 100.9/100 000.[1] Breast cancer is the most common cancer in women in Slovenia as well and in 2016 there were 1386 new cases diagnosed. However, the age-standardized incidence rate in Slovenia is lower than European average rate (68.5/100 000 women).[2,3]

Mammographic screening is one of the established strategies to deal with the breast cancer problem in public healthcare. The Slovenian national mammographic screening program offers biennial screening mammography to all women in the age group 50–69 years.[4]

 doi: 10.2478/raon-2020-0040

However, approximately one sixth of breast cancer patients are diagnosed at age 40 to 49 years, on average with a more advanced stage at the time of diagnosis compared to patients diagnosed in the age group 50–69 years.[2] Despite this fact, in Slovenia there is no organized mammographic screening program in this age group of women due to lack of convincing evidence that population mammographic screening reduces breast cancer mortality in women aged 40–49 years. Namely, according to European guidelines there is conditional recommendation against breast cancer screening for women aged 40 to 45 years, and only conditional recommendation for the screening for the age group 45 to 49 years.[5]

In Slovenia all breast cancer in the age group 40–49 years are diagnosed in regional diagnostic breast clinics whether due to symptomatic disease or as a result of opportunistic screening. Women can be referred to opportunistic screening by their gynaecologists or general practitioners based on family history of breast cancer or other risk factors. Women with high breast cancer risk (i.e. genetic predisposition) may opt for surveillance separately in a dedicated centre.

To overcome the limitations of the population screening in younger women, tailored breast cancer screening limited to women with an above-average breast cancer risk is one of the research options today. Based on the 2018 Slovenian recommendations on breast cancer prevention and treatment a tool is needed to stratify women according to 10-years breast cancer risk in three groups: population risk, moderately increased risk and high-risk group, respectively.[6] Only women at above the population risk should be offered screening before the age of 50.

To improve identification of women at above-average risk of breast cancer, many breast cancer prediction models have been developed in the last three decades.[7] The IBIS software, based on the Tyrer-Cuzick algorithm, is one of the most consistent, both in the general population and in familial setting.[8-10] IBIS calculates breast cancer risk based on classical risk factors including age, family history of breast or ovarian cancer in first- and second-degree relatives, age at menarche and menopause, parity and age at first childbirth.[8] Recently mammographic density and polygenic risk score were added as additional risk factors to be taken into account in the calculation of breast cancer risk.[11,12] However, these two risk factors are very seldom available in routine clinical setting. The IBIS program was developed with breast cancer incidence rates of the United Kingdom and was recently separately adapted for the Swedish and Slovenian populations (S-IBIS software).[13]

The IBIS program was validated on several populations, varying both in age and geographic location.[7,9,10,14,15] However, the performance of the recently adapted S-IBIS in Slovenian population is still unknown. We were particularly interested in S-IBIS performance in two presumably above the average breast cancer risk populations: (i) women aged 40 to 49 years referred for any reason to diagnostic breast centres and (ii) women who were diagnosed with breast cancer between the ages of 40 to 49.

The aim of our study was to conduct S-IBIS calculations in the two aforementioned groups of patients and determine the proportions of three 10-years breast cancer risk groups (population risk, moderately increased and high risk) in both group of patients.

Patients and methods

In this study two groups of patients were included:

1. 357 women aged 40–49 years attending opportunistic screening in 5 diagnostic breast centres in central Slovenia in year 2014;
2. 367 women aged 40–49 at time of breast cancer diagnosis, treated at the Institute of Oncology Ljubljana between 2014 and 2019. Patients are regularly followed up in outpatient clinics of the Institute of Oncology Ljubljana.

All women were asked to answer a questionnaire about established risk factors for breast cancer according to the IBIS requirements and family history of breast and ovarian cancer concerning first- and second-degree relatives (Table 1). Women in the breast cancer group were specifically asked to provide data available at their age of 40. Personal history of breast cancer diagnosis was not included in the risk calculation for the breast cancer group. Mammographic density and polygenic risk score could not be included in the risk calculation due to unavailable data, therefore these fields were left blank. Results of genetic testing were also not included as the testing was usually performed after the diagnosis of breast cancer in the breast cancer group. Women from the Breast centre group did not fill the criteria for genetic testing and the testing was therefore not performed.

Women with known genetic predisposition (i.e. BRCA and other mutations) were not included in the study. The majority of women who are carriers

TABLE 1. Breast cancer risk factors used for 10-year breast cancer risk calculation with S-IBIS software

Risk factor
Age (years)
Height
Weight
Age at menarche (years)
Age at first childbirth
Menopausal status
Hormone replacement therapy use
Benign breast disorder
Family history of breast cancer (breast cancer in first- and second-degree relatives and age at presentation)
Family history of ovarian cancer (ovarian cancer in first-degree relatives and age at presentation)

of a hereditary breast cancer related mutations are already followed up in a dedicated centre and they would not benefit from an improved population screening but may ultimately alter the proportion of women in the low and high-risk groups.

The participants were informed about the meaning and use of the provided data and signed an informed consent.

Based on the acquired data 10-year risk of breast cancer for each woman with the S-IBIS software was calculated.

For the purpose of a separate sub analysis the patients were divided in two subgroups, age 40–44 and age 45–49. In the breast cancer group there were 125 participants in the 40–44 years age group and 242 participants in the 45–49 years group, while in the breast centre group there were 153 participants in the 40–44 years age group and 204 participants in the 45–49 years group.

In breast cancer patient group the personal diagnosis of breast cancer was not included in the calculation of risk.

Breast cancer risk thresholds for the Slovenian population as described in the literature (population risk: below 2%, moderately increased risk: 2–6.5%, high risk: above 6.5%) were taken into account for assessment of performance of the S-IBIS software.[13]

IBM SPSS Statistics v25 was used to generate data analysis. Mann-Whitney and Chi-square tests was used to assess statistically significant differences in baseline data; $p < 0.05$ was considered statistically significant.

The study was approved by the National Ethics Committee.

TABLE 2. Baseline characteristics of participants

	Breast cancer group	Breast Centre group
Age (yaars, mean)*	45.6	44.8
BMI, mean (kg/m2)*	24.3	24.8
Age at menarche (years, mean)	13.0	13.0
Nulliparity	10.5%	11.1%
Age at first childbirth (years, mean)	23.0	23.4
Positive family history for breast and/or ovarian cancer*	48.8%	56.6%

* statistically significant difference was observed between the two groups (p < 0.05); BMI = Body mass index

TABLE 3. Risk stratification for all participants and for age subgroups 40–44 years and 45–49 years based on S-IBIS calculation for breast cancer patients and women screened in Breast centre; risk categories for women aged 40 to 49 as in 2018 Slovenian guidelines

	Population risk (< 2 %)	Moderately increased risk (2–6.5 %)	High risk (> 6.5 %)
Breast cancer group - 10-year breast cancer risk (age 40–49)	60.8 %	37.8 %	1.4 %
Breast centre group - 10-year breast cancer risk (age 40–49)	51.3 %	47.6 %	1.1 %
Breast cancer group - 10-year breast cancer risk (age 40–44)	64.0 %	34.4 %	1.6%
Breast centre group - 10-year breast cancer risk (age 40–44)	58.2%	41.8 %	0.0%
Breast cancer group - 10-year breast cancer risk (age 45–49)	59.1 %	39.7 %	1.2 %
Breast centre group - 10-year breast cancer risk (age 45–49)	46.1 %	51.9%	2.0%

Results

The baseline characteristics of the two groups regarding the breast cancer risk factors are reported in Table 2. Statistically significant differences where noticed between the two groups while analysing age, body mass index (BMI) and positive family history for breast and/or ovarian cancer, with participants in the Breast centre group being younger, with higher BMI and positive family history in more cases.

The risk calculations for the whole population and within each age subgroup are shown in Table 3.

Discussion

S-IBIS risk calculation based on the included participants' data identifies only 48.7% of women referred to Breast centres as above population breast cancer risk (10 years risk > 2%). Furthermore S-IBIS as used in our study identifies as above the population risk 39.2% of women, who were diagnosed with breast cancer. It should be once again noted that some data such as mammographic density and polygenic risk score (PRS) that could be included in the risk calculation, could not be retrieved for the participants of our study. Still, the identification of almost 40% breast cancer patients as at above-average risk is a promising result, that is comparable to results of other studies.[10, 16-19] However it is still worrisome that as much as 60% of patients diagnosed with breast cancer in age group 40–49 would be diagnosed outside the screening program if women were invited to breast cancer screening based on S-IBIS risk calculation as it could be widely available at the present moment (that is, without data about mammographic density and PRS). Therefore our study showed that tailored mammographic screening in the age group 40–49 in Slovenian population cannot be organized based on this form of S-IBIS alone. Assuming the expected less than 100% attendance rate of the invited population and lower mammography sensitivity in this age group, the proportion of diagnosed cancers would be even lower. These data are in clear contrast to current Slovenian screening program in age group 50–69 in which 70% of all cancers in this age group are diagnosed within the screening program with an average 75% attendance rate.[2]

Interestingly, a higher proportion of women were identified as above population risk in healthy women referred to breast centres for opportunistic screening compared to breast cancer patients, 48.7% *vs*. 39.7%, respectively. One of the reasons could be the higher proportion of women with positive family history and higher BMI in the breast centre group. The reason for relatively poor performance of the S-IBIS could be caused also by some personal characteristics of Slovene women that differ from other European populations where IBIS was validated, e.g. the age at first childbirth in Slovenia is lower than European average.[20]

When analysing the S-IBIS performance separately in the 40–44 year and 45–49 year age subgroups, we found that S-IBIS performed slightly better in the age group 45–49 years compared to younger age group (40–44 years). The difference was not big enough however to allow to draw different conclusions between the subgroups studied.

Extension of mammographic screening to women younger than 50 is a matter of debate, although several studies have confirmed that the harms of early screening do not outweighs the benefits. Over-diagnosis and false positive recalls in women younger than 50 years and non-significant lower breast cancer mortality between younger and older breast cancer patients make early breast cancer screening unreliable and unadvisable in the general population.[21,22] However, the problem of early detection of breast cancer in women younger than 50 persists and as previously stated, screening of women at higher-than-average risk of breast cancer seems one of the most feasible solutions. Based on data presented, further steps in refining a breast cancer risk calculation tool will have to be done before a tailored screening is implemented, as the inclusion of more breast cancer risk factors like mammographic density. Mammographic density is considered as a strong risk factor for breast cancer and, as already mentioned, can be included in the S-IBIS calculation.[23-25] Another promising risk factor is the polygenic risk score (PRS) based on the presence of single nucleotide polymorphisms (SNPs) related to breast cancer risk and which can be also included in the S-IBIS calculation.[26-28] At the present moment, there are numerous different sets of SNPs being studied worldwide, none of them yet approved to routine use. Of note, several studies in European populations with higher than Slovenian breast cancer incidence have shown that both factors independently increase the sensitivity of IBIS.[27-30] Due to technical limitations both mammographic density and PRS are not routinely included in S-IBIS calculations throughout Slovenia, therefore currently no data on value of mammographic density and PRS in Slovenian population is available. Data are available for selected breast centres and are yet to be analysed at the time writing this article. Studies with S-IBIS risk calculations that include these risk factors are necessary and will have to be performed to further improve the stratification of women in the breast cancer risk groups and reveal the true potential of the S-IBIS program.

Our study had several limitations. Since it is a cross-sectional study, it lacks follow up and we could not observe the eventual crossover between the two groups. Only follow-up of the Breast centre group until the age of 50 would reveal the percent of overlap between the two groups and the true quality of risk stratification based on risks calculated by S-IBIS. Due to inability to assess the proportion of women undergoing early screening that would develop breast cancer before the age of 50, statistical comparison between the two groups was not performed, as it would lead to false assumptions. Furthermore, the non-systematic accrual of women referred to opportunistic screening in Breast centres can result in high proportion of women at average breast cancer risk in the Breast centre group. Despite these limitations however, our study demonstrated the inability of the S-IBIS alone to reliably stratify women between the breast cancer risk groups. We acknowledge that a prospective study would give clearer and more reliable data, but in the given settings only a retrospective analysis was possible and perhaps necessary to plan a valid perspective study.

Conclusions

In conclusion, risk stratification based on S-IBIS calculation confirmed that at least half of women referred to regional Breast centres have above-average 10-year breast cancer risk and are entitled to regular screening prior to age 50 according to Slovenian guidelines. However, more than half of breast cancer patients aged 40–49 would not be selected for early tailored screening based on S-IBIS calculations with the chosen risk factors. Inclusion of additional risk factors (as mammographic breast density or PRS) into the S-IBIS is warranted in the populations with breast cancer incidence below European average to reliably stratify women into breast cancer risk groups. Tailored mammography screening in age group 40–49 based on S-IBIS alone can not be organized.

Acknowledgment

The study was supported by the research program of the Slovenian research agency P3-0352.

References

1. Ferlay J, Colombet M, Soerjomataram I, Gavin A, Visser O, Bray F, et al. Cancer incidence and mortality patterns in Europe: Estimates for 40 countries and 25 major cancers in 2018. *Eur J Cancer* 2018; **103:** 356-87. doi: 10.1016/j.ejca.2018.07.005
2. Zadnik V, Žagar T. SLORA: Slovenia and Cancer. Epidemiology and Cancer Registry. Institute of Oncology Ljubljana. [cited: 2019 Dec 20]. Available from: www.slora.si
3. Cancer in Slovenia 2016. Ljubljana: Institute of Oncology Ljubljana, Epidemiology and Cancer Registry, Slovenian Cancer Registry; 2019.
4. Krajc M. *National breast cancer screening programme DORA.* Residential public health thesis. [Slovenian]. Ljubljana: Institute of Oncology Ljubljana; 2009. 202 p.
5. Schünemann HJ, Lerda D, Quinn C, Follmann M, Alonso-Coello P, Giorgi Rossi P, et al. Breast cancer screening and diagnosis: a synopsis of the European Breast Guidelines. *Ann Intern Med* 2020; **172:** 46-56. doi: 10.7326/M19-2125
6. Borštnar S, Blatnik A, Perhavec A, Gazić B, Vidergar-Kralj B, Matos E, et al. Recommendations for diagnosis and treatment of patients with breast cancer (Part 1). [Slovenian]. *Onkologija* 2019; **23:** 40-53. doi: 10.25670/oi2019-006on
7. Amir E, Freedman OC, Seruga B, Evans DG. Assessing women at high risk of breast cancer: a review of risk assessment models. *J Natl Cancer Inst* 2010; **102:** 680-91. doi: 10.1093/jnci/djq088
8. Tyrer J, Duffy SW, Cuzick J. A breast cancer prediction model incorporating familial and personal risk factors. *Stat Med* 2004; **23:** 1111-30. doi: 10.1002/sim.1668
9. Tice JA, Bissell MCS, Miglioretti DL, Gard CC, Rauscher GH, Dabbous FM, et al. Validation of the breast cancer surveillance consortium model of breast cancer risk. *Breast Cancer Res Treat* 2019; **175:** 519-23. doi: 10.1007/s10549-019-05167-2
10. Dite GS, MacInnis RJ, Bickerstaffe A, Dowty JG, Allman R, Apicella C, et al. Breast cancer risk prediction using clinical models and 77 independent risk-associated SNPs for women aged under 50 years: Australian breast cancer family registry. *Cancer Epidemiol Biomarkers* 2016; **25:** 359-65. doi: 10.1158/1055-9965.EPI-15-0838
11. Brentnall AR, Harkness EF, Astley SM, Donnelly LS, Stavrinos P, Sampson S, et al. Mammographic density adds accuracy to both the Tyrer-Cuzick and Gail breast cancer risk models in a prospective UK screening cohort. *Breast Cancer Res* 2015; **17:** 147. doi: 10.1186/s13058-015-0653-5
12. Brentnall AR, Evans DG, Cuzick J. Distribution of breast cancer risk from SNPs and classical risk factors in women of routine screening age in the UK. *Br J Cancer* 2014; **110:** 827-8. doi: 10.1038/bjc.2013.747
13. Zadnik V, Krajc M. Development and implementation of personalised breast cancer risk evaluation tool for Slovenian population. [Slovenian]. *Onkologija* 2018; **22:** 6-10. doi: 10.25670/oi2018-016on
14. Laitman Y, Simeonov M, Keinan-Boker L, Liphshitz I, Friedman E. Breast cancer risk prediction accuracy in Jewish Israeli high-risk women using the BOADICEA and IBIS risk models. *Genet Res (Camb)* 2013; **95:** 174-7. doi: 10.1017/S0016672313000232
15. Quante AS, Whittemore AS, Shriver T, Strauch K, Terry MB. Breast cancer risk assessment across the risk continuum: genetic and nongenetic risk factors contributing to differential model performance. *Breast Cancer Res* 2012; **14:** R144. doi: 10.1186/bcr3352
16. Stevanato KP, Pedroso RB, Iora P, dos Santos L, Castilho Pelloso F, de Melo WA, et al. Comparative analysis between the Gail, Tyrer-Cuzick and BRCAPRO models for breast cancer screening in Brazilian population. *Asian Pac J Cancer Prev* 2019; **20:** 3407-13. doi: 10.31557/APJCP.2019.20.11.3407
17. Weiss A, Grossmith S, Cutts D, Mikami SA, Suskin JA, Knust Graichen M, et al. Customized breast cancer risk assessment in an ambulatory clinic: a portal for identifying women at risk. *Breast Cancer Res Treat* 2019; **175:** 229-37. doi: 10.1007/s10549-018-05116-5
18. Coopey SB, Acar A, Griffin M, Cintolo-Gonzalez J, Semine A, Hughes KS. The impact of patient age on breast cancer risk prediction models. *Breast J* 2018; **24:** 592-8. doi: 10.1111/tbj.12976
19. Allman R, Dite GS, Hopper JL, Gordon O, Starlard-Davenport A, Chlebowski R, et al. SNPs and breast cancer risk prediction for African American and Hispanic women. *Breast Cancer Res Treat* 2015; **154:** 583-9. doi: 10.1007/s10549-015-3641-7
20. Mean age of women at birth of first child, 2017. Eurostat. [cited: 2019 Dec 20]. Available at: https://ec.europa.eu/eurostat/web/products-eurostat-news/-/DDN-20190318-1?fbclid=IwAR0j_8KDUqMFY-Tca_wqFn3qHVxk-g4lPSeZb2Vg2zGrBh_B5K8r4hOI-Hys
21. Bucchi L, Ravaioli A, Baldacchini F, Giuliani O, Mancini S, Vattiato R, et al. Annual mammography at age 45-49 years and biennial mammography at age 50-69 years: comparing performance measures in an organised screening setting. *Eur Radiol* 2019; **29:** 5517-27. doi: 10.1007/s00330-019-06050-w
22. van den Ende C, Oordt-Speets AM, Vroling H, van Agt HME. Benefits and harms of breast cancer screening with mammography in women aged 40-49 years: a systematic review. *Int J Cancer* 2017; **141:** 1295-306. doi: 10.1002/ijc.30794
23. Boyd NF, Byng JW, Jong RA, Fishell EK, Little LE, Miller AB, et al. Quantitative classification of mammographic densities and breast cancer risk: results from the Canadian national breast screening study. *J Natl Cancer Inst* 1995; **87:** 670-5. doi: 10.1093/jnci/87.9.670

24. Boyd NF, Guo H, Martin LJ, Sun L, Stone J, Fishell E, et al. Mammographic density and the risk and detection of breast cancer. *N Engl J Med* 2007; **356:** 227-36. doi: 10.1056/NEJMoa062790

25. Byrne C, Schairer C, Wolfe J, Parekh N, Salane M, Brinton LA, et al. Mammographic features and breast cancer risk: effects with time, age, and menopause status. *J Natl Cancer Inst* 1995; **87:** 1622-9. doi: 10.1093/jnci/87.21.1622

26. Mavaddat N, Pharoah PDP, Michailidou K, Tyrer J, Brook MN, Bolla MK, et al. Prediction of breast cancer risk based on profiling with common genetic variants. *J Natl Cancer Inst* 2015; **107:** djv036. doi: 10.1093/jnci/djv036

27. Rudolph A, Song M, Brook MN, Milne RL, Mavaddat N, Michailidou K, et al. Joint associations of a polygenic risk score and environmental risk factors for breast cancer in the Breast Cancer Association Consortium. *Int J Epidemiol* 2018; **47:** 526-36. doi: 10.1093/ije/dyx242

28. Brentnall AR, Evans DG, Cuzick J. Distribution of breast cancer risk from SNPs and classical risk factors in women of routine screening age in the UK. *Br J Cancer* 2014; **110:** 827-8. doi: 10.1038/bjc.2013.747

29. Vachon CM, Scott CG, Tamimi RM, Thompson DJ, Fasching PA, Stone J, et al. Joint association of mammographic density adjusted for age and body mass index and polygenic risk score with breast cancer risk. *Breast Cancer Res* 2019; **21:** 68. doi: 10.1186/s13058-019-1138-8

30. Zhang X, Rice M, Tworoger SS, Rosner BA, Eliassen AH, Tamimi RM, et al. Addition of a polygenic risk score, mammographic density, and endogenous hormones to existing breast cancer risk prediction models: A nested case-control study. *PLoS Med* 2018; **15:** e1002644. doi: 10.1371/journal.pmed.1002644

31. Brentnall AR, van Veen EM, Harkness EF, Rafiq S, Byers H, Astley SM, et al. A case-control evaluation of 143 single nucleotide polymorphisms for breast cancer risk stratification with classical factors and mammographic density. *Int J Cancer* 2020; **146:** 2122-9. doi: 10.1002/ijc.32541

research article

Standard and multivisceral colectomy in locally advanced colon cancer

Artur M. Sahakyan[1,2], Andranik Aleksanyan[1,3], Hovhannes Batikyan[1], Hmayak Petrosyan[2], Mushegh A. Sahakyan[1,4]

[1] Department of Surgery ,N1, Yerevan State Medical University after M.Heratsi, Yerevan, Armenia

[2] Department of General and Abdominal Surgery, ArtMed MRC, Yerevan, Armenia

[3] Clinic of Surgery, Mickaelyan Institute of Surgery, Yerevan, Armenia

[4] The Intervention Center, Oslo University Hospital Rikshospitalet, Oslo, Norway

Radiol Oncol 2020; 54(3): 341-346.

Received 21 February 2020
Accepted 30 April 2020

Correspondence to: Mushegh A. Sahakyan, M.D., Ph.D., The Intervention Center, Oslo University Hospital Rikshospitalet, Sognsvannsveien 20, 0424 Oslo, Norway; E-mail: sahakyan.mushegh@gmail.com

Disclosure: No potential conflicts of interest were disclosed.

Background. Management of locally advanced colon cancer (LACC) is challenging. Surgery is the mainstay of the treatment, yet its outcomes remain unclear, especially in the setting of multivisceral resections. The aim of the study was to examine the outcomes of standard and multivisceral colectomy in patients with LACC.

Patients and methods. Patients demographics, clinical and perioperative data of patients operated within study period 2004–2018 were collected. LACC was defined as stage T4 colon cancer including tumor invasion either through the visceral peritoneum or to the adjacent organs/structures. Accordingly, either standard or multivisceral colectomy (SC and MVC) was performed.

Results. Two hundred and three patients underwent colectomy for LACC. Of those, 112 had SC (55.2%) and 91 (44.8%) had MVC. Severe morbidity and mortality rates were 5.9% and 2.5%, respectively. MVC was associated with an increased blood loss (200 ml *vs.* 100 ml, $p = 0.01$), blood transfusion (22% *vs.* 8.9%, $p = 0.01$), longer operative time (180 minutes *vs.* 140 minutes, $p < 0.01$) and postoperative hospital stay (11 days *vs.* 10 days, $p < 0.01$) compared with SC. The complication-associated parameters were similar. Male gender, presence of ≥ 3 comorbidities, tumor location in the left colon and perioperative blood transfusion were associated with complications in the univariable analysis. In the multivariable model, the presence of ≥ 3 comorbidities was the only independent predictor of complications.

Conclusions. Colectomy with or without multivisceral resection is a safe procedure in LACC. In experienced hands, the postoperative outcomes are similar for SC and MVC. Given the complexity of the latter, these procedures should be reserved to qualified expert centers.

Key words: colectomy; colon cancer; locally advanced; multivisceral; morbidity

Introduction

Colon is the second most common site for cancer both in men and women.[1,2] Significant advances in its treatment have been achieved over the last decades due to the improvements in surgical technique, chemotherapy, targeted therapy and examination of tumor biomarkers.[3,4] Unfortunately, many of these patients are diagnosed relatively late presenting with locally advanced colon cancer (LACC), which is challenging to manage.[5] The definition of LACC is controversial as no uniform approach exists in the literature to date. Some authors qualify stage T3 cancer with extramural invasion ≥ 5 mm and T4 as locally advanced, while others define LACC as stage T4 cancer solely.[6,7]

Multimodal treatment is the standard approach for LACC, although surgery remains its cornerstone. Microscopically complete resection provides satisfactory oncologic outcomes, however, complex multiorgan resection may be required in these patients.[8] The latter is associated with postoperative complications, prolonged hospital stay, increased treatment-associated costs and later start of adjuvant chemotherapy, which may ultimately increase the risk of tumor recurrence.[9] Thus, potential improvement in survival after surgery for LACC should outweigh the aforementioned risks.

This study explores the outcomes of colectomy in patients with LACC. The impact of surgical approaches on postoperative results as well as potential risk factors for complications were evaluated.

TABLE 1. Patient characteristics and perioperative outcomes in patients with T4 colon cancer undergoing colectomy

Variables	(n = 203)
Age, years, mean (± SD)	63.1 (11.6)
Body mass index, kg/m^2, mean (± SD)	27 (4.9)
Female gender, n (%)	87 (42.9%)
Comorbidities, n (%)	21 (10.3%)
ASA score > III, n (%)	5 (2.4%)
Colonic obstruction, n (%)	82 (40.4%)
Hemoglobin, mean (± SD)	111 (29)
Total protein, mean (± SD)	72 (6)
Albumin, mean (± SD)	40 (6)
Tumor location, n (%)	
Right	68 (33.5%)
Left	118 (58.1%)
Transverse colon	17 (8.4%)
T stage, n (%)	
T4a	79 (38.9%)
T4b	124 (61.1%)
N stage, n (%)	
N0	83 (40.9%)
N1	46 (22.7%)
≥ N2	74 (36.4%)
M stage, n (%)	
M0	145 (71.4%)
M1	58 (28.6%)
Tumor size ≥ 6cm, n (%)	169 (83.3%)
Operative time, min, median (range)	160 (60–480)
Estimated blood loss, ml, median (range)	175 (50–900)
Red blood cell transfusion, n (%)	30 (14.8%)
Morbidity (≥ II C–D), n (%)	25 (12.3%)
Severe morbidity (≥ IIIa C–D), n (%)	12 (5.9%)
Anastomosis leakage, n (%)	10 (4.9%)
Relaparotomy, n (%)	10 (4.9%)
Mortality, n (%)	5 (2.5%)
Postoperative stay, days, median (range)	11 (5–44)

ASA = American Society of Anesthesiologists; SD = standard deviation

Patients and methods

Study design and patients

This retrospective observational study included patients with LACC operated at a single surgical unit between 2004 and 2018. Retrospective study was approved by the accredited Institutional Review Board for medical Ethics. LACC was defined as stage T4 (T4a and T4b) colon cancer confirmed on final pathology. Tumor stage was determined and classified based on the criteria suggested by the 8th edition of American Joint Committee on Cancer.[10] Given the diversity of T4a and T4b colon cancers, patients underwent either standard colectomy (SC) or multivisceral colectomy (MVC). Patient demographics, clinical characteristics, imaging findings, lab tests, perioperative and pathology work-up data were prospectively collected and registered in the database. Surgical outcomes and risk factors for postoperative complications were examined. Comparisons were drawn between the outcomes of SC and MVC. Patients diagnosed with tumors other than adenocarcinoma were excluded from the analysis.

The selection criteria for surgery did not change throughout the study period. Normally, all functionally fit patients with no preoperative signs of distant metastases were referred to surgery. However, some patients with metastatic LACC were operated due to life-threatening conditions, such as

TABLE 2. Organs and structures resected during multivisceral colectomies (n = 91) for locally advanced colon cancer

Small bowel	18
Stomach	13
Uterus and/or ovaries	13
Kidney/Ureter/Urinary bladder	11
Liver	11
Gallbladder	3
Pancreas	1
> 1 organ/structure	21
Total	**91**

colon obstruction or bleeding. Of note, colon stenting was not available at our institution during the study period, hence surgery was the only available option. None of the patients had received neoadjuvant chemotherapy. D2 lymphadenectomy was performed routinely. All anastomoses were performed using a hand-sewn uninterrupted suture. Following surgery, the patients were mobilized on a next day. Nasogastric tube was removed on postoperative day 3 and the enteral feeding was started.

Definitions

Tumor size was defined as the largest dimension of the tumor measured microscopically at the pathology work-up. Resection radicality was regarded as R1 if microscopic presence of tumor or tumor involved lymph node was found within 1mm of the resection margin. R2 resection included at least one of the following: macroscopic tumor at the resection margin, distant metastases or peritoneal carcinomatosis.

Postoperative complications were defined and graded according to the classification system suggested by Clavien and Dindo.[11] Complications that were grade II and higher were registered. Grade ≥ III complications were defined as severe. The Comprehensive Complication index was used for a comprehensive assessment of postoperative complications.[12,13] Mortality included all cases of death within 30 days of surgery.

Statistics

Continuous data were presented as mean (± standard deviation) or median (range) depending on data distribution. The two-sample T-test was used to compare means, and the Mann-Whitney *U* test was used for medians. The categorical variables were presented as frequencies (percentages). The Chi-square test or Fisher's exact test were used to compare the categorical data. P-value < 0.05 was considered statistically significant. The aforementioned tests were used in the univariable analysis of risk factors for postoperative complications. Variables significant at p-value < 0.1 were added to the binary logistic regression model to determine the independent predictors of complications.

Results

A total number of 474 patients with colon cancer underwent surgery throughout the study period. Of those, 203 (42.8%) were operated for LACC.

TABLE 3. Outcomes of colectomy for locally advanced colon cancer depending on the type of resection (standard and multivisceral)

Variables	Standard (n = 112)	Multivisceral (n = 91)	p-value
Age, years, mean (±SD)	63.5 (11.7)	62.5 (11.3)	0.57
Body mass index, kg/m², mean (±SD)	27.5 (5.3)	26.2 (4.2)	0.41
Gender, n (%)			0.78
Male	63 (56.2%)	53 (58.2%)	
Female	49 (43.8%)	38 (41.8%)	
Comorbidities, n (%)	98 (87.5%)	84 (92.3%)	0.26
Number of comorbidities, mean (±SD)	2.6 (0.9)	2.6 (1.0)	0.62
Type of comorbidities, n (%)			0.55
Cardiovascular	66 (58.9%)	56 (61.5%)	
Diabetes mellitus	9 (8 %)	3 (3.3%)	
Thrombophlebitis	13 (11.6%)	9 (9.9%)	
ASA score > III, n (%)	1 (0.9%)	4 (4.4%)	0.07
Colonic obstruction, n (%)	54 (48.2%)	28 (30.8%)	0.16
Hemoglobin, g/dl, mean (±SD)	114 (28)	107 (29)	0.11
Total protein, g/dl, mean (±SD)	69 (14.9)	72.8 (5.9)	0.045
Albumin, g/dl, mean (±SD)	40.1 (6.2)	39.2 (6.2)	0.6
CEA, ng/ml, median (range)	3.0 (0.7–267)	7.5 (0.8–1155)	0.52
CA 19-9, U/ml, median (range)	8.6 (0.6–13444)	7.7 (2–2147)	0.96
Tumor location, n (%)			0.07
Right	45 (40.2%)	23 (25.3%)	
Left	60 (53.6%)	58 (63.7%)	
Transverse colon	7 (6.2%)	10 (11%)	
T stage, n (%)			< 0.01
T4a	74 (66.1%)	5 (5.5%)	
T4b	38 (33.9%)	86 (94.5%)	
N stage, n (%)			0.2
N0	45 (40.2%)	38 (41.8%)	
N1	21 (18.8%)	25 (27.5%)	
≥ N2	46 (41.1%)	28 (30.8%)	
M1 stage, n (%)	35 (31.2%)	23 (25.3%)	0.35
Tumor size ≥ 6cm, n (%)	91 (81.2%)	78 (85.7%)	0.4
Operative time, min, median (range)	140 (60–480)	180 (85–390)	< 0.01
Estimated blood loss, ml, median (range)	100 (50-900)	200 (100–600)	0.01
Red blood cell transfusion, n (%)	10 (8.9%)	20 (22.0%)	0.01
Morbidity (≥ II C-D), n (%)	15 (13.4%)	10 (11%)	0.6
Severe morbidity (≥ IIIa C-D), n (%)	8 (7.1%)	4 (4.4%)	0.41
CCI, median (range)	33.7 (20.9–100)	29.6 (20.9–100)	0.33
Anastomosis leakage, n (%)	5 (4.5%)	5 (5.5%)	0.76
Relaparotomy, n (%)	5 (4.5%)	5 (5.5%)	0.76
Mortality, n (%)	2 (1.8%)	3 (3.3%)	0.66
Postoperative stay, days, median (range)	10 (5–44)	11 (7–44)	0.04

ASA = American Society of Anesthesiologists; CA 19-9 = Carbohydrate antigen 19-9; CEA = Carcinoembryonic antigen; CCI = Comprehensive Complication Index

TABLE 4. Univariable analysis of factors associated with postoperative complications

Variables	Complications (n=25)	No complications (n=178)	p-value
Age ≥ 65 years, n (%)	15 (60%)	98 (55.1%)	0.68
Body mass index ≥ 30 kg/m², n (%)	2 (8%)	36 (20.2%)	0.44
Male gender, n (%)	18 (72%)	98 (55.1%)	0.09
Comorbidities, n (%)	1 (4%)	20 (11.2%)	0.48
Number of comorbidities ≥ 3, n (%)	7 (28%)	18 (10.1%)	0.02
Cardiovascular disease n (%)	15 (60%)	107 (60.1%)	0.85
ASA score > III, n (%)	1 (4%)	4 (2.2%)	0.51
Colon obstruction, n (%)	12 (48%)	70 (39.3%)	0.78
Hemoglobin, g/dl, mean (±SD)	111 (27)	111 (28)	0.94
Total protein, g/dl, mean (±SD)	73.3 (5.5)	72.1 (6.2)	0.27
Albumin, g/dl, mean (±SD)	38.5 (4.7)	39.8 (6.5)	0.55
Tumor location, n (%)			0.05
Right	5 (20%)	63 (35.4%)	
Left	20 (80%)	98 (55.1%)	
T stage, n (%)			0.23
T4a	7 (28%)	72 (40.4%)	
T4b	18 (72%)	106 (59.6%)	
N+ disease, n (%)	17 (68%)	103 (57.9%)	0.6
M1 stage, n (%)	9 (36%)	49 (27.5%)	0.38
Tumor size ≥ 6cm, n (%)	21 (84%)	148 (83.1%)	1.0
Estimated blood loss, ml, median (range)	200 (50–900)	100 (100–500)	0.12
Red blood cell transfusion, n (%)	7 (28%)	23 (12.9%)	0.07
≥ 2 organs resected, n (%)	3 (12%)	18 (10.1%)	0.73
Single-layer anastomosis suture, n (%)	15 (60%)	136 (76.4%)	0.13
End-to-end anastomosis, n (%)	9 (36%)	53 (29.8%)	0.57

ASA = American Society of Anesthesiologists

TABLE 5. Multivariable analysis of risk factors for postoperative complications

Variables	Odds ratio (95% confidence interval)	p-value
Male gender	1.88 (0.7–5.04)	0.21
Number of comorbidities ≥ 3	3.1 (1.1–9.2)	0.04
Left-sided tumor	2.2 (0.74–6.48)	0.16
Red blood cell transfusion	1.94 (0.67–5.64)	0.22

Patient characteristics, perioperative data and pathology findings are presented in Table 1. The most common location of LACC was the left colon (58.1%), while 82 (40.4%) patients had colon obstruction. More than one-fourth of the patients (28.6%) had distant metastases at surgery. In patients with non-metastatic LACC (n = 145), the rate of curative resections (R0) was 97%. Morbidity and mortality rates were 12.3% and 2.5%, respectively. Median length of stay was 11 (5–44) days.

SC was performed in 112 (55.2%) patients and MVC in 91 (44.8%). The latter included resections of one (n = 70) or ≥ 2 organs/structures (n = 21) (Table 2). In patients with ≥ 2 organs/structures resected the resection of the small bowel, stomach and pancreas was most often carried out.

A comparative analysis between the outcomes of MVC and SC was performed (Table 3). Preoperative parameters were similar except the significantly higher total protein levels in the MVC group. The latter was almost always performed in patients with T4b adenocarcinoma (94.5% *vs.* 33.9%, p < 0.01). Operative time was significantly longer for MVC (180 minutes *vs.* 140 minutes, p<0.01) and so was the median blood loss (200 ml *vs.* 100 ml, p = 0.01). The red blood cell transfusion rate was significantly higher for MVC - 22% *vs.* 8.9%, p = 0.01. Microscopically complete resection was achieved in a similar number of patients (98.5% *vs.* 95.3%, p = 0.56). Proportions of postoperative complications and their types were comparable between the groups. The length of stay after surgery was longer following MVC (11 days *vs.* 10 days, p = 0.04).

Univariable analysis of factors associated with postoperative complications was performed (Table 4). Male gender, presence of ≥ 3 comorbidities, tumor location in the left colon and red blood cell transfusion were associated with grade ≥ II complications. These factors were analyzed together in the multivariable model (Table 5). The latter demonstrated that only presence of ≥ 3 comorbidities was associated with grade ≥ II morbidity. Specifically, their risk increased more than three times in these patients - OR 3.1 (1.1–9.2), p = 0.038.

Discussion

Our findings indicate that colectomy in patients with LACC is a safe procedure providing satisfactory surgical outcomes when performed in a specialized surgical unit. This is applicable to both SC and MVC. In the literature, postoperative morbidity and mortality rates following surgery for LACC are 25–38% and 3.3–6.9%, respectively.[5,14-17] Hoffman *et al.*, demonstrated that morbidity rate may increase with the use of multiorgan resections.[18] In this series, postoperative morbidity rate was 12.8% including 7.4% severe complications. Although MVC was associated with an increased blood loss, need for blood transfusion, as well as with longer operative time and hospital stay, postoperative morbidity-associated parameters and mortality were comparable to those of SC.

Severe complications were mostly caused by the anastomotic leakage (4.9%), which is consistent with the data in the literature.[14,19] Multiple parameters are found to be associated with the risk of leakage including patient-specific variables, intraoperative complications, surgeon- and technique-related factors. In this report, such analysis was not possible due to the small number of cases. However, when analyzing risk factors for complications technical parameters such as single-layer anastomosis suture or its end-to-end type did not increase the rate of complications. We believe that single-layer suture is a simple technique that significantly expedites the procedure, while the end-to-end anastomosis avoids the need for additional closure of the intestinal stumps on the proximal and/or distal loops. The effectiveness of this technique was reported also by Liu *et al*.[20] Our results do not confirm the association between the postoperative results and blood transfusion suggested by Marinello *et al*.[14] Despite being a significant predictor in the univariable analysis, blood transfusion was not an independent predictor of complications in the multivariable model.

According to the literature, MVC is performed in only 1.2–12% of patients with colon cancer.[14,15,21,22] In our study, MVC was performed in 44.8% of patients with LACC, which accounts for 19.2% of a total number of colon resections for cancer. Higher incidence of MVC in our series can be attributed to strict selection criteria in the aforementioned studies, as well as to a significantly higher proportion of late diagnosed patients in our population. This is confirmed also by the fact that nearly 40% of our patients presented with partial or total colon obstruction prior to surgery.

Intraoperatively, it is not always possible to assess whether or not colectomy will be curative, thus the main goal is to achieve a complete resection of the primary tumor and suspicious adjacent tissues if these are found at surgery.[9] According to the literature, the most common invasion sites for T4b colon cancer are the small bowel, urinary bladder and abdominal wall.[15-17] In this series, most often these patients had tumor ingrowth into ≥ 2 organs, predominantly to the small bowel, distal pancreas and stomach. Tumor invasion into adjacent structure(s) was verified by the pathology examination in about 95% of patients who had undergone MVC. Given that this parameter ranges from 44% to 72.5% in the literature[5,9,15,16], the choice of surgical approach was adequate in this series.

This report has several limitations, including retrospective design with its inherent biases. Furthermore, we did not register grade I complications (according to Clavien-Dindo)[11], which somewhat limits the information on postoperative results of colectomy for LACC. It is also worth mentioning that our data are based on an experience of a specialized center of colorectal surgery, thus the reproducibility of our results is limited and surgical outcomes should be interpreted with caution.

Conclusions

In conclusion, colectomy including MVC is a safe procedure in the setting of LACC. In experienced hands, the postoperative outcomes are acceptable showing no differences between the SC and MVC. However, their oncologic benefits require further investigation. Given the complexity of MVC, these procedures should be reserved to qualified expert centers that are familiar with colorectal procedures as well as with the surgery of other organ systems.

References

1. Teufel A, Gerken M, Hartl J, Itzel T, Fichtner-Feigl S, Stroszczynski C. Benefit of adjuvant chemotherapy in patients with T4 UICC II colon cancer. *BMC Cancer* 2015; **15:** 419. doi: 10.1186/s12885-015-1404-9
2. Sokolov M. Surgical approach in locally advanced colorectal cancer - combined, extended and compound surgery. *Khirurgiia (Sofiia)* 2013; **4:** 29-50. PMID: 24800318
3. Rousseau B, Chibaudel B, Bachet JB, Larsen AK, Tournigand C, Louvet C, et al. Stage II and stage III colon cancer: treatment advances and future directions. *Cancer J* 2010; **16:** 202-9. doi: 10.1097/PPO.0b013e3181ddc5bf
4. Akagi T, Inomata M. Essential advances in surgical and adjuvant therapies for colorectal cancer 2018-2019. *Ann Gastroenterol Surg* 2020; **4:** 39-46. doi: 10.1002/ags3.12307
5. Rosander E, Nordenvall C, Sjövall A, Hjern F, Holm T. Management and outcome after Mmltivisceral resections in patients with locally advanced primary colon cancer. *Dis Colon Rectum* 2018; **61:** 454-60. doi: 10.1097/DCR.0000000000001046
6. Nørgaard A, Dam C, Jakobsen A, Pløen J, Lindebjerg J, Rafaelsen SR. Selection of colon cancer patients for neoadjuvant chemotherapy by preoperative CT scan. *Scand J Gastroenterol* 2014; **49:** 202-8. doi: 10.3109/00365521.2013.862294
7. Ludmir EB, Arya R, Wu Y, Palta M, Willett CG, Czito BG. Role of adjuvant radiotherapy in locally advanced colonic carcinoma in the modern chemotherapy era. *Ann Surg Oncol* 2016; **23:** 856-62. doi: 10.1245/s10434-015-4907-3
8. Gezen C, Kement M, Altuntas YE, Okkabaz N, Seker M, Vural S, et al. Results after multivisceral resections of locally advanced colorectal cancers: an analysis on clinical and pathological T4 tumors. *World J Surg Oncol* 2012; **10:** 39. doi: 10.1186/1477-7819-10-39
9. Lehnert T, Methner M, Pollok A, Schaible A, Hinz U, Herfarth C. Multivisceral resection for locally advanced primary colon and rectal cancer: an analysis of prognostic factors in 201 patients. *Ann Surg* 2002; **235:** 217-25. doi: 10.1097/00000658-200202000-00009

10. Weiser MR. AJCC 8th Edition: Colorectal cancer. *Ann Surg Oncol* 2018; **25:** 1454-5. doi: 10.1245/s10434-018-6462-1

11. Dindo D, Demartines N, Clavien P-A. Classification of surgical complications. *Ann of Surg* 2004; **240:** 205-13. doi: 10.1245/s10434-018-6462-1

12. Slankamenac K, Nederlof N, Pessaux P, de Jonge J, Wijnhoven BP, Breitenstein S, et al. The comprehensive complication index: a novel and more sensitive endpoint for assessing outcome and reducing sample size in randomized controlled trials. *Ann Surg* 2014; **260:** 757-63. doi: 10.1097/SLA.0000000000000948

13. Slankamenac K, Graf R, Barkun J, Puhan MA, Clavien PA. The comprehensive complication index: a novel continuous scale to measure surgical morbidity. *Ann Surg* 2013; **258:** 1-7. doi: 10.1097/SLA.0000000000002132

14. Marinello FG, Baguena G, Lucas E, Frasson M, Hervás D, Flor-Lorente B, et al. Anastomotic leakage after colon cancer resection: does the individual surgeon matter? *Colorectal Dis* 2016; **18:** 562-9. doi: 10.1111/codi.13212

15. Croner RS, Merkel S, Papadopoulos T, Schellerer V, Hohenberger W, Goehl J. Multivisceral resection for colon carcinoma. *Dis Colon Rectum* 2009; **52:** 1381-6. doi: 10.1007/DCR.0b013e3181ab580b

16. Luna-Pérez P, Rodríguez-Ramírez SE, De la Barrera MG, Zeferino M, Labastida S. Multivisceral resection for colon cancer. *J Surg Oncol* 2002; **80:** 100-4. doi: 10.1002/jso.10105

17. Wasmann KATGM, Klaver CEL, van der Bilt JDW, Nagtegaal ID, Wolthuis AM, van Santvoort HC et al. Subclassification of multivisceral resections for T4b colon cancer with relevance for postoperative complications and oncological risks. *J Gastrointest Surg* 2019; [Ahead of print]. doi: 10.1007/s11605-019-04426-3

18. Hoffmann M, Phillips C, Oevermann E, Killaitis C, Roblick UJ, Hildebrand P, et al. Multivisceral and standard resections in colorectal cancer. *Langenbecks Arch Surg* 2012; **397:** 75-84. doi: 10.1007/s00423-011-0854-z

19. Frasson M, Flor-Lorente B, Rodríguez JL, Granero-Castro P, Hervás D, Alvarez Rico MA, et al. Risk factors for anastomotic leak after colon resection for cancer: multivariate analysis and nomogram from a multicentric, prospective, national study with 3193 patients. *Ann Surg* 2015; **262:** 321-30. doi: 10.1097/SLA.0000000000000973

20. Liu Z, Wang G, Yang M, Chen Y, Miao D, Muhammad S et al. Ileocolonic anastomosis after right hemicolectomy for colon cancer: functional end-to-end or end-to-side? *World J Surg Oncol* 2014; **12:** 306. doi: 10.1186/1477-7819-12-306

21. Leijssen LGJ, Dinaux AM, Amri R, Kunitake H, Bordeianou LG, Berger DL. The impact of a multivisceral resection and adjuvant therapy in locally advanced colon cancer. *J Gastrointest Surg* 2019; **23:** 357-66. doi: 10.1002/jso.25610

22. Zhao YZ, Han GS, Lu CM, Ren YK, Li J, Ma PF, et al. Right hemicolectomy and multivisceral resection of right colon cancer: a report of 21 cases. *J Huazhong Univ Sci Technolog Med Sci* 2015; **35:** 255-58. doi: 10.1007/s11596-015-1420-7

research article

Percutaneous image guided electrochemotherapy of hepatocellular carcinoma: technological advancement

Mihajlo Djokic[1], Rok Dezman[2], Maja Cemazar[3,4], Miha Stabuc[2], Miha Petric[1], Lojze M. Smid[5], Rado Jansa[5], Bostjan Plesnik[1], Masa Bosnjak[3], Ursa Lampreht Tratar[3], Blaz Trotovsek[1], Bor Kos[6], Damijan Miklavcic[6], Gregor Sersa[3,7], Peter Popovic[2]

[1] University Medical Centre Ljubljana, Clinical Department of Abdominal Surgery, Ljubljana, Slovenia
[2] University Medical Centre Ljubljana, Clinical Institute of Radiology, Ljubljana, Slovenia
[3] Institute of Oncology Ljubljana, Department of Experimental Oncology, Ljubljana, Slovenia
[4] University of Primorska, Faculty of Health Sciences, Izola, Slovenia
[5] University Medical Centre Ljubljana, Clinical Department of Gastroenterology, Ljubljana, Slovenia
[6] University of Ljubljana, Faculty of Electrical Engineering, Ljubljana, Slovenia
[7] University of Ljubljana, Faculty of Health Sciences, Ljubljana, Slovenia

Radiol Oncol 2020; 54(3): 347-352.

Received 14 Maj 2020
Accepted 1 June 2020

Correspondence to: Prof. Gregor Serša, Ph.D., Institute of Oncology Ljubljana, Department of Experimental Oncology, Zaloška 2, SI-1000 Ljubljana, Slovenia. E-mail: gsersa@onko-i.si and Prof. Peter Popovič, M.D., Ph.D., University Medical Centre Ljubljana, Clinical Institute of Radiology, Zaloška 7, SI-1000 Ljubljana, Slovenia. E-mail: peter.popovic@kclj.si

Mihajlo Djokic and Rok Dezman contributed equally.

Disclosure: Damijan Miklavčič holds patents on electrochemotherapy that have been licensed to IGEA S.p.a (Carpi, Italy) and is also a consultant to various companies with an interest in electroporation-based technologies and treatments. The other authors have no competing interests.

Background. Electrochemotherapy is an effective treatment of colorectal liver metastases and hepatocellular carcinoma (HCC) during open surgery. The minimally invasive percutaneous approach of electrochemotherapy has already been performed but not on HCC. The aim of this study was to demonstrate the feasibility, safety and effectiveness of electrochemotherapy with percutaneous approach on HCC.

Patient and methods. The patient had undergone the transarterial chemoembolization and microwave ablation of multifocal HCC in segments III, V and VI. In follow-up a new lesion was identified in segment III, and recognized by multidisciplinary team to be suitable for minimally invasive percutaneous electrochemotherapy. The treatment was performed with long needle electrodes inserted by the aid of image guidance.

Results. The insertion of electrodes was feasible, and the treatment proved safe and effective, as demonstrated by control magnetic resonance imaging.

Conclusions. Minimally invasive, image guided percutaneous electrochemotherapy is feasible, safe and effective in treatment of HCC.

Key words: electrochemotherapy; hepatocellular carcinoma; percutaneous; minimally invasive; bleomycin

Introduction

Electrochemotherapy is safe and effective treatment of cutaneous tumors and metastases, its application is described in the published Standard Operating procedures, and clinical indications defined in NICE, and several other national guidelines.[1-3]

Electrochemotherapy in treatment of deep-seated tumors, like liver metastases and hepatocellular carcinoma (HCC) proved to be safe and effective.[4-6] The three published studies were done

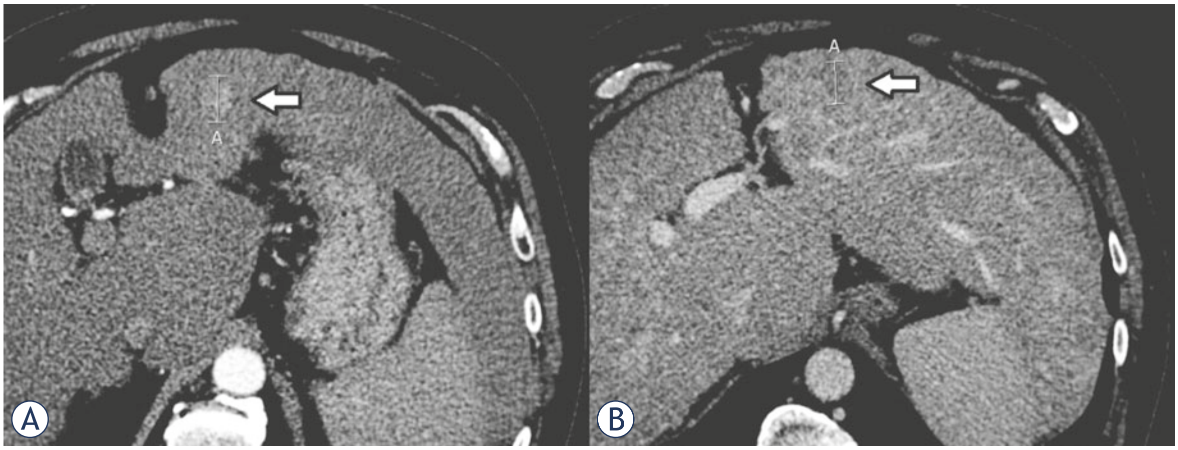

FIGURE 1. A 66- year-old male with hepatocellular carcinoma (HCC). Control CT after drug-eluting bead doxorubicin transarterial chemoembolization (DEBDOX TACE) and microwave ablation (MWA) shows non-target progression in segment III, 18 mm the largest diameter. **(A)** Hypervascular lesion in arterial phase. **(B)** Washout in venous phase.

using electrochemotherapy during open surgery. The surveillance of high-risk population using ultrasound permits to diagnose HCC at an early stage, at which curative treatments can be employed. According to European Association for the Study of Liver (EASL) recommendations, thermal ablation with radiofrequency is the standard of care for patients with Barcelona clinic liver cancer (BCLC) 0 and A, tumors not suitable for surgery. However, in patients with very early stage HCC (BCLC-0) radiofrequency ablation (RFA) in favorable locations can be adopted as first-line therapy even in patients amenable to surgical procedure. Electrochemotherapy is local therapy with similar modes of action as local ablative therapies, e.g. RFA, microwave ablation (MWA) and in particular irreversible electroporation (IRE).[7-9] However, the main difference between electrochemotherapy and other local ablative therapies is that electrochemotherapy combines two modalities, chemotherapy and the application of electric pulses. Thus, the tumor cells are dying not directly due to the application of physical energy, such as in the case of other local thermal ablative therapies or IRE, but due to the action of chemotherapeutic drug, which in the case of bleomycin means that the cells are dying by mitotic cell death.[10] Therefore, electrochemotherapy is effective and safe in treatment of tumors located in close proximity to major hepatic vessels[11-13] and can be performed by image guided percutaneous approach.[14]

Percutaneous approach of electrode insertion is well established in IRE. Several studies demonstrate the feasibility and safety of percutaneous approach of IRE in treatment of liver tumors, including HCC.[9,15-17] Some reports describe percutaneous approach also for electrochemotherapy of cholangiocarcinoma, spine metastases[18,19], lysis of portal vein thrombosis in hepatic hilum, and metastasis from renal cell cancer, however not in treatment of HCC.[20-23] In this report we therefore tested the feasibility, safety and effectiveness of electrochemotherapy with image guided percutaneous approach, in a patient with HCC.

Patient and methods

Sixty six-year old male patient was presented at multidisciplinary team meeting with multifocal HCC in segments III, V, VI in September 2017. At the time that patient was presented he had Child A liver cirrhosis - ethylic etiology, arterial hypertension and diabetes type 2. He was a former smoker and had a history of excessive alcohol consumption. In 2018 he had undergone 1a and 1b drug-eluting bead doxorubicin transarterial chemoembolization (DEBDOX TACE) treatment of hepatic lesions. Two months after the treatment, control computed tomography (CT) showed complete response of the target lesions in segments III and VI and stable disease of the lesion in segment V. Therefore, his documentation was reviewed on hepatopancreaticobiliary (HPB) multidisciplinary team meeting, which concluded that the patient is a candidate for MWA of the lesion in segment V. On control CT scan 1 month after MWA, lesion in segment V was completely avital (complete response), but new lesion, 14 mm in diameter, in segment III was identified. On CT scan 3 months later hypervascular lesion in segment III appeared to be larger - 18 mm in diameter (Figure 1). No signs of extrahepatic disease were found. According to HPB multidisciplinary team meeting, the patient was eligible candidate for percutaneous electrochemotherapy. The patient signed informed consent and was treated in the frame of the clinical study (NCT02291133) approved by the National Ethics Committee (21k/02/14) of the Republic of Slovenia.

Electrochemotherapy was performed according to the standard operating procedures for electrochemotherapy[2] and as described in previous study on electrochemotherapy of HCC[5], performed during the open surgery using cone-beam computed tomography (CBCT) guided percutaneous approach.

Results

Treatment was performed under general anesthesia and deep muscle relaxation. The patient was positioned in supine position. Because the tumor was not visible on ultrasound and CBCT with a contrast agent, we decided for angiography to visualize the lesion. Coeliac truncus was reached through the punction of common femoral artery and left hepatic artery was selectively catheterized. CBCT (Siemens Medical Solutions, Forchheim, Germany) was performed with the administration of non-ionic contrast agent (Ultravist 370®, Bayer HealthCare) through a power injector (Avanta®, Medrad, Bayer HealthCare). CBCT after contrast injection through 2.4 F microcatheter (Progreat®, Terumo Europe N.V.) into segmental branches for liver segment III confirm 18 mm large tumor (Figure 2A). Four electrodes with 3 cm active length were placed percutaneously around the tumor in the form of pseudo-square under stereotactic CBCT guidance according to European Standard Operating Procedures on Electrochemotherapy (ESOPE) recommendations (Figure 2B,C).[2] The distance between the electrodes ranged from 18 to 23 mm (Figure 2B, Figure 3A). Then, bleomycin (Bleomycin medac, Medac, Germany) 30.000 IU in 20 ml of physiological saline; 15 000 IU/m^2, was administered intravenously in bolus lasting 2 minutes. Two trains of 4 electric pulses (duration 100 µs, pulse repetition frequency 1 kHz) of opposite polarity with voltage-to-distance ratio of 1000 V/cm and were delivered between all electrode pairs starting 8 minutes after the bleomycin injection (total number of pulses = 48). The voltages and median currents delivered to each electrode pair are listed in Table 1. Delivery of the electric pulses was synchronized with the ECG, triggered during the refractory phase of the heart.[24] The maximal current amplitude measured during electroporation of the tumor was 40 A. During the treatment, no changes in cardiologic (ECG, pulse rate) and hemodynamic parameters were noticed. After electrode extraction, control CBCT with contrast injection through microcatheter showed area of avital lesion (Figure 2D). The whole procedure from the induction of anesthesia until the end of the application of electric pulses lasted 1 h and 10 minutes.

A numeric reconstruction of the performed treatment, prepared using the treatment planning

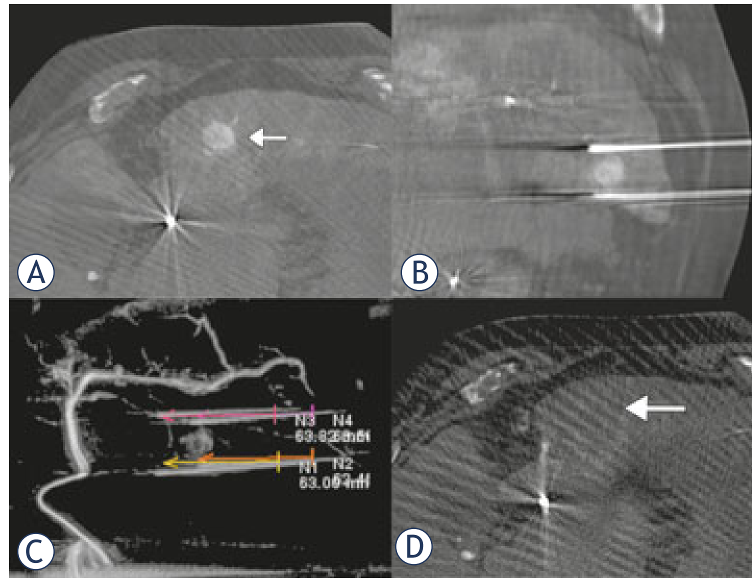

FIGURE 2. A 66- year-old male with hepatocellular carcinoma (HCC). Cone-beam computed tomography (CBCT) demonstrating HCC before the treatment **(A)**. Position of the electrodes in relation to tumor on CBCT. **(B, C)** The absence of the contrast enhancement of the ablated tumor was notable 4 minutes after the electrochemotherapy **(D)**.

TABLE 1. VOLTAGES and currents delivered in the treatment

Electrode pair		Voltage [V]	Current [A]
2	3	2800	38.0
4	1	2800	36.5
1	3	2300	34.5
1	2	2000	29.4
3	4	1800	27.7
2	4	1800	26.5

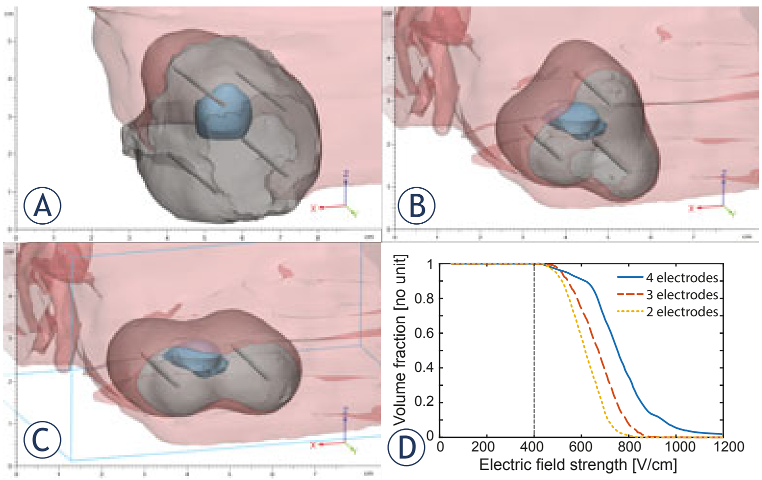

FIGURE 3. Numerical visualization of electric field for successful electrochemotherapy. **(A)** Reconstruction of actual treatment based on cone-beam computed tomography (CBCT) images. **(B)** 3 electrode treatment plan based on pre-treatment CECT. **(C)** 2 electrode treatment plan based on pre-treatment CBCT. **(D)** Electric field histogram showing the volume fraction of tumor tissue covered by electric fields of at least the strength indicated on the horizontal axis for all three treatments shown in panels **A-C**.

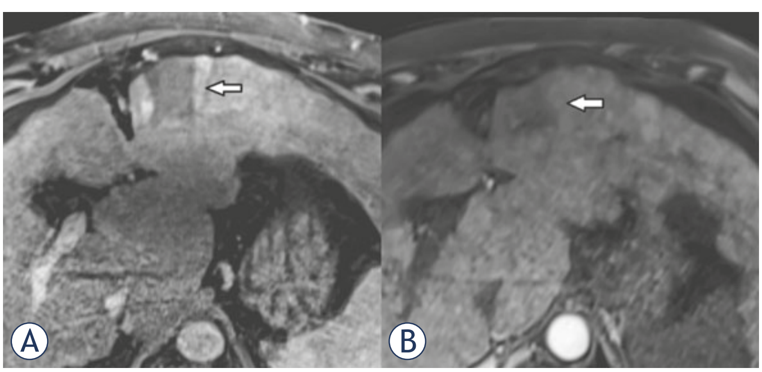

FIGURE 4. A 66- year-old male with hepatocellular carcinoma (HCC). Control MRI of liver 2 months **(A)** and 6 months **(B)** after procedure showing an unenhancing area of ablation – a complete response according to mRECIST criteria.

methods presented in previous work showed that whole tumor area with safety margin (range: 6.2 to 39 mm) was covered, comprising a total volume of 78 cm^3 (Figure 3A).[25] A numerical analysis showed, that a successful treatment would also be possible with a 3 electrode (Figure 3B) and 2 electrode (Figure 3C) configuration. The volumes of obtained lesion are smaller than the actual treatment (26 and 23 cm^3 for the 3 and 2 electrode setup, respectively), but they still achieved a good safety margin (range 3.6 mm to 21.5 mm for 2 electrodes and 5.1 mm to 20.9 mm for 3 electrodes).

Postprocedural course was uneventful, abdominal ultrasound 24 hours post-electrochemotherapy showed normal postinterventional finding - no bleeding, hematoma or fluid collections. Therefore, patient was discharged the day after the procedure with analgesics and antithrombotic prophylaxis.

Two months after percutaneous electrochemotherapy, control magnetic resonance (MRI) of liver showed 36 mm large non enhancing area of ablation necrosis within the treated area - complete response of targeted lesion according to modified Response Evaluation Criteria In Solid Tumors (mRECIST) (Figure 4A). The patient was feeling well, in good physical condition and pain-free.

On the second follow-up, 6 months after the procedure control liver MRI showed complete response of the treated lesion with ablated area decreasing in size, which is in line with expected necrosis resolution dynamics and formation of fibrosis. The lesion was in complete response also 18 months after the treatment, however new HCC foci occurred in other locations.

Discussion

We describe the first case of percutaneous electrochemotherapy of HCC. Minimally invasive, image guide percutaneous electrochemotherapy proved feasible, safe and effective treatment modality, which can be used in selected group of patients with HCC.

The management of HCC has changed in recent years. Percutaneous local ablation is currently considered to be viable treatment for patients with very early HCC, as defined by the BCLC staging system. Indications for percutaneous local ablation include: HCC in BCLC stage A with Child-Pugh class A/B cirrhosis; ECOG performance status of 0-1; ideal tumor size of less than 3 cm and solitary or multiple lesions (up to three lesions). RFA has been the most widely investigated modality of percutaneous ablation. It has been shown that RFA is a safe method with potential drawback due to the heat sink effect. It is believed that 10-25% of patients with HCC may not be eligible for RFA due to this effect.[26]

MWA offers all the benefits of RFA as well as some substantial advantages. Promising results of MWA for HCC have been demonstrated in several studies.[27–29] The advantages of MWA include a larger volume of cellular necrosis, reduction in procedure times, greater temperatures delivered to the target lesion and greater efficacy in lesions in proximity to vascular structures with a reduction in the heat-sink effect compared to RFA.[29] Due to the higher delivered energy a vessel thrombosis as potential complication can occur when tumors adjacent to major vessels are treated. Although extremely rare, these complications have been described.[29]

Electrochemotherapy has already proven effective in treatment of HCC in a series of 17 lesions in 10 patients treated by electrochemotherapy during the open surgery with median tumor size of 24 mm (range 8–41 mm). No treatment related adverse effects or major post-operative complications were observed. The complete response rate at last follow up ranging from 12 to 31 months was 80% per patient and 88% per treated lesion.[5] This response rate of electrochemotherapy is comparable although lower than the response rate achieved by RFA and MWA.[30] Newer studies report the response rate in HCC smaller than 30 mm above 98% for RFA and MWA with low percentage of local recurrence.[31]

The advantage of the electrochemotherapy is that it is effective in treatment of tumors also located in close proximity of the major hepatic vessels. In comparison to RFA electrochemotherapy is not affected by heat sink effect, and this indication was not proven only in the clinical study treating HCC with electrochemotherapy[5], but also in the study treating liver metastases of colorectal cancer by IRE.[32] The safety of treating tumors close to major liver vessels was demonstrated also in the recent study in healthy pigs, where no significant vascular damage/abnormalities were observed in liver vessels, even when the electrodes were inserted through the hepatic or portal vessels.[11]

IRE as an ablation method has also been demonstrated to be effective for treatment of HCC.[15,33] Similar observations were reported for electrochemotherapy, without major complications. IRE, though, is executed percutaneously in many cancer centers, with the aid of image guidance.[34] Due to similar technological approach, electrochemotherapy can also be performed percutaneously. Same principles must be followed - careful pre-treatment planning, image guided electrode insertion and safe delivery of electric pulses with ECG synchronization.[24,35,36] Electrochemotherapy however may offer additional advantages over IRE: shorter treatment duration due to a lower number of pulses required (e.g. 8 vs. 90), the possibility of achieving larger volumes with fewer electrodes and without electrode repositioning.

The advantage of electrochemotherapy in comparison to IRE is its different mode of action. IRE is an ablative technique that by delivering sets of pulses disrupts cell's homeostasis due to cell membrane electroporation leading to cell death. Therefore, the tumor is ablated in the confined area and no selective action on tumor cells is present. IRE being nonthermal ablative technology also elicits strong local immune response and preserves critical structures which is also well established in electrochemotherapy. Electrochemotherapy however acts through three mechanisms. First one is selective cellular cytotoxicity by drug delivered to cells, and cell death due to mitotic catastrophe.[37] In that case tumor safety margins can be wider due to predominantly tumor cell death and sparing of normal tissue. Electrochemotherapy, can therefore be employed also in tumors that are bigger than 3 cm in diameter, which is currently the limit for IRE. The second mode of action is vascular disruption that is well established in electrochemotherapy[38], but not well explored in IRE. And the third is the elicitation of local immune response[39] that could be exploited in combination with immunotherapies.[40,41]

Using percutaneous approach will provide electrochemotherapy broader clinical application in treatment of HCC and other liver tumors/metastases, being minimally invasive, with short hospitalization and good patient's compliance.

Acknowledgement

This work was financially supported by the Slovenian Research Agency (ARRS), grant No. P3-0003 and P2-0249 and grant of University Clinical Center Ljubljana #20180061

References

1. Campana LG, Clover AJ, Valpione S, Quaglino P, Gehl J, Kunte C, et al. Recommendations for improving the quality of reporting clinical electrochemotherapy studies based on qualitative systematic review. *Radiol Oncol* 2016; **50:** 1-13. doi: 10.1515/raon-2016-0006

2. Gehl J, Sersa G, Matthiessen LW, Muir T, Soden D, Occhini A, et al. Updated standard operating procedures for electrochemotherapy of cutaneous tumours and skin metastases. *Acta Oncol* 2018; **57:** 874-82. doi:10.1080/0284186X.2018.1454602

3. Campana LG, Miklavčič D, Bertino G, Marconato R, Valpione S, Imarisio I, et al. Electrochemotherapy of superficial tumors - current status: basic principles, operating procedures, shared indications, and emerging applications. *Semin Oncol* 2019; **46:** 173-91. doi: 10.1053/j.seminoncol.2019.04.002

4. Edhemovic I, Brecelj E, Gasljevic G, Snoj M, Miklavcic D, Gadzijev E, et al. Intraoperative electrochemotherapy of colorectal liver metastases. *J Surg Oncol* 2014; **110:** 320-7. doi: 10.1002/jso.23625

5. Djokic M, Cemazar M, Popovic P, Kos B, Dezman R, Bosnjak M, et al. Electrochemotherapy as treatment option for hepatocellular carcinoma, a prospective pilot study. *Eur J Surg Oncol* 2018; **44:** 651-7. doi: 10.1016/j.ejso.2018.01.090

6. Edhemovic I, Brecelj E, Cemazar M, Boc N, Trotovsek B, Djokic M, et al. Intraoperative electrochemotherapy of colorectal liver metastases: a prospective phase II study. *Eur J Surg Oncol* 2020; Epub ahead of print. doi: 10.1016/j.ejso.2020.04.037
7. Johnson BW, Wright GP. Regional therapies for the treatment of primary and metastatic hepatic tumors: a disease-based review of techniques and critical appraisal of current evidence. *Am J Surg* 2019; **217:** 541-5. doi: 10.1016/j.amjsurg.2018.10.018
8. Lyu C, Lopez-Ichikawa M, Rubinsky B, Chang TT. Normal and fibrotic liver parenchyma respond differently to irreversible electroporation. *HPB* 2019; **21:** 1344-53. doi: 10.1016/j.hpb.2019.01.019
9. Geboers B, Scheffer HJ, Graybill PM, Ruarus AH, Nieuwenhuizen S, Puijk RS, et al. High-voltage electrical pulses in oncology: Irreversible electroporation, electrochemotherapy, gene electrotransfer, electrofusion, and electroimmunotherapy. *Radiology* 2020; **295:** 254-72. doi: 10.1148/radiol.2020192190
10. Miklavčič D, Mali B, Kos B, Heller R, Serša G. Electrochemotherapy: from the drawing board into medical practice. *Biomed Eng Online* 2014; **13:** 29. doi: 10.1186/1475-925X-13-29
11. Brloznik M, Boc N, Sersa G, Zmuc J, Gasljevic G, Seliskar A, et al. Radiological findings of porcine liver after electrochemotherapy with bleomycin. *Radiol Oncol* 2019; **53:** 415-26. doi: 10.2478/raon-2019-0049
12. Zmuc J, Gasljevic G, Sersa G, Edhemovic I, Boc N, Seliskar A, et al. Large liver blood vessels and bile ducts are not damaged by electrochemotherapy with beomycin in pigs. *Sci Rep* 2019; **9:** 3649. doi: 10.1038/s41598-019-40395-y.
13. Gasljevic G, Edhemovic I, Cemazar M, Brecelj E, Gadzijev EM, Music MM, et al. Histopathological findings in colorectal liver metastases after electrochemotherapy. *PLoS One* 2017; **12:** e0180709. doi: 10.1371/journal.pone.0180709.
14. Probst U, Fuhrmann I, Beyer L, Wiggermann P. Electrochemotherapy as a new modality in interventional oncology: a review. *Technol Cancer Res Treat* 2018; **17:** 1533033818785329. doi: 10.1177/1533033818785329
15. Sutter O, Calvo J, N'kontchou G, Nault J-C, Ourabia R, Nahon P, et al. Safety and efficacy of irreversible electroporation for the treatment of hepatocellular carcinoma not amenable to thermal ablation techniques. *Radiology* 2017; **284:** 877-86. doi: 10.1148/radiol.2017161413
16. Kalra N, Gupta P, Gorsi U, Bhujade H, Chaluvashetty SB, Duseja A, et al. Irreversible electroporation for unresectable hepatocellular carcinoma: initial experience. *Cardiovasc Intervent Radiol* 2019; **42:** 584-90. doi: 10.1007/s00270-019-02164-2
17. Kalra N. Locoregional treatment for hepatocellular carcinoma: the best is yet to come. *World J Radiol* 2015; **7:** 306-18. doi: 10.4329/wjr.v7.i10.306
18. Gasbarrini A, Campos WK, Campanacci L, Boriani S. Electrochemotherapy to metastatic spinal melanoma: a novel treatment of spinal metastasis? *Spine* 2015; **40:** E1340-6. doi: 10.1097/BRS.0000000000001125
19. Cornelis FH, Ben Ammar M, Nouri-Neuville M, Matton L, Benderra MA, Gligorov J, et al. Percutaneous image-guided electrochemotherapy of spine metastases: initial experience. *Cardiovasc Intervent Radiol* 2019; **42:** 1806-9. doi: 10.1007/s00270-019-02316-4
20. Tarantino L, Busto G, Nasto A, Nasto RA, Tarantino P, Fristachi R, et al. Electrochemotherapy of cholangiocellular carcinoma at hepatic hilum: a feasibility study. *Eur J Surg Oncol* 2018; **44:** 1603-9. doi: 10.1016/j.ejso.2018.06.025
21. Cindrič H, Kos B, Tedesco G, Cadossi M, Gasbarrini A, Miklavčič D. Electrochemotherapy of spinal metastases using transpedicular approach - a numerical feasibility study. *Technol Cancer Res Treat* 2018; **17:** 1533034618770253. doi: 10.1177/1533034618770253
22. Tarantino L, Busto G, Nasto A, Fristachi R, Cacace L, Talamo M, et al. Percutaneous electrochemotherapy in the treatment of portal vein tumor thrombosis at hepatic hilum in patients with hepatocellular carcinoma in cirrhosis: a feasibility study. *World J Gastroenterol* 2017; **23:** 906-18. doi: 10.3748/wjg.v23.i5.906
23. Cornelis FH, Cindrič H, Kos B, Fujimori M, Petre EN, Miklavčič D, et al. Peritumoral metallic implants reduce the efficacy of irreversible electroporation for the ablation of colorectal liver metastases. *Cardiovasc Intervent Radiol* 2020; **43:** 84-93. doi: 10.1007/s00270-019-02300-y
24. Mali B, Gorjup V, Edhemovic I, Brecelj E, Cemazar M, Sersa G, et al. Electrochemotherapy of colorectal liver metastases - an observational study of its effects on the electrocardiogram. *Biomed Eng Online* 2015; **14 Suppl 3**: S5. doi: 10.1186/1475-925X-14-S3-S5
25. Lu DS, Raman SS, Limanond P, Aziz D, Economou J, Busuttil R, et al. Influence of large peritumoral vessels on outcome of radiofrequency ablation of liver tumors. *J Vasc Interv Radiol* 2003; **14:** 1267-74. doi: 10.1097/01.rvi.0000092666.72261.6b
26. Baker EH, Thompson K, McKillop IH, Cochran A, Kirks R, Vrochides D, et al. Operative microwave ablation for hepatocellular carcinoma: a single center retrospective review of 219 patients. *J Gastrointest Oncol* 2017; **8:** 337-46. doi: 10.21037/jgo.2016.09.06
27. Baker EH, Thompson K, McKillop IH, Cochran A, Kirks R, Vrochides D, et al. Operative microwave ablation for hepatocellular carcinoma: a single center retrospective review of 219 patients. *J Gastrointest Oncol* 2017; **8:** 337-46. doi: 10.21037/jgo.2016.09.06
28. Wang T, Lu XJ, Chi JC, Ding M, Zhang Y, Tang XY, et al. Microwave ablation of hepatocellular carcinoma as first-line treatment: long term outcomes and prognostic factors in 221 patients. *Sci Rep* 2016; **6:** 32728. doi: 10.1038/srep32728
29. Ding J, Jing X, Liu J, Wang Y, Wang F, Wang Y, et al. Complications of thermal ablation of hepatic tumours: comparison of radiofrequency and microwave ablative techniques. *Clin Radiol* 2013; **68:** 608-15. doi: 10.1016/j.crad.2012.12.008
30. Lucchina N, Tsetis D, Ierardi AM, Giorlando F, Macchi E, Kehagias E, et al. Current role of microwave ablation in the treatment of small hepatocellular carcinomas. *Ann Gastroenterol* 2016; **29:** 460-5. doi: 10.20524/aog.2016.0066
31. Ding J, Jing X, Liu J, Wang Y, Wang F, Wang Y, et al. Comparison of two different thermal techniques for the treatment of hepatocellular carcinoma. *Eur J Radiol* 2013; **82:** 1379-84. doi: 10.1016/j.ejrad.2013.04.025
32. Distelmaier M, Barabasch A, Heil P, Kraemer NA, Isfort P, Keil S, et al. Midterm safety and efficacy of irreversible electroporation of malignant liver tumors located close to major portal or hepatic veins. *Radiology* 2017; **285:** 1023-31. doi: 10.1148/radiol.2017161561
33. Pompili M, Francica G. Irreversible electroporation for hepatic tumors. *J Ultrasound* 2019; **22:** 1-3. doi: 10.1007/s40477-019-00367-4
34. Mafeld S, Wong JJ, Kibriya N, Stenberg B, Manas D, Bassett P, et al. Percutaneous irreversible electroporation (IRE) of hepatic malignancy: a bi-institutional analysis of safety and outcomes. *Cardiovasc Intervent Radiol* 2019; **42:** 577-83. doi: 10.1007/s00270-018-2120-z
35. Mali B, Jarm T, Corovic S, Paulin-Kosir MS, Cemazar M, Sersa G, et al. The effect of electroporation pulses on functioning of the heart. *Med Biol Eng Comput* 2008; **46:** 745-57. https://doi.org/10.1007/s11517-008-0346-7
36. Ball C, Thomson KR, Kavnoudias H. Irreversible electroporation: a new challenge in "out of operation theatre" anaesthesia. *Anesth Analg* 2010; **110:** 1305-9. doi: 10.1213/ANE.0b013e3181d27b30
37. Mekid H, Tounekti O, Spatz A, Cemazar M, Kebir E, Mir LM. In vivo evolution of tumour cells after the generation of double-strand DNA breaks. *Br J Cancer* 2003; **88:** 1763-71. doi: 10.1038/sj.bjc.6600959
38. Markelc B, Sersa G, Cemazar M. Differential mechanisms associated with vascular disrupting action of electrochemotherapy: intravital microscopy on the level of single normal and tumor blood vessels. *PLoS One* 2013; **8:** e59557. doi: 10.1371/journal.pone.0059557
39. Calvet CY, Famin D, André FM, Mir LM. Electrochemotherapy with bleomycin induces hallmarks of immunogenic cell death in murine colon cancer cells. *Oncoimmunology* 2014; **3:** e28131. doi: 10.4161/onci.28131
40. Sersa G, Teissie J, Cemazar M, Signori E, Kamensek U, Marshall G et al. Electrochemotherapy of tumors as in situ vaccination boosted by immunogene electrotransfer. *Cancer Immunol Immunother* 2015; **64:** 1315-27. doi: 10.1007/s00262-015-1724-2
41. Heppt MV, Eigentler TK, Kähler KC, Herbst RA, Göppner D, Gambichler T, et al. Immune checkpoint blockade with concurrent electrochemotherapy in advanced melanoma: a retrospective multicenter analysis. *Cancer Immunol Immunother* 2016; **65:** 951-9. doi: 10.1007/s00262-016-1856-z

research article

Consolidation radiotherapy for patients with extended disease small cell lung cancer in a single tertiary institution: impact of dose and perspectives in the era of immunotherapy

Karmen Stanic[1,2], Martina Vrankar[1,2], Jasna But-Hadzic[1,2]

[1] Department of Radiotherapy, Institute of Oncology Ljubljana, Ljubljana, Slovenia

[2] Faculty of Medicine, University of Ljubljana, Ljubljana, Slovenia

Radiol Oncol 2020; 54(3): 353-363.

Received 9 March 2020
Accepted 4 July 2020

Correspondence to: Assist. Prof. Jasna But-Hadžić, M.D. PhD., Institute of Oncology Ljubljana, Department of Radiotherapy, Zaloška 2, 1000 Ljubljana. E-mail: jbut@onko-i.si

Disclosure: No potential conflicts of interest were disclosed.

Background. Consolidation radiotherapy (cRT) in extended disease small cell lung cancer (ED-SCLC) showed improved 2-year overall survival in patients who responded to chemotherapy (ChT) in CREST trial, however results of two meta - analysis were contradictive. Recently, immunotherapy was introduced to the treatment of ED-SCLC, making the role of cRT even more unclear. The aim of our study was to access if consolidation thoracic irradiation improves survival of ED-SCLC patients treated in a routine clinical practice and to study the impact of cRT dose on survival. We also discuss the future role of cRT in the era of immunotherapy.

Patients and methods. We retrospectively reviewed 704 consecutive medical records of patients with small cell lung cancer treated at the Institute of Oncology Ljubljana from January 2010 to December 2014 with median follow up of 65 months. We analyzed median overall survival (mOS) of patients with ED-SCLC treated with ChT only and those treated with ChT and cRT. We also compared mOS of patients treated with different consolidation doses and performed univariate and multivariate analysis of prognostic factors.

Results. Out of 412 patients with ED-SCLC, ChT with cRT was delivered to 74 patients and ChT only to 113 patients. Patients with cRT had significantly longer mOS compared to patients with ChT only, 11.1 months (CI 10.1–12.0) *vs.* 7.6 months (CI 6.9–8.5, $p < 0.001$) and longer 1-year OS (44% *vs.* 23%, $p = 0.0025$), while the difference in 2-year OS was not significantly different (10% *vs.* 5%, $p = 0.19$). The cRT dose was not uniform. Higher dose with 45 Gy (in 18 fractions) resulted in better mOS compared to lower doses 30–36 Gy (in 10–12 fractions), 17.2 months *vs.* 10.3 months ($p = 0.03$) and statistically significant difference was also seen for 1-year OS (68% *vs.* 30%, $p = 0.01$) but non significant for 2-year OS (18% *vs.* 5%, $p = 0.11$).

Conclusions. Consolidation RT improved mOS and 1-year OS in ED-SCLC as compared to ChT alone. Higher dose of cRT resulted in better mOS and 1-year OS compared to lower dose. Consolidation RT, higher number of ChT cycles and prophylactic cranial irradiation (PCI) were independent prognostic factors for better survival in our analysis. For patients who received cRT, only higher doses and PCI had impact on survival regardless of number of ChT cycles received. Role of cRT in the era of immunotherapy is unknown and should be exploited in further trials.

Key words: small cell lung cancer; ED-SCLC; radiotherapy; consolidation radiotherapy; immunotherapy

Introduction

Small cell lung cancer (SCLC) represents only small proportion of lung cancer but is an aggressive disease and unfortunately diagnosed already in advanced stage in majority of patients.[1] In Slovenia 15.3% of lung cancer patients were diagnosed with SCLC in 2014, and majority had metastatic dis-

doi: 10.2478/raon-2020-0046

ease.[2] In recent years, percentage of patients with metastatic disease has slightly increased, but this might only be due to better staging with incorporation of PET/CT and brain MRI.[3,4]

SCLC is highly chemo-sensitive disease and standard treatment for metastatic patients is platinum based chemotherapy (ChT), usually combined with etoposide or irinotecan.[5,6] Almost 75% of the patients have persisting intra-thoracic disease after treatment with ChT and addition of chest radiotherapy (RT) aimed to improve progression free survival (PFS) and overall survival (OS) in those patients.[7] Prospective randomized CREST study suggested survival benefit of added thoracic RT in addition to PCI for ED-SCLC patients who respond to ChT; however, OS at 1-year, which was the primary endpoint of the study, was not significantly improved.[8] Prospective RTOG 0937 study also failed to show 1-year survival benefit, though disease progression was delayed.[9] On the other hand, some retrospective studies showed benefit of consolidation RT (cRT).[10-13] None of the prospective and only rare retrospective studies specifically researched the effect of radiation dose on survival.

In addition, selective patients might benefit from prophylactic cranial irradiation (PCI), which showed increase in overall survival if added to ED-SCLC after ChT.[14] In spite of that, the median overall survival (mOS) of metastatic disease remains poor, ranging from 8 to13 months, with only 5% of patients being alive at 2 years.[15] Recently, immunotherapy with atezolizumab or durvalumab added to ChT without chest irradiation has shown increased mOS in first line treatment of patients with metastatic SCLC, therefore in the future the role of radiotherapy would need to be reconsidered.[16,17]

The aim of our study was to access if cRT improves survival of ED-SCLC patients treated in a routine clinical practice of tertiary single centre and to study the impact of cRT dose on survival. We also discuss whether the cRT still has the role in the treatment of ED SCLC in the era of immunotherapy.

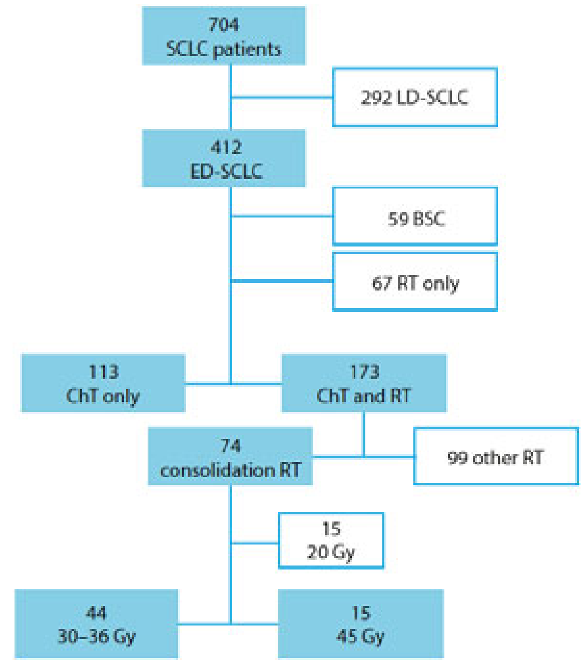

FIGURE 1. Diagram of patients' selection process.

Patients and methods

We retrospectively reviewed medical records of consecutive patients with SCLC treated at the Institute of Oncology Ljubljana during the five year period, from January 2010 to December 2014. Median follow up was 65 months.

Not all metastatic SCLC patients were referred to our center for treatment; however, during the period studied, we were the only radiotherapy center in the country and all patients that needed irradiation, based on multidisciplinary tumor board decision, were treated at our institution. Only patients who had at least stable disease or regression of disease after chemotherapy were eligible for thoracic consolidation radiotherapy. The decision about the dose was at the discretion of radiation oncologist and based on the volume of the tumor and performance status of the patient since during the time period studied there was no uniform dose suggested in any of the guidelines.

Diagram in Figure 1 outlines the selection process. During 5 year period 704 consecutive patients with SCLC were treated at the Institute of oncology Ljubljana, 412 with extended disease and 292 with locally advanced disease. Among all ED-SCLC patients, 59 (14.3%) were treated with BSC, 67 (16.2%) patients with RT only, 113 (27.4%) with ChT only and 173 (41.9%) with combined ChT and RT. RT was either consolidation RT (cRT), delivered to 74 patients or any other type of RT which included urgent RT, partly concurrent ChT or RT that was prematurely closed due to any reason (99 patents).

The following parameters were recorded: demographic and clinical characteristics, date of diagnosis, TNM stage, treatment characteristics, including chemotherapy and radiation therapy details, metastatic locations and date of death or last follow up.

Chemotherapy

Of Majority (47.5%) of patients received all 6 planned cycles of chemotherapy, 66 patients (35.3%) received less than 4 cycles of ChT. Etoposide with platinum was the most frequent combination (83.8%), the rest received anthracycline based ChT. In the group with cRT were less patients who received 4 ChT cycles or less.

Radiotherapy

Radiotherapy with linear accelerators (photon beam 6-10MV), based on 3D CT-based conformal radiation therapy planning, started after ChT. There was no difference in frequency of patients who started before (29 patients) and after 4 weeks (25 patients) of ChT completion. Prophylactic cranial irradiation was delivered with two opposed lateral fields with the dose of 25 Gy in 10 fractions using 2D planning and 6MV photon beam energy.

Statistical analysis

The primary endpoints in this analysis were mOS, 1-year and 2-year OS of ED-SCLC patients treated with ChT only versus patients treated with ChT and cRT and those receiving higher *vs.* lower dose of cRT. Median OS was calculated from the time of diagnosis to the time of death due to any cause or last follow up visit. Kaplan-Meier (KM) method and log-rank test were used for comparison of survival curves between different groups. Cox proportional hazards algorithm was used for univariate and multivariate analysis. Association between subgroups and clinico-pathological characteristics of patients were tested using chi-square method. All p values reported were based on 2 side hypothesis. The statistical analysis was computed using SPSS v.20 statistical package.

Ethical consideration

This survey was approved by Institutional Ethics Committee and Institutional Review Board in December 2017.

Results

We performed two analysis. In our first analysis we included 187 patients, 113 patients treated with Cht only were compared to 74 patients treated with ChT and cRT. Different fractionation schemes were

TABLE 1. Patients' characteristics: chemotherapy only *vs.* chemotherapy with consolidation radiotherapy

		ChT only	ChT with cRT	p
		n (%)	n (%)	
Gender	187 (100)	113 (60.4)	74 (39.6)	
Male	126 (67.4)	81 (71.1)	45 (60.1)	0.12
Female	61 (32.6)	32 (28.9)	29 (39.9)	
Age				
median (range)	63 (42-80)	61 (42-80)	63 (47-80)	0.24
< 65	122 (65.2)	70 (61.9)	52 (70.3)	
> 65	65 (34.8)	43 (38.1)	22 (29.7)	
Number of ChT cycles*				
< 4	66 (35.3)	51 (47.2)	15 (20)	**<0.001**
> 4	113 (60.4)	57 (52.8)	56 (80)	
T stage				0.23
T1–2	32 (17.1)	20(17.7)	12 (16.2)	
T3-4	122 (65.2)	69 (61)	53 (71.6)	
Tx	33 (17.7)	24 (21.3)	9 (12.2)	
N stage				0.56
N0–2	71 (38)	40 (35.4)	31(41.9)	
N3	91(48.7)	56 (49.6)	35 (47.3)	
Nx	25 (13.3)	17 (15)	8 (10.8)	
Metastases location**				
Brain	44 (23.5)	28 (24.8)	16 (21.6)	0.61
Liver	86 (46)	57 (50.4)	29 (39.2)	0.13
Bone	42 (22.5)	28 (24.8)	14 (18.9)	0.34
Adrenal gland	38 (20.3)	23 (20.4)	15 (20.3)	0.98
Other	92 (49.2)	62 (54.9)	30 (40.5)	0.06
Number of metastatic locations				
1	105 (56.1)	55 (48.7)	50 (67.6)	**0.01**
> 2	82 (43.9)	58 (51.3)	24 (23.4)	
PCI				
Yes	41 (21.9)	20 (17.6)	21 (28.4)	0.08
no	146 (78.1)	93 (82.4)	53 (71.6)	

* for 8 patients we were not able to retrieve the exact number of cycles from medical records, percentage of patient is calculated only for those with known number of cycles (179);

** some patients had more than 1 metastatic location, percentages are calculated as part of all patients in a group;

ChT = chemotherapy; cRT = consolidation radiotherapy; PCI = prophylactic cranial irradiation

TABLE 2. Patients' characteristics: higher *vs.* lower dose of radiotherapy

	All	45 Gy	30-36 Gy	p
	n (%)	n (%)	n (%)	
Gender	59	15	44	
Male	35 (60)	6 (40)	29 (65.9)	0.078
Female	24 (40)	9 (60)	15 (34.1)	
Age				
median	62 (42–76)	60 (54–73)	62 (42–76)	0.12
< 65	42 (71.2)	13 (68.7)	29 (65.9)	
> 65	17 (28.8)	2 (13.3)	15 (34.1)	
Number of ChT cycles				
< 4	12 (20.3)	2 (13.3)	10 (22.7)	0.37
> 4	44 (74.6)	13 (68.7)	31 (70.5)	
unknown	3 (5.1)	0 (0)	3 (6.8)	
PS before RT				0.66
0-1	22 (37.3)	5 (33.3)	17 (38.6)	
2–3	7 (11.8))	1 (6.67)	6 (13.6)	
unknown	30 (50.9)	9 (0.6)	21 (47.8)	
T stage				0.15
T1–2	8 (13.6)	4 (26.7)	4 (9.1)	
T3–4	42 (71.2)	8 (53.3)	34 (77.3)	
Tx	9 (15.3)	3 (20)	6 (13.6)	
N stage				0.69
N0–2	24 (40.7)	7 (46.7)	17 (38.6)	
N3	29 (49.2)	6 (40)	23 (52.3)	
Nx	6 (10.1)	2 (13.3)	4 (9.1)	
Metastases location*				
Brain	14 (23.7)	5 (33.3)	9 (20.5)	0.31
Liver	27 (45.7)	6 (40)	21 (47.7)	0.60
Bone	13 (22)	3 (30)	10 (22.7)	0.82
Adrenal gland	15 (25.4)	3 (30)	12 (27.3)	0.57
Other	21 (35.6)	3 (30)	19 (43.2)	0.10
Number of metastatic locations				
1	34 (57.6)	10 (66.7)	24 (54.5)	0.41
> 2	25 (42.4)	5 (33.3)	20 (45.4)	
Timing of RT**				0.15
< 4 weeks after ChT	17 (53.1)	6 (75)	11 (45.9)	
> 4 weeks after ChT	15 (46.9)	2 (25)	13 (54.1)	
PCI				
Yes	17 (28.8)	5 (33.3)	12 (27.3)	0.65

* some patients had more than one metastatic site;

** for 31 missing patients no reliable data of the completion chemotherapy date could be retrieved from the medical records;

Ch =- chemotherapy; Gy = Gray; N = lymph nodes; PS = performance status; RT = radiotherapy; T = tumour

used for cRT. The doses in cRT were not uniform, therefore we divided them into 3 groups: below 30 Gy, 30–36 Gy and 45 Gy. Only 59 patients with doses above 30 Gy were included in our second analysis of dose comparison.

Patient characteristics

Baseline characteristics of 187 patients, divided to those with ChT only and those who also received cRT are presented in Table 1. The two groups were balanced regarding gender, age, T and N stage and metastatic locations. However, lower number of patients received 4 or less cycles of ChT and had 2 or more metastases present at diagnosis in ChT plus cRT group.

Table 2 present baseline characteristics of 59 patients who received > 30 Gy cRT, comparing those with higher dose (45 Gy) cRT and lower dose (30–36 Gy). In summary, median age was 63 years, more than half were men. Majority of patients were younger than 65 years. Unfortunately, reliable PS could not be retrieved from medical records for half of the patients and more than 10% of patients had PS 2-3 before cRT. Non-significantly more patients had larger tumors (T3-4) and more extended lymph node disease (N3) in the group treated with lower dose RT. For more than 10% of patients with central tumors, the size of tumor (T) or nodal status could not be determined. Fifty-eight percent of patients had one metastatic site. The most frequent site of metastases were liver. Less than third of patients had PCI.

Survival data

Median OS of patients who had either BSC or RT only was poor, 1.86 and 2.42 months, respectively. Patients who had any form of additional chest irradiation (173 patients) had significantly better mOS than 113 patients with ChT only (9.9m *vs.* 7.6m, p = 0.002).

Consolidation RT was delivered to 74 patients. Those patients had significantly longer mOS compared to 113 patients with ChT only as presented in Figure 2, 11.1 months (CI 10.1–12.0) *vs.* 7.6 months (CI 6.9–8.5), p < 0.001. They also had significantly longer 1-year OS (44% *vs.* 23%, p = 0.0025), but non significantly longer 2-year OS (10% *vs.* 5%, p = 0.19).

Univariate survival analysis (UVA) for patients with or without cRT included the following variables: cRT, gender, age, number of ChT cycles, T and N stage, metastatic location, number of metastatic locations and PCI. Presence of cRT, female gender, number of ChT cycles (4 or less and more than 4) and PCI were significant in univariate analysis and were tested in multivariate analysis (MVA) (Table 3). Except for gender, they were all independent predictors of better survival.

In the group of 59 patients irradiated with cRT ≥ 30 Gy patients irradiated with 45 Gy had better mOS compared to patients irradiated with doses 30–36 Gy, 17.2 months *vs.* 10.3 months, p = 0.03. (Figure 3) Patients with higher dose of consolidation RT had significantly longer 1-year OS (68%) than those with lower dose (30%), p = 0.01, but non-significantly longer 2-year OS (18% *vs.* 5%, p = 0.11).

In the group of patients with cRT, we made another analysis. We included gender, age categories, PS before RT, RT dose, T and N stage, metastatic locations, number of ChT cycles, number of metastatic lesions, PCI and timing of RT in UVA. Statistically significant predictors of longer mOS were PCI irradiation and higher RT dose. Both were analyzed in MVA (Table 4) and remained independent predictors of improved survival. (PCI HR = 0.51, 95% CI 0.27–0.96; higher RT dose HR = 0.47, 95% CI 0.25–0.87).

Discussion

Thoracic irradiation has never been considered such an important part of ED-SCLC treatment as chemotherapy. Since the pivotal study of Jeremic *et al.* two decades ago, who were the first to show importance of RT in ED SCLC, only lately introduction of modern RT techniques with less toxicity rose interest again for the use of RT.[18]

Survival of patients with chemotherapy only and those who also had consolidation radiotherapy

Our analysis showed that cRT significantly improved mOS compared to patients who had ChT only, 11.1 months *vs.* 7.6 months. Those patients also had significantly longer 1-year OS (44% *vs.* 23%) and non-significantly longer 2-year OS (10% *vs.* 5%). Apart from cRT, independent predictors of survival were also PCI and higher number of ChT cycles delivered. Unfortunately, the response to ChT could not be included to our analysis, as due to retrospective nature of this study the response to ChT was not uniformly evaluated.

How results of our study compares to others is presented in Table 5. In a retrospective study of 119 patients by Zhu *et al.*, survival results were much better than in our analysis, with mOS of 17 months for patients in ChT plus cRT group and 9.3 months for those with ChT only, and 2-year OS of 35% and 17%, respectively. They delivered higher cRT dose (range 40–60 Gy) and had comparable mOS (17.2 months) as our group of patients irradiated with 45

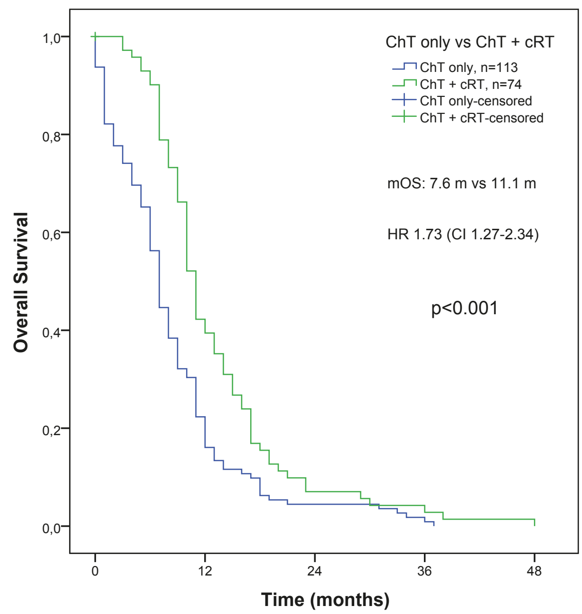

FIGURE 2. Overall survival of patients treated with chemotherapy (Cht only) *vs.* chemotherapy and consolidation radiotherapy (ChT + cRT).

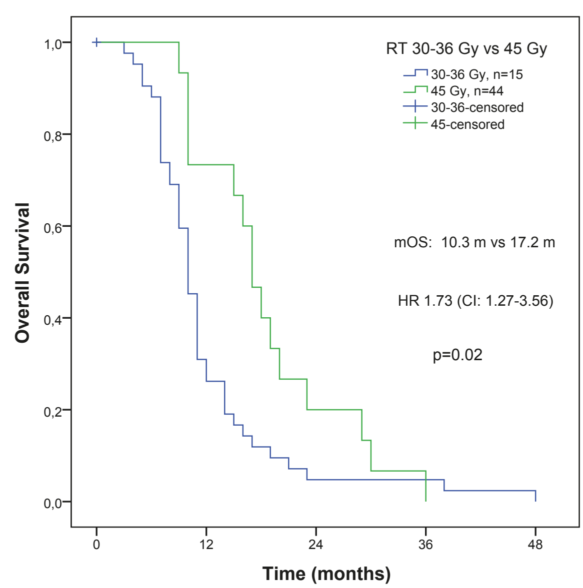

FIGURE 3. Overall survival of patients treated with higher (45 Gy) *vs.* lower (30-36 Gy) dose of irradiation.

TABLE 3. Univariate and multivariate analysis of overall survival for patients with cRT vs no cRT (n = 187)

	p	Univariate analysis	p	Multivariate analysis
		HR (95% CI)		HR (95% CI)
cRT	**< 0.001**	**1.73 (1.27–2.34)**	**0.01**	**1.52 (1.10–2.09)**
no				
yes				
Gender	**0.042**	**1.17 (1.00–1.37)**	0.68	1.03 (0.87–1.21)
Male				
Female				
Age	0.25	1.19 (0.88–1.62)		
> 65				
< 65				
Number of cycles received	**< 0.001**	**3.23 (2.33–4.47)**	**< 0.001**	**3.11 (2.22–4.35)**
< 4				
> 4				
T stage	0.98	1.00 (0.67–1.50)		
T1, 2				
T3, 4				
N stage	0.16	1.08 (0.96–1.22)		
N0-2				
N3				
Metastases location				
Brain no/yes	0.61	0.91 (0.64–1.29)		
Liver no/yes	0.40	1.13 (0.84–1.52)		
Bone no/yes	0.75	0.94 (0.67-1.33)		
Adrenal gland no/yes	0.62	1.09 (0.76–1.57)		
Other no/yes	0.18	1.21 (0.90–1.63)		
Number of metastatic locations	0.68	1.06 (0.79–1.42)		
1				
> 2				
PCI	**< 0.001**	**0.49 (CI 0.32–0.76)**	**0.015**	**1.59 (1.09–2.32)**
No				
Yes				

cRT = consolidation radiotherapy; N = lymph nodes; PCI = prophylactic cranial irradiation; T = tumour

Gy.[10] Study by Yee *et al.* included only 33 patients, all with PCI and cRT (40 Gy), but their reported mOS of 8.3 months is lower than ours.[11] Another small retrospective study of 19 patients with cRT 40 Gy in 15 fraction reported mOS 14 months with 1-year and 2-year OS 58% and 14%.[12] Difference in the results of these studies show that survival benefit could not be attributed to RT only, but also to the increased chances of those patients who remained in a better shape and fitter at the time of disease progression to receive subsequent lines of chemotherapy. Data from SEER analysis on almost 7000 patients also provide evidence that radiotherapy for thoracic lesion and any metastatic sites could significantly improve the OS, except for brain metastasis.[13]

Three prospective randomized trials researched impact of RT on survival in ED SCLC.[8,9,18] Trial by Jeremic *et al.* differs in many ways from more recently reported studies. They used accelerated hyperfractionation (54 Gy in 36 fractions) with concomitant ChT after 3 cycles of induction ChT and additional 2 cycles after RT in one group or after 5 cycles of ChT in another, both groups also eligible for PCI. They studied combined modality treatment rather than cRT. The reported mOS was excellent for those who received RT early (17 months) as compared to those who received late RT (6–8 months).[18] Another concern regarding hyperfractionated RT is that is delivered twice daily (BID) and is technically challenging for patients with bilateral mediastinal lesions, which represented the majority in our population. Further, patients selected for combined modality treatment, which incorporates BID RT must have excellent performance status and baseline pulmonary function. In our study more than 10% of patients had PS 2-3 before cRT and unfortunately in more than half of patients PS could not be reliably retrieved from medical records.

Phase III EORTC study (CREST) included patents with PS 0–2 without brain and pleural metastases. Responders after 4–6 cycles of ChT and residual disease in the thorax were treated with irradiation of 30 Gy in 10 fractions.[8] Contrary to our results, no benefit was shown for added RT after ChT regarding mOS, which reported to be 8 months in both groups and for 1-year OS (33% for ChT with cRT *vs.* 28% for ChT group only). However, they reported significant difference in 2-year OS 13% *vs.* 3% (p = 0.004). It should, however, be noted that mOS was calculated from the randomization while mOS from diagnosis (as calculated in our analysis) was 12 months.

More aggressive thoracic irradiation was given in RTOG 0937 trial with 45 Gy in 15 fractions.[9] Reported median OS (15.8 months) was better than anticipated and much better than in CREST and our study. Unlike all other studies, they reported better mOS for ChT only group (15.8 months) than for ChT plus RT group (13.8 months), though the difference was not statistically significant. 1-year OS was similar, surprisingly higher for ChT only than for ChT plus cRT group (60.1% *vs.* 50.8%).

Two meta-analyses were published. The first, published by Palma *et al.* in 2015 included 2 studies with 604 patients, while the second published in 2019 by Rathod *et al.* added also 86 patients from prematurely closed RTOG 0937 data.[19,20] First meta-analysis found increased OS ($p = 0.01$), while the second failed to show improvement in overall survival by adding cRT to ChT, ($p = 0.36$).

Effect of consolidation radiotherapy dose on survival

We found that patients who had been irradiated with higher dose (45 Gy in 18 fractions) had better mOS compared to those who received lower doses 30–36 Gy (in 10–12 fractions), 17.2 months *vs.* 10.3 months. Patients with higher dose of cRT had better 1-year OS (68%) than those with lower dose (30%) and also better 2-year OS (18% *vs.* 5%).

Not many studies looked into dose difference for cRT. In retrospective study including 306 patients of whom 170 received cRT, those with higher RT dose (BED > 50 Gy) had longer 2y-OS, 32.3% *vs.* 17% ($p < 0.001$), respectively.[21] In recently published retrospective analysis of National Cancer Database that included 3280 patients they also reported that patients treated with the dose at least 45 Gy had better survival; 1-year OS was 58.1% and 2-year OS was 25.2% compared to 43.8% and 15.1% for lower dose.[22] Our results for 1-year OS compare favorable, but 2-year OS data are lower, suggesting our subsequent treatments were not as effective.

In CREST study, cRT dose used was 30 Gy in 10 fractions. The relative high intrathoracic failure rate of 42% indicated that this dose might be insufficient to eliminate all the residual disease. In additional analysis from CREST study, for patients with complete intrathoracic response no benefit of TRT was observed. They concluded that TRT should be offered to patients with a good or partial response after chemotherapy, but not to those without residual disease in the thorax. It appears that the greater the volume of the residual disease in the thorax is, the higher dose is needed to eliminate the tumor.

TABLE 4. Univariate and multivariate analysis of overall survival for higher *vs.* lower dose of consolidation radiotherapy

	p	Univariate analysis HR (95% CI)	p	Multivariate analysis HR (95% CI)
Dose	**0.023**	**0.49 (0.27–0.90)**	**0.018**	**0.47 (0.25–0.87)**
45 Gy				
30-36 Gy				
Gender	0.17	1.4 (0.86–2.27)		
Male				
Female				
Age	0.38	1.25 (0.75–2.09)		
> 65				
< 65				
PS before RT	0.089	1.94 (0.90–4.18)		
2–3				
0–1				
Number of ChT cycles	0.065	1.78 (0.96–3.31)		
< 4				
> 4				
T stage	0.34	0.72 (0.37–1.40)		
T1–2				
T3–4				
N stage	0.28	1.32 (0.79–2.20)		
N0–2				
N3				
Metastases location				
Brain da/ne	0.52	1.2 (0.68–2.11)		
Liver da/ne	0.39	1.22 (0.76–1.92)		
Bone da/ne	0.46	1.24 (0.70–2.21)		
Adrenal gland da/ne	0.98	0.99 (0.59–1.67)		
Other	0.84	0.95 (0.58–1.56)		
Number of metastatic locations	0.43	0.82 (0.51–1.33)		
1				
> 2				
Timing of RT	0.71	1.13 (0.59–2.16)		
< 4 weeks after ChT				
> 4 weeks after ChT				
PCI	**0.04**	**0.56 (CI 0.32–0.97)**	**0.037**	**0.51 (0.27–0.95)**
Yes				
No				

ChT = chemotherapy; cRT = consolidation radiotherapy; N = lymph nodes; PS = performance status; RT = radiatiotherapy; T = tumour

TABLE 5. Trials of consolidation radiotherapy (cRT) in extended disease small cell lung cancer (ED-SCLC)

Author/Trial, reference	Publication year	Type of study	Patients -years enrolled	Number of patients	Patient selection	Thoracic irradiation dose scheme	mOS	1-year OS	2-year OS
Jeremic[18]	1999	P	1988–1993	109	ED-SCLC with CR at metastatic sites and at least PR in thorax	54 Gy in 36 fractions, BID	17 m vs. 11 m* P = 0.041	65% vs. 46% P ≤ 0.05	38% vs. 28% P ≤ 0.05
Slotman (CREST)[8]	2015	P	2009–2012	495	ED-SCLC with any response to ChT	30 Gy in 10 fractions	8 m vs. 8 m	33% vs. 28% P = 0.066	13% vs. 3% P = 0.004
Gore (RTOG 0937)[9]	2017	P	2010–2016	97	ED-SCLC (1-4 extracranial m., any response to ChT	40 Gy in 15 fractions	15.8 m vs. 13.8 m P = 0.21	50.8% vs. 60.1% P = 0.21	NR
Zhu[10]	2011	R	2003–2006	119	ED-SCLC	40–60 Gy	17 m vs. 9.3 m P = 0.014	NR	35% vs. 17%
Giuliani[12]	2011	R	2005–2009	19	ED-SCLC with minimal metastatic disease	36–45 Gy	14 m	58%	14%
Yee[11]	2012	R	2008–2009	32	ED-SCLC	40 Gy in 15 fractions	8.3 m	NR	NR
Zhan[13] (SEER database)	2018	R	2010–2012	6812	ED-SCLC from SEER database	Different, not reported	9 m vs. 7 m; P < 0.001 8 m vs. 6 m for polymetastases P < 0.05	NR	NR
Stanic	2020	R	2010–2014	187	ED-SCLC	30–45 Gy	11.1 m vs. 7.6 m P < 0.001	44% vs. 23% P = 0.0025	10% vs. 5% P = 0.19

* group 1 CR/PR and RT vs. group 2 CR/PR, no RT;

BID = twice daily; ChT = chemotherapy; CR = complete response; ED-SCLC = extended disease small cell lung cancer; m = months; mOS = median overall survival; NR-not reported; OS = overall survival; P = prospective; PR = partial response; R = retrospective

However, dose restrictions to the organs at risk and consequent toxicity limit the actual received dose.

Number of metastases was not predictive factor for survival in our analysis. Contrary to that, in recent retrospective publications it was shown that tumor burden of metastatic disease should be taken into account when treating ED SCLC patients, since those with ≥2 metastases had significantly worse outcome than those with only one metastasis.[23,24]

No difference of timing was found in our survival analysis if RT started before or after 4 weeks after ChT completion. In RTOG 0937 trial and one retrospective Chinese study also no difference was found in survival for patients who received RT early or late.[9,25] On the contrary, meta-analysis for limited SCLC, showed that earlier or shorter RT brings 7.7% advantage in 5-year survival.[26]

In our study PCI was independent predictor of better survival, although only 21.9% of patients received one. Our previous publication, focused on impact of PCI on survival in patients with LD-SCLC, also showed that only low number of patients (6%) actually received PCI in routine clinical setting, nevertheless OS was improved with PCI.[27] As our analysis is retrospective, this reflects real clinical situation. However, the reason why such a low number of patients actually received PCI is unclear. PCI as independent predictor of survival was reported also in retrospective study by Xu *et al*.[21] PCI in ED-SCLC was studied in EORTC conducted prospective study that showed reduced incidence of symptomatic brain metastases and improved 1-year OS (27% *vs.* 13.3%, HR 0.68, p = 0.003). That study, however, was highly criticized due to the insufficient imaging prior to PCI.[9] Japanese prospective study evaluated 224 patients with ED-SCLC who performed MRI prior to randomization to PCI or observation with MRI.[28] The study was terminated prematurely due to lower rate of brain metastases in PCI arm (40%) *vs.* MRI observation only (64%), but they found no significant difference in 1-year OS. None of our patients had MRI prior to PCI and only one third had CT evaluation, indicating that imaging in routine clinical practice should improve. In CREST study PCI dose was not uniform (20–30 Gy in 5–15 fractions) with unusual hypofractionated dose (20 Gy in 5 fraction) used in majority of patients (62%).[8] It was delivered concurrently with thoracic irradiation in 88% of patients, while other studies used sequential approach and uniform dose of 25 Gy in 10 fractions.[9,18] Difference in pre-PCI imaging and dose delivered as well as timing of PCI show diversified approach on this not fully researched area.[29]

Consolidation radiotherapy and immunotherapy

Immunotherapy (IT) has been successfully incorporated into the treatment of metastatic non-small cell lung cancer (NSCLC) either as combination of ChT and IT or as mono-IT and lately also in stage III as consolidation treatment after concomitant chemoradiotherapy.[30-39]

Recently, two randomized studies confirmed efficacy of IT also for the treatment in ED-SCLC. IMpower 133 study was the first to show improved OS in patients treated with atezolizumab combined with ChT (12.3 months) as compared to ChT plus placebo (10.3 months). 1-year OS rate was 51.7% in the atezolizumab group and 38.2% in the placebo group.[16] Consolidation RT was not permitted, while patients could have PCI. The same criteria about cRT and PCI were also applied in CASPIAN study with durvalumab.[17] Again, IT combination showed increased results, mOS in ChT-IT arm was 13 months and 10.3 months in ChT only arm and 1-year OS was 54% *vs.* 40%, respectively. Though PCI was allowed in the non IT group, only 8% of patients received it. If the inclusion of immunotherapy would prove to reduce the incidence of brain metastases in ES-SCLC considerably in future trials as suggested from present studies, then PCI and consequently neurotoxic sequels could be omitted in the future. The decision about skipping cRT might be more challenging. Survival data from current studies has not shown superior survival in first line treatment with ChT-IT in ED-SCLC compared to studies with ChT and cRT. Could cRT be combined with IT during the consolidation phase? First reported data indicate that the combination is tolerable, however trials are still ongoing and safety as well as survival results are expected in the future.[40] As previously reported, the use of thoracic RT may enhance the effect of IT by influencing the immune system and its interactions with cancer cells and tumors, recruiting anti-tumor immune cells, increasing the exposure of tumor antigens, and improving cross-presentation of these antigens to the adaptive immune system.[41-43]

Beside retrospective nature of our analysis we should acknowledge several other limitations of our research. The irradiation dose was not specified by the protocol or any other department regulation and the decision was under the discretion of treating physician. Larger tumors (T3-4, N3) were more frequently irradiated with lower dose, but this does not necessarily mean that larger tumors would not be feasible to the treatment with larger doses. Unfortunately, we were not able to retrieve reliable information about PS before RT in half of patients, reflecting real clinical practice. This would be valuable information as treatment decision in clinical practice is greatly influenced by PS and consequently might influence survival data. Due to the fact that not all patients were treated with ChT in our institution, PS before ChT could not be included in UVA and MVA. Also, the response to initial Cht as one of the main prognostic factors of cRT efficacy according to the published data, is missing, since not all the patients were treated at our institution. However, all the patients were discussed at the MTB before the treatment which at least partially reduces this shortcoming.

Conclusions

Our analysis has shown that cRT improved mOS as compared to ChT alone of the ED-SCLC patients treated at our institution. Consolidation RT, higher number of ChT cycles and profilactic cranial irradiation (PCI) were independent prognostic factors for better survival. For patients who received cRT, only higher doses and PCI had impact on survival regardless of number of ChT cycles received. Whether cRT and PCI will still be players in the era of immunotherapy is unknown and will be shown in further trials.

References

1. van Meerbeeck JP, Fennell DA, De Ruysscher DK. Small-cell lung cancer. *Lancet* 2011; **378:** 1741-55. doi: 10.1016/S0140-6736(11)60165-7
2. Cancer in Slovenia 2014. Ljubljana: Institute of Oncology Ljubljana, Epidemiology and Cancer Registry, Cancer Registry of Republic of Slovenia; 2017.
3. Mitchell MD, Aggarwal C, Tsou AY, Torigian DA, Treadwell JR. Imaging for the pretreatment staging of small cell lung cancer: a systematic review. *Acad Radiol* 2016; **23:** 1047-56. doi: 10.1016/j.acra.2016.03.017

4. Niho S, Fujii H, Murakami K, Nagase S, Yoh K, Goto K, et al. Detection of unsuspected distant metastases and/or regional nodes by FDG-PET [corrected] scan in apparent limited-disease small-cell lung cancer. *Lung Cancer* 2007; **57:** 328-33. doi.org/10.1016/j.lungcan.2007.04.001

5. Früh M, De Ruysscher D, Popat S, Crinò L, Peters S, Felip E, on behalf of the ESMO Guidelines Working Group. Small-cell lung cancer (SCLC): ESMO Clinical Practice Guidelines for diagnosis, treatment and follow-up. *Ann Oncol* 2013; **24(Suppl 6):** vi99-105. doi: 10.1093/annonc/mdt178

6. National Comprehensive Cancer Network. NCCN guidelines version 2.2020. Small cell lung cancer Nov 15 2019. [Cited 2020 Feb 15]. Available from: https://www.nccn.org/professionals/physician_gls/pdf/sclc.pdf

7. Slotman B, Faivre-Finn C, Kramer G, Rankin E, Snee M, Hatton M, et al. Prophylactic cranial irradiation in extensive small-cell lung cancer. *N Engl J Med* 2007; **357:** 664-72. doi: 10.1056/NEJMoa071780

8. Slotman BJ, van Tinteren H, Praag JO, Knegjens JL, El Sharouni SY5 Hatton M, et al. Use of thoracic radiotherapy for extensive stage small-cell lung cancer: a phase 3 randomised controlled trial. *Lancet* 2015; **385:** 36-42. doi: 10.1016/S0140-6736(14)61085-0

9. Gore EM, Hu C, Sun AY, Grimm DF, Ramalingam SS, Dunlap NE, et al. Randomized phase II study comparing prophylactic cranial irradiation alone to prophylactic cranial irradiation and consolidative extracranial irradiation for extensive-disease small cell lung cancer (ED SCLC): NRG Oncology RTOG 0937. *J Thorac Oncol* 2017; **12:** 1561-70. doi: 10.1016/j.jtho.2017.06.015

10. Zhu H, Zhou Z, Wang Y, Bi N, Feng Q, Li J, et al. Thoracic radiation therapy improves the overall survival of patients with extensive-stage small cell lung cancer with distant metastasis. *Cancer* 2011; **117:** 5423-31. doi: 10.1002/cncr.26206

11. Yee D, Butts C, Reiman A, Joy A, Smylie M, Fenton D, et al. Clinical trial of post-chemotherapy consolidation thoracic radiotherapy for extensive-stage small cell lung cancer. *Radiother Oncol* 2012; **102:** 234-8. doi: 10.1016/j.radonc.2011.08.042

12. Giuliani ME, Atallah S, Sun A, et al. Clinical outcomes of extensive stage small cell lung carcinoma patients treated with consolidative thoracic radiotherapy. *Clin Lung Cancer* 2011; **12:** 375-9. doi: 10.1016/j.cllc.2011.03.028

13. Zhang R, Li P, Li Q, Qiao Y, Xu T, Ruan P, et al. Radiotherapy improves the survival of patients with extensive-disease small-cell lung cancer: a propensity score matched analysis of surveillance, epidemiology, and end results database. *Cancer Manag Res* 2018; **10:** 6525-35. doi: 10.2147/CMAR.S174801

14. Jeremic B, Gomez-Caamano A, Dubinsky P, Cihoric N, Casas F, Filipovic N. Radiation therapy in extensive stage small cell lung cancer. *Front Oncol* 2017; **7:** 169. doi: 10.3389/fonc.2017.00169

15. Alvarado-Luna G, Morales-Espinosa D. Treatment for small cell lung cancer, where are we now?-a review. *Transl Lung Cancer Res* 2016; **5:** 26-38. doi: 10.3978/j.issn.2218-6751.2016.01.13.

16. Horn L, Mansfield AS, Szczęsna A, Havel L, Krzakowski M, Hochmair MJ, et al. First-line atezolizumab plus chemotherapy in extensive-stage small-cell lung cancer. *N Engl J Med* 2018; **379:** 2220-9. doi: 10.1056/NEJMoa1809064

17. Paz-Ares L, Dvorkin M, Chen Y, Reinmuth N, Hotta K, Trukhin D, et al. Durvalumab plus platinum–etoposide versus platinum-etoposide in first-line treatment of extensive-stage small-cell lung cancer (CASPIAN): a randomised, controlled, open-label, phase 3 trial. *Lancet* 2019; **394:** 1929-39. doi: 10.1016/S0140-6736(19)32222-6

18. Jeremic B, Shibamoto Y, Nikolic N, Milicic B, Milisavljevic S, Dagovic A, et al. Role of radiation therapy in the combined modality treatment of patients with extensive disease small-cell lung cancer: a randomized study. *J Clin Oncol* 1999; **17:** 2092-9. doi: 10.1200/JCO.1999.17.7.2092

19. Palma DA, Warner A, Louie AV, Senan S, Slotman B, Rodrigues GB. Thoracic radiotherapy for extensive stage small-cell lung cancer: a meta-analysis. *Clin Lung Cancer* 2016; **17:** 239-44. doi: 10.1016/j.cllc.2015.09.00

20. Rathod S, Jeremic B, Dubey A, Giuliani M, Bashir B, Chowdhury A, et al. Role of thoracic consolidation radiation in extensive stage small cell lung cancer: A systematic review and meta-analysis of randomised controlled trials. *Eur J Cancer* 2019; **110:** 110-9. doi: 10.1016/j.ejca.2019.01.003

21. Xu LM, Zhao LJ, Charles B , Simone CB 2nd, Cheng C, Kang M, et al. Receipt of thoracic radiation therapy and radiotherapy dose are correlated with outcomes in a retrospective study of three hundred and six patients with extensive stage small-cell lung cancer. *Radiother Oncol* 2017; **125:** 331-7. doi: 10.1016/j.radonc.2017.10.005

22. Hasan S, Renz P, Turrisi A, Colonias A, Finley G, Wegner RE. Dose escalation and associated predictors of survival with consolidative thoracic radiotherapy in extensive stage small cell lung cancer (SCLC): A National Cancer Database (NCDB) propensity-matched analysis. *Lung Cancer* 2018; **124:** 283-90. doi: 10.1016/j.lungcan.2018.08.016

23. Xu LM, Cheng C, Kang M, Luo J, Gong LL, Pang QS, et al. Thoracic radiotherapy (TRT) improved survival in both oligo- and polymetastatic extensive stage small cell lung cancer. *Sci Rep* 2017; **7:** 9255. doi: 10.1038/s41598-017-09775-0

24. Fukui T, Itabashi M, Ishihara M, Hiyoshi Y, Kasajima M, Igawa S, et al. Prognostic factors affecting the risk of thoracic progression in extensive-stage small cell lung cancer. *BMC Cancer* 2016; **16:** 197. doi:10.1186/s12885-016-2222-4

25. Luo J, Xu L, Zhao L, Cao Y, Pang Q, Wang J, et al. Timing of thoracic radiotherapy in the treatment of extensive-stage small-cell lung cancer: important or not? *Radiat Oncol* 2017; **12:** 42. doi: 10.1186/s13014-017-0779-y

26. De Ruysscher D, Lueza B, Le Péchoux C, Johnson DH, O'Brien M, Murray N, et al. Impact of thoracic radiotherapy timing in limited-stage small-cell lung cancer: usefulness of the individual patient data meta-analysis. *Ann Oncol* 2016; **27:** 1818-28. doi: 10.1093/annonc/mdw263

27. Stanic K, Kovac V. Prophylactic cranial irradiation in patients with small-cell lung cancer: the experience at the Institute of Oncology Ljubljana. *Radiol Oncol* 2010; **44:** 180-6. doi: 10.2478/v10019-010-0038-4

28. Takahashi T, Yamanaka T, Seto T, Harada H, Nokihara H, Saka H, et al. Prophylactic cranial irradiation versus observation in patients with extensive-disease small-cell lung cancer: a multicentre, randomised, open-label, phase 3 trial. *Lancet Oncol* 2017; **18:** 663-71. doi: 10.1016/S1470-2045(17)30230-9

29. Rusthoven CG, Kavanagh BD. Prophylactic cranial irradiation (PCI) versus active MRI surveillance for small cell lung cancer: the case for equipoise. *J Thorac Oncol* 2017; **12:** 1746-54. doi: 10.1016/j.jtho.2017.08.016

30. Hui R, Gandhi L, Costa EC, Felip E, Ahn MJ, Eder JP, et al. Long-term OS for patients with advanced NSCLC enrolled in the KEYNOTE-001 study of pembrolizumab (pembro). *J Clin Oncol* 2016; **34:** Abstr nr 9026.

31. Garon EB, Rizvi NA, Hui R, Leighl N, Balmanoukian AS, Eder JP, et al. Pembrolizumab for the treatment of non-small-cell lung cancer. *N Engl J Med* 2015; **372:** 2018-28. doi: 10.1056/NEJMoa1501824

32. Herbst RS, Baas P, Kim DW, Felip E, Pérez-Gracia JL, Han JY, et al. Pembrolizumab versus docetaxel for previously treated, PD-L1-positive, advanced non-small-cell lung cancer (KEYNOTE-010): a randomised controlled trial. *Lancet* 2016; **387:** 1540-50. doi: 10.1016/S0140-6736(15)01281-7

33. Reck M, Rodríguez-Abreu D, Robinson AG, Hui R, Csőszi T, Fülöp A, et al. Pembrolizumab versus chemotherapy for PD-L1-positive non-small-cell lung cancer. *N Engl J Med* 2016; **375:** 1823-33. doi: 10.1056/NEJMoa1606774

34. Langer CJ, Gadgeel SM, Borghaei H, Papadimitrakopoulou VA, Patnaik A, Powell SF, et al. Carboplatin and pemetrexed with or without pembrolizumab for advanced, non-squamous non-small-cell lung cancer: a randomised, phase 2 cohort of the open-label KEYNOTE-021 study. *Lancet Oncol* 2016; **17:** 1497-508. doi: 10.1016/S1470-2045(16)30498-3

35. Brahmer J, Reckamp KL, Baas P, Crinò L, Eberhardt WE, Poddubskaya E, et al. Nivolumab versus docetaxel in advanced squamous-cell non-small-cell lung cancer. *N Engl J Med* 2015; **373:** 123-35. doi: 10.1056/NEJMoa1504627

36. Borghaei H, Paz-Ares L, Horn L, Spigel DR, Steins M, Ready NE, et al. Nivolumab versus docetaxel in advanced nonsquamous non-small-cell lung cancer. *N Engl J Med* 2015; **373:** 1627-39. doi: 10.1056/NEJMoa1507643

37. Fehrenbacher L, Spira A, Ballinger M, Kowanetz M, Vansteenkiste J, Mazieres J, et al. Atezolizumab versus docetaxel for patients with previously treated non-small-cell lung cancer (POPLAR): a multicentre, open-label, phase 2 randomised controlled trial. *Lancet* 2016; **387:** 1837-46. doi: 10.1016/S0140-6736(16)00587-0

38. Antonia SJ, Villegas A, Daniel D, Vicente D, Murakami S, Hui R, et al. Overall survival with durvalumab after chemoradiotherapy in stage III NSCLC. *N Engl J Med* 2018; **379:** 2342-50. doi: 10.1056/NEJMoa1809697

39. Antonia SJ, Villegas A, Daniel D, Vicente D, Murakami S, Hui R, et al. Durvalumab after chemoradiotherapy in stage III non–small-cell lung cancer. *N Engl J Med* 2017; **377:** 1919-29. doi: 10.1056/NEJMoa1709937

40. Verma V, Cushman TR, Selek U, Tang C, Welsh JW. Safety of Combined Immunotherapy and Thoracic Radiation Therapy: Analysis of 3 Single-Institutional Phase I/II Trials. *Int J Radiat Oncol Biol Phys* 2018; **101:** 1141-8. doi: 10.1016/j.ijrobp.2018.04.054

41. Demaria S, Golden EB, Formenti SC. Role of local radiation therapy in cancer immunotherapy. *JAMA Oncol* 2015; **1:** 1325-32. doi: 10.1001/jamaoncol.2015.2756

42. Vrankar M, Stanic K. Long-term survival of locally advanced stage III non-small cell lung cancer patients treated with chemoradiotherapy and perspectives for the treatment with immunotherapy. *Radiol Oncol* 2018; **52:** 281-8. doi: 10.2478/raon-2018-0009

43. Sharabi AB, Lim M, DeWeese TL, Drake CG. Radiation and checkpoint blockade immunotherapy: radiosensitisation and potential mechanisms of synergy. *Lancet Oncol* 2015; **16:** e498-509. doi: 10.1016/S1470-2045(15)00007-8

research article

Assessment of set-up errors in the radiotherapy of patients with head and neck cancer: standard vs. individual head support

Sabina Androjna[1], Valerija Zager Marcius[1,2], Primoz Peterlin[1], Primoz Strojan[1,3]

[1] Department of Radiotherapy, Institute of Oncology Ljubljana, Ljubljana, Slovenia
[2] Faculty of Health Sciences, University of Ljubljana, Ljubljana, Slovenia
[3] Faculty of Medicine, University of Ljubljana, Ljubljana, Slovenia

Radiol Oncol 2020; 54(3): 364-370.

Received 17 February 2020
Accepted 3 May 2020

Correspondence to: Prof. Primož Strojan, M.D., Ph.D., Institute of Oncology Ljubljana, Zaloška 2, SI-1000 Ljubljana, Slovenia.
E-mail: pstrojan@onko-i.si

Disclosure: No potential conflicts of interest were disclosed.

Background. The aim of the study was to (a) compare the accuracy of two different immobilization strategies for patients with head and neck tumors, and (b) compare the set-up errors on treatment units with different portal imaging systems.

Patients and methods. Variations in the position of the isocenter (IC) relative to the reference point determined on the computed tomography simulator were measured in a vertical (anterior-posterior), longitudinal (superior-inferior), and lateral (medial-lateral) direction in 120 head and neck cancer patients irradiated with curative intent. Depending on the treatment unit (unit A - 2D/2D image previews; unit B - 2D image previews) and the time of irradiation, patients were divided into 6 groups of 20 patients. In patients irradiated in 2014, standard head supports were used (groups 1 and 2), whereas in those treated in 2015 and 2017 (groups 3–6) individual head supports were employed. The clinical-to-planning target volume safety margin was calculated according to the formula proposed by Van Herk.

Results. In total, 2,454 portal images and 3,681 set-up errors were analysed. Implementation of individual head supports in 2015 resulted in a statistically significant reduction in the average inter-fraction displacement in the vertical direction and in decreased number of IC displacements in the vertical and longitudinal direction (applies to both treatment units). The largest reduction of the safety margin was calculated in the longitudinal direction and the safety margins were larger for unit B than for unit A.

Conclusions. The use of individual head supports and a more advanced imaging system were found to increase set-up precision.

Key words: head and neck radiotherapy; immobilization; head support; set-up errors

Introduction

The basic tools for the immobilization of patients with head and neck (HN) tumors during radiotherapy are thermoplastic masks with a 5-point pinning system and supporting system for the head. These immobilization aids largely, but not completely, prevent major shifts during irradiation. Due to its regular use, the head support can shrink and deform over time, which leads to deviations in the position of the HN compared to the reference position determined on the computed tomography (CT) simulator (Figure 1). To overcome this problem, patient-specific head supports were introduced (*i.e.*, customized head support that are moulded to the patient's anatomy), which proved to effectively reduce systematic and random errors.[1-4]

At the Institute of Oncology Ljubljana, the majority of HN cancer patients are irradiated on two similar treatment units with slightly different imaging capabilities. Commercially available head supports have been used since the 1990s (CIVCO, Coralville, Iowa, USA), whereas patient-specific head supports have never been introduced in routine practice. Until 2015, all patients irradiated on a particular treatment unit shared the same set of head supports (*i.e.*, standard head support). In order to reduce the set-up error, this policy was changed in 2015 and it was ensured that the same head support was used for a given patient from the CT simulator throughout the irradiation course (*i.e.*, individual head support). Regular quality checks of head supports were performed: the difference between the heights of used and unused supports was not allowed to exceed 3 mm.

In the present study, two hypotheses were tested: (1) Deviations recorded by portal imaging system will be smaller in patients using individual head supports compared to those with standard ones; (2) The treatment unit with a more advanced portal imaging system will allow for a more accurate positioning of patients.

Patients and methods

Between January 2014 and October 2017, 120 HN cancer patients irradiated with curative intent were included in this retrospective non-interventional study. Patients were irradiated on either of the two low-energy linear accelerators equipped with MV imaging systems: unit A - Unique Performance Edition; and unit B - Clinac DBX (both: Varian Medical Systems, Palo Alto, California, USA). Depending on the treatment unit (A or B), the time of irradiation, and the type of head support used, patients were divided into 6 groups of 20 patients. Because individual head supports were introduced into routine practice in 2015, the consistency of results related to their use over time was verified in two time periods (2015 and 2017) and, consequently, in two independent groups of patients:

- Group 1 – linear accelerator A, 2014 (standard head support)
- Group 2 – linear accelerator B, 2014 (standard head support)
- Group 3 – linear accelerator A, 2015 (individual head support)
- Group 4 – linear accelerator B, 2015 (individual head support)
- Group 5 – linear accelerator A, 2017 (individual head support)
- Group 6 – linear accelerator B, 2017 (individual head support)

Variations in the position of the isocenter (IC) relative to the reference point determined on the CT simulator (*i.e.*, set-up errors) were measured in a vertical (anterior-posterior), longitudinal (superior-inferior), and lateral (medial-lateral) direction.

Simulation procedure

At the CT simulator, the most appropriate head support was selected from the commercially available set of items of various heights and contours, offering a comprehensive range of neck angulations (CIVCO, Coralville, Iowa, USA), according to the curvature of patient's neck and occiput. The Kneefix™ and the Armaflex™ cushion were placed under the knees and the back and pelvis, respectively, and the head was additionally fixed with a thermoplastic 5-point Posicast® mask (all: CIVCO, Coralville, Iowa, USA). Radio-opaque markers (Beekley Medical, Bristol, Connecticut, USA) were used for three-point marking of the IC origin. CT scanning from 2 cm above the top of the head to the tracheal bifurcation (slice thickness: 2 mm) was accomplished using an intravenous administration of iodine contrast medium by power injector, followed by tattooing the thoracic skin for the central alignment of the patient.

Geometric verification

Patients on the treatment units were pre-positioned into the IC, based on the room lasers before the set up imaging. Portal images were taken according to the Extended No Action Level (eNAL) protocol.[5] The PortalVision computer program with

FIGURE 1. The example of shrinkage (right) of the head support.

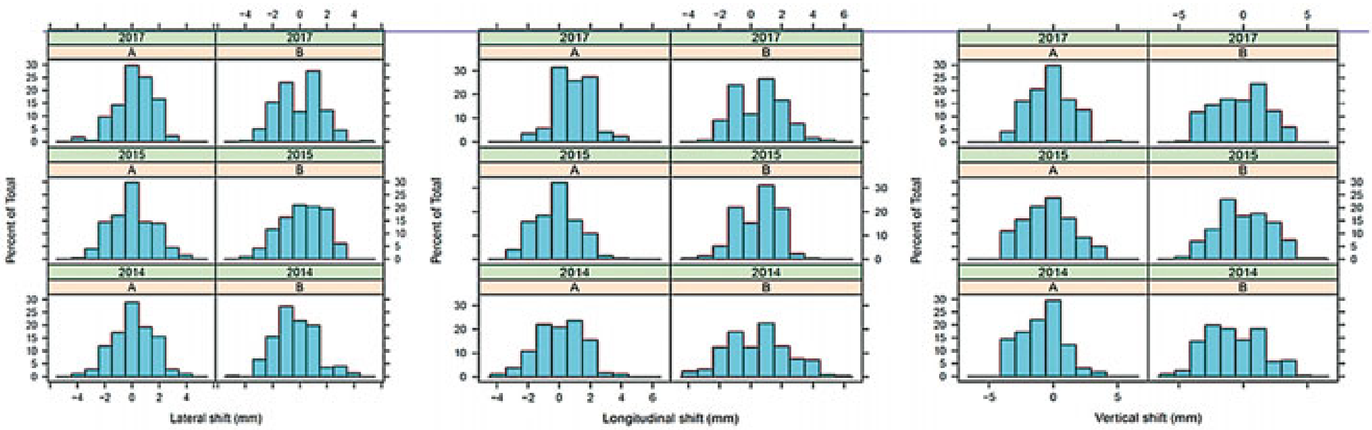

FIGURE 2. Inter-fraction displacements by axis and period.

the AutoMatching registration procedure (Varian Medical Systems, Palo Alto, California, USA) was used to calculate the size and direction of the displacement. Electronic portal images acquired with gantry at 0° (anteroposterior projection) and 90° (or 270°, lateral projection) were compared with digitally reconstructed radiographs (DRRs). Portal images were obtained using the Varian's EPID PortalVision using an amorphous silicon plane detector aS1000 (resolution of 1024 × 768 pixels, unit A) or aS500 (resolution 512 × 384 pixels, unit B). Whereas unit A allows simultaneous patient position alignment in all three directions using 2D/2D image matching, unit B requires the radiographers to combine the position corrections obtained from two separate orthogonal 2D image matchings.

Statistical analysis

The study protocol was approved by the Protocol Review Board of the Institute of Oncology Ljubljana on April 4, 2017.

Testing set-up error distributions for normality was done using the Shapiro-Wilk test. As Shapiro-Wilk test did not support the normality hypothesis in any of the distribution, non-parametric Mann-Whitney U-test (two-sample rank-sum test) was employed for comparing median values in distributions instead of two-sided Student's t-test. For the same reason, non-parametric modified Levene's test (using median instead of mean) was used to test the equality of variances in set-up error distributions. Statistical calculations were performed using the GNU R statistical program.[7] The sample size of 350 measurements per time period was calculated with the G*Power software, considering a = 0.05, b = 0.8 and the effect size of 0.267, which was calculated on the basis of averages and standard deviations of similar studies.[1,2,6,8] For comparison with published studies, the clinical target volume (CTV) – planning target volume (PTV) safety margin was calculated according to the formula proposed by Van Herk.[9] The differences at $p < 0.05$ were considered statistically significant.

Results

In total, 2454 portal images and 3681 set-up errors were analysed: 828, 832, and 794 portal images obtained in 2014, 2015, and 2017, respectively. We first analysed the data sets for the presence of large set-up errors. The proportion of displacements smaller than 3 mm and smaller than 5 mm were 85% and 99.1%, respectively in the 2014 set, when standard head supports were employed. The introduction of individual head supports in 2015 increased these figures to 89% and 99.6%, respectively, and in a most recent data set from 2017 they were further increased to 90% and 99.6%, respectively.

Inter-fraction set-up errors registered in units A and B at different periods are shown in Table 1 and Figure 2. The difference in distribution of inter-fraction displacements were tested using Mann-Whitney U-test. In four cases, the test showed that the distribution obtained in one year differ significantly ($p < 0.05$) from those obtained in the other two years. For unit A, set-up error distributions in the vertical direction obtained in 2014 and in the longitudinal direction obtained in 2017 differ from the other two years. For unit B, set-up error distributions in the vertical direction in the year 2014 and in the lateral direction in the year 2014 differ from the other two years. Comparing the vertical shift distribution for the unit A in the years 2014 and 2015 shows significant difference (Mann-Whitney U =

TABLE 1. Inter-fraction displacements recorded on units A and B at different periods

	2014 Standard head support			2015 Individual support			2017 Individual support		
	VRT	LNG	LAT	VRT	LNG	LAT	VRT	LNG	LAT
UNIT A									
Average displacement – M [mm]	- 0.86	0.05	0.05	- 0.47*	- 0.24*	- 0.05	- 0.16*	0.88	0.18
Systematic error – Σ [mm]	0.66	1.04	0.88	0.91	0.79	0.95	0.82	0.59	0.83
Random error – σ [mm]	1.49	1.21	1.37	1.56	1.28	1.38	1.28	1.14	1.2
UNIT B									
Average displacement – M [mm]	- 0.60	0.46	- 0.43	- 0.02*	0.51	0.25	- 0.18*	0.46	- 0.02
Systematic error – Σ [mm]	1.09	0.80	0.82	0.92	0.74	0.94	0.93	0.69	0.88
Random error – σ [mm]	1.77	1.83	1.47	1.77	1.22	1.41	1.71	1.56	1.44

LAT = lateral (medial-lateral); LNG = longitudinal (superior-inferior); VRT = vertical (anterior-posterior)

*p < 0.05 (2014 vs. 2015 or 2014 vs. 2017)

16293, n1 = 187, n2 = 201, p = 0.02, Hodges-Lehmann estimator (HLΔ) = -0.000012, 95% confidence interval (CI) is (-0.999974, -0.000010)). The difference in distributions is even more pronounced between the sets for the year 2014 and 2017 (U = 12918.5, n1 = 187, n2 = 175, p < 0.001, HLΔ = -0.999982, 95% CI (-0.999989, -0.000059). Comparing the distributions for the years 2015 and 2017 did not show a significant difference. Comparing the longitudinal shift distributions for the unit A also doesn't show a significant difference; however, comparing the distributions for the years 2014 and 2017 does show a significant difference (U = 11230, n1 = 187, n2 = 175, p < 0.001, HLΔ = -0.999982, 95% CI (-1.000066, -0.999956)), and so does the comparison for the years 2015 and 2017 (U = 10171.5, n1 = 201, n2 = 175, p < 0.001, HLΔ = -1.000006, 95% CI (-1.000032, -0.999955)). Neither comparison for the lateral shifts for the unit A showed significance. Comparing the vertical shift distributions for the unit B also shows significant difference between the sets for the years 2014 and 2015 (U = 19637.5, n1 = 227, n2 = 215, p < 0.001, HLΔ = -0.999931, 95% CI (-1.000049, -0.000042)), as well as between the sets for the years 2014 and 2017 (U = 21674, n1 = 227, n2 = 222, p < 0.01, HLΔ = -0.000046, 95% CI (-0.999990, -0.000025)), while the difference between data sets for the years 2015 and 2017 is not significant. In unit B, none of the differences in the longitudinal shift distribution is considered significant. Comparing the lateral shift distributions shows significance between the data sets for the years 2014 and 2015 (U = 18998, n1 = 227, n2 = 215, p < 0.01, HLΔ = -0.999942, 95% CI (-0.999980, -0.000042)) and for the years 2014 and 2017 (U = 22030, n1 = 227, n2 = 222, p < 0.02, HLΔ = -0.000058, 95% CI (-0.999953, -0.000040)), while the distributions of lateral shifts between 2015 and 2017 is not considered significant. Comparing the variances of the distributions (which correspond to the systematic error Σ and the random error σ combined) only shows significant differences in five cases: in unit A the vertical shift distributions for the years 2015 and 2017 differ significantly (Levene's F = 6.3082, DF = 386, p < 0.02), as well as longitudinal

TABLE 2. Number of IC displacements and of gross errors at treatment units in relation to time for both units. In the brackets, the most prevalent direction of applied movements is indicated

	Isocenter movements			Gross errors
	VRT	LNG	LAT	
	Unit A / unit B (direction)	Unit A / unit B (direction)	Unit A / unit B (direction)	
2014 – standard head support	11 / 15 (P)	5 / 15 (I)	4 / 5 (L)	2 / 5
2015 – individual head support	12 / 13 (P)	3 / 6 (I)	9 / 8 (R)	0 / 1
2017 – individual head support	5 / 14 (P)	7 / 10 (I)	6 / 7 (L)	0 / 1

I = inferior; L = left; LAT = lateral (medial-lateral); LNG = longitudinal (superior-inferior); P = posterior; R = right; VRT = vertical (anterior-posterior)

TABLE 3. Clinical target volume - planning target volume (CTV-PTV) safety margins for units A and B at different periods (calculated according to van Herk[8])

	CTV-PTV safety margin [mm]		
	VRT	LNG	LAT
UNIT A			
2014 – standard head support	2.7	3.4	3.2
2015 – individual head support	3.4	2.9	3.3
2017 – individual head support	2.9	2.3	2.9
UNIT B			
2014 – standard head support	4.0	3.3	3.1
2015 – individual head support	3.5	2.7	3.3
2017 – individual head support	3.5	2.8	3.2

LAT = lateral (medial-lateral); LNG = longitudinal (superior-inferior); VRT = vertical (anterior-posterior)

shift distributions for the years 2014 and 2017 ($F = 9.2817$, $DF = 360$, $p < 0.01$). In unit B, all three comparisons of longitudinal shift distributions show significant difference: between the sets for 2014 and 2015 ($F = 24.5077$, $DF = 440$, $p < 0.001$), between the sets for 2014 and 2017 ($F = 9.1372$, $DF = 447$, $p < 0.01$), and between the sets for 2015 and 2017 ($F = 4.5802$, $DF = 435$, $p = 0.03$). In Table 2, the number of IC displacements for both units together at different periods are presented, as well as the number of recorded gross errors (> 5 mm). Most of the IC shifts were made in the posterior, inferior and in the left direction. With the implementation of individual head supports, their number decreased, except for the lateral direction, and the number of gross errors was also reduced.

The CTV-PTV safety margins calculated from the population set-up errors for units A and B at different periods are shown in Table 3. In unit A, the largest reduction of the safety margin after implementation of individual head supports was calculated in the longitudinal direction (2014 *vs.* 2015, by 0.6; and 2014 *vs.* 2015, 1.2 mm), whereas in the lateral direction, the margin did not change substantially. On the contrary, in the vertical direction the margin increased by 0.7 mm (2014 *vs.* 2015) and by 0.2 mm (2014 *vs.* 2017). In unit B, a general trend toward a reduction in the safety margins resulted from the employment of individual head supports. In addition, the average reduction of the safety margins was also larger in unit B. The most significant reductions (2014 *vs.* 2015 and 2017) were observed in the vertical (by 0.4 and 0.5 mm) and longitudinal directions (by 0.6 and 0.5 mm). In the lateral direction, the size of the safety margin did not increase substantially (by 0.3 and 0.1 mm).

Discussion

In the present study, individual head supports were found to significantly reduce inter-fraction displacements in the vertical direction, specifically in the posterior direction, compared to the standard head supports. Reduction of average displacement in vertical direction recorded between 2014 and 2017 on units A and B was 0.70 mm and 0.42 mm, respectively. This observation pointed to the shrinkage of material, *i.e.* polyurethane foam, as a possible reason for the observed displacements due to the prolonged and frequent use of head supports.

Comparing the three periods, the systematic error did not change significantly for either unit. In the vertical direction, the systematic error recorded on unit A increased by an average of 0.15 mm, while on unit B it decreased by approximately the same extent. A negligible increase over the time was observed in the lateral direction, on average by less than 0.1 mm. It seems that the use of head supports and the shrinkage of the material they are made of influenced mainly the rotational set-up errors of the head in the sagittal plane, rather than the head displacements to the left or to the right.[1] In the longitudinal direction, the systematic error was reduced over time on both treatment units. Similarly, by abolishing the standard head supports, a statistically non-significant decrease in the size of the random error was recorded on unit A in all three directions. On unit B, the random error remained practically unchanged in two directions; in the longitudinal direction, its change was negligible.

Our observations are in line with those of other authors. A reduction of systematic and random errors in all directions was calculated by Van Lin *et al.*[1] when customized and the standard head supports were compared. A decrease was most notable in the longitudinal direction and least marked in the lateral direction, which is the pattern comparable to that found in our study. McKernan *et al.* showed a reduction in setup error by on average 1.3 mm with the use of customized head supports instead of standard ones.[4] Similarly, Houweling *et al.* reported that the use of customized head supports reduced systematic errors by at least 20% and random errors by at least 25%.[2] They indicated a decrease in inter-fraction set-up errors by 40%;

most statistically significant displacements were recorded in the lateral direction. However, in this particular direction we recorded the smallest set-up errors. The observed discrepancy could be due to sample characteristics: this was significantly smaller (n = 22) in the study of Houweling *et al.* than in our study (n = 120). Thus, their results are less likely to adequately represent the characteristics of the population. To the contrary, in the study of Howlin *et al.*, the difference in set-up errors between patients with customized and standard head supports was not significant in any direction.[6]

Furthermore, our calculations of the estimated margins from CTV to PTV were also comparable to those reported in the literature. Humphreys *et al.* used a customized immobilization system: the estimated margins in lateral, longitudinal and vertical directions were 2.9, 2.6 and 3.3 mm, respectively.[3] The authors used the same formula as we did.[9] Similarly, Van Lin *et al.* suggested that with a customized head support and appropriate correction protocol, suitable CTV-PTV margins would be 3 mm in the vertical and longitudinal directions and 4 mm in the lateral direction.[1] However, we observed that the CTV-PTV safety margins were larger for unit B than for unit A, which confirms our second hypothesis that the treatment unit with a more advanced portal imaging system allows for more accurate positioning of patients.

Humphreys *et al.*[3] reported 94% of displacements smaller than 3 mm and 99% smaller than 5 mm, which is comparable to the results of this study. In addition, individual head supports reduced the number of IC set-up errors in our patients, particularly in the vertical direction, and also of gross errors by 66%; all but two of the latter were recorded in the posterior direction. In unit A, which was equipped with a more advanced portal imaging system, fewer IC displacements and fewer gross errors were documented than in unit B.

In addition, there were some differences across the study groups recorded in the size of inter-fraction displacements (unit A: longitudinal displacement, 2014 *vs.* 2017), number of IC displacements (unit A: longitudinal axis, 2014 *vs.* 2015 *vs.* 2017), and in the size of CTV-PTV margin (unit A: vertical axis, 2014 *vs.* 2015 *vs.* 2017), which are not in line with the expected greater accuracy when using individual head rests. However, these differences are small and, as such, seem to be of questionable importance for day-to-day clinical work. We are aware that there may be more causes for registered set-up errors that may also influence the calculation of the CTV-PTV margin; imprecision in daily set-up and patient movements when lying on the table of treatment unit are just two of the potential sources.[10] As measurements within each of the six study groups were made within a relatively short time (*i.e.* 10–12 weeks) and with constant RTT teams, it can be argued that the results of the group measurements were consistent. Of course, over the 2015–2017 period, there were changes in the composition of RTT teams, which could affect our calculations. Other causative factors for set-up errors would be different technical errors (inaccuracies in the in-room laser calibration or of the imaging IC, procedure of the matching process and its quality) or those originated from the thermoplastic mask itself, changes in the patient anatomy (due to weight loss or volume reduction/swelling of the tumor or specific organs-at-risk), or different physiological processes (swallowing respiration). However, we were able to account for these factors only in the context of a regular quality assurance program; their detailed analysis is beyond the scope of this study. The impact of eventual changes in the departmental protocol used to position patients on irradiation units is negligible, since no significant protocol changes occurred during the study period.

Conclusions

When compared to standard head supports, the introduction of individual head supports reduced inter-fraction set-up errors in the vertical direction and the number of gross errors; in some directions, also the number of IC displacements and the size of the CTV-PTV safety margin were reduced. A more advanced imaging system with a better spatial resolution contributed to a reduction in the systematic and random errors.

Acknowledgement

This work was financially supported by the Slovenian Research Agency (program no. P3-0307).

References

1. Van Lin EN, van der Vight L, Huizenga H, Kaanders JHAM, Visser AG. Set-up improvement in head and neck radiotherapy using a 3D off-line EPID-based correctioon protocol and a customised head and neck support. *Radiother Oncol* 2003; **68:** 137-48. doi: 10.1016/S0167-8140(03)00134-8

2. Houweling AC, van der Meer S, van der Wal E, Terhaard CHJ, Raaijmakers CPJ. Improved immobilization using an individual head support in head-and-neck cancer patients. *Radiother Oncol* 2010; **96:** 100-3. doi: 10.1016/j.radonc.2010.04.014

3. Humphreys M, Guerrero Urbano MT, Mubata C, Miles E, Harrington KJ, Bidmead M, et al. Assessment of a customised immobilisation system for head and neck IMRT using electronic portal imaging. *Radiother Oncol* 2005; **77:** 39-44. doi: 10.1016/j.radonc.2005.06.039

4. McKernan B, Bydder S, Ebert M, Waterhouse D, Joseph D. A simple and inexpensive method to routinely produce customized neck supports for patient immobilization during radiotherapy. *J Med Imaging Radiat Oncol* 2008; **52:** 611-6. doi: 10.1111/j.1440-1673.2008.02024

5. De Boer HC, Heijmen BJ. eNAL: an extenstion of the NAL setup correction protocol for effective use of weekly follow-up measurements. *Int J Radiat Oncol Biol Phys* 2007; **67:** 1586-95. doi: 10.1016/j.ijrobp.2006.11.050

6. Howlin C, O'Shea E, Dunne M, Mullaney L, McGarry M, Clayton-Lea A, et al. A randomized controlled trial comparing customized versus standard headrests for head and neck radiotherapy immobilization in terms of set-up errors, patient comfort and staff satisfaction. *Radiography* 2015; **21:** 74-83. doi: 10.1016/j.radi.2014.07.009

7. R Core Team. *R: a language and environment for statistical computing.* Vienna: R Foundation for Statistical Computing; 2018.

8. Faul F, Erdfelder E, Lang AG, Buchner A. G*Power 3: a flexible statistical power analysis program for the social, behavioral, and biomedical sciences. *Behav Res Methods* 2007; **39:** 175-91. doi: 10.3758/bf03193146

9. Van Herk M. Errors and margins in radiotherapy. *Semin Radiat Oncol* 2004; **14:** 52-64. doi: 10.1053/j.semradonc.2003.10.003

10. International Atomic Energy Agency. Introduction of image guided radiotherapy into clinical practice. In: *IAEA Human Health Reports No. 16.* Vienna: International Atomic Energy Agency; 2019.

Radiol Oncol 2020; 54(3): 253-262.
doi: 10.2478/raon-2020-0035

Transarterijska embolizacija zunanje karotidne arterije pri zdravljenju življenje ogrožajoče krvavitve, nastale zaradi maksilofacialne poškodbe

Langel Č, Lovrič D, Zabret U, Mirković T, Gradišek P, Mrvar-Brečko A, Šurlan Popovič K

Izhodišča. Huda krvavitev zaradi maksilofacialne poškodbe je redka, a življenje ogrožajoča. Bolnike, pri katerih osnovne metode zdravljenja ne zadoščajo za zaustavitev krvavitve, lahko zdravimo s transarterijsko embolizacijo zunanje karotidne arterije ali njenih vej. Objavljeni tovrstni primeri niso pogosti, kar je presenetljivo glede na razmeroma visoko incidenco maksilofacialnih poškodb. Zato domnevamo, da o transarterijski embolizaciji bodisi premalo poročamo, bodisi jo premalo uporabljamo ali oboje. Ob tem je zelo malo strokovnih objav o uporabi novih neadhezivnih tekočih embolizacijskih sredstev za transarterijsko embolizacijo v področju zunanje karotidne arterije.

Bolniki in metode. S pomočjo pregleda zbirke PubMed smo zbrali objave o transarterijski embolizaciji v področju zunanje karotidne arterije v okviru tope (tj. nepenetrantne) maksilofacialne poškodbe. Zabeležili smo mesto poškodbe v povirju zunanje karotidne arterije, mesto embolizacije, izbrano embolizacijsko sredstvo in učinkovitost ter varnost postopka transarterijske embolizacije. Naredili smo tudi pregled napovednih dejavnikov preživetja. Na koncu smo dodali prikaz primera iz slovenske terciarne ustanove, pri katerem smo za transarterijsko embolizacijo v področjih obeh karotidnih arterij uporabili novo embolizacijsko sredstvo obarjajočo hidrofobno tekočino za injiciranje PHIL (ang. *precipitating hydrophobic injectable liquid*).

Zaključki. Pregled 205 primerov je pokazal, da je transarterijska embolizacija učinkovita v 79,4–100 %; pomembni zapleti so se pojavljali v 2–4%. Napovedni dejavniki, statistično značilno povezani z višjo stopnjo preživetja, so bili: uspešna zaustavitev krvavitve, vrednost ≥ 8 po Glasgowski lestvici kome, vrednost ≤ 32 po točkovalniku resnosti poškodbe ISS (ang. *injury severity score*) ter indeks šoka ≤ 1,1 pred transarterijsko embolizacijo in ≤ 0,8 po njej. PHIL dopušča hitro in hkrati filigransko vbrizganje, kar omogoča pomemben prihranek časa v življenje ogrožajočih okoliščinah in zmanjšuje verjetnost nenamernega injiciranja v potencialno nevarne anastomoze med zunanjo in notranjo karotidno arterijo.

Radiol Oncol 2020; 54(3): 263-271.
doi: 10.2478/raon-2020-0045

Zdravljenje intrahepatičnega holangiokarcinoma. Od resekcije do paliativnega zdravljenja

Bartolini I, Risaliti M, Fortuna L, Agostini C, Novella Ringressi M, Taddei A, Muiesan P

Izhodišča. Intrahepatični holangiokarcinom je za hepatocelularnim karcinomom drugi najpogostejši primarni rak jeter. Intrahepatični holangiokarcinom predstavlja 20 % rakov od vseh holangiokarcinomov. Njegova incidence in tudi mortaliteta narašča. Kirurška resekcija je edina kurativna metoda zdravljena kljub visoki stopnji ponovitve bolezni, ki je do 80 %. Ponovitve te bolezni v intrahepatičnem prostoru je možno še enkrat operirati s kurativnim namenom, vendar v majhnem odstotku bolnikov. Žal je diagnoza pri večini bolnikov pozna zaradi pomanjkanja specifičnih simptomov in operacija ni možna. Indikacije za transplantacijo jeter pa so še vedno kontroverzne. V zadnjem času je več poročil o izboljšanju uspeha zdravljenja z neodjuvantnim zdravljenjem s kemoterapijo, vendar v zelo selektivnih primerih. Zato mora transplantacija jeter ostati kot možnost zdravljenja predvsem v kliničnih študijah. V paliativnih primerih, ko kirurški poseg ni mogoč, lahko uporabimo kemoterapijo, radioterapijo in loko-regionalne ablativne tehnike, kot so radiofrekvenčna ablacija in trans-arterijska kemoembolizacija ali radioembolizacija.

Zaključki. Pričujoči pregled je osredotočen na kirurško zdravljenje intrahepatičnega holangiokarcinoma. Pomembni so potencialni napovedni dejavniki, ki lahko pomagajo pri izbiri primernega zdravljenja.

Radiol Oncol 2020; 54(3): 272-277.
doi: 10.2478/raon-2020-0031

Konsenzusni molekularni podtipi (CMS) v personalizirani medicini metastatskega raka debelega črevesa in danke

Reberšek M

Izhodišča. Rak debelega črevesa in danke je eden najpogostejših rakov na svetu. Metastatski rak debelega črevesa in danke je še vedno neozdravljiva bolezen pri večini bolnikov. Preživetje bolnikov se je izboljšalo, ko smo jih pričeli zdraviti z novo sistemsko kemoterapijo v kombinaciji s tarčno terapijo. Pri nekaterih bolnikih lahko s kombiniranim zdravljenjem s sistemsko terapijo in kirurgijo dosežemo zazdravitve ali celo ozdravitve. Novo znanje o kompleksni heterogenosti raka debelega črevesa in danke z vidika genetike, epigenetike, transkriptomije in mikrookolja, kot tudi z vidika napovednih in kliničnih značilnosti je privedlo do razvrstitve raka debelega črevesa in danke v različne molekularne podtipe. Imenujemo jih konsenzusni molekularni podtipi (CMS). Klasifikacija CMS bo v prihodnosti onkologom olajšala odločitev, katero sistemsko kemoterapijo, tarčno terapijo, v kateri kombinaciji in v katerem zaporedju bodo izbrali za vsakega posameznega bolnika.

Zaključki. CMS so pri metastatskem raku debelega črevesa in danke novo orodje, ki vključuje znanja o kliničnih in molekularnih značilnostih, tumorskem mikrookolju in signalnih poteh ter omogoča personalizirano, bolniku prilagojeno zdravljenje.

Radiol Oncol 2020; 54(3): 278-284.
doi: 10.2478/raon-2020-0034

Napovedna vloga pozitronskoemisijske tomografije in računalniške tomografije pri žleznem raku pljuč stadija I

Carretta A, Bandiera A, Muriana P, Viscardi S, Ciriaco P, Samanes Gajate AM, Arrigoni G, Lazzari C, Gregorc V, Negri G

Izhodišča. Veljavna patološka klasifikacija žleznega raka pljuč vključuje histološke podtipe z različnimi napovednimi dejavniki, ki lahko vplivajo na različne kirurške pristope. Namen raziskave je bil oceniti napovedno vlogo parametrov računalniške tomografije (CT) in pozitronskoemisijske tomografije (PET) pri razvrščanju bolnikov z žleznim rakom pljuč stadija I.

Bolniki in metode. Retrospektivno smo pregledali 58 bolnikov s pljučnim rakom stadija I in s patološko diagnozo žlezni rak oz. adenokarcinom, ki smo jih kirurško zdravili. Adenokarcinom *in situ* in minimalno invazivni adenokarcinom smo opredelili kot neinvazivni žlezni rak. Drugi histološki tipi so bili označeni kot invazivni žlezni rak. Ocenili smo vlogo parametrov, ki smo jih pridobili s CT slikanjem: razmerje gostote mlečnega stekla, stopnjo izginotja tumorja in konsolidacijski premer. Ocenili smo tudi napovedno vloga naslednjih parametrov PET: maksimalno vrednost standardiziranega privzema (SUV)max, SUVindeks (razmerje med SUVmax in jetrnim SUV), metabolični volumen tumorja, skupno glikolizo lezije.

Rezultati. Sedem bolnikov je imelo neinvazivni, 51 pa invazivni žlezni rak. Petletno preživetje brez bolezni za neinvazivni in invazivni žlezni rak sta bili 100% in 100%, preživetje, specifično za raka pa 70 % in 91 %. Univariatna analiza je pokazala pomembno razliko v vrednostih SUVmax, SUV indeks, razmerja gostote mlečnega stekla in razmerja stopnje izginotja tumorja med skupinami neinvazivnega in invazivnega žleznega raka. Optimalne vrednosti za napoved invazivnih rakov so bile 2,6 za SUVmax, 0,9 za SUVindeks, 40 % za razmerje gostote mlečnega stekla in 56 % kot mejna vrednost za stopnjo izginotja tumorja. Skupna glikoliza lezije, SUVmax, SUVindeks so pomembno korelirali s preživetjem specifičnim za raka.

Zaključki. Parametri slikovnih preiskav CT in PET se lahko razlikujejo med neinvazivnimi in invazivnimi žleznimi raki stadija I. Če bi te izsledke lahko potrdili v večjih raziskavah, bi lahko dodatno vplivali na izbiro najustreznejšega kirurškega zdravljenja.

Radiol Oncol 2020; 54(3): 285-294.
doi: 10.2478/raon-2020-0042

Radiomske značilnosti slik [^{18}F]FDG PET pri imunoterapiji (iRADIOMICS) napovejo odziv bolnikov z nedrobnoceličnim pljučnim rakom na zdravljenje s pembrolizumabom

Valentinuzzi D, Vrankar M, Boc N, Ahac V, Zupančič Ž, Unk M, Škalič K, Žagar I, Studen A, Simončič U, Eickhoff J, Jeraj R

Izhodišča. Zaviralci imunskih kontrolnih točk so spremenili obravnavo bolnikov z rakom. Kljub temu pa še vedno obstaja potreba po neinvazivnih slikovnih bioloških označevalcih, s katerimi bi lahko napovedali, kateri bolniki ne bodo odgovorili na zdravljenje. Namen raziskave je bil proučiti, ali radiomske značilnosti slik [^{18}F]FDG PET pri imunoterapiji napovejo odgovor bolnikov z metastatskim nedrobnoceličnim pljučnim rakom na zdravljenje s pembrolizumabom bolje od trenutnih tumorskih označevalcev, ki jih uporabljamo v klinični praksi.

Bolniki in metode. V raziskavo smo vključili 30 bolnikov, ki smo jih zdravili s pembrolizumabom. Z [^{18}F]FDG PET/CT smo jih slikali pred začetkom zdravljenja, po enem mesecu in po štirih mesecih. Analizirali smo povezave šestih robustnih radiomskih metrik primarnih tumorjev s celokupnim preživetjem, za kar smo uporabili Mann-Whitney U-test, Coxovo regresijsko analizo sorazmernih tveganj in analizo krivulje ROC. iRADIOMICS smo oblikovali na podlagi univariatnega in multivariatnega logističnega modela z najbolj obetajočimi metrikami. Napovedno moč iRADIOMICS smo primerjali z napovedno močjo deleža tumorskih celic (*angl. tumour proportion score* [TPS]) z izraženim PD-L1 ter z iRECIST, za kar smo uporabili analizo krivulje ROC. Natančnosti napovedi smo ocenili s petkratno navzkrižno validacijo.

Rezultati. Največjo napovedno moč so imele radiomske metrike pred zdravljenjem, npr. poudarek na majhnem teku (*angl. small run emphasis*) (Mann-Whitney U-test, p = 0,001; razmerje tveganj [HR] = 0,46, p = 0,007; ploščina pod krivuljo [AUC] = 0.85 [95 % interval zaupanja [CI] 0.69–1.00). Multivariatni iRADIOMICS se je izkazal kot boljši od trenutnih standardov tako s stališča napovedne moči kot časovno, če primerjamo naslednje AUC (95 % CI) in natančnosti napovedi (standardne deviacije): iRADIOMICS (pred zdravljenjem), 0,90 (0,78–1,00), 78 % (18 %); TPS PD-L1 (pred terapijo) 0,60 (0,37–0,83), 53 % (18 %); iRECIST (1. mesec), 0,79 (0,62–0,95), 76 % (16 %); iRECIST (4. mesec), 0.86 (0.72–1.00), 76 % (17 %).

Zaključki. Multivariatni iRADIOMICS se je pokazal kot obetajoč slikovni biološki označevalec, ki bi lahko bolje napovedal odgovor na zdravljenje z imunoterapijo pri bolnikih z metastatskim nedrobnoceličnim pljučnim rakom. Bolnikom, katerim bi iRADIOMICS napovedal, da najverjetneje ne bodo odgovorili na zdravljenje s pembrolizumabom, bi lahko ponudili drugačno vrsto zdravljenja.

Radiol Oncol 2020; 54(3): 295-300.
doi: 10.2478/raon-2020-0033

Izboljšanje primarne učinkovitosti mikrovalovne ablacije malignih tumorjev jeter s pomočjo robotskega navigacijskega sistema

Schaible J, Pregler B, Verloh N, Einspieler I, Bäumler W, Zeman F, Schreyer A, Stroszczynski C, Beyer L

Izhodišča. Namen raziskave je bil primerjati primarno učinkovitost robotsko vodene mikrovalovne ablacije jetrnih tumorjev z ročno vodeno.

Bolniki in metode. Naredili smo retrospektivno analizo mikrovalovnih ablacij, ki smo jih izvedli v enem centru, na 368 tumorjih, pri 192 bolnikih (36 žensk, 156 moških, sredna starost 63 let). 119 ablacij smo opravili med 8/2011 in 03/2014 z ročno vodeno tehniko, 249 ablacij pa med 04/2014 in 11/2018 z robotsko vodeno tehniko. Evaluacijo z ultrazvokom, kompjutersko tomografijo ali magnetno resonanco smo naredili 6 mesecev po posegu.

Rezultati. Učinkovitost robotsko vodene mikrovalovne ablacije je bila značilno bolj učinkovita v primerjavi z ročno vodeno ablacijo (88 % *vs*. 76 %; p = 0,013). Multipla logistična regresija je pokazala, da je velikost tumorjev pod 3 cm premera pozitiven napovedni dejavnik za učinek zdravljenja, prav tako je robotsko vodena ablacija pozitiven napovedni dejavnik za popolno ablacijo jetrnih tumorjev.

Zaključki. Mala velikost tumorjev in robotsko vodena mikrovalovna ablacija jetrnih tumorjev sta bila pozitivna napovedna dejavnika za primarno tehnično učinkovitost mikrovalovne ablacije.

Radiol Oncol 2020; 54(3): 301-310.
doi: 10.2478/raon-2020-0037

Gliomi stopnje II in III. Primerjava med dinamičnim magnetnoresonančnim slikanjem s kontrastom in magnetnoresonančnim slikanjem z znotraj-vokselnim nekoherentnih premikanjem

Wang X, Cao M, Chen H, Ge J, Suo S, Zhou Y

Izhodišča. Vpliv mutacije izocitrat dehidrogenaze 1 (*IDH1*) na tvorbo novih žil je lahko pri gliomih povezan s tkivno perfuzijo. Trenutno potreba po injiciranju kontrastnega sredstva in s tem podaljšanim časom slikanja omejujeta uporabo perfuzijskih tehnik. V raziskavi, smo uporabili izpeljano perfuzijsko frakcijo (ang. *simplified perfusion fraction - SPF*]) iz poenostavljenega nekoherentnega gibanja znotraj voksla (ang. *intravoxel incoherent motion* - IVIM), ki smo ga izračunali iz difuzijsko obteženega slikanja (ang: *diffusion-weighted imaging* - DWI) z uporabo le treh b-vrednosti, da bi kvantitativno ocenili spremembe tkivne perfuzije, povezane z *IDH1*, pri gliomih II–III stopnje po Svetovni zdravstveni organizaciji (WHO). Poleg tega smo s primerjavo natančnosti med dinamičnim magnetnoresonančni slikanjem s kontrastom (MRI DCE) in popolnim magnetno resonančnim slikanjem MRI IVIM poskušali najti optimalne slikovne označevalce za napoved statusa mutacije *IDH1*.

Bolniki in metode. Prospektivno smo pregledali 30 bolnikov in uporabili DCE in DWI z več vrednostmi b. Vse parametre smo primerjali med bolniki z gliomi stopnje II in III po WHO z mutiranim *IDH1* in nemutiranim *IDH1*. Uporabili smo Mann-Whitney U test, vključno s K^{trans}, v_e in v_p in konvencionlanim navideznim koeficientom ($ADC_{0,1000}$) pridobljenim z MRI DCE, perfuzijsko frakcijo pridobljeno z IVIM (*f*), difuzijski koeficient (*D*), navidezni-difuzijski koeficient (*D**), in *SPF*. Diagnostično uspešnost smo ovrednotili z analizo lastnosti delovanja sprejemnika (ang. *receiver operating characteristic* - ROC).

Rezultati. Med vsemi perfuzijskimi in difuzijskimi parametri smo ugotovili statistično pomembne razlike med bolniki z gliomi stopnje II–III stopnje po WHO (P < 0,05). Gliomi z nemutiranim *IDH1* so imeli občutno višje perfuzijske vrednosti (P < 0,05) in nižje difuzijske vrednosti (P < 0,05). Med vsemi parametri je večjo diagnostično učinkovitost pokazal *SPF* (območje pod krivuljo 0,861), z 94,4 % občutljivostjo in 75,0 % specifičnostjo.

Zaključki. DWI, DCE in IVIM MRI lahko neinvazivno pomagajo pri razlikovanju statusov mutacije *IDH1* pri bolnikih z gliomi stopnje II in II po WHO. Poenostavljeni *SPF*, ki smo ga izpeljali iz DWI, je pokazal zelo dobro diagnostično učinkovitost.

Radiol Oncol 2020; 54(3): 311-316.
doi: 10.2478/raon-2020-0041

Možnosti ultrazvočno vodene, vakumsko asistirane evakuacije velikih hematomov v dojki

Almasarweh S, Sudah M, Joukainen S, Okuma H, Vanninen R, Masarwah A

Izhodišča. V literaturi je hematom v dojki velikokrat podcenjena in zanemarjena post-proceduralna komplikacija. Sodoben način zdravljenja predstavljata kirurški ali konzervativni pristop, medtem ko imajo perkutani posegi manjšo vlogo. Preučevali smo učinkovitost vakumsko asistirane evakuacije pri zdravljenju klinično pomembnih velikih hematomih dojke kot alternativnim načinom kirurškemu zdravljenju.

Bolniki in metode. Retrospektivno smo analizirali bolnice iz zadnjih 4 let, ki so imele interventni poseg na dojki (kirurški ali perkutani) in so kasneje razvile klinično pomemben velik hematom. Poizkusno smo jih zdravili z vakumsko asistirano evakuacijo hematoma. Interventno zdravljenje je bilo uspešno, če smo odstranili več kot 50 % volumna hematoma in dosegli zmanjšanje bolničinih simptomov. Vse bolnice smo klinično ali ultrazvočno sledili v različnih intervalih glede na resnost simptomov.

Rezultati. V raziskavo smo vključili 11 bolnic. Povprečni največji diameter hematoma je bil 7,9 cm in povprečna površina hematoma je bila 32,4 cm^2. Povprečno trajanje posega je bilo 40,5 min. Pri vseh bolnicah je bila vakumsko asistirana evakuacija hematoma uspešna in brez zapletov. Kontrolni pregledi niso pokazali večjega hematoma ali formacije seroma.

Zaključki. Raziskava je pokazala, da je vakumsko asistirana evakuacija hematoma uspešen in varen način zdravljenja in zato lahko predstavlja alternativo kirurškemu zdravljenju pri velikih, klinično pomembnih hematomih, ne glede na etiologijo ali trajanje. Poseg je manj tvegan, manj stresen in cenejši, lahko ga opravimo tudi ambulantno v primerjavi z kirurškim zdravljenjem.

Radiol Oncol 2020; 54(3): 317-328.
doi: 10.2478/raon-2020-0047

Analiza molekulskih vzorcev povezanih s celičnimi poškodbami po elektroporaciji celic in vitro

Polajžer T, Jarm T, Miklavčič D

Izhodišča. Imunogena celična smrt je ena od oblik celične smrti tumorskih celic, pri kateri se iz celic sproščajo molekule imenovane molekulski vzorci povezani s poškodbami (DAMPs). Te molekule aktivirajo celice imunskega sistema. Posledično se lahko aktivirata tako prirojeni kot pridobljeni imunski sistem, kar vodi v uničenje preostalih spremenjenih celic. Aktivacija imunskega sistema je pomembna komponenta zdravljenja tumorskih tkiv z elektrokemoterapijo in ireverzibilno elektroporacijo. V študiji smo raziskali, če in kdaj po elektroporaciji celic *in vitro* se sprostijo specifične molekule DAMP.

Materiali in metode. Suspenzijo hrčkovih ovarijskih celic (CHO) smo izpostavili 100 µs dolgim električnim pulzom. Prisotnost molekul DAMP, kot so ATP, kalretikulin, nukleinske kisline in sečna kislina, smo analizirali v različnih časovnih točkah po izpostavitvi električnim pulzom različnih amplitud. Za vrednotenje statistične korelacije med količino molekul DAMP in deležem permeabiliziranih ter preživelih celic, oziroma reverzibilno ter ireverzibilno elektroporiranih celic smo uporabili Pearsonov korelacijski koeficient.

Rezultati. Sproščanje molekul DAMP se v splošnem povečuje z naraščajočo amplitudo pulzov, pri tem pa se sama koncentracija molekul lahko razlikuje v različnih časovnih točkah po izpostavitvi električnim pulzom. Večinoma izločanje molekul DAMP bolj korelira z deležem odmrlih celic, kot deležem permeabiliziranih celic. V analiziranih vzorcih nismo uspeli potrditi prisotnosti sečne kisline.

Zaključki. Sproščanje molekul DAMP lahko služi kot označevalec za napoved celične smrti. Stabilnost nekaterih molekul DAMP je časovno odvisna, kar je potrebno upoštevati pri načrtovanju poskusov analize molekul DAMP po izpostavitvi električnim pulzom.

Radiol Oncol 2020; 54(3): 329-334.
doi: 10.2478/raon-2020-0048

Vpliv epidemije COVID-19 na diagnostiko in zdravljenje raka v Sloveniji. Prvi rezultati

Zadnik V, Mihor A, Tomšič S, Žagar T, Bric N, Lokar K, Oblak I

Izhodišča. Pandemija COVID-19 je otežila dostop do zdravstvenih storitev in zmanjšala njihovo uporabo po vsem svetu. V Sloveniji je bila epidemija uradno razglašena od sredine marca do sredine maja 2020. Z odlokom vlade so bile ustavljene vse nenujne zdravstvene storitve, vendar je bila onkološka dejavnost navedena kot izjema. Obvladovanje raka je odvisno tudi od drugih zdravstvenih storitev in ker se je med epidemijo vedenje ljudi predvidoma spremenilo, smo analizirati, ali je epidemija COVID-19 vplivala na diagnostiko in zdravljenje raka v Sloveniji.

Metode. Iz treh virov smo analizirali rutinske podatke v obdobju od novembra 2019 do maja 2020: (1) iz podatkov Registra raka Republike Slovenije smo analizirali prijavnice rakavih bolezni iz patohistoloških izvidov in kliničnih obravnav, prispele iz Onkološkega inštituta Ljubljana in UKC Maribor; (2) iz sistema e-Napotnica smo analizirali podatke o vseh napotnicah v Sloveniji, izdanih za onkološke storitve, stratificirane po vrsti zdravstvene dejavnosti; in (3) iz administrativnih virov Onkološkega inštituta Ljubljana smo analizirali podatke o številu ambulantnih obiskov glede na vrsto obiskov in podatkov o številu opravljenih diagnostičnih slikovnih preiskav.

Rezultati. V primerjavi s povprečjem v obdobju november 2019 – februar 2020 je bilo aprila 2020 43 % in 29 % manj registriranih prijavnic rakavih bolezni iz patohistoloških izvidov in kliničnih obravnav; 33 %, 46 % in 85 % manj napotitev na prve onkološke preglede, kontrolne onkološke preglede in genetska svetovanja; 19 % (53 %), 43 % (72 %) in 20 % (21 %) manj prvih (in kontrolnih) ambulantnih obiskov v sektorjih za radioterapijo, kirurgijo in internistično onkologijo Onkološkega inštituta Ljubljana ter 48 %, 76 % in 42 % manj opravljenih rentgenskih, mamografskih in ultrazvočnih preiskav na Onkološkem inštitutu Ljubljana, v tem vrstnem redu. Število opravljenih preiskav CT in MRI ni bilo znižano.

Zaključki. Pomemben upad prvih napotitev na onkološke storitve, prvih ambulantnih obiskov in opravljenih slikovnih preiskav na Onkološkem inštitutu Ljubljana ter prijavnic rakave bolezni v aprilu 2020 nakazuje na možnost zamika pri diagnozi raka za nekatere bolnike v času prvega porasta okužb s SARS-CoV-2 v Sloveniji. Vzrokov za zamik ne poznamo, verjetno so povezani s spremenjenim vedenjem bolnikov (spremembe v iskanju zdravstvene pomoči), razmišljanji in praksami zdravnikov in/ali upravljanjem zdravstvenega sistema v času epidemije. Upad kontrolnih napotitev in kontrolnih ambulantnih obiskov je najverjetneje posledica odločitve Onkološkega inštituta Ljubljana, da do dva meseca prestavi nenujne preglede bolnikov, naročenih za spremljanje po zaključenem zdravljenju.

Radiol Oncol 2020; 54(3): 335-340.
doi: 10.2478/raon-2020-0040

Ocena ogroženosti za raka dojk z napovednim modelom ogroženosti S-IBIS pri slovenskih ženskah v starostni skupini 40-49 let

Oblak T, Zadnik V, Krajc M, Lokar K, Žgajnar J

Izhodišča. Z izračunom 10-letne ogroženosti za raka dojk s programom S-IBIS smo želeli določiti delež nadpovprečno ogroženih preiskovank starih 40 do 49 let v populaciji bolnic z rakom dojk ter žensk, obravnavanih v Centrih za bolezni dojk (CBD). Rak dojk je najpogostejši rak pri ženskah v Sloveniji, njegova incidence pa je pod evropskim povprečjem. Napovedni model ogroženosti za raka dojk S-IBIS temelji na angleškem Tyrer-Cuzickovem algoritmu, vendar upošteva slovenske incidenčne podatke za raka dojk. V Sloveniji razmišljamo o uvedbi presejalnega programa za raka dojk za nadpovprečno ogrožene ženske v starosti 40 do 49 let. S-IBIS je potencialno orodje za prepoznavo bolj ogroženih žensk, ki bi bile vabljene v prilagojeno presejanje.

Bolniki in metode. Pri 367 bolnicah, ki so zbolele za rakom dojk v starosti od 40 do 49 let, in pri 357 zdravih ženskah, ki so bile obravnavane v CBD, smo izračunali 10-letno ogroženost za rakom dojk s programom S-IBIS. V posamezni podskupini smo izračunali delež žensk z nadpovprečno ogroženostjo za razvoj raka dojk.

Rezultati. Pri 48,7 % žensk iz CBD ter 39,2 % bolnic smo izračunali nadpovprečno 10-letno ogroženost za razvoj raka dojk. Ženske iz CBD so imele pozitivno družinsko anamnezo za raka dojk v večjem deležu kot bolnice ($p < 0,05$).

Zaključek. Za zanesljivo razvrstitev žensk v razrede ogroženosti za razvoj raka dojk, bo potrebno vključiti dodatne dejavnike ogroženosti v S-IBIS.

Radiol Oncol 2020; 54(3): 341-346.
doi: 10.2478/raon-2020-0032

Standardna in multivisceralna kolektomija pri lokalno napredovalem raku debelega črevesa

Sahakyan AM, Aleksanyan A, Batikyan H, Petrosyan H, Sahakyan MA

Izhodišča. Obravnava lokalno napredovalega raka debelega črevesa je še vedno izziv. Kirurško zdravljenje je temeljno zdravljenje, vendar so rezultati razmeroma nejasni, zlasti pri multivisceralnih resekcijah. Cilj raziskave je bil preučiti rezultate standardne in multivisceralne kolektomije pri bolnikih z lokalno napredovalim rakom debelega črevesa.

Bolniki in metode. Zbrali smo demografske, klinične in perioperativne podatke o bolnikih, operiranih v obdobju 2004–2018. Lokalno napredovali rak debelega črevesa smo opredelili rak v stadiju T4, kjer je tumor preraščal visceralni peritonej ali sosednje organe oz. strukture. Glede na preraščanje smo izvedli bodisi standardno bodisi multivisceralno kolektomijo.

Rezultati. V raziskavo smo vključili 203 bolnikov, ki smo jim naredili kolektomijo zaradi lokalno napredovalega raka debelega črevesa. Med njimi smo 112 bolnikom naredili standardno (55,2 %) in 91 (44,8 %) multivisceralno kolektomijo. Resno obolevnost in umrljivost smo ugotovili 5,9 % pri standardni kolektomiji in 2,5 % pri multivisceralni kolektomiji. Ta je bila povezana s povečano izgubo krvi (200 ml proti 100 ml, p = 0,01), z več transfuzij krvi (22 % proti 8,9 %, p = 0,01), daljšim operativnim časom (180 minut proti 140 minut, p < 0,01) in z daljšo pooperativno hospitalizacijo (11 dni proti 10 dni, p <0,01) v primerjavi s standardno kolektomijo. Parametri, povezani z zapleti so bili podobni v obeh skupinah. Univariatna analiza je pokazala, da so bili moški spol, prisotnost ≥ 3 komorbidnosti, lokacija tumorja v levem debelem črevesu in perioperativna transfuzija krvi povezani s pooperativnimi zapleti. Multivariatna analiza pa je pokazala, da je bila prisotnost ≥ 3 komorbidnosti edini neodvisni napovedni dejavnik zapletov.

Zaključki. Kolektomija z multivisceralno resekcijo ali brez nje je varen postopek pri obravnavi lokalno napredovalega raka debelega črevesa. Pooperativni rezultati med standardno in multivisceralno kolektomijo so podobni v primeru, da resekcijo naredi izkušen kirurški tim, zato bi morali multivisceralno kolektomijo opravljati zgolj za to strokovno usposobljeni centri.

Radiol Oncol 2020; 54(3): 347-352.
doi: 10.2478/raon-2020-0038

Perkutana slikovno vodena elektrokemoterapija hepatocelularnega raka

Djokić M, Dežman R, Čemažar M, Štabuc M, Petrič M, Šmid LM, Janša R, Plesnik B, Bošnjak M, Lampreht Tratar U, Trotovšek B, Kos B, Miklavčič D, Serša G, Popovič P

Izhodišča. Elektrokemoterapija med operacijskim posegom je učinkovita pri zdravljenju metastaz raka debelega črevesa in danke kot tudi hepatocelularnega raka. Slikovno vodeno elektrokemoterapijo s perkutanim pristopom so že izvedli, vendar ne pri hepatocelularnem raku. Zato je bil namen pričujoče raziskave preveriti izvedljivost, varnost in učinkovitost elektrokemoterapije s perkutanim pristopom pri zdravljenju hepatocelularnega raka.

Bolnik in metode. Bolniku smo naredili transarterijsko kemoembolizacijo, kot tudi mikrovalovno ablacijo več lezij hepatocelularnega raka v III., V. in VI. jetrnem segmentu. Ob sledenju bolnika smo ugotovili novo lezijo v II. jetrnem segmentu. Na multidisciplinarnem timu smo ocenili, da je primerna za minimalno invazivni perkutani pristop elektrokemoterapije. Zdravljenje smo izvedli z dolgo igelnimi elektrodami, ki smo jih vstavili s kotrolo slikovne diagnostike.

Rezultati. Zdravljenje smo izvedli brez zapletov in je bilo varno in učinkovito, kar smo dokazali s kontrolnim slikanjem z magnetno resonanco.

Zaključki. Minimalno invaziven perkutani pristop elektrokemoterapije s kotrolo slikovne diagnostike je izvedljiv, varen in učinkovit pri zdravljenju hepatocelularnega raka.

Radiol Oncol 2020; 54(3): 353-363.
doi: 10.2478/raon-2020-0046

Konsolidacijska radioterapija pri bolnikih z razširjenim drobnoceličnim rakom pljuč v terciarni ustanovi. Vpliv sevalne doze in perspektive v dobi imunoterapije

Stanič K, Vrankar M, But-Hadžić J

Izhodišča. Konsolidacijska radioterapija pri razširjenem drobnoceličnem pljučnem raku (ED-SCLC) je bila povezana z boljšim dvoletnim celokupnim preživetjem pri bolnikih, ki so se v raziskavi CREST odzvali na kemoterapijo, rezultati dveh metaanaliz pa so bili nasprotujoči. Pred kratkim so uvedli imunoterapijo za zdravljenje ED-SCLC, zaradi česar je vloga konsolidacijske radioterapije še bolj nejasna. Cilj študije je bil raziskati, ali konsolidacijsko obsevanje prsnega koša izboljša preživetje bolnikov z ED-SCLC, ki jih zdravimo v rutinski klinični praksi, in preučiti vpliv odmerka konsolidacijske radioterapije na preživetje. Razpravljamo tudi o prihodnji vlogi konsolidacijske radioterapije v dobi imunoterapije.

Bolniki in metode. Retrospektivno smo pregledali zdravstveno dokumentacijo 704 zaporednih bolnikov z drobnoceličnim rakom pljuč, ki smo jih od januarja 2010 do decembra 2014 zdravili na Onkološkem inštitutu Ljubljana. Srednji čas spremljanja bolnikov je bil 65 mesecev. Analizirali smo srednje celokupno preživetje bolnikov z ED-SCLC, ki smo jih zdravili samo s kemoterapijo, ter tistih, ki smo jih zdravili s kemoterapijo in konsolidacijsko radioterapijo. Primerjali smo tudi srednje preživetje bolnikov, ki smo jih zdravili z različnimi konsolidacijskimi dozami obsevanja in izvedli univariatno in multivariatno analizo napovednih dejavnikov.

Rezultati. Od 412 bolnikov z ED-SCLC je prejelo kemoterapijo s konsolidacijsko radioterapijo 74 bolnikov, samo kemoterapijo pa 113 bolnikov. Bolniki s konsolidacijsko radioterapijo so imeli bistveno daljše srednje preživetje v primerjavi z bolniki zdravljenimi samo s kemoterapijo, 11,1 mesecev (interval zaupanja [CI] 10,1–12,0) v primerjavi s 7,6 meseca (CI 6,9–8,5, $p < 0,001$) in daljše enoletno celokupno preživetje (44 % v primerjavi s 23 %, $p = 0,0025$), medtem ko se razlika v dvoletnem celokupnem preživetju ni značilno razlikovala (10 % v primerjavi s 5 %, $p = 0,19$). Doza konsolidacijske radioterapije ni bila enotna. Višja sevalna doza 45 Gy (v 18 frakcijah) je izboljšala srednje celokupno preživetje v primerjavi z nižjo dozo 30–36 Gy (v 10–12 frakcijah), 17,2 meseca v primerjavi z 10,3 meseca ($p = 0,03$). Statistično značilno razliko smo opazili tudi pri 1-letnem celokupnem preživetju (68 % v primerjavi s 3 0%, $p = 0,01$) in neznačilno razliko pri dvoletnem celokupnem preživetju (18 % v primerjavi s 5 %, $p = 0,11$).

Zaključki. Konsolidacijska radioterapija je izboljšala srednje celokupno preživetje in enoletno celokupno preživetje pri bolnikih z ED-SCLC v primerjavi s samo kemoterapijo. Višja sevalna doza konsolidacijske radioterapije je bila povezana z daljšim celokupnim preživetjem in enoletnim celokupnim preživetjem v primerjavi z nižjo dozo. Konsolidacijska radioterapija, večje število krogov kemoterapije in profilaktično obsevanje glave so bili neodvisni napovedni dejavniki za boljše preživetje v naši analizi. Pri bolnikih, ki so prejeli konsolidacijsko radioterapijo, so na preživetje vplivali le višji odmerki in profilaktično obsevanje glave, ne glede na število prejetih krogov kemoterapije. Vloga konsolidacijske radioterapije v obdobju imunoterapije ni znana in bi jo veljalo raziskati.

Radiol Oncol 2020; 54(3): 364-370.
doi: 10.2478/raon-2020-0036

Ocena nastavitvenih napak pri obsevanju bolnikov z rakom glave in vratu. Standardne in individualne podlage za glavo

Androjna S, Žager Marciuš V, Peterlin P, Strojan P

Izhodišča. Cilj raziskave je bil (a) primerjati natančnost dveh različnih imobilizacijskih strategij pri bolnikih s tumorji glave in vratu; in (b) primerjati nastavitvene napake na terapevtskih enotah z različnimi sistemi za portalno slikanje.

Bolniki in metode. Variacije v legi izocentra (IC) glede na referenčno točko, določeno na CT simulatorju smo merili v vertikalni (anteriorno-posteriorno), longitudinalni (superiorno-inferiorno) in lateralni (medialno-lateralno) smeri pri 120 bolnikih z rakom glave in vratu. Bolnike smo obsevali z namenom ozdravitve in jih, odvisno od terapevtske enote (enota A – 2D/2D slikovni predogled; enota B – 2D slikovni predogled) in obdobje obsevanja razdelili v 6 skupin po 20 bolnikov. Pri tistih, ki smo jih obsevali v letu 2014, smo uporabljali standardne podlage za pod glavo in vrat (skupini 1 in 2), pri tistih, ki smo jih obsevali leta 2015 in 2017 (skupine 3-6) pa smo uporabljali individualne podlage za za pod glavo in vrat. Varnostni rob med kliničnim in planirnim tarčnim volumnom smo izračunali po formuli, ki jo je predlagal Van Herk.

Rezultati. Analizirani smo skupaj 2.454 portalnih slik in 3.681 nastavitvenih napak. Z uvedbo individualnih podlag za za pod glavo in vrat v letu 2015 smo statistično značilno zmanjšali povprečni medfrakcijski odklon v vertikalni smeri in zmanjšali število odklonov izocentra v vertikalni in longitudinalni smeri (velja za obe terapevtski enoti). Največje zmanjšanje varnostnega robu smo izračunali v longitudinalni smeri, varnostni robovi pa so bili večji za enoto B kot enoto A.

Zaključki. Ugotovili smo, da uporaba individualnih podlag za pod glavo in vrat in bolj naprednega slikovnega sistema povečuje natančnost nastavitve pri obsevanju bolnikov z rakom glave in vratu.

FUNDACIJA DR. J. CHOLEWA

Fundacija "Docent dr. J. Cholewa"
je neprofitno, neinstitucionalno in nestrankarsko
združenje posameznikov, ustanov in organizacij, ki želijo
materialno spodbujati in poglabljati raziskovalno
dejavnost v onkologiji.

Dunajska 106

1000 Ljubljana

IBAN: SI56 0203 3001 7879 431

FUNDACIJA
DR. J. CHOLEWA

Activity of "Dr. J. Cholewa" Foundation for Cancer Research and Education – a report for the third quarter of 2020

Dr. Josip Cholewa Foundation for cancer research and education continues with its planned activities in the third quarter of 2020. Its primary focus remains the provision of grants, scholarships, and other forms of financial assistance for basic, clinical and public health research in the field of oncology. In parallel, it also makes efforts to provide financial and other support for the organisation of congresses, symposia and other forms of meetings to spread the knowledge about prevention and treatment of cancer, and finally about rehabilitation for cancer patients. In Foundation's strategy, the spread of knowledge should not be restricted only to the professionals that treat cancer patients, but also to the patients themselves and to the general public.

The Foundation continues to provide support for »Radiology and Oncology«, a quarterly scientific magazine with a respectable impact factor that publishes research and review articles about all aspects of cancer. The magazine is edited and published in Ljubljana, Slovenia. »Radiology and Oncology« is an open access journal available to everyone free of charge. Its long tradition represents a guarantee for the continuity of international exchange of ideas and research results in the field of oncology for all in Slovenia that are interested and involved in helping people affected by many different aspects of cancer.

The Foundation will continue with its activities in the future, especially since the problems associated with cancer affect more and more people in Slovenia and elsewhere. Ever more treatment that is successful reflects in results with longer survival in many patients with previously incurable cancer conditions. Thus adding many new dimensions in life of cancer survivors and their families.

Borut Štabuc, M.D., Ph.D.

Andrej Plesničar, M.D., M.Sc.

Viljem Kovač M.D., Ph.D.

TANTUM VERDE®

benzidaminijev klorid

Za lajšanje bolečine in oteklin v ustni votlini in žrelu, ki so posledica radiomukozitisa

Bistvene informacije iz Povzetka glavnih značilnosti zdravila

Tantum Verde 1,5 mg/ml oralno pršilo, raztopina
Tantum Verde 3 mg/ml oralno pršilo, raztopina
Sestava 1,5 mg/ml: 1 ml raztopine vsebuje 1,5 mg benzidaminijevega klorida, kar ustreza 1,34 mg benzidamina. V enem razpršku je 0,17 ml raztopine. En razpršek vsebuje 0,255 mg benzidaminijevega klorida, kar ustreza 0,2278 mg benzidamina. **Sestava 3 mg/ml:** 1 ml raztopine vsebuje 3 mg benzidaminijevega klorida, kar ustreza 2,68 mg benzidamina. V enem razpršku je 0,17 ml raztopine. En razpršek vsebuje 0,51 mg benzidaminijevega klorida, kar ustreza 0,4556 mg benzidamina. **Terapevtske indikacije:** Samozdravljenje: Lajšanje bolečine in oteklin pri vnetju v ustni votlini in žrelu, ki so lahko posledica okužb in stanj po operaciji. Po nasvetu in navodilu zdravnika: Lajšanje bolečine in oteklin v ustni votlini in žrelu, ki so posledica radiomukozitisa. **Odmerjanje in način uporabe:** Odmerjanje 1,5 mg/ml: Odrasli: 4 do 8 razprškov 2- do 6-krat na dan (vsake 1,5 do 3 ure). Pediatrična populacija: Mladostniki, stari od 12 do 18 let: 4-8 razprškov 2- do 6-krat na dan. Otroci od 6 do 12 let: 4 razprški 2- do 6-krat na dan. Otroci, mlajši od 6 let: 1 razpršek na 4 kg telesne mase; do največ 4 razprške 2- do 6-krat na dan. Odmerjanje 3 mg/ml: Uporaba 2- do 6-krat na dan (vsake 1,5 do 3 ure). Odrasli: 2 do 4 razprški 2- do 6-krat na dan. Pediatrična populacija: Mladostniki, stari od 12 do 18 let: 2 do 4 razprški 2- do 6-krat na dan. Otroci od 6 do 12 let: 2 razprška 2- do 6-krat na dan. Otroci, mlajši od 6 let: 1 razpršek na 8 kg telesne mase; do največ 2 razprška 2- do 6-krat na dan. Starejši bolniki, bolniki z jetrno okvaro in bolniki z ledvično okvaro: Uporabo oralnega pršila z benzidaminijevim kloridom se svetuje pod nadzorom zdravnika. Način uporabe: Za orofaringealno uporabo. Zdravilo se razprši v usta in žrelo. **Kontraindikacije:** Preobčutljivost na učinkovino ali katero koli pomožno snov. **Posebna opozorila in previdnostni ukrepi:** Če se simptomi v treh dneh ne izboljšajo, se mora bolnik posvetovati z zdravnikom ali zobozdravnikom, kot je primerno. Benzidamin ni priporočljiv za bolnike s preobčutljivostjo nasalicilno kislino ali druga nesteroidna protivnetna zdravila. Pri bolnikih, ki imajo ali so imeli bronhialno astmo, lahko pride do bronhospazma, zato je potrebna previdnost. To zdravilo vsebuje majhne količine etanola (alkohola), in sicer manj kot 100 mg na odmerek. To zdravilo vsebuje metilparahidroksibenzoat (E218). Lahko povzroči alergijske reakcije (lahko zapoznele). Zdravilo z jakostjo 3 mg/ml vsebuje makrogolglicerol hidroksistearat 40. Lahko povzroči želodčne težave in drisko. **Medsebojno delovanje z drugimi zdravili in druge oblike interakcij:** Študij medsebojnega delovanja niso izvedli. **Nosečnost in dojenje:** O uporabi benzidamina pri nosečnicah in doječih ženskah ni zadostnih podatkov. Uporaba zdravila med nosečnostjo in dojenjem ni priporočljiva. **Vpliv na sposobnost vožnje in upravljanja strojev:** Zdravilo v priporočenem odmerku nima vpliva na sposobnost vožnje in upravljanja strojev. **Neželeni učinki:** Neznana pogostnost (ni mogoče oceniti iz razpoložljivih podatkov): anafilaktične reakcije, preobčutljivostne reakcije, odrevenelost, laringospazem, suha usta, navzea in bruhanje, angioedem, fotosenzitivnost, pekoč občutek v ustih. Neposredno po uporabi se lahko pojavi občutek odrevenelosti v ustih in v žrelu. Ta učinek se pojavi zaradi načina delovanja zdravila in po kratkem času izgine. **Način in režim izdaje zdravila:** BRp-Izdaja zdravila je brez recepta v lekarnah in specializiranih prodajalnah.

Imetnik dovoljenja za promet: Aziende Chimiche Riunite Angelini Francesco – A.C.R.A.F. S.p.A., Viale Amelia 70, 00181 Rim, Italija **Datum zadnje revizije besedila:** 14. 10. 2019

Pred svetovanjem ali izdajo preberite celoten Povzetek glavnih značilnosti zdravila.

Samo za strokovno javnost.

Datum priprave informacije: november 2019

Odgovoren za trženje: Bonifar d.o.o.

ANGELINI

PR/BSI/BEN/2019/012

KEYTRUDA®
(pembrolizumab, MSD)

Pomaga spreminjati pričakovanja o preživetju

• pri metastatskem NSCLC [*,1,2]
• in napredovalem melanomu[3]

*NSCLC – non-small cell lung cancer

Reference: 1. Gandhi L, Rodríguez-Abreu D, Gadgeel S, et. al.; for the KEYNOTE-189 investigators. Pembrolizumab plus chemotherapy in metastatic non–small-cell lung cancer. N Engl J Med. 2018;378(22):2078–2092. **2.** Keytruda EU SmPC **3.** Hamid O, Robert C, Daud A, et. al. 5-year survival outcomes for patients with advanced melanoma treated with pembrolizumab in KEYNOTE-001. Annals of Oncology 2019; 30: 582-588.

SKRAJŠAN POVZETEK GLAVNIH ZNAČILNOSTI ZDRAVILA

Pred predpisovanjem, prosimo, preberite celoten Povzetek glavnih značilnosti zdravila! Ime zdravila: KEYTRUDA 25 mg/ml koncentrat za raztopino za infundiranje vsebuje pembrolizumab. **Terapevtske indikacije: Zdravilo KEYTRUDA je kot samostojno zdravljenje indicirano za zdravljenje:** napredovalega (neoperabilnega ali metastatskega) melanoma pri odraslih; za adjuvantno zdravljenje odraslih z melanomom v stadiju III, ki se je razširil na bezgavke, po popolni kirurški odstranitvi; metastatskega nedrobnoceličnega pljučnega raka (NSCLC) v prvi liniji zdravljenja pri odraslih, ki imajo tumorje z ≥ 50 % izraženostjo PD-L1 (TPS) in brez pozitivnih tumorskih mutacij EGFR ali ALK; lokalno napredovalega ali metastatskega NSCLC pri odraslih, ki imajo tumorje z ≥ 1 % izraženostjo PD-L1 (TPS) in so bili predhodno zdravljeni z vsaj eno shemo kemoterapije, bolniki s pozitivnimi tumorskimi mutacijami EGFR ali ALK so pred prejemom zdravila KEYTRUDA morali prejeti tudi tarčno zdravljenje; odraslih bolnikov s ponovljenim ali neodzivnim klasičnim Hodgkinovim limfomom (cHL), pri katerih avtologna presaditev matičnih celic (ASCT) in zdravljenje z brentuksimabom vedotinom (BV) nista bila uspešna, in odraslih bolnikov, ki za presaditev niso primerni, zdravljenje z BV pa pri njih ni bilo uspešno; lokalno napredovalega ali metastatskega urotelijskega raka pri odraslih, predhodno zdravljenih s kemoterapijo, ki je vključevala platino; lokalno napredovalega ali metastatskega urotelijskega raka pri odraslih, ki niso primerni za zdravljenje s kemoterapijo, ki vsebuje cisplatin in imajo tumorje z izraženostjo PD-L1 ≥ 10, ocenjeno s kombinirano pozitivno oceno (CPS); ponovljenega ali metastatskega ploščatoceličnega raka glave in vratu (HNSCC) pri odraslih, ki imajo tumorje z ≥ 50 % izraženostjo PD-L1 (TPS), in pri katerih je bolezen napredovala med zdravljenjem ali po zdravljenju s kemoterapijo, ki je vključevala platino. Zdravilo KEYTRUDA je kot samostojno zdravljenje ali v kombinaciji s kemoterapijo s platino in 5-fluorouracilom (5-FU) indicirano za prvo linijo zdravljenja metastatskega ali neoperabilnega ponovljenega ploščatoceličnega raka glave in vratu pri odraslih, ki imajo tumorje z izraženostjo PD-L1 s CPS ≥ 1. Zdravilo KEYTRUDA je v kombinaciji s pemetreksedom in kemoterapijo na osnovi platine indicirano za prvo linijo zdravljenja metastatskega neploščatoceličnega NSCLC pri odraslih, pri katerih tumorji nimajo pozitivnih mutacij EGFR ali ALK; v kombinaciji s karboplatinom in bodisi paklitakselom bodisi nab-paklitakselom je indicirano za prvo linijo zdravljenja metastatskega ploščatoceličnega NSCLC pri odraslih; v kombinaciji z aksitinibom je indicirano za prvo linijo zdravljenja napredovalega raka ledvičnih celic (RCC) pri odraslih. **Odmerjanje in način uporabe:** Testiranje PD-L1 pri bolnikih z NSCLC, urotelijskim rakom ali HNSCC: Za samostojno zdravljenje z zdravilom KEYTRUDA je priporočljivo opraviti testiranje izraženosti PD-L1 tumorja z validirano preiskavo, da izberemo bolnike z NSCLC ali predhodno nezdravljenim urotelijskim rakom. Bolnike s HNSCC je treba za samostojno zdravljenje z zdravilom KEYTRUDA ali v kombinaciji s kemoterapijo s platino in 5-fluorouracilom (5-FU) izbrati na podlagi izraženosti PD-L1, potrjene z validirano preiskavo. Odmerjanje: Priporočeni odmerek zdravila KEYTRUDA za samostojno zdravljenje je bodisi 200 mg na 3 tedne ali 400 mg na 6 tednov, apliciran z intravensko infuzijo v 30 minutah. Priporočeni odmerek za kombinirano zdravljenje je 200 mg na 3 tedne, apliciran z intravensko infuzijo v 30 minutah. Za uporabo v kombinaciji glejte povzetke glavnih značilnosti sočasno uporabljenih zdravil. Če se uporablja kot del kombiniranega zdravljenja skupaj z intravensko kemoterapijo, je treba zdravilo KEYTRUDA aplicirati prvo. Bolnike je treba zdraviti do napredovanja bolezni ali nesprejemljivih toksičnih učinkov. Pri adjuvantnem zdravljenju melanoma je treba zdravilo uporabljati do ponovitve bolezni, pojava nesprejemljivih toksičnih učinkov oziroma mora zdravljenje trajati do enega leta. Če je aksitinib uporabljen v kombinaciji s pembrolizumabom, se lahko razmisli o povečanju odmerka aksitiniba nad začetnih 5 mg v presledkih šest tednov ali več. Pri bolnikih starih ≥ 65 let, bolnikih z blago do zmerno okvaro ledvic, bolnikih z blago okvaro jeter prilagoditev odmerka ni potrebna. Odložitev odmerka ali ukinitev zdravljenja: Zmanjšanje odmerka zdravila KEYTRUDA ni priporočljivo. Za obvladovanje neželenih učinkov je treba uporabo zdravila KEYTRUDA zadržati ali ukiniti, prosimo, glejte celoten Povzetek glavnih značilnosti zdravila. **Kontraindikacije:** Preobčutljivost na učinkovino ali katero koli pomožno snov. **Povzetek posebnih opozoril, previdnostnih ukrepov, interakcij in neželenih učinkov:** Imunsko pogojeni neželeni učinki (pnevmonitis, kolitis, hepatitis, nefritis, endokrinopatije, neželeni učinki na kožo in drugi): Pri bolnikih, ki so prejemali pembrolizumab, so se pojavili imunsko pogojeni neželeni učinki, vključno s hudimi in smrtnimi primeri. Večina imunsko pogojenih neželenih učinkov, ki so se pojavili med zdravljenjem s pembrolizumabom, je bila reverzibilnih in so jih obvladali s prekinitvami uporabe pembrolizumaba, uporabo kortikosteroidov in/ali podporno oskrbo. Pojavijo se lahko tudi po zadnjem odmerku pembrolizumaba in hkrati prizadanejo več organskih sistemov. V primeru suma na imunsko pogojene neželene učinke je treba poskrbeti za ustrezno oceno za potrditev etiologije oziroma izključitev drugih vzrokov. Glede na izrazitost neželenega učinka je treba zadržati uporabo pembrolizumaba in uporabiti kortikosteroide – za natančna navodila, prosimo, glejte Povzetek glavnih značilnosti zdravila Keytruda. Zdravljenje s pembrolizumabom lahko poveča tveganje za zavrnitev pri prejemnikih presadkov čvrstih organov. Pri bolnikih, ki so prejemali pembrolizumab, so poročali o hudih z infuzijo povezanih reakcijah, vključno s preobčutljivostjo in anafilaksijo. Pembrolizumab se iz obtoka odstrani s katabolizmom, zato presnovnih medsebojnih delovanj zdravil ni pričakovati. Uporabi sistemskih kortikosteroidov ali imunosupresivov pred uvedbo pembrolizumaba se je treba izogibati, ker lahko vplivajo na farmakodinamično aktivnost in učinkovitost pembrolizumaba. Vendar pa je kortikosteroide ali druge imunosupresive mogoče uporabiti za zdravljenje imunsko pogojenih neželenih učinkov. Kortikosteroide je mogoče uporabiti tudi kot premedikacijo, če je pembrolizumab uporabljen v kombinaciji s kemoterapijo, kot antiemetično profilakso in/ali za ublažitev neželenih učinkov, povezanih s kemoterapijo. Ženske v rodni dobi morajo med zdravljenjem s pembrolizumabom in vsaj še 4 mesece po zadnjem odmerku pembrolizumaba uporabljati učinkovito kontracepcijo, med nosečnostjo in dojenjem se ga ne sme uporabljati. Varnost pembrolizumaba pri samostojnem zdravljenju so v kliničnih študijah ocenili pri 5.884 bolnikih z napredovalim melanomom, kirurško odstranjenim melanomom v stadiju III (adjuvantno zdravljenje), NSCLC, cHL, urotelijskim rakom ali HNSCC s štirimi odmerki (2 mg/kg na 3 tedne, 200 mg na 3 tedne in 10 mg/kg na 2 ali 3 tedne). V tej populaciji bolnikov je mediani čas opazovanja znašal 7,3 mesece (v razponu od 1 dneva do 31 mesecev), najpogostejši neželeni učinki zdravljenja s pembrolizumabom so bili utrujenost (32 %), navzea (20 %) in diareja (20 %). Večina poročanih neželenih učinkov pri samostojnem zdravljenju je bila po izrazitosti 1. ali 2. stopnje. Najresnejši neželeni učinki so bili imunsko pogojeni neželeni učinki in hude z infuzijo povezane reakcije. Varnost pembrolizumaba pri kombiniranem zdravljenju s kemoterapijo so ocenili pri 1.067 bolnikih NSCLC ali HNSCC, ki so v kliničnih študijah prejemali pembrolizumab v odmerkih 200 mg, 2 mg/kg ali 10 mg/kg na vsake 3 tedne. V tej populaciji bolnikov so bili najpogostejši neželeni učinki naslednji: anemija (50 %), navzea (50 %), utrujenost (37 %), zaprtost (35%), diareja (30 %), nevtropenija (30 %), zmanjšanje apetita (28 %) in bruhanje (25 %). Pri kombiniranem zdravljenju s pembrolizumabom je pri bolnikih z NSCLC pojavnost neželenih učinkov 3. do 5. stopnje znašala 67 %, pri zdravljenju samo s kemoterapijo pa 66 %, pri kombiniranem zdravljenju s pembrolizumabom pri bolnikih s HNSCC 85 % in pri zdravljenju s kemoterapijo v kombinaciji s cetuksimabom 84 %. Varnost pembrolizumaba v kombinaciji z aksitinibom so ocenili v klinični študiji pri 429 bolnikih z napredovalim rakom ledvičnih celic, ki so prejemali 200 mg pembrolizumaba na 3 tedne in 5 mg aksitiniba dvakrat na dan. V tej populaciji bolnikov so bili najpogostejši neželeni učinki diareja (54 %), hipertenzija (45 %), utrujenost (38 %), hipotiroidizem (35 %), zmanjšan apetit (30 %), sindrom palmarno-plantarne eritrodisestezije (28 %), navzea (28 %), zvišanje vrednosti ALT (27 %), zvišanje vrednosti AST (26 %), disfonija (25 %), kašelj (21 %) in zaprtost (21 %). Pojavnost neželenih učinkov 3. do 5. stopnje je bila med kombiniranim zdravljenjem s pembrolizumabom 76 % in pri zdravljenju s sunitinibom samim 71 %. Za celoten seznam neželenih učinkov, prosimo, glejte celoten Povzetek glavnih značilnosti zdravila. **Način in režim izdaje zdravila**: H – Predpisovanje in izdaja zdravila je le na recept, zdravilo se uporablja samo v bolnišnicah. **Imetnik dovoljenja za promet z zdravilom:** Merck Sharp & Dohme B.V., Waarderweg 39, 2031 BN Haarlem, Nizozemska. **Datum zadnje revizije besedila:** 2. junij 2020.

MSD

Merck Sharp & Dohme inovativna zdravila d.o.o.,
Šmartinska cesta 140, 1000 Ljubljana
tel: +386 1/ 520 42 01, fax: +386 1/ 520 43 50

Pripravljeno v Sloveniji, junij 2020; SI-KEY-00118 EXP: 06/2022
Samo za strokovno javnost.
H - Predpisovanje in izdaja zdravila je le na recept, zdravilo pa se uporablja samo v bolnišnicah. Pred predpisovanjem, prosimo, preberite celoten Povzetek glavnih značilnosti zdravila Keytruda, ki je na voljo pri naših strokovnih sodelavcih ali na lokalnem sedežu družbe.

▼ **Lonsurf®**

trifluridin/tipiracil

Več časa za trenutke, ki štejejo

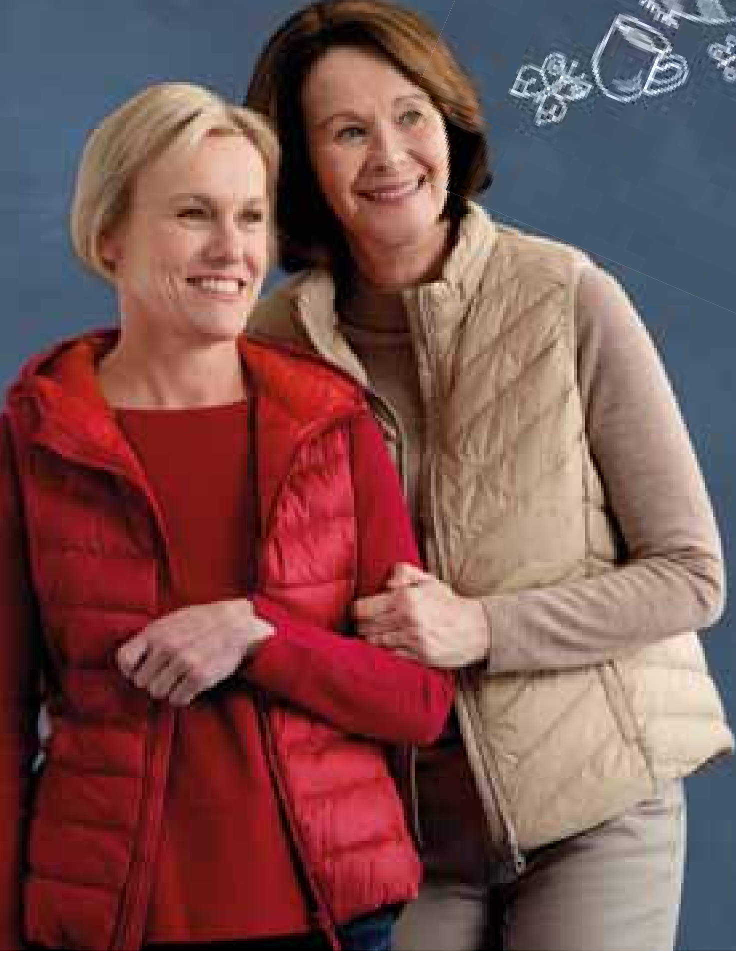

Kolorektalni rak

Zdravilo Lonsurf je indicirano v monoterapiji za zdravljenje odraslih bolnikov z metastatskim kolorektalnim rakom (KRR), ki so bili predhodno že zdravljeni ali niso primerni za zdravljenja, ki so na voljo. Ta vključujejo kemoterapijo na osnovi fluoropirimidina, oksaliplatina in irinotekana, zdravljenje z zaviralci žilnega endotelijskega rastnega dejavnika (VEGF – Vascular Endothelial Growth Factor) in zaviralci receptorjev za epidermalni rastni dejavnik (EGFR – Epidermal Growth Factor Receptor).

Rak želodca

Zdravilo Lonsurf je indicirano v monoterapiji za zdravljenje odraslih bolnikov z metastatskim rakom želodca vključno z adenokarcinomom gastro-ezofagealnega prehoda, ki so bili predhodno že zdravljeni z najmanj dvema sistemskima režimoma zdravljenja za napredovalo bolezen.

Družba Servier ima licenco družbe Taiho za zdravilo Lonsurf®. Pri globalnem razvoju zdravila sodelujeta obe družbi in ga tržita na svojih določenih področjih.

SERVIER

Skrajšan povzetek glavnih značilnosti zdravila: Lonsurf 15 mg/6,14 mg filmsko obložene tablete in Lonsurf 20 mg/8,19 mg filmsko obložene tablete

▼ Za to zdravilo se izvaja dodatno spremljanje varnosti. Tako bodo hitreje na voljo nove informacije o njegovi varnosti. Zdravstvene delavce naprošamo, da poročajo o katerem koli domnevnem neželenem učinku zdravila. **SESTAVA*: Lonsurf 15 mg/6,14 mg:** Ena filmsko obložena tableta vsebuje 15 mg trifluridina in 6,14 mg tipiracila (v obliki klorida). **Lonsurf 20 mg/8,19 mg**: Ena filmsko obložena tableta vsebuje 20 mg trifluridina in 8,19 mg tipiracila (v obliki klorida). **TERAPEVTSKE INDIKACIJE*:** Kolorektalni rak – zdravilo Lonsurf je indicirano v monoterapiji za zdravljenje odraslih bolnikov z metastatskim kolorektalnim rakom, ki so bili predhodno že zdravljeni ali niso primerni za zdravljenja, ki so na voljo. Ta vključujejo kemoterapijo na osnovi fluoropirimidina, oksaliplatina in irinotekana, zdravljenje z zaviralci žilnega endotelijskega rastnega dejavnika (VEGF – Vascular Endothelial Growth Factor) in zaviralci receptorjev za epidermalni rastni dejavnik (EGFR – Epidermal Growth Factor Receptor). Rak želodca – zdravilo Lonsurf je indicirano v monoterapiji za zdravljenje odraslih bolnikov z metastatskim rakom želodca vključno z adenokarcinomom gastro-ezofagealnega prehoda, ki so bili predhodno že zdravljeni z najmanj dvema sistemskima režimoma zdravljenja za napredovalo bolezen. **ODMERJANJE IN NAČIN UPORABE*:** Priporočeni začetni odmerek zdravila Lonsurf pri odraslih je 35 mg/m^2/odmerek peroralno dvakrat dnevno na 1. do 5. dan in 8. do 12. dan vsakega 28-dnevnega cikla zdravljenja, najpozneje 1 uro po zaključku jutranjega in večernega obroka (20 mg/m^2/odmerek dvakrat dnevno pri bolnikih s hudo ledvično okvaro). Odmerjanje, izračunano glede na telesno površino, ne sme preseči 80 mg/odmerek. Možne prilagoditve odmerka glede na varnost in prenašanje zdravila: dovoljena so zmanjšanja odmerka na najmanjši odmerek 20 mg/m^2 dvakrat dnevno (oz. 15 mg/m^2 dvakrat dnevno pri bolnikih s hudo ledvično okvaro). Potem ko je bil odmerek zmanjšan, povečanje ni dovoljeno. **KONTRAINDIKACIJE*:** Preobčutljivost na zdravilni učinkovini ali katero koli pomožno snov. **OPOZORILA IN PREVIDNOSTNI UKREPI*:** Supresija kostnega mozga: Pred uvedbo zdravljenja in po potrebi za spremljanje toksičnosti zdravila, najmanj pred vsakim ciklom zdravljenja, je treba pregledati celotno krvno sliko. Zdravljenja ne smete začeti, če je absolutno število nevtrofilcev < 1,5 x 10^9/l, če je število trombocitov < 75 x 10^9/l ali če se je pri bolniku zaradi predhodnih zdravljenj pojavila klinično pomembna nehematološka toksičnost 3. ali 4. stopnje, ki še traja. Bolnike je treba skrbno spremljati zaradi morebitnih okužb, uvesti je treba ustrezne ukrepe, kot je klinično indicirano. Toksičnost za prebavila: Potrebna je uporaba antiemetikov, antidiaroikov ter drugih ukrepov, kot je klinično indicirano. Če je potrebno, prilagodite odmerke. Ledvična okvara: Zdravilo Lonsurf ni primerno za uporabo pri bolnikih s končno stopnjo ledvične okvare. Bolnike z ledvično okvaro je potrebno med zdravljenjem skrbno spremljati; bolnike z zmerno ali hudo ledvično okvaro je treba zaradi hematološke toksičnosti bolj pogosto spremljati. Jetrna okvara: Uporaba zdravila Lonsurf pri bolnikih z obstoječo zmerno ali hudo jetrno okvaro ni priporočljiva. Proteinurija: Pred začetkom zdravljenja in med njim je priporočljivo spremljanje proteinurije z urinskimi testnimi lističi. Pomožne snovi: Zdravilo vsebuje laktozo. **INTERAKCIJE*:** Zdravila, ki medsebojno delujejo z nukleozidnimi prenašalci CNT1, ENT1 in ENT2, zaviralci OCT2 ali MATE1, substrati humane timidin-kinaze (npr. zidovudinom), hormonskimi kontraceptivi. **PLODNOST*, NOSEČNOST IN DOJENJE*:** Ni priporočljivo. **KONTRACEPCIJA*:** Ženske in moški morajo uporabljati učinkovito metodo kontracepcije med zdravljenjem in do 6 mesecev po zaključku zdravljenja. **VPLIV NA SPOSOBNOST VOŽNJE IN UPRAVLJANJA STROJEV*:** Med zdravljenjem se lahko pojavijo utrujenost, omotica ali splošno slabo počutje. **NEŽELENI UČINKI*:** *Zelo pogosti:* nevtropenija, levkopenija, anemija, trombocitopenija, zmanjšan apetit, diareja, navzea, bruhanje, utrujenost. *Pogosti:* okužba spodnjih dihal, febrilna nevtropenija, limfopenija, hipoalbuminemija, disgevzija, periferna nevropatija, dispneja, bolečina v trebuhu, zaprtje, stomatitis, bolezni ustne votline, hiperbilirubinemija, sindrom palmarne plantarne eritrodisestezije, izpuščaj, alopecija, pruritus, suha koža, proteinurija, pireksija, edem, vnetje sluznice, splošno slabo počutje, zvišanje jetrnih encimov, zvišanje alkalne fosfataze v krvi, zmanjšanje telesne mase. *Občasni:* septični šok, infekcijski enteritis, pljučnica, okužba žolčevoda, gripa, okužba sečil, gingivitis, herpes zoster, tinea pedis, okužba s kandido, bakterijska okužba, okužba, nevtropenična sepsa, okužba zgornjih dihal, konjunktivitis, bolečina zaradi raka, pancitopenija, granulocitopenija, monocitopenija, eritropenija, levkocitoza, monocitoza, dehidracija, hiperglikemija, hiperkaliemija, hipokaliemija, hipofosfatemija, hipernatriemija, hiponatriemija, hipokalciemija, protin, anksioznost, nespečnost, nevrotoksičnost, disestezija, hiperestezija, hipoestezija, sinkopa, parestezija, pekoč občutek, letargija, omotica, glavobol, zmanjšana ostrina vida, zamegljen vid, diplopija, katarakta, suho oko, vrtoglavica, neugodje v ušesu, angina pektoris, aritmija, palpitacije, embolija, hipertenzija, hipotenzija, vročinski oblivi, pljučna embolija, plevralni izliv, izcedek iz nosu, disfonija, orofaringealna bolečina, epistaksa, kašelj, hemoragični enterokolitis, krvavitev v prebavilih, akutni pankreatitis, ascites, ileus, subileus, kolitis, gastritis, refluksni gastritis, ezofagitis, moteno praznjenje želodca, abdominalna distenzija, analno vnetje, razjede v ustih, dispepsija, gastroezofagealna refluksna bolezen, proktalgija, bukalni polip, krvavitev dlesni, glositis, parodontalna bolezen, bolezen zob, siljenje na bruhanje, flatulenca, slab zadah, hepatotoksičnost, razširitev žolčnih vodov, luščenje kože, urtikarija, preobčutljivostne reakcije na svetlobo, eritem, akne, hiperhidroza, žulj, bolezni nohtov, otekanje sklepov, artralgija, bolečina v kosteh, mialgija, mišično-skeletna bolečina, mišična oslabelost, mišični krči, bolečina v okončinah, ledvična odpoved, neinfektivni cistitis, motnje mikcije, hematurija, levkociturija, motnje menstruacije, poslabšanje splošnega zdravstvenega stanja, bolečina, občutek spremembe telesne temperature, kseroza, nelagodje, zvišanje kreatinina v krvi, podaljšanje intervala QT na elektrokardiogramu, povečanje mednarodnega umerjenega razmerja (INR), podaljšanje aktiviranega parcialnega tromboplastinskega časa (aPTČ), zvišanje sečnine v krvi, zvišanje laktatne dehidrogenaze v krvi, znižanje celokupnih proteinov, zvišanje C-reaktivnega proteina, zmanjšan hematokrit. *Post-marketinške izkušnje:* intersticijska bolezen pljuč. **PREVELIKO ODMERJANJE*:** Neželeni učinki, o katerih so poročali v povezavi s prevelikim odmerjanjem, so bili v skladu z uveljavljenim varnostnim profilom. Glavni pričakovani zaplet prevelikega odmerjanja je supresija kostnega mozga. **FARMAKODINAMIČNE LASTNOSTI*:** *Farmakoterapevtska skupina:* zdravila z delovanjem na novotvorbe, antimetaboliti, oznaka ATC: L01BC59. Zdravilo Lonsurf sestavljata antineoplastični timidinski nukleozidni analog, trifluridin, in zaviralec timidin-fosforilaze (TPaze), tipiracilijev klorid. Po privzemu v rakave celice timidin-kinaza fosforilira trifluridin. Ta se v celicah nato presnovi v substrat deoksiribonukleinske kisline (DNA), ki se vgradi neposredno v DNA ter tako preprečuje celično proliferacijo. TPaza hitro razgradi trifluridin in njegova presnova po peroralni uporabi je hitra zaradi učinka prvega prehoda, zato je v zdravilo vključen zaviralec TPaze, tipiracilijev klorid. **PAKIRANJE*:** 20 filmsko obloženih tablet. **NAČIN PREDPISOVANJA IN IZDAJE ZDRAVILA:** Rp/Spec. **Imetnik dovoljenja za promet:** Les Laboratoires Servier, 50, rue Carnot, 92284 Suresnes cedex, Francija. **Številka dovoljenja za promet z zdravilom:** EU/1/16/1096/001 (Lonsurf 15 mg/6,14 mg), EU/1/16/1096/004 (Lonsurf 20 mg/8,19 mg). **Datum zadnje revizije besedila: april 2020. *Pred predpisovanjem preberite celoten povzetek glavnih značilnosti zdravila. Celoten povzetek glavnih značilnosti zdravila in podrobnejše informacije so na voljo pri: Servier Pharma d.o.o., Podmilščakova ulica 24, 1000 Ljubljana, tel: 01 563 48 11, www.servier.si.**

Datum priprave informacije: april 2020.
LNF AD1 C2 19/20 Samo za strokovno javnost.

Instructions for authors

The editorial policy

Radiology and Oncology is a multidisciplinary journal devoted to the publishing original and high quality scientific papers and review articles, pertinent to diagnostic and interventional radiology, computerized tomography, magnetic resonance, ultrasound, nuclear medicine, radiotherapy, clinical and experimental oncology, radiobiology, medical physics and radiation protection. Therefore, the scope of the journal is to cover beside radiology the diagnostic and therapeutic aspects in oncology, which distinguishes it from other journals in the field.

The Editorial Board requires that the paper has not been published or submitted for publication elsewhere; the authors are responsible for all statements in their papers. Accepted articles become the property of the journal and, therefore cannot be published elsewhere without the written permission of the editors.

Submission of the manuscript

The manuscript written in English should be submitted to the journal via online submission system Editorial Manager available for this journal at: **www.radioloncol.com**.

In case of problems, please contact Sašo Trupej at **saso.trupej@computing.si** or the Editor of this journal at **gsersa@onko-i.si**

All articles are subjected to the editorial review and when the articles are appropriated they are reviewed by independent referees. In the cover letter, which must accompany the article, the authors are requested to suggest 3-4 researchers, competent to review their manuscript. However, please note that this will be treated only as a suggestion; the final selection of reviewers is exclusively the Editor's decision. The authors' names are revealed to the referees, but not vice versa.

Manuscripts which do not comply with the technical requirements stated herein will be returned to the authors for the correction before peer-review. The editorial board reserves the right to ask authors to make appropriate changes of the contents as well as grammatical and stylistic corrections when necessary. Page charges will be charged for manuscripts exceeding the recommended length, as well as additional editorial work and requests for printed reprints.

Articles are published printed and on-line as the open access (**https://content.sciendo.com/raon**).

All articles are subject to 900 EUR + VAT publication fee. Exceptionally, waiver of payment may be negotiated with editorial office, upon lack of funds.

Manuscripts submitted under multiple authorship are reviewed on the assumption that all listed authors concur in the submission and are responsible for its content; they must have agreed to its publication and have given the corresponding author the authority to act on their behalf in all matters pertaining to publication. The corresponding author is responsible for informing the coauthors of the manuscript status throughout the submission, review, and production process.

Preparation of manuscripts

Radiology and Oncology will consider manuscripts prepared according to the Uniform Requirements for Manuscripts Submitted to Biomedical Journals by International Committee of Medical Journal Editors (www.icmje.org). The manuscript should be written in grammatically and stylistically correct language. Abbreviations should be avoided. If their use is necessary, they should be explained at the first time mentioned. The technical data should conform to the SI system. The manuscript, excluding the references, tables, figures and figure legends, must not exceed 5000 words, and the number of figures and tables is limited to 8. Organize the text so that it includes: Introduction, Materials and methods, Results and Discussion. Exceptionally, the results and discussion can be combined in a single section. Start each section on a new page, and number each page consecutively with Arabic numerals. For ease of review, manuscripts should be submitted as a single column, double-spaced text.and must have continuous line numbering.

The Title page should include a concise and informative title, followed by the full name(s) of the author(s); the institutional affiliation of each author; the name and address of the corresponding author (including telephone, fax and E-mail), and an abbreviated title (not exceeding 60 characters). This should be followed by the abstract page, summarizing in less than 250 words the reasons for the study, experimental approach, the major findings (with specific data if possible), and the principal conclusions, and providing 3-6 key words for indexing purposes. Structured abstracts are required. Slovene authors are requested to provide title and the abstract in Slovene language in a separate file. The text of the research article should then proceed as follows:

Introduction should summarize the rationale for the study or observation, citing only the essential references and stating the aim of the study.

Materials and methods should provide enough information to enable experiments to be repeated. New methods should be described in details.

Results should be presented clearly and concisely without repeating the data in the figures and tables. Emphasis should be on clear and precise presentation of results and their significance in relation to the aim of the investigation.

Discussion should explain the results rather than simply repeating them and interpret their significance and draw conclusions. It should discuss the results of the study in the light of previously published work.

Charts, Illustrations, Images and Tables

Charts, Illustrations, Images and Tables must be numbered and referred to in the text, with the appropriate location indicated. Charts, Illustrations and Images, provided electronically, should be of appropriate quality for good reproduction. Illustrations and charts must be vector image, created in CMYK color space, preferred font "Century Gothic", and saved as .AI, .EPS or .PDF format. Color charts, illustrations and Images are encouraged, and are published without additional charge. Image size must be 2.000 pixels on the longer side and saved as .JPG (maximum quality) format. In Images, mask the identities of the patients. Tables should be typed double-spaced, with a descriptive title and, if appropriate, units of numerical measurements included in the column heading. The files with the figures and tables can be uploaded as separate files.

References

References must be numbered in the order in which they appear in the text and their corresponding numbers quoted in the text. Authors are responsible for the accuracy of their references. References to the Abstracts and Letters to the Editor must be identified as such. Citation of papers in preparation or submitted for publication, unpublished observations, and personal communications should not be included in the reference list. If essential, such material may be incorporated in the appropriate place in the text. References follow the style of Index Medicus, DOI number (if exists) should be included.

All authors should be listed when their number does not exceed six; when there are seven or more authors, the first six listed are followed by "et al.". The following are some examples of references from articles, books and book chapters:

Dent RAG, Cole P. In vitro maturation of monocytes in squamous carcinoma of the lung. *Br J Cancer* 1981; **43:** 486-95. doi: 10.1038/bjc.1981.71

Chapman S, Nakielny R. *A guide to radiological procedures*. London: Bailliere Tindall; 1986.

Evans R, Alexander P. Mechanisms of extracellular killing of nucleated mammalian cells by macrophages. In: Nelson DS, editor. *Immunobiology of macrophage.* New York: Academic Press; 1976. p. 45-74.

Authorization for the use of human subjects or experimental animals

When reporting experiments on human subjects, authors should state whether the procedures followed the Helsinki Declaration. Patients have the right to privacy; therefore the identifying information (patient's names, hospital unit numbers) should not be published unless it is essential. In such cases the patient's informed consent for publication is needed, and should appear as an appropriate statement in the article. Institutional approval and Clinical Trial registration number is required. Retrospective clinical studies must be approved by the accredited Institutional Review Board/Committee for Medical Ethics or other equivalent body. These statements should appear in the Materials and methods section.

The research using animal subjects should be conducted according to the EU Directive 2010/63/EU and following the Guidelines for the welfare and use of animals in cancer research (Br J Cancer 2010; 102: 1555 – 77). Authors must state the committee approving the experiments, and must confirm that all experiments were performed in accordance with relevant regulations.

These statements should appear in the Materials and methods section (or for contributions without this section, within the main text or in the captions of relevant figures or tables).

Transfer of copyright agreement

For the publication of accepted articles, authors are required to send the License to Publish to the publisher on the address of the editorial office. A properly completed License to Publish, signed by the Corresponding Author on behalf of all the authors, must be provided for each submitted manuscript.

The non-commercial use of each article will be governed by the Creative Commons Attribution-NonCommercial-NoDerivs license.

Conflict of interest

When the manuscript is submitted for publication, the authors are expected to disclose any relationship that might pose real, apparent or potential conflict of interest with respect to the results reported in that manuscript. Potential conflicts of interest include not only financial relationships but also other, non-financial relationships. In the Acknowledgement section the source of funding support should be mentioned. The Editors will make effort to ensure that conflicts of interest will not compromise the evaluation process of the submitted manuscripts; potential editors and reviewers will exempt themselves from review process when such conflict of interest exists. The statement of disclosure must be in the Cover letter accompanying the manuscript or submitted on the form available on **www.icmje.org/coi_disclosure.pdf**

Page proofs

Page proofs will be sent by E-mail to the corresponding author. It is their responsibility to check the proofs carefully and return a list of essential corrections to the editorial office within three days of receipt. Only grammatical corrections are acceptable at that time.

Open access

Papers are published electronically as open access on **https://content.sciendo.com/raon**, also papers accepted for publication as E-ahead of print.

BISTVENI PODATKI IZ POVZETKA GLAVNIH ZNAČILNOSTI ZDRAVILA

XALKORI 200 mg, 250 mg trde kapsule

Sestava in oblika zdravila: Ena kapsula vsebuje 200 mg ali 250 mg krizotiniba. **Indikacije:** Monoterapija za: - prvo linijo zdravljenja odraslih bolnikov z napredovalim nedrobnoceličnim pljučnim rakom (NSCLC – *Non-Small Cell Lung Cancer*), ki je ALK (anaplastična limfomska kinaza) pozitiven; - zdravljenje odraslih bolnikov s predhodno zdravljenim, napredovalim NSCLC, ki je ALK pozitiven; - zdravljenje odraslih bolnikov z napredovalim NSCLC, ki je ROS1 pozitiven. **Odmerjanje in način uporabe:** Zdravljenje mora uvesti in nadzorovati zdravnik z izkušnjami z uporabo zdravil za zdravljenje rakavih bolezni. Preverjanje prisotnosti ALK in ROS1: Pri izbiri bolnikov za zdravljenje je treba pred zdravljenjem opraviti točno in validirano preverjanje prisotnosti ALK ali ROS1. Odmerjanje: Priporočeni odmerek je 250 mg dvakrat na dan (500 mg na dan), bolniki pa morajo zdravilo jemati brez prekinitev. Če bolnik pozabi vzeti odmerek, ga mora vzeti takoj, ko se spomni, razen če do naslednjega odmerka manjka manj kot 6 ur. V tem primeru bolnik pozabljenega odmerka ne sme vzeti. *Prilagajanja odmerkov:* Glede na varnost uporabe zdravila pri posameznem bolniku in kako bolnik zdravljenje prenaša, utegne biti potrebna prekinitev in/ali zmanjšanje odmerka pri bolnikih, ki se zdravijo s krizotinibom 250 mg peroralno dvakrat na dan (za režim zmanjševanja odmerka glejte poglavje 4.2 v povzetku glavnih značilnosti zdravila). Za prilagajanje odmerkov pri *hematološki in nehematološki toksičnosti* (povečanje vrednosti AST, ALT, bilirubina; ILD/pnevmonitis; podaljšanje intervala QTc, bradikardija, bolezni oči) glejte preglednici 1 in 2 v poglavju 4.2 povzetka glavnih značilnosti zdravila. *Okvara jeter:* Pri zdravljenju pri bolnikih z okvaro jeter je potrebna previdnost. Pri blagi okvari jeter prilagajanje začetnega odmerka ni priporočeno, pri zmerni okvari jeter je priporočeni začetni odmerek 200 mg dvakrat na dan, pri hudi okvari jeter pa 250 mg enkrat na dan (za merila glede klasifikacije okvare jeter glejte poglavje 4.2 v povzetku glavnih značilnosti zdravila). *Okvara ledvic:* Pri blagi in zmerni okvari prilagajanje začetnega odmerka ni priporočeno. Pri hudi okvari ledvic (ki ne zahteva peritonealne dialize ali hemodialize) je začetni odmerek 250 mg peroralno enkrat na dan; po vsaj 4 tednih zdravljenja se lahko poveča na 200 mg dvakrat na dan. *Starejši bolniki (≥ 65 let):* Prilagajanje začetnega odmerka ni potrebno. *Pediatrična populacija:* Varnost in učinkovitost nista bili dokazani. Način uporabe: Kapsule je treba pogoltniti cele, z nekaj vode, s hrano ali brez nje. Ne sme se jih zdrobiti, raztopiti ali odpreti. Izogibati se je treba uživanju grenivk, grenivkinega soka ter uporabi šentjanževke. **Kontraindikacije:** Preobčutljivost na krizotinib ali katerokoli pomožno snov. **Posebna opozorila in previdnostni ukrepi:** Določanje statusa ALK in ROS1: Pomembno je izbrati dobro validirano in robustno metodologijo, da se izognemo lažno negativnim ali lažno pozitivnim rezultatom. Hepatotoksičnost: V kliničnih študijah so poročali o hepatotoksičnosti, ki jo je povzročilo zdravilo (vključno s primeri s smrtnim izidom). Delovanje jeter, vključno z ALT, AST in skupnim bilirubinom, je treba preveriti enkrat na teden v prvih 2 mesecih zdravljenja, nato pa enkrat na mesec in kot je klinično indicirano. Ponovitve preverjanj morajo biti pogostejše pri povečanjih vrednosti stopnje 2, 3 ali 4. Intersticijska bolezen pljuč (ILD)/pnevmonitis: Lahko se pojavi huda, življenjsko nevarna ali smrtna ILD/pnevmonitis. Bolnike s simptomi ILD/pnevmonitisa je treba spremljati, zdravljenje pa prekiniti ob sumu na ILD/pnevmonitis. Podaljšanje intervala QT: Opažali so podaljšanje intervala QTc. Pri bolnikih z obstoječo bradikardijo, podaljšanjem intervala QTc v anamnezi ali predispozicijo zanj, pri bolnikih, ki jemljejo antiaritmike ali druga zdravila, ki podaljšujejo interval QT, ter pri bolnikih s pomembno obstoječo srčno boleznijo in/ali motnjami elektrolitov je treba krizotinib uporabljati previdno; potrebno je redno spremljanje EKG, elektrolitov in delovanja ledvic; preiskavi EKG in elektrolitov je treba opraviti čimbližje uporabi prvega odmerka, potem se priporoča redno spremljanje. Če se interval QTc podaljša za 60 ms ali več, je treba zdravljenje s krizotinibom začasno prekiniti in se posvetovati s kardiologom. Bradikardija: Lahko se pojavi simptomatska bradikardija (lahko se razvije več tednov po začetku zdravljenja); izogibati se je treba uporabi krizotiniba v kombinaciji z drugimi zdravili, ki povzročajo bradikardijo; pri simptomatski bradikardiji je treba prilagoditi odmerek. Srčno popuščanje: Poročali so o hudih, življenjsko nevarnih ali smrtnih neželenih učinkih srčnega popuščanja. Bolnike je treba spremljati glede pojavov znakov in simptomov srčnega popuščanja in ob pojavu simptomov zmanjšati odmerjanje ali prekiniti zdravljenje. Nevtropenija in levkopenija: V kliničnih študijah so poročali o nevtropeniji, levkopeniji in febrilni nevtropeniji; spremljati je treba popolno krvno sliko (pogostejše preiskave, če se opazijo abnormalnosti stopnje 3 ali 4 ali če se pojavi povišana telesna temperatura ali okužba). Perforacija v prebavilih: V kliničnih študijah so poročali o perforacijah v prebavilih, v obdobju trženja pa o smrtnih primerih perforacij v prebavilih. Krizotinib je treba pri bolnikih s tveganjem za nastanek perforacije v prebavilih uporabljati previdno; bolniki, pri katerih se razvije perforacija v prebavilih, se morajo prenehati zdraviti s krizotinibom; bolnike je treba poučiti o prvih znakih perforacije in jim svetovati, naj se nemudoma posvetujejo z zdravnikom. Vplivi na ledvice: V kliničnih študijah so opazili zvišanje ravni kreatinina v krvi in zmanjšanje očistka kreatinina. V kliničnih študijah in v obdobju trženja so poročali tudi o odpovedi ledvic, akutni odpovedi ledvic, primerih s smrtnim izidom, primerih, ki so zahtevali hemodializo in hiperkaliemiji stopnje 4. Vplivi na vid: V kliničnih študijah so poročali o izpadu vidnega polja stopnje 4 z izgubo vida. Če se na novo pojavi huda izguba vida, je treba zdravljenje prekiniti in opraviti oftalmološki pregled. Če so motnje vida trdovratne ali se poslabšajo, je priporočljiv oftalmološki pregled. Histološka preiskava, ki ne nakazuje adenokarcinoma: Na voljo so le omejeni podatki pri NSCLC, ki je ALK in ROS1 pozitiven in ima histološke značilnosti, ki ne nakazujejo adenokarcinoma, vključno s ploščatoceličnim karcinomom (SCC). **Medsebojno delovanje z drugimi zdravili in druge oblike interakcij:** Izogibati se je treba sočasni uporabi z močnimi zaviralci CYP3A4, npr. atazanavir, ritonavir, kobicistat, itrakonazol, ketokonazol, posakonazol, vorikonazol, klaritromicin, telitromicin in eritromicin (razen če morebitna korist za bolnika odtehta tveganje, v tem primeru je treba bolnike skrbno spremljati glede neželenih učinkov krizotiniba), ter grenivko in grenivkinim sokom, saj lahko povečajo koncentracije krizotiniba v plazmi. Izogibati se je treba sočasni uporabi z močnimi induktorji CYP3A4, npr. karbamazepin, fenobarbital, fenitoin, rifampicin in šentjanževka, saj lahko zmanjšajo koncentracije krizotiniba v plazmi. Učinek zmernih induktorjev CYP3A4, npr. efavirenz in rifabutin, še ni jasen, zato se je treba sočasni uporabi s krizotinibom izogibati. Zdravila, katerih koncentracije v plazmi lahko krizotinib spremeni (midazolam, alfentanil, cisaprid, ciklosporin, derivati ergot alkaloidov, fentanil, pimozid, kinidin, sirolimus, takrolimus, digoksin, dabigatran, kolhicin, pravastatin: sočasni uporabi s temi zdravili se je treba izogibati oziroma izvajati skrben klinični nadzor; bupropion, efavirenz, peroralni kontraceptivi, raltegravir, irinotekan, morfin, nalokson, metformin, prokainamid).

XALKORI®
KRIZOTINIB

Zdravila, ki podaljšujejo interval QT ali ki lahko povzročijo Torsades de pointes (antiaritmiki skupine IA (kinidin, disopiramid), antiaritmiki skupine III (amiodaron, sotalol, dofetilid, ibutilid), metadon, cisaprid, moksifloksacin, antipsihotiki) – v primeru sočasne uporabe je potreben skrben nadzor intervala QT. Zdravila, ki povzročajo bradikardijo (nedihidropiridinski zaviralci kalcijevih kanalčkov (verapamil, diltiazem), antagonisti adrenergičnih receptorjev beta, klonidin, gvanfacin, digoksin, meflokin, antiholinesteraze, pilokarpin) – krizotinib je treba uporabljati previdno. **Plodnost, nosečnost in dojenje:** Ženske v rodni dobi se morajo izogibati zanositvi. Med zdravljenjem in najmanj 90 dni po njem je treba uporabljati ustrezno kontracepcijo (velja tudi za moške). Zdravilo lahko škoduje plodu in se ga med nosečnostjo ne sme uporabljati, razen če klinično stanje matere ne zahteva takega zdravljenja. Matere naj se med jemanjem zdravila dojenju izogibajo. Zdravilo lahko zmanjša plodnost moških in žensk. **Vpliv na sposobnost vožnje in upravljanja strojev:** Lahko se pojavijo simptomatska bradikardija (npr. sinkopa, omotica, hipotenzija), motnje vida ali utrujenost; potrebna je previdnost. **Neželeni učinki:** Najresnejši neželeni učinki so bili hepatotoksičnost, ILD/pnevmonitis, nevtropenija in podaljšanje intervala QT. Najpogostejši neželeni učinki (≥ 25 %) so bili motnje vida, navzea, diareja, bruhanje, edem, zaprtje, povečane vrednosti transaminaz, utrujenost, pomanjkanje apetita, omotica in nevropatija. Ostali zelo pogosti (≥ 1/10 bolnikov) neželeni učinki so: nevtropenija, anemija, levkopenija, disgevzija, bradikardija, bolečina v trebuhu in izpuščaj. **Način in režim izdaje:** Predpisovanje in izdaja zdravila je le na recept, zdravilo pa se uporablja samo v bolnišnicah. Izjemoma se lahko uporablja pri nadaljevanju zdravljenja na domu ob odpustu iz bolnišnice in nadaljnjem zdravljenju. **Imetnik dovoljenja za promet:** Pfizer Europe MA EEIG, Boulevard de la Plaine 17, 1050 Bruxelles, Belgija. **Datum zadnje revizije besedila:** 31.10.2019.

Pred predpisovanjem se seznanite s celotnim povzetkom glavnih značilnosti zdravila.

Vir: 1. Povzetek glavnih značilnosti zdravila Xalkori, 31.10.2019

XAR-01-20 Samo za strokovno javnost

Pfizer Luxembourg SARL, GRAND DUCHY OF LUXEMBOURG, 51, Avenue J.F. Kennedy, L-1855,
Pfizer podružnica Ljubljana, Letališka cesta 29a, 1000 Ljubljana

Radiology and Oncology | Ljubljana | Slovenia | https://content.sciendo.com/raon

ISSN 1318 - 2099